



University  
of Glasgow

Greig, Fiona Helen (2013) *The involvement of modified lipids in vascular injury and disease*. PhD thesis.

<http://theses.gla.ac.uk/4229/>

Copyright and moral rights for this thesis are retained by the author

A copy can be downloaded for personal non-commercial research or study

This thesis cannot be reproduced or quoted extensively from without first obtaining permission in writing from the Author

The content must not be changed in any way or sold commercially in any format or medium without the formal permission of the Author

When referring to this work, full bibliographic details including the author, title, awarding institution and date of the thesis must be given

# **The Involvement of Modified Lipids in Vascular Injury and Disease**

**Fiona Helen Greig  
BSc (Hons)**

Submitted in fulfilment of the requirements of the degree of Doctor of  
Philosophy in the Institute of Cardiovascular and Medical Sciences,  
University of Glasgow

Institute of Cardiovascular and Medical Sciences  
College of Medical, Veterinary and Life Sciences  
University of Glasgow

© F.H. Greig 2013

## **Author's Declaration**

I declare that this thesis has been written solely by me with the research entirely generated by myself with the exception of the small vessel wire myography using oxidised phospholipids which was in collaboration with Ms. Amy Bolsworth, Melissa Craft and Lisa McArthur. This thesis has also not been previously submitted for a higher degree. The research was carried out principally in the Institute of Cardiovascular and Medical Sciences at the University of Glasgow, under the supervision of Dr. Simon Kennedy. With the exception of initial cell culture experiments and mass spectrometry which were performed at the Strathclyde Institute of Pharmacy and Biomedical Sciences at the University of Strathclyde, Glasgow, mass spectrometry analysis of arteries was carried out in the School of Life and Health Sciences at the Aston University, Birmingham, all under the supervision of Dr. Corinne M. Spickett.

Fiona H. Greig

January 2013

# Acknowledgements

First and foremost I would like to thank my supervisors, Dr. Simon Kennedy and Dr. Corinne Spickett for all their support, guidance, advice and the opportunities I've had over the course of my PhD. I would also like to acknowledge the British Heart Foundation for their support and funding of this project.

There are many people whose help over the years has been invaluable and greatly appreciated, both at the Universities of Glasgow and Strathclyde. I would like to thank all the members of the Kennedy and Spickett groups past and present for helping me with just about everything especially Dr. Dave Farmer, Ian Watt and Dr. Norsyahida Mohd Fauzi. A special thanks goes to Dr. Marie-Ann Ewart who has put up with my incessant chatting and endless questions over the last few years but who always has time for me. I would also like to thank Professor Andy Pitt and Dr. Ana Reis for their help with mass spectrometry and Margaret Nilsen for her help and advice with all things immunohistochemistry related.

I have made some amazing friends during the course of my PhD and I would like to thank them all for putting up with me and attempting to keep me sane whilst constantly making me laugh over the last few years. A huge thanks goes to AK Johansen, Clare McKinney and Emma Wallace for always having time for a talk or a wine depending on the situation. I couldn't have got through it without you. I would also like to thank all my friends outside of science for their support despite having no idea what it is I actually do and reminding me there is a world out there.

Finally, I would like to thank my family for all the advice, encouragement and "inspirational" talks over the years and even listening to the occasional rant. I couldn't have done it without you.

# Table of Contents

Author's Declaration.....	ii
Acknowledgements.....	iii
Table of Contents.....	iv
List of Figures.....	ix
List of Tables.....	xiii
List of Publications.....	xiv
List of Abbreviations and Definitions.....	xv
Abstract.....	xix
CHAPTER 1.....	1
GENERAL INTRODUCTION.....	1
1.1    Cardiovascular system.....	2
1.1.1    Structural organisation.....	2
1.1.2    Structure of the arterial wall.....	2
1.1.3    Vascular smooth muscle function.....	2
1.1.4    Cardiovascular disease.....	3
1.2    Atherosclerosis.....	4
1.2.1    Classification of atherosclerotic lesions.....	4
1.2.2    Pathophysiology of atherosclerosis.....	5
1.2.3    Atherosclerosis and hypertension.....	10
1.2.4    Animal models of atherosclerosis.....	10
1.3    Modification of phospholipids and LDL in atherosclerosis.....	12
1.3.1    LDL particles.....	12
1.3.2    Oxidation of LDL.....	13
1.3.3    Physiological effects of oxidised phospholipids.....	15
1.3.4    MPO.....	21
1.3.5    Formation and physiological activity of chlorinated lipids.....	22
1.4    Treatments for atherosclerosis.....	25
1.4.1    Pharmacological treatment of atherosclerosis.....	26
1.4.2    Surgical intervention in the treatment of atherosclerosis.....	26
1.5    Restenosis.....	28
1.5.1    Pathophysiology of restenosis.....	28
1.5.2    Potential involvement of modified lipids in restenosis.....	32
1.5.3    Current and future treatments for restenosis.....	33
1.6    Adenosine monophosphate-activated protein kinase.....	34
1.6.1    Regulatory mechanism and signalling of AMPK.....	34
1.6.2    Involvement of AMPK in vascular disease.....	35

1.7	Aims of this thesis .....	39
CHAPTER 2 .....		40
GENERAL MATERIALS AND METHODS .....		40
Materials.....		41
2.1	Chemicals and Reagents.....	41
Methods.....		41
2.2	Lipid preparation and synthesis.....	41
2.2.1	Chlorohydrin formation .....	41
2.2.2	Measurement of stability of chlorohydrins .....	42
2.2.3	Quantification of phospholipids by ESMS .....	42
2.2.4	Alpha-chloro fatty aldehyde synthesis .....	42
2.3	Tissue culture .....	43
2.3.1	Maintenance of primary cell cultures.....	43
2.3.2	Rabbit aortic smooth muscle cells .....	43
2.3.3	Measurement of cell proliferation.....	44
2.3.4	Assessment of cell viability .....	45
2.3.5	Measurement of cell migration .....	45
2.4	Western blotting .....	46
2.4.1	Treatment of rabbit aortic smooth muscle cells .....	46
2.4.2	Preparation of mouse aorta and liver .....	46
2.4.3	Quantification of protein concentration .....	46
2.4.4	SDS PAGE.....	47
2.4.5	Immunoblotting.....	48
2.4.6	Quantification of expression of protein.....	48
2.5	Small vessel wire myography.....	48
2.5.1	Cumulative concentration-response curve .....	49
2.6	Animal models .....	51
2.6.1	C57BL/6 mice .....	51
2.6.2	ApoE <sup>-/-</sup> mice .....	51
2.6.3	Mouse carotid artery injury model.....	51
2.6.4	AICAR administration .....	54
2.6.5	Haemodynamic measurements.....	54
2.6.6	Measurement of plasma MPO.....	54
2.7	Histology .....	56
2.7.1	Fixation .....	56
2.7.2	Haematoxylin and eosin staining .....	57
2.7.3	Immunohistochemistry.....	57
2.8	Detection of lipids in murine arteries .....	59
2.8.1	Lipid extraction from mouse carotid arteries and aortae .....	59

2.8.2	Quantification of lipids by ESMS .....	59
2.9	Statistical analysis .....	60
CHAPTER 3	.....	61
THE INFLUENCE OF MODIFIED LIPIDS ON VSMCs	.....	61
3.1	Introduction .....	62
3.1.1	Aims .....	63
3.2	Methods .....	64
3.2.1	Lipid preparation and analysis .....	64
3.2.2	VSMC proliferation .....	64
3.2.3	VSMC viability .....	64
3.2.4	Western blotting .....	64
3.2.5	VSMC migration .....	65
3.2.6	Statistical analysis .....	65
3.3	Results .....	66
3.3.1	Detection and assessment of the stability of phospholipid chlorohydrins .....	66
3.3.2	Effect of pretreatment of modified lipids on VSMC proliferation and viability .....	66
3.3.3	Effect of chronic incubation of modified lipids on VSMC proliferation and viability .....	78
3.3.4	Effect of modified lipids on VSMC migration .....	78
3.4	Discussion .....	87
3.5	Conclusions .....	91
CHAPTER 4	.....	92
THE IMPACT OF AMPK SIGNALLING ON THE EFFECTS OF MODIFIED LIPIDS IN VSM	.....	92
4.1	Introduction .....	93
4.1.1	Aims .....	94
4.2	Methods .....	95
4.2.1	Smooth muscle proliferation .....	95
4.2.2	Smooth muscle viability .....	95
4.2.3	Western blotting .....	95
4.2.4	Small vessel wire myography .....	97
4.2.5	Statistical analysis .....	98
4.3	Results .....	99
4.3.1	Effect of AMPK activation or inhibition in VSMCs .....	99
4.3.2	Effect of AMPK activation or inhibition prior to modified lipid treatment on VSMC proliferation and viability .....	102
4.3.3	Effect of AMPK activation or inhibition prior to modified lipid incubation on AMPK $\alpha$ and ACC expression .....	109
4.3.4	Effect of modified lipid incubation of AICAR-induced relaxation .....	114

4.4	Discussion .....	117
4.5	Conclusions .....	121
CHAPTER 5 .....		122
THE OCCURRENCE OF MODIFIED LIPIDS IN NEOINTIMA FORMATION IN MICE .....		122
5.1	Introduction .....	123
5.1.1	Aims .....	124
5.2	Methods .....	125
5.2.1	Carotid artery injury .....	125
5.2.2	MPO assay .....	125
5.2.3	Histology .....	125
5.2.4	Detection of lipids in carotid arteries .....	126
5.2.5	Statistical analysis .....	126
5.3	Results .....	127
5.3.1	Extent of neointima formation in C57BL/6 and ApoE <sup>-/-</sup> mice after vascular injury .....	127
5.3.2	Structural composition of neointima in C57BL/6 and ApoE <sup>-/-</sup> mice after vascular injury .....	130
5.3.3	Occurrence of modified lipids in neointima formation after vascular injury.....	134
5.3.4	Role of AMPK in neointima formation .....	145
5.4	Discussion .....	148
5.5	Conclusions .....	153
CHAPTER 6 .....		154
THE EFFECT OF AMPK ACTIVATION IN HEALTHY AND ATHEROSCLEROTIC MICE.....		154
6.1	Introduction .....	155
6.1.1	Aims .....	156
6.2	Methods .....	157
6.2.1	Chronic AICAR administration .....	157
6.2.2	Haemodynamic measurements.....	157
6.2.3	Western blotting .....	158
6.2.4	MPO assay .....	158
6.2.5	Detection of lipids in aortae by ESMS.....	158
6.2.6	Statistical analysis .....	158
6.3	Results .....	159
6.3.1	Effect of chronic AICAR administration on blood pressure and weight in healthy and atherosclerotic mice.....	159
6.3.2	Effect of chronic AICAR treatment on expression of AMPK $\alpha$ and ACC in mouse aorta and liver .....	169

6.3.3	Effect of AICAR administration on modified lipids in healthy and atherosclerotic mice .....	174
6.4	Discussion .....	184
6.5	Conclusions .....	189
CHAPTER 7 .....		191
GENERAL DISCUSSION.....		191
7.1	Conclusions .....	199
List of References .....		200
Appendices.....		230

# List of Figures

Figure 1.1 – Formation of foam cells and plaques in atherosclerosis and the importance of VSMCs in disease progression. ....	9
Figure 1.2 – Sources and physiological effects of LDL and phospholipid oxidation. ....	20
Figure 1.3 – Formation of phospholipid chlorohydrins. ....	24
Figure 1.4 – Vascular remodelling processes involved in restenosis. ....	31
Figure 1.5 – AMPK activation and its cardio and vasculoprotective functions. ....	38
Figure 2.1 – Representative BSA standard curve. ....	47
Figure 2.2 – Representative diagram of mouse carotid artery mounted in small vessel wire myograph. ....	49
Figure 2.3 – <i>In vivo</i> experimental design. ....	53
Figure 2.4 – Representative MPO standard curve. ....	55
Figure 2.5 – Photograph of QTRAP® 5500 mass spectrometer. ....	60
Figure 3.1 – Illustration of chemotactic cell migration assay. ....	65
Figure 3.2 – Stability of SOPC and SLPC ClOH over 72 hour period. ....	68
Figure 3.3 – Immunostaining of primary cell culture for $\alpha$ SMA. ....	69
Figure 3.4 – Effect of increasing concentrations of FCS on BrdU incorporation in proliferating VSMCs in culture. ....	69
Figure 3.5 – Effect of 2 hour pretreatment of SOPC ClOH on VSMC proliferation and viability. ....	70
Figure 3.6 – Effect of 2 hour pretreatment with 2-ClHDA on VSMC proliferation and viability. ....	71
Figure 3.7 – Effect of 2 hour pretreatment with PGPC on VSMC proliferation and viability. ....	72
Figure 3.8 – Effect of 2 hour pretreatment with POVPC on VSMC proliferation and viability. ....	73
Figure 3.9 – Effect of 2 hour pretreatment of chlorinated lipids on VSMC morphological changes and caspase 3 expression. ....	74
Figure 3.10 – Effect of 2 hour pretreatment of oxidised lipids on VSMC morphological changes and caspase 3 expression. ....	75
Figure 3.11 – Effect of 6 hour pretreatment with chlorinated lipids and selected oxidised phospholipid on VSMC viability. ....	76
Figure 3.12 – Effect of HOCl incubation on VSMC proliferation. ....	77
Figure 3.13 – Effect of chronic treatment of SOPC ClOH on VSMC proliferation and viability. ....	79
Figure 3.14 – Effect of chronic treatment of 2-ClHDA on VSMC proliferation and viability. ....	80
Figure 3.15 – Effect of chronic treatment of PGPC on VSMC proliferation and viability. ....	81

Figure 3.16 – Effect of chronic treatment of POVPC on VSMC proliferation and viability. .....	82
Figure 3.17 – Effect of prior incubation of chlorinated lipids on FCS-induced VSMC migration. ....	83
Figure 3.18 – Effect of prior incubation of oxidised lipids on FCS-induced VSMC migration. ....	84
Figure 3.19 – Effect of incubation of chlorinated lipids during FCS-induced VSMC migration. ....	85
Figure 3.20 – Effect of incubation of oxidised lipids during FCS-induced VSMC migration. ....	86
Figure 4.1 – Schematic diagram of <i>in vitro</i> VSMC experiments for AMPK activation or inhibition prior to modified lipid incubation.....	96
Figure 4.2 – Representative myography recording for AICAR-induced relaxation.....	97
Figure 4.3 – Effect of AMPK activation or inhibition on VSMC proliferation and viability. .....	100
Figure 4.4 – Effect of AMPK activators and inhibitors on AMPK $\alpha$ and ACC expression in VSMCs.....	101
Figure 4.5 – Effect of AMPK activation prior to 2 hour chlorinated lipid treatment on VSMC proliferation and viability. ....	103
Figure 4.6 – Effect of AMPK activation prior to 2 hour oxidised phospholipid treatment on VSMC proliferation and viability. ....	104
Figure 4.7 – Effect of AMPK inhibition prior to 2 hour chlorinated lipid treatment on VSMC proliferation and viability. ....	105
Figure 4.8 – Effect of AMPK inhibition prior to 2 hour oxidised phospholipid treatment on VSMC proliferation and viability. ....	106
Figure 4.9 – Effect of AMPK activation and inhibition prior to 2 hour SOPC ClOH incubation on AMPK $\alpha$ and ACC expression. ....	110
Figure 4.10 – Effect of AMPK activation and inhibition prior to 2 hour 2-ClHDA incubation on AMPK $\alpha$ and ACC expression. ....	111
Figure 4.11 – Effect of AMPK activation and inhibition prior to 2 hour PGPC incubation on AMPK $\alpha$ and ACC expression. ....	112
Figure 4.12 – Effect of AMPK activation and inhibition prior to 2 hour POVPC incubation on AMPK $\alpha$ and ACC expression. ....	113
Figure 4.13 – Effect of modified lipid incubation on U46619-induced contraction in mouse carotid arteries. ....	115
Figure 4.14 – Effect of modified lipid incubation on AICAR-induced relaxation in mouse carotid arteries. ....	116
Figure 5.1 – Neointimal growth in the carotid arteries of C57BL/6 and ApoE <sup>-/-</sup> mice after sham-operated and carotid artery injury procedure. ....	128
Figure 5.2 – Circumference of carotid arteries of sham-operated and injured C57BL/6 and ApoE <sup>-/-</sup> mice. ....	129
Figure 5.3 – Aortic sections from C57BL/6 and ApoE <sup>-/-</sup> mice after carotid artery injury..... .....	129

Figure 5.4 – $\alpha$ SMA staining in left carotid arteries of sham-operated and injured C57BL/6 and ApoE <sup>-/-</sup> mice. ....	131
Figure 5.5 – Ki67 staining in left carotid arteries of sham-operated and injured C57BL/6 and ApoE <sup>-/-</sup> mice. ....	132
Figure 5.6 – Active caspase 3 staining in left carotid arteries from sham-operated and injured C57BL/6 and ApoE <sup>-/-</sup> mice. ....	133
Figure 5.7 – Effect of carotid artery injury on MPO plasma content of C57BL/6 and ApoE <sup>-/-</sup> mice. ....	136
Figure 5.8 – Detection of PCs and SMs from left and right carotid arteries of sham-operated and injured C57BL/6 and ApoE <sup>-/-</sup> mice.....	137
Figure 5.9 – Detection of chain-shortened PCs from left and right carotid arteries of sham-operated and injured C57BL/6 and ApoE <sup>-/-</sup> mice.....	138
Figure 5.10 – Detection of PEs from left and right carotid arteries of sham-operated and injured C57BL/6 and ApoE <sup>-/-</sup> mice. ....	139
Figure 5.11 – Detection of PSs from left and right carotid arteries of sham-operated and injured C57BL/6 and ApoE <sup>-/-</sup> mice. ....	140
Figure 5.12 – Detection of PIs from left and right carotid arteries of sham-operated and injured C57BL/6 and ApoE <sup>-/-</sup> mice. ....	141
Figure 5.13 – Detection of cholesterol and cholesteryl esters from left and right carotid arteries of sham-operated and injured C57BL/6 and ApoE <sup>-/-</sup> mice.....	142
Figure 5.14 – Total AMPK $\alpha$ staining in left carotid arteries from sham-operated and injured C57BL/6 and ApoE <sup>-/-</sup> mice. ....	146
Figure 5.15 – Phosphorylated AMPK $\alpha$ staining in left carotid arteries from sham-operated and injured C57BL/6 and ApoE <sup>-/-</sup> mice. ....	147
Figure 6.1 – Representative arterial blood pressure trace from cannulation of the left common carotid artery. ....	157
Figure 6.2 – Effect of AICAR dosing on mean arterial pressure of C57BL/6 and ApoE <sup>-/-</sup> mice.....	161
Figure 6.3 – Effect of AICAR dosing on diastolic pressure of C57BL/6 and ApoE <sup>-/-</sup> mice. ....	162
Figure 6.4 – Effect of AICAR dosing on systolic pressure of C57BL/6 and ApoE <sup>-/-</sup> mice. ....	163
Figure 6.5 – Effect of AICAR dosing on pulse pressure of C57BL/6 and ApoE <sup>-/-</sup> mice...164	164
Figure 6.6 – Effect of AICAR dosing on heart rate of healthy and atherosclerotic mice..165	165
Figure 6.7 – Effect of 14 day dosing regimen on body weight of C57BL/6 and ApoE <sup>-/-</sup> mice.....	166
Figure 6.8 – Effect of AICAR dosing on organ weight of C57BL/6 and ApoE <sup>-/-</sup> mice. ...167	167
Figure 6.9 – Effect of AICAR dosing on phosphorylated and total AMPK $\alpha$ expression in aortae of C57BL/6 and ApoE <sup>-/-</sup> mice. ....	170
Figure 6.10 – Effect of AICAR dosing on phosphorylated and total ACC expression in aortae of C57BL/6 and ApoE <sup>-/-</sup> mice. ....	171
Figure 6.11 – Effect of AICAR dosing on phosphorylated and total AMPK $\alpha$ expression in liver of C57BL/6 and ApoE <sup>-/-</sup> mice.....	172

Figure 6.12 – Effect of AICAR dosing on phosphorylated and total ACC expression in liver of C57BL/6 and ApoE <sup>-/-</sup> mice.....	173
Figure 6.13 – Effect of AICAR treatment on MPO content of C57BL/6 and ApoE <sup>-/-</sup> mouse plasma. ....	176
Figure 6.14 – Detection of PCs and SMs from aortae of vehicle- and AICAR-treated C57BL/6 and ApoE <sup>-/-</sup> mice. ....	177
Figure 6.15 – Detection of chain-shortened PCs from aortae of vehicle- and AICAR-treated C57BL/6 and ApoE <sup>-/-</sup> mice.....	178
Figure 6.16 – Detection of PEs from aortae of vehicle- and AICAR-treated C57BL/6 and ApoE <sup>-/-</sup> mice. ....	179
Figure 6.17 – Detection of PSs from aortae of vehicle- and AICAR-treated C57BL/6 and ApoE <sup>-/-</sup> mice. ....	180
Figure 6.18 – Detection of PIs from aortae of vehicle- and AICAR-treated C57BL/6 and ApoE <sup>-/-</sup> mice. ....	181
Figure 6.19 – Detection of cholesterol and cholesteryl esters from aortae of vehicle- and AICAR-treated C57BL/6 and ApoE <sup>-/-</sup> mice.....	182
Figure 7.1 – Schematic diagram of the proposed interaction of modified lipids and AMPK signalling in VSMCs. ....	195

## List of Tables

Table 2.1 – Summary of antibodies and dilutions used for immunoblotting.....	50
Table 2.2 – Sequence for processing samples for histological analysis. ....	56
Table 2.3 – Summary of antibodies, dilutions and length of incubations used for immunohistochemistry.....	58
Table 4.1 – Percentage of proliferating or viable VSMCs after AMPK activation or inhibition prior to 2 hour incubation with increasing concentrations of chlorinated lipids. ....	107
Table 4.2 – Percentage of proliferating or viable VSMCs after AMPK activation or inhibition prior to 2 hour incubation with increasing concentrations of oxidised phospholipids. ....	108
Table 5.1 – Body and organ weight measurements of C57BL/6 and ApoE <sup>-/-</sup> mice before and 14 days after carotid artery injury procedure. ....	127
Table 5.2 – Relative abundances of detected phospholipid species in left common carotid arteries of sham-operated and injured C57BL/6 and ApoE <sup>-/-</sup> mice.....	143
Table 5.3 – Relative abundances of detected phospholipid species in right common carotid arteries of sham-operated and injured C57BL/6 and ApoE <sup>-/-</sup> mice.....	144
Table 6.1 – Weight and haemodynamic measurements of C57BL/6 and ApoE <sup>-/-</sup> mice before and after 14 days of AICAR administration. ....	168
Table 6.2 – Relative abundances of detected phospholipid species in aortae of vehicle- and AICAR-treated C57BL/6 and ApoE <sup>-/-</sup> mice.....	183

## List of Publications

**F.H. Greig**, S. Kennedy and C.M. Spickett (2012) Physiological effects of oxidized phospholipids and their cellular signaling mechanisms in inflammation. *Free Radic Biol Med*, **52**, 266-280. [Appendix 1]

A. Robaszkiewicz, **F.H. Greig**, A.R. Pitt, C.M. Spickett, G. Bartosz and M. Soszyński (2010) Effect of phosphatidylcholine chlorohydrins on human erythrocytes. *Chem Phys Lipids*, **163**, 639-647. [Appendix 2]

Abstracts:

**F.H. Greig**, M.A. Ewart, C.M. Spickett and S. Kennedy (2012) Enhanced cell death by oxidized phospholipids in vascular smooth muscle cells via activation of AMP-activated protein kinase. *Arterioscler Thromb Vasc Biol*, **32**(5), A181.

**F.H. Greig**, C.M. Spickett and S. Kennedy (2011) Influence of modified phospholipids on vascular cell function in restenosis. *pA<sub>2</sub> online*, **9**(3), A110P.

## List of Abbreviations and Definitions

$\alpha$ SMA	Alpha smooth muscle actin
2-CIHDA	2-chlorohexadecanal
A-769662	6,7-dihydro-4-hydroxy-3-(2'-hydroxy[1,1'-biphenyl]-4-yl)-6-oxo-thieno[2,3- <i>b</i> ]pyridine-5-carbonitrile (AMPK activator)
ABCA1	ATP binding cassette transporter A1
ABCG1	ATP binding cassette transporter G1
ACC	Acetyl-coA carboxylase
AICAR	5-aminoimidazole-4-carboxamide-1- $\beta$ -D-ribofuranoside (AMPK activator)
AMP	Adenosine monophosphate
AMPK	AMP-activated protein kinase
AMPK $\alpha$ 1 <sup>-/-</sup>	Mice deficient in AMPK $\alpha$ 1
AMPK $\alpha$ 2 <sup>-/-</sup>	Mice deficient in AMPK $\alpha$ 2
ANOVA	Analysis of variance
ApoB-100	Apolipoprotein B-100
ApoE	Apolipoprotein E
ApoE <sup>-/-</sup>	Mice deficient in ApoE
ATP	Adenosine triphosphate
BHT	Butylated hydroxytoluene
BrdU	Bromodeoxyuridine
BSA	Bovine serum albumin
Ca <sup>2+</sup>	Calcium
CABG	Coronary artery bypass grafting
CAD	Coronary artery disease
CAMKK $\beta$	Calcium-calmodulin-dependent kinase kinase $\beta$
Compound C	6-[4-(2-piperidin-1-yl-ethoxy)-phenyl]-3-pyridin-4-yl-pyrazolo[1,5- <i>a</i> ]-pyrimidine (AMPK inhibitor)
COX-2	Cyclooxygenase-2

CVD	Cardiovascular disease
CVS	Cardiovascular system
DAB	3,3-diaminobenzidine
DES	Drug-eluting stents
DPPE	1,2-dipalmitoyl- <i>sn</i> -glycero-3-phosphocholine
DTT	Dithiothreitol
ECL	Enhanced chemiluminescence
ECM	Extracellular matrix
EDTA	Ethylenediamine tetra-acetic acid
EEL	Exterior elastic lamina
ELISA	Enzyme-linked immunosorbent assay
ER	Endoplasmic reticulum
ESMS	Electrospray mass spectrometry
FCS	Foetal calf serum
GAPDH	Glyceraldehyde-3-phosphate dehydrogenase
H&E	Haematoxylin and eosin
H <sub>2</sub> O <sub>2</sub>	Hydrogen peroxide
HBSS	Hanks' balanced salt solution
HCAEC	Human coronary artery endothelial cell
HDL	High density lipoproteins
HMG-CoA	Hydroxymethylglutaryl-CoA
HPLC	High performance liquid chromatography
HOCl	Hypochlorous acid
HRP	Horseradish peroxidase
HUVEC	Human umbilical vein endothelial cell
i.p.	Intraperitoneal
IDL	Intermediate density lipoproteins
IL	Interleukin
Ki67	Nuclear proliferative marker

LDL	Low density lipoproteins
LDLr <sup>-/-</sup>	Mice deficient in low density lipoprotein receptor
LKB1	Liver kinase B1
LPC	Lysophosphatidylcholine
m/z	Mass-to-charge ratio
MAPK	Mitogen-activated protein kinase
MCP-1	Monocyte chemotactic protein-1
MI	Myocardial infarction
MKP-1	Mitogen-activated protein kinase phosphatase-1
mmLDL	Minimally-modified low density lipoproteins
MMP	Matrix metalloproteinase
MPO	Myeloperoxidase
NO	Nitric oxide
NOS	Nitric oxide synthase
oxLDL	Oxidised low density lipoproteins
oxPAPC	Oxidised 1-palmitoyl-2-arachidonoyl- <i>sn</i> -glycero-3-phosphocholine
PAPC	1-palmitoyl-2-arachidonoyl- <i>sn</i> -glycero-3-phosphocholine
PBS	Phosphate buffered saline
PC	Phosphatidylcholine
PCI	Percutaneous coronary intervention
PDGF	Platelet derived growth factor
PE	Phosphatidylethanolamine
PGPC	1-palmitoyl-2-glutaroyl- <i>sn</i> -glycero-3-phosphocholine
PI	Phosphatidylinositol
POVPC	1-palmitoyl-2-oxoaleroyl- <i>sn</i> -glycero-3-phosphocholine
PS	Phosphatidylserine
PTCA	Percutaneous transluminal coronary angioplasty
ROS	Reactive oxygen species
SDS PAGE	Sodium dodecyl sulphate polyacrylamide gel electrophoresis

SEM	Standard error of the mean
SLPC	1-stearoyl-2-linoleoyl- <i>sn</i> -glycero-3-phosphocholine
SM MHC	Smooth muscle myosin heavy chain
SM MLC	Smooth muscle myosin light chain
SM	Sphingomyelin
SMase	Sphingomyelinase
SOPC	1-stearoyl-2-oleoyl- <i>sn</i> -glycero-3-phosphocholine
SOPC ClOH	1-stearoyl-2-oleoyl- <i>sn</i> -glycero-3-phosphocholine chlorohydrin
TBST	Tris-buffered saline solution with Tween-20
TLR	Toll-like receptor
TMB	Tetra-methylbenzidine
U46619	9,11-dideoxy-11 $\alpha$ ,9 $\alpha$ -epoxymethanoprostaglandin F <sub>2<math>\alpha</math></sub> (thromboxane A <sub>2</sub> receptor agonist)
VCAM-1	Vascular cell adhesion molecule-1
VLDL	Very low density lipoproteins
VPO1	Vascular peroxidase 1
VSM	Vascular smooth muscle
VSMC	Vascular smooth muscle cell
ZMP	Zeatin riboside-5-monophosphate

## Abstract

Atherosclerosis is characterised by the deposition and accumulation of modified lipids in the subendothelial space of the arterial wall, as well as vascular remodelling leading to atherosclerotic plaque formation. Restenosis is a known complication of the surgical interventions used to treat atherosclerosis and results in neointimal thickening, in part by the action of vascular smooth muscle cells (VSMCs). Various physiological effects have previously been attributed to the action of oxidised low density lipoproteins leading to an exacerbation of the inflammatory response and vascular remodelling processes in atherosclerosis and restenosis. Little is known to date about the effects of individual modified lipids generated by the action of phagocytic myeloperoxidase (MPO) on these processes. The aim of the present study was to investigate the biological effects of modified lipids, both chlorinated and oxidised species, in vascular injury and disease, focussing primarily on their effects on vascular smooth muscle (VSM). Primary VSMCs were used to examine the effects of these modified lipids at a cellular level.

Chlorinated lipids, phospholipid chlorohydrins and alpha-chloro fatty aldehydes were found to have a limited effect on VSMC proliferation, viability or migration whereas, oxidised phospholipids caused a concentration-dependent reduction in all of these vascular remodelling processes. As AMP-activated protein kinase (AMPK) has recently been implicated in vascular disease and found to exert anti-apoptotic effects, the impact of AMPK signalling on the effects of the modified lipids in VSM was assessed. Activation of AMPK prior to incubation of 1-stearoyl-2-oleoyl-*sn*-glycero-3-phosphocholine chlorohydrin resulted in an increase in VSMC proliferation while a greater level of VSMC death was observed after treatment with the oxidised phospholipid, 1-palmitoyl-2-oxoaleroyl-*sn*-glycero-3-phosphocholine than with the lipids alone. The occurrence of these modified lipids in neointima formation was subsequently investigated using a carotid artery injury model in healthy and atherosclerotic mice (mice deficient in apolipoprotein E, ApoE<sup>-/-</sup>). Neointimal growth and levels of plasma MPO were increased in ApoE<sup>-/-</sup> mice resulting in elevated levels of lysophosphatidylcholines and altered relative proportions of phosphatidylcholines (PCs) in injured carotid arteries compared to their contralateral uninjured right carotid arteries. Finally, *in vivo* AMPK activation by administration of 5-aminoimidazole-4-carboxamide-1-β-D-ribofuranoside (AICAR) in healthy and atherosclerotic mice and its effect on the lipid profile of the aorta were characterised. Chronic AMPK activation resulted in a reduction in mean arterial and diastolic pressures

as well as a dramatic increase in pulse pressure in ApoE<sup>-/-</sup> mice compared to their saline-treated littermates. Plasma MPO was elevated in AICAR-treated ApoE<sup>-/-</sup> mice with an alteration in the relative intensities of PCs in aortae of AMPK activated ApoE<sup>-/-</sup> mice.

The present study is the first report of divergent effects of different classes of modified lipids on vascular remodelling processes and how these processes may be modulated by AMPK signalling in VSM in atherosclerosis. In addition, this study has generated novel data on the relative changes in distribution of PCs in carotid arteries after vascular injury as well as in aortic tissue of healthy and atherosclerotic mice after AMPK activation. Additional analysis is required to confirm these differences which could offer further insight into the involvement of modified lipids in vascular diseases. This study has also highlighted a novel interaction of AMPK signalling and modified lipids in VSM and could therefore provide novel therapeutic targets in the treatment of both atherosclerosis and restenosis.

# **CHAPTER 1**

## **GENERAL INTRODUCTION**

## **1.1 Cardiovascular system**

### **1.1.1 Structural organisation**

The cardiovascular system (CVS) transports and distributes essential substances such as gases, nutrients and hormones to various cells and tissues in the body through its intricate network of blood vessels. It is also responsible for the clearance of by-products of metabolism and is crucial in the maintenance of body temperature by transport of heat as well as monitoring the water content of cells. The main components of this circulatory system are the heart, blood and blood vessels. Oxygenated blood from the lungs is ejected from the left ventricle of the heart and flows through the aorta to be distributed to the peripheral tissues. The muscular aorta undergoes repeated arterial branching, ultimately resulting in the formation of thin-walled capillaries which allow for diffusion of gases and metabolites between the blood and cells of the body.

### **1.1.2 Structure of the arterial wall**

The arterial wall is made up of three concentric layers: the tunica intima, tunica media and tunica adventitia with each layer composed of phenotypically distinct cell types (Levick, 2003). The innermost layer, the tunica intima, exists as a monolayer of endothelial cells attached to a thin layer of connective tissue; the basal lamina. Endothelial cells encircle the lumen of the vessel and are in constant contact with blood releasing vasoactive agents such as the potent vasodilators prostacyclin and nitric oxide (NO). The tunica media consists chiefly of vascular smooth muscle cells (VSMCs) arranged helically in a matrix of collagen and elastin fibres with the internal and external elastic lamina (EEL) marking the boundaries of the layer. The tunica media is responsible for regulating the arterial diameter and therefore vascular tone, as it is the only vascular layer capable of producing a contractile response. The outermost layer, the tunica adventitia, is a connective tissue-rich sheath containing collagen and elastin fibres with no distinct outer border. The adventitia aids in the stability and anchoring of the vessel and contains tiny blood vessels called the vasa vasorum which supplies nourishment to the medial layer.

### **1.1.3 Vascular smooth muscle function**

Vascular smooth muscle (VSM) is continuously active with the concentration of cytosolic calcium ( $\text{Ca}^{2+}$ ) being the major determinant of vasoconstriction or vasodilation (Levick, 2003). The movement of  $\text{Ca}^{2+}$  in the cytosol results from a change in membrane potential

or the activation of receptors by contractile agents (Rang *et al.*, 2007). This results in the production of inositol 1,4,5-trisphosphate (IP<sub>3</sub>) and diacylglycerol from the hydrolysis of phosphatidyl inositol-bisphosphate by phospholipase C. Following activation, IP<sub>3</sub> causes Ca<sup>2+</sup> release from its internal store, the sarcoplasmic reticulum (SR) via the IP<sub>3</sub> receptor. The calcium-binding protein calmodulin forms a complex with Ca<sup>2+</sup> which in turn activates myosin light chain kinase. The activated enzyme phosphorylates smooth muscle myosin light chain (SM MLC), a process driven by adenosine triphosphate (ATP). This results in the interaction of SM MLC with alpha smooth muscle actin (αSMA) filaments, initiating crossbridge cycling and the generation of force which in turn produces contraction. For relaxation to occur, the level of free cytosolic Ca<sup>2+</sup> must decrease which occurs by the movement of Ca<sup>2+</sup> back into the lumen of the SR via the sarco/endoplasmic reticulum Ca<sup>2+</sup>-ATPase (SERCA) pump with the hydrolysis of ATP. Thus, VSM regulates the luminal diameter of the vessel and therefore is fundamental in vascular tone as well as arterial blood flow and pressure.

#### **1.1.4 Cardiovascular disease**

The term cardiovascular disease (CVD) encompasses all diseases involving the heart and circulatory system including coronary artery disease (CAD), hypertension and stroke. CVD remains the leading cause of premature death (in people below the age of 75) in the U.K. today, claiming 28 % of men and 20 % of women in 2008 ([www.heartstats.org](http://www.heartstats.org), 2012). CVD is a multifactorial disease with interactions of both genetic and environmental risk factors including lifestyle, smoking and diet, playing their part in the prevalence of the disease. CAD and stroke are two of the biggest killers and the unhealthy diet of many people living in the West of Scotland results in an extremely high incidence, with the highest death rate from CAD in the U.K. occurring in this region. In contrast, there is a low occurrence of CVD and reduced mortality rate within the French population despite a high intake of saturated fats in their diet, known as the “French paradox” (Criqui and Ringel, 1994). This is attributed to the high consumption of red wine, containing molecules such as the antioxidant resveratrol which is thought to be beneficial in the prevention of CVD (reviewed in Lippi *et al.* (2010)). With CAD responsible for around a third of all deaths in the U.K., it has been reported to cost the health care system around £3.2 billion in primary patient care in 2006 with this value increasing up to £3.9 billion with the addition of loss of productivity costs ([www.heartstats.org](http://www.heartstats.org), 2012). Although the numbers of people with CVD has been falling in recent years, there is still a vital need for continued research within this area leading to new prevention strategies and treatments.

## 1.2 Atherosclerosis

One of the major causes of both CAD and stroke can arise from the same common problem; the presence of atherosclerosis in the vasculature. Atherosclerosis is a progressive disease characterised by a thickening and hardening of the arterial wall, affecting large (aorta) and medium-sized (carotid, coronary, *etc.*) muscular and elastic arteries of the CVS (Ross, 1999a). The narrowing or complete occlusion of the luminal area of these arteries results in reduced blood flow and depending on the artery affected can ultimately lead to myocardial infarction (MI) or stroke. High plasma levels of circulating cholesterol-containing lipoproteins such as low density lipoproteins (LDL) is a primary risk factor as disease progression is attributed to lipid deposition and accumulation within the subendothelial space. The pathology of atherosclerosis matures over many years from the initial fatty streak, which can occur from childhood, up to an advanced, complex lesion. However, most clinical manifestations are not observed until the disease has progressed extensively and there is a large reduction in the diameter of the arterial lumen, usually presenting clinically as angina-like symptoms.

### 1.2.1 Classification of atherosclerotic lesions

In the early nineties, the American Heart Association's Committee on Vascular Lesions devised a numerical classification of atherosclerotic plaques by consideration of the composition and structure of the lesions (Stary *et al.*, 1992, Stary *et al.*, 1994, Stary *et al.*, 1995). Both type I and II lesions refer to small lipid deposits in the arterial wall, usually termed early lesions. Type I lesions are the first detectable lipid deposits observed in the intima of muscular arteries and are not usually visible to the naked eye. In contrast, type II lesions include the formation of fatty streaks in atherosclerosis-prone regions which are usually the first recognisable characteristic of atherosclerosis. Typically, areas susceptible to lesion formation are arterial bifurcation points that are subjected to high pressure and turbulent flow. Type III lesions manifest as the link between early and advanced plaque formation and termed the transitional lesion. These lesions accumulate additional extracellular lipid pools in the medial layer causing greater intimal thickening. The first plaques classified as advanced are type IV lesions due to the formation of an extensive extracellular lipid core while type V lesions also contain fibrous connective tissue. These forms of plaques are largely responsible for the morbidity and mortality associated with atherosclerosis. Large complicated lesions have now been classified as type VI, VII and VIII lesions with the presence of surface disruptions and the predominance of calcification

and fibrous tissue respectively, which carry a high risk of thrombotic events due to the rupture of the fibrous cap of vulnerable plaques (Stary, 2000). In some cases, this can lead to acute closure of the vessel, resulting in a MI or can, in subacute cases, cause transient ischaemic events as seen in patients with unstable angina.

### **1.2.2 Pathophysiology of atherosclerosis**

Atherosclerosis is now widely acknowledged as an inflammatory disease with the first step in disease progression believed to occur via dysfunction of the endothelium (Ross, 1999b). This can occur at regions of arterial branching where there is turbulent flow and is enhanced by a combination of endogenous factors including elevated levels of modified LDL as well as environmental factors such as free radicals present in tobacco smoke (Bassiouny *et al.*, 1994, Ross, 1999a). Chronic infections have also been suggested to initiate damage to the intima of the vessel (reviewed in Libby *et al.* (1997)). Compensatory mechanisms that change the homeostatic control of the endothelium subsequently occur to overcome the initial damage (Ross, 1999a). Damage to the endothelium and the presence of high plasma levels of circulating LDL leads to deposition of these lipids in the subendothelial space of the arterial wall (Davignon and Ganz, 2004). Cholesterol-rich LDL is then subjected to oxidative and enzymatic attack which will be discussed in greater detail in Section 1.3.2 (Skalen *et al.*, 2002). The modification of LDL results in the activation of endothelial cells which leads to the expression of inflammatory cell adhesion molecules and the recruitment of blood-borne monocytes (Shih *et al.*, 1999, Glass and Witztum, 2001). This facilitates the adherence of leukocytes to the damaged endothelium and results in the transmigration of these cells into the intimal layer by the action of chemokines such as monocyte chemoattractant protein-1 (MCP-1). Once inside the arterial wall, migrated monocytes mature into activated intimal macrophages by the action of macrophage colony-stimulating factor which also results in the up-regulation of scavenger receptors (Yan and Hansson, 2007). Macrophages internalise oxidised LDL (oxLDL) particles in an uncontrolled manner giving rise to lipid-laden foam cells. An illustration of the foam cell and subsequent atherosclerotic plaque formation is presented in Figure 1.1. Macrophage foam cells secrete a variety of pro-inflammatory products such as cytokines and reactive oxygen species (ROS) which worsen the inflammatory response, as well as resulting in VSMCs proliferation and migration (Libby, 2002). Accumulation of foam cells results in the formation of fatty streaks, the type II plaques which consist mainly of inflammatory cells (Stary *et al.*, 1994). The artery can then undergo positive vascular remodelling causing the lumen to be unaffected, thereby negating the effect on blood flow.

However, these fatty streaks continue to grow with the accumulation of more foam cells, dead macrophages, lipids and VSMCs forming advanced atherosclerotic plaques. These lesions contain fibrous connective tissue which forms a fibrous cap and, with the addition of inflammatory cells, lipids and debris over time becomes thinner and more vulnerable, exposing the inner layer which is pro-thrombotic (Ross, 1999a). Fibrous cap erosion can occur in numerous ways including inflammation which leads to apoptosis as well as the absence of  $\text{Ca}^{2+}$  in the fibrous cap causing it to become weak and fragile (Mitra *et al.*, 2004). This results in exposure of the necrotic lipid core to circulating blood causing thrombosis formation and a potentially fatal cardiovascular event.

### **1.2.2.1 Inflammatory cell recruitment**

Both monocytes and macrophages are influential in the development of atherosclerotic plaques and present at every stage of atherogenesis (reviewed in Moore and Tabas (2011)). Monocyte recruitment has been shown to be a rate-limiting step in the formation of lesions as they are responsible for the secretion of multiple pro-inflammatory agents including cytokines, chemokines and matrix metalloproteinases (MMPs) (Ross, 1995, 1999a). This is significant as these extravasated inflammatory cells can then multiply within the lesion leading to the release of additional cytokines and chemokines. This in turn attracts more inflammatory cells to the site of action causing further damage to the endothelium (Ross, 1999a). This forms the basis of the response-to-injury hypothesis where the inflammation begins as a protective measure and then due to the continued response can become detrimental to the vessel (Ross, 1999b). In atherosclerotic mice, monocyte attachment has been observed through all phases of atherosclerosis (Reddick *et al.*, 1994). This process occurs through the binding of these inflammatory cells to various vascular adhesion molecules such as P-selectin, vascular cell adhesion molecule-1 (VCAM-1) and intracellular adhesion molecule-1 (ICAM-1), expressed on the endothelium. Mice deficient in VCAM-1 display reduced atherosclerosis while the loss of ICAM-1 or P-selectin is protective against atherosclerosis highlighting the importance of these adhesion molecules in disease progression (Collins *et al.*, 2000). Selectins present on the endothelial surface attract and capture circulating leukocytes and monocytes which are then activated by endothelial chemokines. This promotes rolling of the activated cells resulting in firm adhesion followed by transmigration into the intima (Muller, 2003). Once inside the arterial wall, monocytes mature to activated macrophages with the overexpression of scavenger receptors, notably the scavenger receptor class A (SRA) and the class B scavenger receptor, CD36 (Kunjathoor *et al.*, 2002). This leads to the uncontrolled uptake

of oxLDL by macrophages and the formation of lipid-loaded foam cells, a prerequisite for the development of atherosclerosis (Suzuki *et al.*, 1997). However, alternative mechanisms of lipid uptake may also be in operation as hyperlipidaemic mice lacking in SR-A and CD36 still demonstrate macrophage foam cell formation and atherosclerotic lesions (Moore *et al.*, 2005). The increased quantity of leukocytes such as neutrophils can also provide a source for the modification of lipids, discussed in detail in Section 1.3. Taken together, this highlights the inflammatory nature of atherosclerosis and the need for inflammatory cell recruitment for disease progression.

### 1.2.2.2 Involvement of VSMCs

While inflammatory cells are essential in the development of foam cells and fatty streaks, VSMCs become more dominant as atherosclerosis progresses (Raines and Ross, 1993). In a normal adult blood vessel, the VSMC doubling time is greater than 80 years whereas in atherosclerosis this is reduced to about 20 years and found to be only about 4 weeks in vein grafts. The phenotype of intimal VSMCs within atherosclerotic lesions is found to differ significantly from their medial counterparts (Mosse *et al.*, 1985). Medial VSMCs usually express high levels of smooth muscle myosin heavy chain (SM MHC) and  $\alpha$ SMA as these proteins are involved in the contractile function of the cell (Owens *et al.*, 2004). In contrast, intimal VSMCs have a high proliferative index and express much lower levels of SM MHC and  $\alpha$ SMA. VSMCs exhibit this plasticity as they are not terminally differentiated and can therefore undergo phenotypic switching from a quiescent “contractile” phenotype to an active “synthetic” state, displayed in Figure 1.1 (Campbell and Campbell, 1994, Gomez and Owens, 2012). This can occur in response to numerous pro-inflammatory and atherogenic stimuli including components of the extracellular matrix (ECM), cytokines and modified lipids (Thyberg and Hultgardh-Nilsson, 1994, Hautmann *et al.*, 1997, Pidkovka *et al.*, 2007). In addition to macrophages, VSMCs are responsible for a significant number of lipid-loaded foam cells in atherosclerosis due to increased expression of scavenger receptors facilitating more efficient lipid uptake and foam cell formation (Stary *et al.*, 1994, Rong *et al.*, 2003). VSMCs are also key producers of ECM in both healthy and atherosclerotic vessels with synthetic VSMCs able to produce up to 25 to 46 times more collagen and therefore able to synthesis large amounts of ECM, contributing to vascular remodelling (Doran *et al.*, 2008, Ang *et al.*, 1990).

Synthetic VSMCs also assist in remodelling as they are able to migrate and proliferate more readily than their contractile counterparts. VSMCs undergo proliferation in a

regulated cell cycle. Quiescent VSMCs are usually maintained in a nonproliferative phase, gap 0 (G0) and only enter interphase, firstly to the gap 1 (G1) checkpoint when stimulated after injury or disease. During this time, all the factors necessary for DNA replication are produced and assembled for the synthetic (S) phase after which VSMCs enter another gap phase, G2, in preparation for mitosis (M). Restriction points at the G1-S and G2-M junctions ensure orderly cell cycle progression controlled by cyclins and other regulatory proteins (Dzau *et al.*, 2002). Although an important component of atherosclerosis, the proliferation rate of VSMCs in lesions has been revealed to be relatively low using antibodies to cell cycle-related proteins with a similar result observed with macrophages (Gordon *et al.*, 1990). VSMC proliferation can be induced by a variety of mechanisms including mechanical stress and growth factors (reviewed in Rivard and Andres (2000)). A lower proliferative index may suggest a greater role of migratory VSMCs from the medial layer in remodelling of the arterial wall. There are a variety of signal transduction pathways found to induce traction force and therefore VSMC migration, reviewed in Gerthoffer (2007). These include activation of the p38 mitogen-activated protein kinase (MAPK) and Rho-activated protein kinase (ROCK). VSMC migration occurs by subsequent remodelling of the cytoskeleton and a change in the matrix adhesiveness resulting in activation of motor proteins in the VSMC. There is also a link between migration and proliferation as VSMCs were found to migrate in the G1 phase but not in later stages of the cell cycle (Fukui *et al.*, 2000).

In addition to proliferation and migration, cell death plays a critical role in vascular remodelling and contributes to the pathophysiology of atherosclerosis (Gibbons and Dzau, 1994). Programmed cell death or apoptosis is an intrinsic mechanism of cell suicide involving cell shrinkage and chromatin condensation with subsequent fragmentation of DNA. Defective or inappropriate apoptosis plays a role in remodelling of the vasculature in atherosclerosis (Bennett and Boyle, 1998, Mallat and Tedgui, 2000). Apoptosis in VSMCs and macrophages can promote inflammation, accelerate atherosclerosis as well as alter the composition of atherosclerotic lesions (Clarke *et al.*, 2008, Ait-Oufella *et al.*, 2007). There are a variety of triggers including both intrinsic and extrinsic signals, which are thought to induce VSMC apoptosis in atherosclerotic lesions. Similar to proliferation and migration, there are numerous pathways involved in VSMC apoptotic signalling including activation of the caspase cascade (reviewed in Bennett and Boyle (1998) and Mallat and Tedgui (2000)). Collectively, this emphasises the significance of VSMCs in the development and progression of atherosclerosis as well as in arterial remodelling.

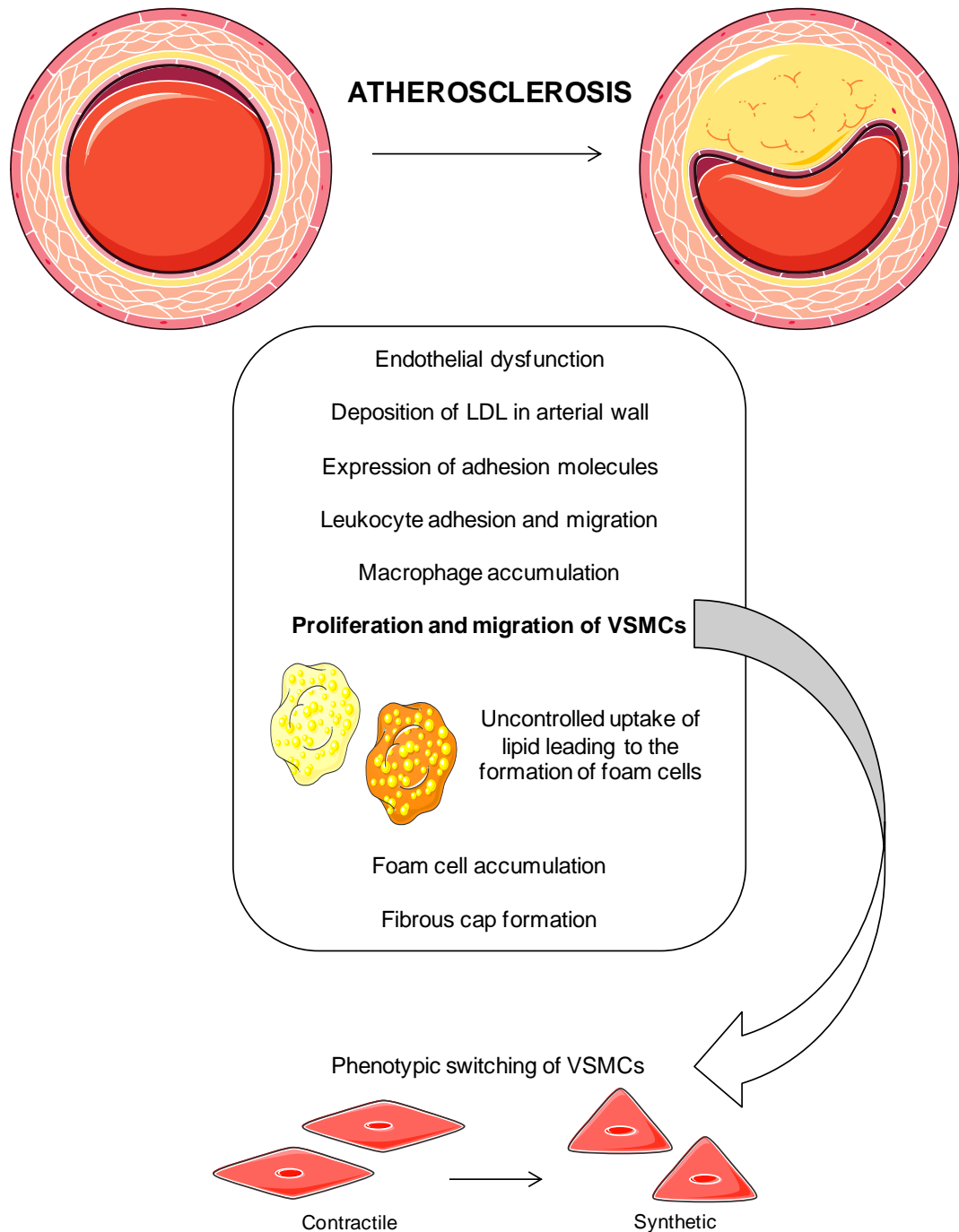


**Figure 1.1 – Formation of foam cells and plaques in atherosclerosis and the importance of VSMCs in disease progression.**

The large clear lumen of a normal artery is drastically reduced after the formation of an advanced atherosclerotic plaque. Lesion formation occurs after endothelial dysfunction which causes the expression of adhesion molecules and in turn, the migration of inflammatory cells to the site of injury. This results in the accumulation of macrophages as well as the proliferation and migration of VSMCs after phenotypic switching from a contractile to a synthetic state. Lipid-laden foam cells are then formed by the uncontrolled uptake of deposited lipid by macrophages and VSMCs. This results in the formation of fatty streaks which develop into advanced atherosclerotic plaques with the addition of a fibrous cap.

### **1.2.3 Atherosclerosis and hypertension**

Atherosclerosis and hypertension are closely related but separate cardiovascular disorders which combined leads to an extremely high risk of CAD and MI (Lithell, 1994). Similar to atherosclerosis, hypertension is a multifactorial process involving the interaction of genetic and environmental factors resulting in an elevation of arterial blood pressure. Hypertension is both a predisposing risk factor and a consequence of atherosclerosis and causes VSMCs in the arterial wall to grow either by hyperplasia, an increase in number or hypertrophy, an increase in mass (Dzau and Gibbons, 1988). The mechanisms of this synergistic effect between atherosclerosis and hypertension are not well understood. Previous clinical trials have shown a strong correlation between hypertension and the risk of developing atherosclerosis highlighted by the predominance of atherosclerotic plaques in areas of the vasculature subjected to high pressures and turbulent flow (Kannel *et al.*, 1986, Alexander, 1995). LDL from hypertensive patients is also more vulnerable to oxidation *in vitro* than LDL isolated from normotensive patients (Maggi *et al.*, 1993). In animal models, angiotensin II-induced hypertension increased plaque area in the thoracic aorta of atherosclerotic mice compared to their healthy wild type counterparts (Weiss *et al.*, 2001). Both atherosclerosis and hypertension have also been shown to enhance oxidative stress within the arterial wall leading to an exacerbated phenotype which can further accelerate atherosclerotic progression (Alexander, 1995).

### **1.2.4 Animal models of atherosclerosis**

As atherosclerosis is a highly complex multifactorial disease, it has proved difficult to produce an animal model with all the characteristics required. Previously, the majority of animal models available for research were large animals such as dogs, pigs and rabbits. Dogs are not ideal models as they do not develop spontaneous atherosclerosis and large modification of their diet as well as concomitant thyroid suppression was needed in order to produce lesions (Geer, 1965). Similar to dogs, rabbits do not develop spontaneous atherosclerosis; however, they respond quickly to dietary cholesterol manipulation and produce vascular lesions (Schenk *et al.*, 1966, Drobnik *et al.*, 2000). Pigs fed with cholesterol were found to exhibit similar distribution and morphology to human atherosclerotic lesions making them a desirable model (Ratcliffe and Luginbuhl, 1971). However, the cost, as well as the difficulties in handling due to their size and weight, has made the pig model an impractical choice for many researchers. The handling issues were overcome by the development of mini pigs; however, these animals are still very expensive

and difficult to obtain (Swindle *et al.*, 1988). Mice are ideal experimental models in the pursuit of finding and testing new therapeutic agents due to their small size, short breeding time, ready availability and simple husbandry. For atherosclerosis research, the major drawback is that mice are highly resistant to atherosclerosis. The plasma cholesterol in mice is mainly found in the anti-atherogenic high density lipoproteins (HDL) and low levels in proatherogenic LDL and very low density lipoproteins (VLDL), which is in contrast to humans who are high in LDL and low in HDL. The only exception to this is the C57BL/6 mouse strain which when fed on a high cholesterol diet develops lesions. This strain of mouse is one of the most widely used in the production of experimental models of human diseases as a genetic background. Transgenic and knockout mice became the focus in the development of a suitable atherosclerotic mouse model with the first genetically altered models of atherosclerosis being created in the early nineties.

#### **1.2.4.1 Mice deficient in apolipoprotein E**

In both mice and humans, apolipoprotein E (ApoE) is one of the major genes involved in determining plasma lipid levels and is synthesised in the liver, brain and other tissues. It is also a structural component of all lipoprotein particles except LDL and acts as a ligand for the LDL receptor and LDL receptor-related proteins thereby promoting the specific uptake of atherogenic particles from the circulation. In 1992, mice deficient in ApoE (ApoE<sup>-/-</sup>) were generated by the inactivation of ApoE by gene targeting in mouse embryonic stem cells (Piedrahita *et al.*, 1992, Plump *et al.*, 1992). Targeting plasmids were used which replaced part of the apoE gene and disrupted its structure. The homozygous animals created appeared to be healthy, displayed normal development and were comparable in body weight to wild type mice. However, major differences were observed in relation to the lipid and lipoprotein profiles in the ApoE<sup>-/-</sup> mice. The total plasma cholesterol levels were dramatically increased and were up to five times higher than their wild type littermates. This was due to the loss of clearance of the excess lipoproteins from the plasma resulting in an altered lipoprotein profile with ApoE<sup>-/-</sup> mice having a high level of atherogenic VLDL (Jawien *et al.*, 2004). ApoE<sup>-/-</sup> mice develop spontaneous atherosclerosis, with the first signs of the disease occurring at about 6 to 8 weeks of age. These include monocyte adhesion, disruption of the subendothelial elastic lamina and initial foam cell formation which is accelerated further by high fat feeding (Nakashima *et al.*, 1994, Coleman *et al.*, 2006). Previous studies have shown ApoE<sup>-/-</sup> mice to exhibit similar blood pressure recordings to control mice (Gervais *et al.*, 2003, Hartley *et al.*, 2000). However, continuous blood pressure measurements over a 24 hour period revealed

ApoE<sup>-/-</sup> mice to have elevated systolic and diastolic pressures as well as increased heart rate compared to C57BL/6 control mice and an elimination of circadian cycles (Pelat *et al.*, 2003). This highlights the ApoE<sup>-/-</sup> mouse as an attractive animal model due to the benefits of using a mouse model as well as displaying a similar morphology to human atherosclerosis progression. In addition, mice deficient in the LDL receptor (LDLr<sup>-/-</sup>) is another mouse model used in the investigation of familial hypercholesterolaemia. LDLr<sup>-/-</sup> mice were developed in 1993 and show a more modest change in total plasma cholesterol levels compared to ApoE<sup>-/-</sup> mice (Ishibashi *et al.*, 1993). The use of mouse models of atherosclerosis has greatly accelerated research within this area.

### **1.3 Modification of phospholipids and LDL in atherosclerosis**

Lipid deposition and accumulation is one of the hallmarks of atherosclerosis. There are a large number of potential targets for phospholipid modification *in vivo* as phospholipids are the major components of both cellular membranes and circulating plasma lipoproteins. Glycerophospholipids are a class of phospholipids containing a phosphatidyl group linked to a glycerol molecule, which is substituted with two fatty acids. These phospholipids are classified depending on the alkyl chains attached to the phosphatidyl group. Phosphatidylcholines (PCs) are the most abundant species with phosphatidylethanolamines (PEs) and sphingomyelins (SMs) also contributing a substantial proportion. Phosphatidylserines (PSs) are less abundant and found normally in the inner leaflet of the plasma membrane while phosphatidylinositols (PIs) are usually cellular rather than circulating lipoprotein components. Apoptotic cells and bodies have been reported to contain increased levels of biologically active phospholipid oxidation products, highlighting the occurrence of oxidative damage in vascular disease (Huber *et al.*, 2002). With regard to lipoproteins, most research has focussed on the formation of oxidised phospholipids in LDL particles in CVD and atherosclerosis.

#### **1.3.1 LDL particles**

Lipoproteins are lipid-protein complexes and their primary function is as a method of transport for lipids and primarily cholesterol in the blood due to their insoluble nature. LDL is formed in a two step process with a variable fraction of each of the lipoproteins being formed at each step (Havel, 1984). The liver synthesises VLDL which is secreted into the bloodstream where lipoprotein lipases in peripheral capillaries partially hydrolyse the molecule causing the lipolytic removal of most of the triglycerides present in VLDL.

After lipolysis occurs, the particles are called intermediate density lipoproteins (IDL). IDL is then transported back to the liver where further transformation can occur with the removal of more triglycerides and alteration of the protein component forming LDL particles which transport exogenous and endogenous cholesterol to peripheral tissues. LDL leaves the bloodstream through capillary pores or across the endothelium by vesicular transport to target tissues. Any cholesterol that is not used is removed by active transport mediated by the ATP-binding cassette transporters, ABCG1 and ABCA1 and is absorbed by HDL and subsequently cleared by the liver by reverse cholesterol transport to maintain physiological levels of circulating cholesterol (Martini, 2006, Berne *et al.*, 2004).

The LDL particle is complex containing several different components and proposed to be a three-layer spherical molecule usually about 25 nm in diameter. It comprises a polar hydrophilic outer surface, interfacial layer and non-polar hydrophobic core (Hevonoja *et al.*, 2000). One LDL particle is known to contain approximately 600 molecules of free cholesterol, 1600 molecules of cholesteryl esters, 185 molecules of triglycerides in the core and the outer surface layer comprising of around 700 phospholipid molecules, mainly PCs and SM with about 450 and 185 molecules respectively (Gotto *et al.*, 1986). LDL particles also contain other phospholipids such as lysophosphatidylcholines, PEs and PIs to a much lesser extent. In addition to the lipids present, LDL contains a protein component of one molecule of apolipoprotein B-100 (ApoB-100) which is made up of 4536 amino acid residues and wraps around the surface of the particle (Yang *et al.*, 1986, Knott *et al.*, 1986). LDL particles are a heterogeneous group of molecules and vary in both diameter and density from about 18 to 25 nm and 1.019 to 1.063 g/ml respectively (Kumar *et al.*, 2011). This is important as small dense LDL particles have been identified as an emerging cardiovascular risk factor by the National Cholesterol Education Program Adult Treatment Panel III (2002) as they are more susceptible to oxidative modification than more buoyant particles of LDL (Chait *et al.*, 1993). The unsaturated nature of the fatty acyl chains of phospholipids present in the LDL particle such as cholesteryl esters, triglycerides and phospholipids means these molecules are particularly vulnerable to oxidation as well as the protein component, ApoB-100.

### **1.3.2 Oxidation of LDL**

LDL isolated from plasma of normolipidaemic patients was first found to induce cell death in cultured human vascular cells while HDL had no detrimental effects (Hessler *et al.*, 1979). Structural modification of LDL was thought to be required in order for the particle

to induce pro-atherosclerotic effects as native LDL was taken up by macrophages at a rate that was insufficient to produce lipid-laden cells (Brown and Goldstein, 1983). Another group found that incubation with native LDL did not lead to foam cell formation and later found that cultured cells could modify LDL to a form that was recognised by macrophage scavenger receptors (Henriksen *et al.*, 1981, 1983). These structural changes were found to be due to oxidative modification of the LDL particles (Steinbrecher *et al.*, 1990). The oxidative hypothesis of atherosclerosis was then proposed whereby oxidative modification of LDL is essential for the formation and progression of the disease due to uptake and accumulation of oxLDL by macrophages (Witztum, 1994). The term oxLDL, does not describe a well characterised molecular species as different laboratories use different conditions and mechanisms of oxidation which leads to different extents to which LDL will become oxidised. There are also large variations due to the heterogeneous nature of the native LDL particles. Depending on the mechanism of oxidation as well as the length of incubation, oxidation of LDL can refer to modification of all components of the particle including lipids and protein. However, the term minimally-modified LDL (mmLDL) usually refers to a particle where the lipids and not the protein component is oxidised.

### 1.3.2.1 Sources of LDL and phospholipid oxidation

The potential sources of LDL and phospholipid oxidation are shown in Figure 1.2 including a selection of biological effects attributed to these modifications, discussed in Section 1.3.3. Many cell types, including vascular cells such as endothelial cells and VSMCs as well as inflammatory cells such as leukocytes, can modify LDL *in vitro* (reviewed in Witztum and Steinberg (1991)). One of the principal methods of oxidation is via the action of enzymes, both by direct enzymatic attack and their production of reactive species. The enzyme, 12/15-lipoxygenase acts directly by catalysing the oxygenation of arachidonic acid at carbon 12 and/or carbon 15 and is capable of oxidising both LDL and phospholipids. 12/15-lipoxygenase and apoE double knockout mice fed on a high fat diet had reduced atherosclerotic plaque formation compared with ApoE<sup>-/-</sup> mice expressing the enzyme, indicating its importance *in vivo* (Cyrus *et al.*, 1999). There are also a number of enzymes involved in the production of free radicals with the ability to modify LDL including myeloperoxidase (MPO), NADPH oxidase (Griendling *et al.*, 2000) and nitric oxide synthase (NOS) (Vasquez-Vivar *et al.*, 1998). The mechanism of modification of both LDL and phospholipids by the phagocytic enzyme, MPO is of particular interest to this study and will be discussed further in Section 1.3.4. Exogenous sources including smoking, UV radiation and atmospheric pollution also have the potential to modify LDL

and phospholipids with tobacco smoking containing a large quantity of free radicals in both the gas and tar phase (Church and Pryor, 1985). A commonly used *in vitro* model for producing oxLDL is the exposure of LDL particles to transition metals. Incubation of LDL with copper or iron leads to extensive oxidation of the particles (Steinbrecher *et al.*, 1984, Heinecke *et al.*, 1984); however the contribution of this source of oxidation *in vivo* is thought to be relatively low. Furthermore, iron-containing haemoglobin is another source for LDL modification by oxidatively cross-linking with ApoB-100 (Ziouzenkova *et al.*, 1999). The different mechanisms of oxidation have also been implicated at different stages of atherosclerosis, for example, 12/15-lipoxygenase which is thought to be important in early plaque formation (reviewed in Gaut and Heinecke (2001)). Together, this highlights different mechanisms and sources available *in vivo* for the modification of LDL and phospholipids which causes a variety of physiological effects witnessed in the progression of atherosclerosis.

### **1.3.3 Physiological effects of oxidised phospholipids**

Oxidised 1-palmitoyl-2-arachidonoyl-*sn*-glycero-3-phosphocholine (oxPAPC) is often used as a model system for the biological effects of oxLDL, as it was found to mimic some of its actions *in vitro* (Watson *et al.*, 1997). 1-palmitoyl-2-glutaroyl-*sn*-glycero-3-phosphocholine (PGPC) and 1-palmitoyl-2-oxovaleroyl-*sn*-glycero-3-phosphocholine (POVPC) are the truncated products formed from the autoxidation of 1-palmitoyl-2-arachidonoyl-*sn*-glycero-3-phosphocholine (PAPC), present in mmLDL and could be critical markers in the progression of atherosclerosis (Watson *et al.*, 1997). As mentioned earlier, phenotypic switching of VSMCs from a contractile state to a synthetic one is influential in the primary stages of the disease (Owens *et al.*, 2004). Oxidised phospholipids, POVPC and PGPC induced phenotypic switching of VSMCs with the transformation of these cells occurring both *in vitro* and *in vivo* (Pidkovka *et al.*, 2007). The oxidised phospholipids were found to decrease expression of  $\alpha$ SMA and SM MHC as well as induce nuclear translocation of a known smooth muscle repressor gene, Krüppel-like transcription factor 4 (Klf4) (Pidkovka *et al.*, 2007). POVPC was also found to induce Klf4 expression directly in cultured VSMCs (Yoshida *et al.*, 2008). Furthermore, exposure of anti-inflammatory M2 macrophages to oxLDL results in the switching of these cells to a pro-inflammatory status causing the accumulation of oxLDL and the enhanced secretion of MCP-1 (van Tits *et al.*, 2011). Oxidised phospholipids and LDL are implicated in nearly every stage of the pathogenesis of atherosclerosis.

### 1.3.3.1 Remodelling processes

Remodelling of the vasculature in atherosclerosis involves various cellular processes such as VSMC proliferation, apoptosis, migration, leukocyte adhesion and formation of ECM (Gibbons and Dzau, 1994). The physiological effects of oxidised phospholipids have previously been investigated in terms of proliferation and apoptosis of VSMCs while very little on the effects of these lipids on migration or production of ECM has been examined. A biphasic response has been reported for oxidised phospholipid effects on remodelling processes with a proliferative action observed at lower concentrations and apoptosis predominating at higher levels (Auge *et al.*, 2002). The length of exposure of these biological active lipids with VSMCs is also an important factor with longer treatments resulting in oxidised phospholipid-induced apoptosis (Chahine *et al.*, 2009). This suggests a balance exists in VSMCs between proliferative and apoptotic effects of oxidised phospholipids which is an important feature of both atherosclerosis and restenosis; a common side effect of cardiological interventions to treat atherosclerosis, characterised by the proliferation and migration of VSMCs (Section 1.5).

Proliferation of vascular cells within vessels is essential for the progression and formation of atherosclerotic plaques. POVPC, but not PGPC, was suggested to be the component of mmLDL responsible for stimulating proliferation of VSMCs by activating the production of lactosylceramide resulting in the phosphorylation of p44 MAPK (Chatterjee *et al.*, 2004). POVPC topically applied to mouse carotid arteries *in vivo* induced significant VSMC proliferation while no effect was observed with PGPC treatment and it has been suggested that while POVPC works through the MAPK pathway, PGPC works through protein kinase C (Johnstone *et al.*, 2009, Chatterjee *et al.*, 2004, Leitinger, 2005). This is in line with the truncated products of oxPAPC reported to localise in different cellular compartments with PGPC found in lysosomes while POVPC formed covalent adducts with components of the plasma membrane (Moumtzi *et al.*, 2007). An inhibitory action of oxidised phospholipids has also been observed where VSMC growth was inhibited by PGPC and to a greater extent, POVPC (Fruhirth *et al.*, 2006). In addition to the effects of individual oxidised phospholipids, oxLDL has been reported to stimulate VSMC proliferation by increased expression of regulatory proteins involved in entry into and progression through the cell cycle (Zettler *et al.*, 2003). VSMC proliferation stimulated by oxLDL, also induced the E-cadherin/ $\beta$ -catenin/T-cell factor pathway, which is influential in cell adhesion and therefore the inflammatory response (Bedel *et al.*, 2008). A stimulatory effect on human coronary artery endothelial cell (HCAEC) proliferation has

also been observed at a low concentration of oxLDL (Yu *et al.*, 2011). In addition to the effects observed in vascular cells, oxLDL stimulated macrophage proliferation leading to the activation of extracellular signal-regulated kinase 1/2 and MAPK (Senokuchi *et al.*, 2004). Oxidised phospholipids can therefore induce proliferation of vascular cells and macrophages, which leads to the activation of several pathways involved in the immune response.

As discussed earlier, defective or inappropriate apoptosis in the vasculature during atherosclerosis impacts greatly on remodelling processes (Bennett and Boyle, 1998, Mallat and Tedgui, 2000). VSMCs are competent phagocytes and are capable of engulfing damaged VSMCs undergoing apoptosis; however, this process is greatly reduced by oxLDL or hyperlipidaemia *in vivo* (Clarke *et al.*, 2010). This observation is emphasised by the fact that high levels of oxidised lipids are found in apoptotic cells leading to the release of interleukin-1 (IL-1) which further exacerbates the inflammatory response (Chang *et al.*, 2004, Clarke *et al.*, 2010). In addition to VSMCs, macrophages incubated with oxLDL were shown to activate apoptotic signalling pathways (Hardwick *et al.*, 1996). These effects were also witnessed after incubation with PGPC and POVPC (Stemmer *et al.*, 2012). Conversely, oxLDL has also been implicated in the survival of macrophages by preventing the production of ceramide via the inhibition of acid sphingomyelinase (SMase) activity (Hundal *et al.*, 2003). In contrast to the proliferative actions observed with individual oxidised phospholipids, POVPC and PGPC have also been shown to induce apoptosis by the phosphorylation of MAPK and activation of the acid form of SMase (Fruhworth *et al.*, 2006, Loidl *et al.*, 2003). Ceramide, a hydrolysis product of SMase, mimics the action of mmLDL and activates caspase 3 signalling and apoptosis (Loidl *et al.*, 2004). LDLr<sup>-/-</sup> mice crossed with programmed cell death-1 receptor knockout mice, exhibited an increase in atherosclerotic lesion size as well as a compositional change with plaques containing more macrophages and T-cells compared with control LDLr<sup>-/-</sup> mice (Bu *et al.*, 2011). OxLDL has also been found to up-regulate expression of the lectin-like endothelial receptor for oxLDL and incubation with HCAECs induced apoptosis in a concentration- and time-dependent manner (Li and Mehta, 2000). The activation of caspase signalling pathways after oxLDL incubation has also been observed in endothelial cells, similar to VSMCs (Chen *et al.*, 2004).

In addition to the effects of oxidised phospholipids on other remodelling processes, POVPC and PGPC have been found to activate VSMC migration and type VIII collagen expression, involved in the compositional change of ECM in atherosclerotic lesions (Al-

Shawaf *et al.*, 2010, Cherepanova *et al.*, 2009). Collectively, this suggests that oxidised phospholipids are not only involved in the production of foam cells but also in a change in the vessel architecture witnessed in the formation of atherosclerotic plaques by their effects on vascular remodelling.

### 1.3.3.2 Endothelial function and inflammatory cell adhesion

Endothelial dysfunction is believed to be an early event in atherosclerosis with oxidised phospholipid-induced apoptosis contributing to this but some less severe effects of oxidised phospholipids have been also been associated with it. OxPAPC treatment of endothelial cells activated more than 1000 genes and produced a range of chemokines including MCP-1, IL-6 and IL-8, involved in both cell adhesion and migration (Gargalovic *et al.*, 2006). NO is crucial in the regulation of arterial tone and oxLDL was found to rapidly reduce the intracellular levels; however, it did not affect the ability of endothelial NOS to produce the signalling molecule (Cominacini *et al.*, 2001). Endothelial cells treated with oxPAPC induced the production of the pro-inflammatory cytokine, IL-8 and this effect was sustained for up to 24 hours (Yeh *et al.*, 2001). Subsequently, a NOS inhibitor, *N*-nitro-L-arginine methyl ester, has been found to reduce the oxPAPC-induced IL-8 transcription (Gharavi *et al.*, 2006). Furthermore, sterol-regulatory element-binding proteins, transcription factors involved in cholesterol metabolism, are activated by oxPAPC and bind to the IL-8 promoter region resulting in increased IL-8 production (Yeh *et al.*, 2004).

Adhesion and transmigration of inflammatory cells into the subendothelial space is also vital in the formation of lipid-laden foam cells and atherosclerosis. In a static adhesion system, both oxPAPC and POVPC induced adhesion of monocytic U937 cells and human peripheral blood monocytes to human umbilical vein endothelial cells (HUVECs) (Huber *et al.*, 2006). In human aortic endothelial cells, oxPAPC induced expression of mitogen-activated protein kinase phosphatase-1 (MKP-1) which mediates the production of MCP-1 and oxPAPC-induced monocyte adhesion was prevented by inhibition of MKP-1 (Reddy *et al.*, 2001). *In vivo* effects have also been reported with oxPAPC applied topically in a pluronic gel to the mouse carotid artery; inducing atherosclerosis-related gene expression in the vessel wall and also monocyte adhesion in isolated arteries (Furnkranz *et al.*, 2005). Shear stress should also be taken into consideration in adhesion studies as although oxPAPC induced adhesion of monocytes to bovine aortic endothelial cells, high shear stress significantly reduced the effect of oxPAPC as did, to a lesser extent, low shear (Hsiai

*et al.*, 2001). Both endothelial dysfunction and inflammatory cell adhesion are known to be critical in atherosclerosis and contribute to disease progression, in part by the action of oxidised phospholipids.

### **1.3.3.3 Anti-inflammatory effects of oxidised phospholipids**

In addition to the pro-inflammatory effects which are routinely reported, there are also anti-inflammatory actions associated with oxidised phospholipids, primarily via toll-like receptor (TLR) signalling (reviewed in Erridge and Spickett (2007)). OxPAPC, POVPC and hydroxyalkenal-containing phospholipids prevent the inflammatory actions of lipopolysaccharide including neutrophil binding to endothelial cells and E-selectin up-regulation via NF- $\kappa$ B activation (Subbanagounder *et al.*, 2002, Leitinger *et al.*, 1999, Bochkov *et al.*, 2002). OxPAPC, as well as its truncated products PGPC and POVPC have also been reported to inhibit the activation of TLR2 and TLR4 (Erridge *et al.*, 2008, Walton *et al.*, 2003). In addition to the anti-inflammatory effects observed *in vitro*, oxidised phospholipids have also been found to inhibit the inflammatory responses to TLR2 and TLR4 agonists *in vivo*. This occurs by competitively inhibiting the interaction with accessory proteins that interact directly with bacterial lipids resulting in an inhibition in the production of tumour necrosis factor- $\alpha$  and other inflammatory mediators (Bochkov *et al.*, 2002, Ma *et al.*, 2004, Erridge *et al.*, 2008). Taken together, this shows a plethora of physiological effects of oxidised phospholipids in inflammatory conditions, in particular atherosclerosis.

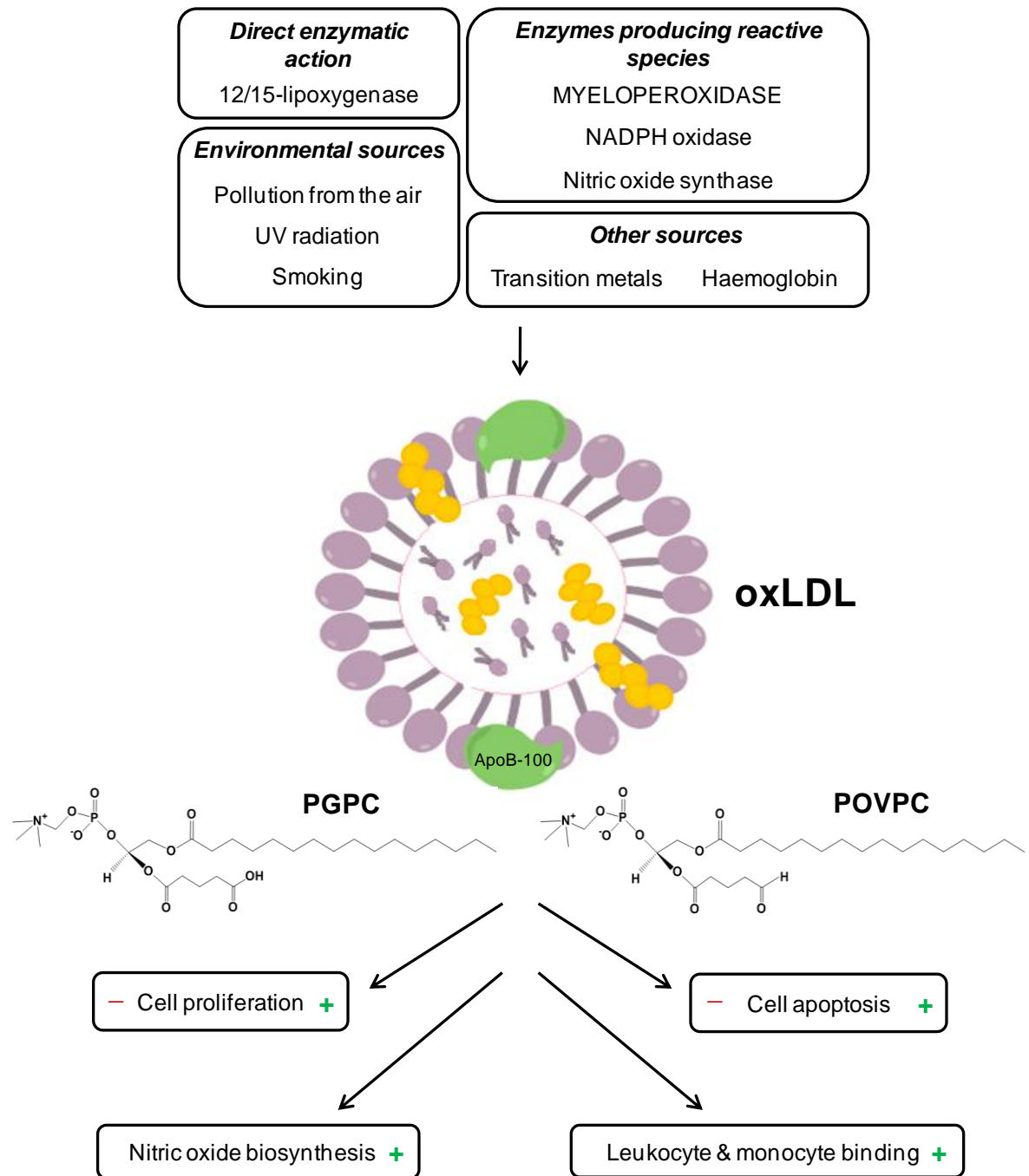


**Figure 1.2 – Sources and physiological effects of LDL and phospholipid oxidation.**

LDL can be oxidised by a number of mechanisms including direct enzymatic attack or by the production of reactive species by enzymes such as MPO which is significant in this study. Other sources of oxidation include transition metals and haemoglobin as well as environmental factors such as smoking. The truncated oxidised phospholipids, PGPC and POVPC have been found to mimic the biological effects of oxLDL *in vitro* and therefore could be the active components of the particle. Some of these biological effects include changes to cell proliferation, apoptosis and induction of leukocyte and monocyte binding. Adapted from Greig *et al.* (2012).

### 1.3.4 MPO

MPO is a tetrameric haem-containing enzyme of about 150 kDa, localised in intracellular granules of circulating neutrophils and monocytes as well as activated macrophages (Klebanoff, 1980, 2005). It is one of the primary mechanisms for modification of phospholipids. It also generates reactive oxidants which can cause both lipid and protein oxidation and is therefore thought to contribute to the inflammatory state in a number of diseases including CVD and neurodegenerative disorders. Patients with unstable CAD were found to have increased levels of MPO in comparison with stable CAD and control patients while individuals with a deficiency in MPO have displayed a drastically reduced rate of CVD compared to people with normal functioning MPO (Zhang *et al.*, 2001, Samsamshariat *et al.*, 2011, Kutter *et al.*, 2000). In atherosclerosis, the active form of MPO is present within human lesions and also modifies LDL into a form that is readily taken up by macrophages via the CD36 scavenger receptor, aiding in the formation of foam cells (Daugherty *et al.*, 1994, Podrez *et al.*, 1999, Podrez *et al.*, 2000b). Atherosclerotic lesions of LDLr<sup>-/-</sup> mice were also found to contain an accumulation of neutrophils which stained positively for MPO (van Leeuwen *et al.*, 2008). However, LDLr<sup>-/-</sup> mice deficient in MPO had exacerbated atherosclerosis with 50 % larger lesions than the control group suggesting a protective role of MPO in plaque formation (Brennan *et al.*, 2001). This could be explained by potential species differences with murine MPO being less influential in lesion formation in mice or levels observed in mice being between 10 to 20 % less compared to human samples (Noguchi *et al.*, 2000, Rausch and Moore, 1975). In contrast, macrophages from hypercholestromic mice expressing human MPO were found to promote atherosclerotic progression (McMillen *et al.*, 2005). Expression of the human MPO promoter polymorphism with G at position -463 (which has been linked with higher mRNA and protein expression of MPO) in LDLr<sup>-/-</sup> male mice resulted in larger aortic plaques as well as an increase in serum cholesterol compared to control males (Kumar *et al.*, 2004, Castellani *et al.*, 2006). MPO has also been suggested to play a role in plaque rupture due to its co-localisation with the MMP-7, pro-matrixin and subsequent activation (Fu *et al.*, 2001). Furthermore, MPO has been found to affect the protective mechanisms involved in the clearance of modified lipids. It causes site-specific oxidation of apolipoprotein A-I, present in HDL in human atherosclerotic lesions resulting in the production of dysfunctional HDL which can no longer promote cholesterol efflux (Shao *et al.*, 2006, Shao *et al.*, 2012). This highlights the impact of MPO in atherosclerosis and has led to the suggestion that MPO could be used as a useful prognostic tool in predicting the risk of CVD (Baldus *et al.*, 2003, Brennan *et al.*, 2003, Brennan and Hazen, 2003).

### 1.3.4.1 Hypochlorous acid

One of the major reactions that MPO catalyses is the formation of hypochlorous acid (HOCl) from hydrogen peroxide ( $H_2O_2$ ); formed from the dismutation of superoxide, and chloride (Schultz and Kaminker, 1962). Each component of the MPO/ $H_2O_2$ /chloride system is needed for the oxidation process; however HOCl was also found to generate the same products alone (Heinecke *et al.*, 1994). Subsequently, chloride has been shown to be the chlorinating intermediate needed for modification of targets (Hazen *et al.*, 1996, Panasenko *et al.*, 2007). HOCl-modified proteins have been found in atherosclerotic lesions *in vivo* and detected in VSM, monocytes/macrophages and endothelial cells as well as the ECM (Hazell *et al.*, 1996, Woods *et al.*, 2003b). Furthermore, tissue isolated from human atherosclerotic lesions had six-fold higher levels of 3-chlorotyrosine, a marker for MPO chlorination, than normal aortic intima (Hazen and Heinecke, 1997). The occurrence of HOCl-modified epitopes has also been shown to increase in relation to the severity of the atherosclerotic lesion (Malle *et al.*, 2000). The anion of HOCl,  $OCl^-$ , has been found in high concentrations of up to 300  $\mu M$  at sites of inflammation in rheumatoid arthritis due to the presence of neutrophils releasing MPO (Katrantzis *et al.*, 1991). Similar to MPO, HOCl modification of HDL impairs reverse cholesterol transport and therefore prevents the clearance of high levels of circulating cholesterol-containing lipoproteins (Marsche *et al.*, 2002). MPO was previously thought to be the only route for producing chlorinated species under both physiological and pathophysiological conditions *in vivo* (reviewed in Podrez *et al.* (2000a) and Nicholls and Hazen (2005)); however, a newly identified haem-containing peroxidase, vascular peroxidase 1 (VPO1), has also been found to catalyse the production of HOCl by a similar mechanism to MPO (Cheng *et al.*, 2008). Angiotensin II significantly increased the level of HOCl which was found to induce a 40 % increase in VSMC proliferation compared to control as well as the expression of VPO1 in cultured VSMCs (Shi *et al.*, 2011). Together, this suggests that there is a high probability of chlorinated products being formed in inflammatory conditions and in particular, atherosclerotic lesions.

### 1.3.5 Formation and physiological activity of chlorinated lipids

HOCl is an oxidising and chlorinating compound and reacts rapidly with a number of biological targets including DNA, proteins and lipids (Prutz, 1996). Modification of ApoB-100, the major protein present in LDL, by HOCl transforms the lipoprotein into a form which is then taken up by macrophages in an uncontrolled manner (Hazell and Stocker, 1993). In response to the MPO system, protein oxidation of ApoB-100 is thought

to occur rapidly with the lipid oxidation of LDL occurring as a secondary reaction over a prolonged period of time (Hazell *et al.*, 1994, Hazell *et al.*, 1999, Jerlich *et al.*, 1998). Even though the modification of lipids could occur at a slower rate than other biological compounds such as protein, there is still a high concentration of lipid targets available for modification due to the abundance of plasma membranes and lipoproteins *in vivo*. Additionally, in inflammatory conditions when the concentration of HOCl is greatly increased, lipid modification is more prevalent than at lower concentrations of HOCl (reviewed in Malle *et al.* (2006)). It is thought that the formation of chlorinated lipids in atherosclerotic plaques could contribute to the pathology of atherosclerosis in a similar manner to oxidised phospholipids.

### 1.3.5.1 Phospholipid chlorohydrins

The predominant products formed from the action of MPO-derived HOCl on unsaturated ester phospholipids are chlorohydrins with the reaction occurring in two steps (Figure 1.3). HOCl is added across the double bond by electrophilic attack with the chloronium ion polarising the bond which is added to one of the carbon atoms (Winterbourn *et al.*, 1992). The double bond is then no longer unsaturated with the other carbon atom becoming positively charged where the remaining hydroxide ion (OH<sup>-</sup>) is added. Water can be subsequently lost from the molecule with the exchange of hydrogen for chlorine in comparison to the native lipid. HOCl causes the formation of mono- and bis-chlorohydrins when incubated with mono- or di-unsaturated PCs and with polyunsaturated lipids; mono-chlorohydrins are the first products formed and longer incubation times are needed for the production of bis-chlorohydrins (Arnhold *et al.*, 2001). Lysophospholipids are also formed from this reaction and occur by the loss of a fatty acid chain from the lipid with the probability of occurrence increasing with the degree of unsaturation of the molecule (Arnhold *et al.*, 2002). The reaction for chlorohydrin formation has been found to be pH dependent with optimal conditions at about pH 6, as at a pH lower than 7.4, chlorohydrins were the only significant products formed (Winterbourn *et al.*, 1992, Arnhold *et al.*, 2001). Chlorohydrins have been detected after treatment with the MPO system or HOCl with LDL and cultured cells (Jerlich *et al.*, 2000, Spickett *et al.*, 2001). Cholesterol is another target for MPO-derived HOCl forming cholesterol  $\alpha$ - and  $\beta$ -chlorohydrins (van den Berg *et al.*, 1993, Heinecke *et al.*, 1994). Electrospray mass spectrometry (ESMS) is routinely utilised for monitoring chlorohydrin formation as well as the conversion of native lipids to their respective chlorohydrins as it limits the breakdown of the molecules in comparison to other methods such as gas chromatography-mass spectrometry (Carr *et al.*, 1996). The

addition of HOCl across the unsaturated bond of a phospholipid causes an increase in the mass-to-charge ratio ( $m/z$ ) of 52 indicating the formation of a mono-chlorohydrin.

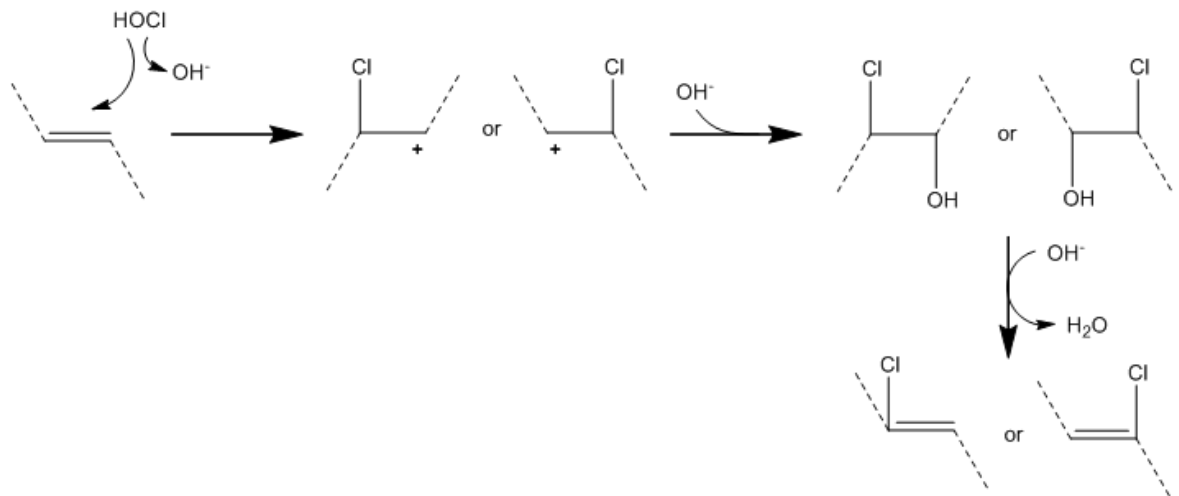


**Figure 1.3 – Formation of phospholipid chlorohydrins.**

HOCl is added across unsaturated bonds of phospholipids by electrophilic attack forming phospholipid chlorohydrins. Adapted from Spickett (2007).

Phospholipid chlorohydrins have demonstrated toxicity in a number of cell types including myeloid and endothelial cells by depletion of ATP levels as well as activation of the caspase 3 signalling cascade (Dever *et al.*, 2003, Vissers *et al.*, 1999, Vissers *et al.*, 2001). This is thought to occur due to the high polarity of chlorohydrins leading to disruption of the plasma membrane after treatment (Carr *et al.*, 1996, Carr *et al.*, 1997). Furthermore, pro-inflammatory effects have been observed with chlorohydrins inducing leukocyte adhesion in C57BL/6 and ApoE<sup>-/-</sup> mice via the up-regulation of P-selectin (Dever *et al.*, 2006, Dever *et al.*, 2008). Phospholipid chlorohydrins have also been found to alter the biophysical properties of erythrocytes after suspected incorporation into the plasma membrane (Robaszkiewicz *et al.*, 2010). Similar to the CVS, HOCl modification of SM in dopaminergic PC12 neurons *in vitro* caused a decrease in cell viability suggesting potential neurotoxic properties (Nusshold *et al.*, 2010). Chlorohydrins of oleic acid have also been detected in plasma in human patients as well as in a rat model of acute pancreatitis (Franco-Pons *et al.*, 2013). Although, phospholipid chlorohydrins have yet to be observed in diseased vessels *in vivo*, lysophosphatidylcholine-chlorohydrins have been detected in human atherosclerotic plaques with a 60-fold increase in human tissue compared to control (Messner *et al.*, 2008b). While smooth muscle is an integral component of atherosclerotic plaques and vascular remodelling, there are currently no studies researching the effects of phospholipid chlorohydrins on these processes in relation to VSMCs.

### 1.3.5.2 Alpha-chloro fatty aldehydes

Plasmalogens are present in the plasma membrane of mammalian cells and in particular vascular cells in the CVS including VSM (Gross, 1984, Ford and Gross, 1989, Hazen *et al.*, 1993). They contain a vinyl ether linkage between the *sn*-1 aliphatic chain and the glycerol backbone and play a role in regulation of transmembrane ion channels and the storage of arachidonic acid (Ford and Gross, 1989, Ford and Hale, 1996). The vinyl ether bond of plasmalogens has been found to be susceptible to attack by MPO-derived HOCl forming alpha-chloro fatty aldehydes including 2-chlorohexadecanal (2-CIHDA) and also lysophospholipids (Albert *et al.*, 2001). The amount of lysophospholipids formed is found to increase with the degree of unsaturation of the native plasmalogen (Lessig *et al.*, 2007). Activation of neutrophils in the presence of bovine pulmonary artery endothelial cells resulted in the modification of endothelial plasmalogens producing 2-CIHDA which also acts as a neutrophil chemoattractant (Thukkani *et al.*, 2002). Chlorinating species produced by the MPO system have also been found to modify plasmalogens present within LDL particles forming alpha-chloro fatty aldehydes and these compounds have been detected in human atherosclerotic lesions *in vivo* as well as lysophosphatidylcholine species (Thukkani *et al.*, 2003a, Thukkani *et al.*, 2003b). 2-CIHDA is reported to be a natural inhibitor of endothelial NO biosynthesis at low micromolar concentrations and found to accumulate in rat hearts subjected to MI where it also caused myocardial damage (Marsche *et al.*, 2004, Thukkani *et al.*, 2005). In the murine brain, inflammation resulting from a single systemic injection of endotoxin generated 2-CIHDA as a result of HOCl attack of membrane plasmalogens (Ullen *et al.*, 2010). 2-CIHDA can also be oxidised to its respective chlorinated fatty acids by endothelial cells and these metabolites have also been found *in vivo* (Wildsmith *et al.*, 2006, Anbukumar *et al.*, 2010). Alpha-chloro fatty aldehydes and their metabolites also displayed pro-inflammatory actions causing increased expression of cyclooxygenase-2 (COX-2) in HCAECs and could be influential in atherosclerosis development (Messner *et al.*, 2008a). However like phospholipid chlorohydrins, very little is known about the effects of alpha-chloro fatty aldehydes on VSM function, a cell type crucial in the atherosclerotic phenotype.

## 1.4 Treatments for atherosclerosis

The rupture of a vulnerable advanced atherosclerotic lesion leads to thrombus formation which can result in the complete occlusion of a coronary artery and therefore MI. Patient survival depends on the restoration of the coronary blood flow as well as the time taken to

achieve this. However, the first clinical manifestations of atherosclerosis are usually evident as angina-like symptoms such as chest, shoulder or neck pain as well as shortness of breath on exertion. This results from the formation of atherosclerotic plaques reducing blood flow through the artery and can be up to 70 % occluded before symptoms occur (Brown *et al.*, 1982). There are a variety of treatments for atherosclerosis including both surgical and pharmacological, which have varying degrees of success.

### **1.4.1 Pharmacological treatment of atherosclerosis**

There are currently no optimal pharmacological therapies in the treatment of atherosclerosis as knowledge of the mechanisms of plaque progression and destabilisation are incomplete (Stoll and Bendszus, 2006). Drugs are typically used in combination with lifestyle changes including modification of the patient's diet and increasing the amount of daily exercise. Therapeutic strategies are mainly designed to prevent lesion progression and plaque rupture and therefore to halt and maintain atherosclerotic plaque stability. These include the use of inhibitors of the renin-angiotensin system to prevent lesion progression through a reduction in MCP-1 and macrophage infiltration as well as Ca<sup>2+</sup> channel blockers; however, both have shown minimal success in patients (Enseleit *et al.*, 2001, MacMahon *et al.*, 2000, Pitt *et al.*, 2000). Drugs to inhibit thrombus formation such as anti-platelet therapy and anti-coagulants are used to maintain an anti-thrombotic environment and inhibitors of MMPs could be a novel tool in maintaining atherosclerotic plaque stability (Rang *et al.*, 2007, George, 2000). Lipid-lowering drugs are used as primary prevention in the treatment of atherosclerosis for patients who are at a high risk of a cardiovascular event due to elevated levels of serum cholesterol. Statins are inhibitors of hydroxymethylglutaryl-CoA (HMG-CoA) reductase, a rate-limiting enzyme in cholesterol biosynthesis. This results in the decreased production of cholesterol in the liver and an up-regulation of LDL receptor synthesis with subsequent clearance of circulating LDL from the plasma (Rang *et al.*, 2007). As mentioned previously, MPO has been highlighted as a potential biomarker for CVD and a recent study found rosuvastatin to significantly reduce MPO levels as well as oxLDL in stable heart failure patients (Andreou *et al.*, 2010). Inhibitors of MPO could provide a novel strategy in atherosclerosis therapy leading to a reduction in the formation of modified lipids and therefore lesion progression.

### **1.4.2 Surgical intervention in the treatment of atherosclerosis**

In addition to pharmacological therapies, surgical interventions are routinely used for the restoration of blood flow through an atherosclerotic vessel. One method of

revascularisation to treat arterial occlusion is coronary artery bypass grafting (CABG). This involves the transplantation of a healthy segment of a blood vessel from another part of the body to the diseased artery, bypassing the obstructed portion and thereby restoring blood flow to the myocardium. The blood vessels routinely used in this procedure as a coronary conduit are either a small artery (the internal thoracic artery) or a peripheral vein (the saphenous vein) (Martini, 2006). Endarterectomies can also be used where the atherosclerotic artery is removed and replaced with plastic tube grafts although this procedure is not always possible.

Percutaneous coronary intervention (PCI) was introduced in 1979 as a less invasive alternative to CABG surgery in the treatment of occluded arteries in atherosclerosis (Gruntzig *et al.*, 1979). Percutaneous transluminal coronary angioplasty (PTCA) involves the insertion of a catheter through a large peripheral artery under anaesthesia or more commonly now, just under light sedation. The catheter is advanced and guided to the stenotic artery followed by controlled inflation of a distensible balloon at the tip which dilates the vessel (Gruntzig *et al.*, 1979). This results in a widening of the lumen of the diseased artery and restoration of blood flow, providing relief from the angina-like symptoms associated with atherosclerosis. The major drawback associated with PCI is restenosis of the treated vessel where the previously occluded artery narrows again after PTCA resulting in the loss of the beneficial effects of the treatment (discussed in further detail in Section 1.5). The consequence of this is a recurrence of the angina-like symptoms and a need for repeated revascularisation of the affected artery. Angiographic restenosis is defined as the presence of greater than 50 % occlusion of the lumen in the previously stenotic artery (Teirstein *et al.*, 1997). Originally, the rate of restenosis was high after balloon angioplasty due to vessel recoil and became a common complication, occurring in up to 50 % of patients and usually developing within the first 6 months (Fischman *et al.*, 1994). This led to the introduction of intravascular bare-metal stents in the late 1980s to combat the problem of restenosis as elastic recoil is minimal during stent deployment due to the rigid scaffolding of the stent in comparison with PTCA (Sigwart *et al.*, 1987).

Bare-metal stents are a small tubular mesh of stainless steel or cobalt-chromium and are positioned in the stenotic vessel in a similar manner to PTCA with the insertion of a catheter through a peripheral artery. The catheter is then advanced to the affected artery where controlled inflation of the balloon occurs resulting in expansion and deployment of the stent which in turn widens the lumen of the artery. The use of bare-metal stents resulted in a reduction in the incidence of restenosis by 20 to 30 %; however, signs of

restenosis still occurred as little as 5 months after stent deployment in selected patients and therefore remains an important complication of the treatment (Fattori and Piva, 2003, Moussa *et al.*, 1997). Additional detrimental factors have also been found with the use of stents in comparison with PTCA including under expansion during implantation, late stent thrombosis or hypersensitivity to one of the components of the stent (Jukema *et al.*, 2012b).

## 1.5 Restenosis

Despite the improvements in revascularisation techniques, the major limitation affecting the long-term success of all forms of PCI is the formation of neointimal thickening. Restenosis is thought to be a consequence of exaggerated wound healing after vascular injury to restore adequate blood flow in stenotic vessels. The recurrence of luminal narrowing results from neointimal hyperplasia and rapid vascular remodelling of the treated vessel with excessive VSMC proliferation and migration as well as ECM production, presented diagrammatically in Figure 1.4. The condition is observed clinically as the presentation of recurrent angina and similar to atherosclerotic plaques, the lesions have been divided into four groups by angiographic classification. Lesions of less than 10 mm in length are classified as focal class I whereas diffuse class II, III and IV lesions are characterised as being greater than 10 mm in length (Mehran *et al.*, 1999). One of the first detailed models of restenosis was proposed by Forrester *et al.* (1991), highlighting platelet aggregation, inflammatory cell infiltration as well as ECM remodelling and medial VSMC modulation and proliferation as markers of the response. This model was modified by Libby *et al.* (1992) who suggested a cascade mechanism after vascular injury and highlighted the importance of inflammation in the restenotic phenotype. Murine models as well as larger animals such as rabbits and pigs are routinely used in restenosis research using wire-, balloon- or stent-induced injury of the endothelium of the carotid, coronary, femoral or subclavian arteries, to initiate neointima formation and restenosis development (Lindner *et al.*, 1993, Kantor *et al.*, 1999, Hadoke *et al.*, 1995).

### 1.5.1 Pathophysiology of restenosis

A complex cascade of events leads to restenosis. These mechanisms can be divided into an “early” (days to weeks) phase and a “late” (days or weeks to months) stage. The initial consequences after placement of the stent are stretch of the entire artery as well as endothelium denudation which stimulates an acute inflammatory response (Costa and

Simon, 2005). Compression of the atherosclerotic lesion exposes the subendothelial pro-thrombogenic core of the plaque to circulating blood and often results in dissection of the medial and occasionally, the adventitial layer of the arterial wall (Inoue and Node, 2009). Following this, deposition of platelets and fibrin at the site of injury results in rapid thrombus formation and leukocyte recruitment which are early indicators of the onset of restenosis (Libby and Simon, 2001). Activation of platelets leads to the expression of adhesion molecules on their surface such as P-selectin. This results in the adhesion of circulating leukocytes and monocytes and their subsequent transmigration by the action of chemical gradients of chemokines such as MCP-1 and growth factors (Welt and Rogers, 2002). These are released from resident macrophages and VSMCs within the arterial wall. Activated platelets at the site of injury secrete growth factors such as platelet derived growth factor (PDGF) that stimulate VSMC proliferation and migration (Walker *et al.*, 1986). Damage to the endothelium therefore triggers an aggressive form of atherosclerosis due to acute platelet and fibrin deposition with the activation of these platelets leading to the release of a variety of inflammatory and growth mediators resulting in thrombus formation and vasoconstriction (Welt and Rogers, 2002). These pro-inflammatory responses are sustained for several weeks following injury of the vessel and lead to the proliferation of vascular components such as VSMCs and ECM which are key features of the late phase of restenosis (Libby *et al.*, 1992).

The cellular proliferation phase involves phenotypic modulation of medial VSMCs as they migrate to form the neointima; a process similar to fibrous cap formation in atherosclerosis (Mitra and Agrawal, 2006). The late stage of restenosis typically occurs days to weeks after the initial vascular injury and lasts up to 6 months. Quiescent contractile VSMCs become stimulated by the mechanical injury and inflammatory response which triggers the progression through the G1/S transition of the cell cycle (Tanner *et al.*, 1998, Nabel, 2002). VSMCs closest to the region of injury undergo maximal apoptosis with surviving VSMCs migrating towards the arterial lumen (Perlman *et al.*, 1997, Hanke *et al.*, 1990). In addition, dead or damaged vascular cells release growth factors such as basic fibroblast growth factor and epidermal growth factor which act as mitogens for medial VSMC proliferation as well as migration (Lindner and Reidy, 1991, Casscells, 1992). Non-dividing VSMCs as well as proliferating VSMCs can migrate to the intima after vascular injury (Clowes and Schwartz, 1985). In an atherosclerotic rabbit model, cell proliferation was found to peak 4 days earlier than apoptosis after angioplasty with apoptosis inversely correlated with restenosis (Durand *et al.*, 2002). In contrast, balloon injury in healthy rabbits displayed an increase in VSMC apoptosis via caspase 3 after 24 hours followed by

significant proliferation 28 days after injury (Spiguel *et al.*, 2010). This is in agreement with a study using carotid balloon injury in the ApoE<sup>-/-</sup> mouse model where apoptosis was increased 1 hour after injury while proliferation rates peaked at 7 days and were still elevated up to 28 days following surgery (Matter *et al.*, 2006). VSMC proliferation is thought to be maximal at 5 to 7 days after injury with around 10 to 20 % of the total medial VSMCs proliferating. In addition to VSMCs, there is evidence of proliferating cells from a myeloid lineage within restenotic tissue (Welt and Rogers, 2002).

As mentioned previously, VSMCs are key producers of ECM and during the chronic proliferative phase, VSMCs are also responsible for increasing the volume of intimal tissue by a coordinated increase in ECM synthesis (Inoue and Node, 2009). This results in fewer cellular components and can last for several months (Lee *et al.*, 1993). ECM is the major component of mature restenotic plaques with a shift towards ECM synthesis rather than VSMC proliferation (Schwartz *et al.*, 1992). Partial re-endothelialisation of the injured surface also occurs during this phase with growth factors such as vascular endothelial growth factor facilitating endothelial regrowth (Brindle, 1993). Complete re-endothelialisation is possible as quickly as 30 days after PCTA; however, regenerated endothelium may be dysfunctional or may also never fully regrow depending on the extent of denudation (Hamon *et al.*, 1995, Weidinger *et al.*, 1990).

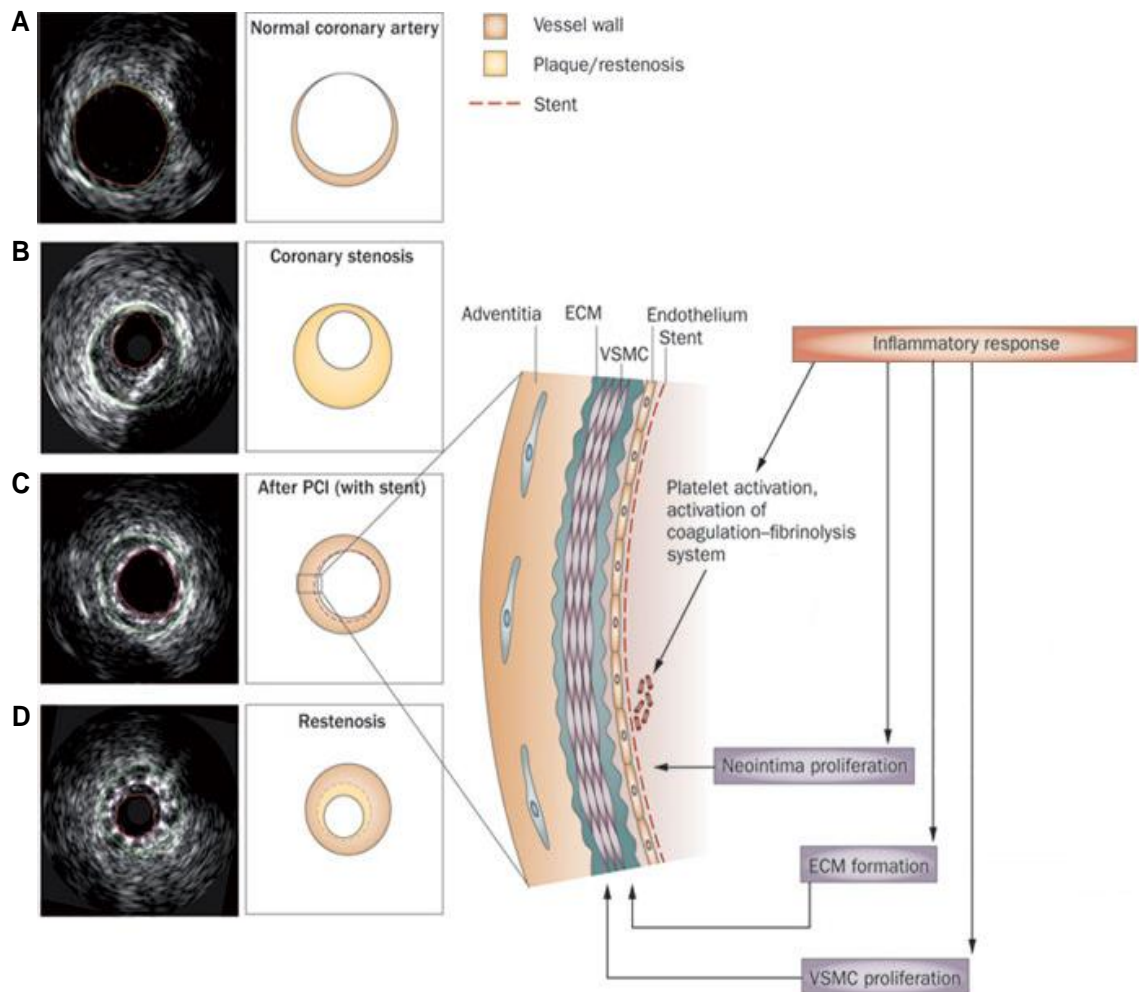


**Figure 1.4 – Vascular remodelling processes involved in restenosis.**

Intravascular ultrasound images (left) and schematic representations (right) depict the progression from a normal healthy coronary artery (A) to coronary stenosis due to the formation of an advanced atherosclerotic plaque (B) followed by the restoration of normal blood flow by widening of the lumen after stent deployment (C) to the subsequent restenosis (D). The vascular remodelling processes which occur after PCI include an inflammatory response which stimulates thrombus formation and neointimal proliferation from ECM formation and VSMC proliferation. Adapted from Jukema *et al.* (2012b).

### **1.5.2 Potential involvement of modified lipids in restenosis**

Mechanical injury to the atherosclerotic artery during stent deployment results in compression and damage to the plaque with exposure and disruption of the modified lipid-containing core, suggesting a potential lipid involvement in restenosis. The total plasma cholesterol levels in ApoE<sup>-/-</sup> mice were found to be markedly elevated after carotid balloon injury which was in parallel with neointima formation (Matter *et al.*, 2006). In contrast, vascular remodelling was impaired after coronary balloon angioplasty in hypercholesterolaemic mini pigs causing a reduction in VSMC migration with the effects attributed to the action of oxLDL (Theilmeier *et al.*, 2002). Restenosis is an inflammatory condition which relies on the recruitment of leukocytes such as neutrophils, which are a source of MPO. This could therefore lead to an increase in the production of modified lipids in the neointima. Balloon-injured vessels showed a significant increase in leukocyte adhesion 24 hours following injury in rabbit subclavian arteries as well as up-regulation of adhesion molecules such as P-selectin (Kennedy *et al.*, 2000). There is also evidence of sustained inflammation with inflammatory cells remaining in close proximity to the stents in rabbit iliac arteries up to 28 days after placement (Kennedy *et al.*, 2004, Coats *et al.*, 2008). Increased leukocyte adhesion has also been demonstrated up to 28 days following surgery in a wire injury mouse model (Tennant *et al.*, 2008). Neutropaenic rabbits, which have a low number of neutrophils, were found to have a significantly reduced level of neointima formation after 28 days (Miller *et al.*, 2001). Furthermore, arterial segments from ApoE<sup>-/-</sup> mice treated *in vitro* with a phospholipid chlorohydrin formed from the action of the MPO system, displayed an increase in leukocyte adhesion in a concentration-dependent manner as well as an increase in P-selectin expression (Dever *et al.*, 2008). Stent deployment also results in neutrophil activation, which is associated with neointimal thickening (Inoue *et al.*, 2006). VSMC proliferation was evident 24 hours after the topical application of POVPC to mouse carotid arteries *in vivo* (Johnstone *et al.*, 2009). In addition to oxidised phospholipids, an increase in the presence of MPO and HOCl-modified proteins has been found to correlate with an increase in the intima-to-media ratio in human iliac arteries (Hazell *et al.*, 2001). HOCl was also found to mediate neointimal hyperplasia in a time- and dose-dependent manner, initially causing apoptosis followed by vascular proliferation in a rat model of balloon injury (Yang *et al.*, 2006). Together, this highlights the importance of inflammatory cell recruitment in neointima formation in injured vessels and with the presence of LDL and inflammatory cells could lead to the production of significant quantities of modified lipids in the vessel wall. However, very

little is known about the potential involvement of these modified lipids, both oxidised and chlorinated species, in the development of restenotic lesions.

### **1.5.3 Current and future treatments for restenosis**

Several therapeutic options have been proposed and implemented to increase the long-term success of PCI and reduce the incidence of restenosis. One of the most promising advances in the treatment of restenosis was the development of drug-eluting stents (DES). The drug is encapsulated in a polymer which allows the drug to diffuse slowly over time or the polymer is degraded in order to release the drug which has been directly coated onto the surface on the stent. DES provide a combination of mechanical support with the controlled release of drugs capable of potentially reducing neointima formation. DES coated with anti-proliferative drugs have shown to be beneficial with paclitaxel, effectively reducing neointimal hyperplasia after 4 weeks in a porcine model of coronary restenosis and in rabbit iliac arteries (Heldman *et al.*, 2001, Drachman *et al.*, 2000). In addition, local delivery of anti-proliferative agents has also proved effective in reducing hyperactivity of injured vessels to constrictor agents in porcine coronary arteries (Kennedy *et al.*, 2006). Immunosuppressive drugs such as rapamycin and anti-platelet therapies have proved to be beneficial causing a reduction in neointima formation (reviewed in Costa and Simon (2005) and Fattori and Piva (2003)). Drugs targeting other areas in the development of restenosis such as inhibition of inflammatory chemokines and ECM deposition have also resulted in reduced neointima formation in animal models (Grassia *et al.*, 2009, Backes *et al.*, 2010). After the introduction of DES, patients experienced lower rates of target vessel and lesion revascularisation as well as MI and death compared to the use of bare-metal stents (Hannan *et al.*, 2008). However, other studies have found DES to correlate with higher rates of reappearance of stenosis (Steinberg *et al.*, 2009). Although clinical application of DES has proved difficult with differences present between animal models and humans, this form of treatment still results in a widely successful outcome compared to bare-metal stents with a reduction in restenosis and neointima formation leading to target vessel revascularisation. However, restenosis remains a complication in a number of patients after surgical intervention in the treatment of atherosclerosis. This had led to the investigation of novel potential therapies such as biodegradable stents and endothelial progenitor cell capturing stents to reduce neointima formation after PCI (reviewed in Jukema *et al.* (2012a)).

## 1.6 Adenosine monophosphate-activated protein kinase

In hyperproliferative diseases like atherosclerosis and restenosis, adenosine monophosphate-activated protein kinase (AMPK) may play an important role due to the increased number of cells present. AMPK has been shown to be involved in a plethora of cardio and vasculoprotective functions including stimulation leading to a reduction in monocyte adhesion to endothelial cells and cholesterol synthesis in the liver (reviewed in Ewart and Kennedy (2012)). A selection of the physiological effects which result from AMPK activation are displayed in Figure 1.5. AMPK is a key regulator of cellular energy homeostasis and involved in the maintenance of energy stores. The enzyme was first discovered in 1973 and is now commonly referred to as a cellular “fuel gauge” (Beg *et al.*, 1973, Carlson and Kim, 1973, Hardie and Carling, 1997). AMPK is a highly conserved heterotrimeric complex consisting of a catalytic  $\alpha$  subunit and two regulatory subunits;  $\beta$  and  $\gamma$ , with each subunit having two or more isoforms which are expressed in different cell and tissue types (Davies *et al.*, 1994, Stapleton *et al.*, 1994). For the catalytic domain, the  $\alpha 1$  subunit predominates in the vasculature while in cardiac and skeletal muscle, the  $\alpha 2$  subunit is the primary isoform (Stapleton *et al.*, 1997, Davis *et al.*, 2006). In contrast, equal distributions of  $\alpha 1$  and  $\alpha 2$  subunits are found in the liver (Woods *et al.*, 1996).

### 1.6.1 Regulatory mechanism and signalling of AMPK

Activation of AMPK occurs via phosphorylation of the threonine residue at position 172 in the activation loop of the catalytic  $\alpha$  domain contained within the N-terminus (Hawley *et al.*, 1996). The regulatory  $\gamma$  subunits contain areas termed “Bateman domains” with the capacity to bind one molecule of either adenosine monophosphate (AMP) or ATP (Cheung *et al.*, 2000, Bateman, 1997, Scott *et al.*, 2004). ATP occupies these domains in well energised cells with AMPK in an inactive locked state. However, when there is a depletion of ATP and an elevation of AMP levels, for example during periods of stress such as hypoxia or glucose deprivation, AMP competitively displaces ATP leading to the phosphorylation of AMPK at the threonine residue. The binding of AMP to the Bateman domains induces a conformational change of AMPK and also makes it a less desirable substrate for AMPK phosphatases resulting in an increased proportion of phosphorylated AMPK (Scott *et al.*, 2004, Towler and Hardie, 2007). AMPK is subsequently dephosphorylated by the action of protein phosphatases when the stores of cellular energy have increased and the cell is no longer stressed. AMPK activation can also occur by alternative upstream kinase pathways termed AMPK kinases, including the tumour

suppressor protein, liver kinase B1 (LKB1) and calcium/calmodulin-dependent protein kinase kinase  $\beta$  (CAMKK $\beta$ ) (Woods *et al.*, 2003a, Hurley *et al.*, 2005). In addition to endogenous activation, AMPK can be modulated by pharmacological agents such as activation by 5-aminoimidazole-4-carboxamide-1- $\beta$ -D-ribofuranoside (AICAR) that mimics the action of AMP. AICAR is transported inside the cell via the adenosine transporter where it is phosphorylated to form the AMP analogue, zeatin riboside-5-monophosphate (ZMP) (Merrill *et al.*, 1997). A-769662 is another extremely potent AMPK activator which directly stimulates the enzyme by mimicking the effects of AMP as well as inhibiting de-phosphorylation (Göransson *et al.*, 2007). AMPK signalling directly regulates a number of enzymes involved in energy consumption within the cell such as acetyl-coA carboxylase (ACC) which is directly phosphorylated by AMPK leading to the inhibition of enzyme activity and reduced fatty acid synthesis (reviewed in Hardie (2004)).

### **1.6.2 Involvement of AMPK in vascular disease**

Pathologies of the CVS such as atherosclerosis, restenosis and hypertension evoke stress signals in vascular tissue leading to potential changes in cellular energy thus AMPK has been implicated in the progression of several diseases (Motoshima *et al.*, 2006, Li and Keaney, 2010). In atherosclerosis, activation of AMPK by AICAR results in a reduction in endoplasmic reticulum (ER) stress and inhibition of macrophage proliferation, both induced by high levels of circulating oxLDL (Dong *et al.*, 2010, Ishii *et al.*, 2009). The expression of serine/threonine protein phosphatase 2A, one of the enzymes responsible for the inactivation of AMPK, was increased 40-fold by incubation of human monocytes with oxLDL (Kang *et al.*, 2006). AICAR treatment has also been found to reduce ER stress and protect endothelial cells against the effects of modified LDL (Dong *et al.*, 2010). AMPK activation has also been found to exert anti-apoptotic effects in a number of cell types including endothelial cells, therefore promoting cell survival (Ido *et al.*, 2002, Kim *et al.*, 2008, Liu *et al.*, 2010). In addition, AMPK has been associated with inflammatory cells such as neutrophils, which are the primary source of MPO and involved in the modification of LDL (Alba *et al.*, 2004). AMPK activation attenuated neutrophil activity and metformin, an anti-diabetic drug known to activate AMPK, decreased MPO levels in lung tissue (Zhao *et al.*, 2008, Tsoyi *et al.*, 2011). In addition, AMPK has been implicated in reverse cholesterol transport, as activation increased protein levels of ABCG1 and ABCA1 resulting in cholesterol efflux from foam cells derived from macrophages as well as reduced plaque formation in ApoE<sup>-/-</sup> mice (Li *et al.*, 2010a, Li *et al.*, 2010b). Therapeutic agents used in the treatment of atherosclerosis such as statins have also been

shown to partially mediate their effects through the action of AMPK, as reviewed in Ewart and Kennedy (2011). Incubation with atorvastatin increased phosphorylation of AMPK and its downstream target ACC, both *in vitro* and *in vivo* (Sun *et al.*, 2006). In addition, AMPK is implicated in restenosis. Mice deficient in AMPK $\alpha$ 2 (AMPK $\alpha$ 2<sup>-/-</sup>) had a dramatic increase in the formation of neointima after wire injury of the carotid artery compared to wild type controls (Song *et al.*, 2011). This is in agreement with another study where a reduction in AMPK activity led to an increase in neointima development after arterial injury in a murine model (Yu *et al.*, 2012). Local administration of the AMPK activator, AICAR also reduced neointima formation 2 weeks after balloon injury in rat carotid arteries (Stone *et al.*, 2013). Furthermore, endothelium-selective expression of constitutively-active AMPK was protective against vascular injury and promoted re-endothelialisation in a murine diabetic model (Li *et al.*, 2012).

The activation of AMPK is also been associated with hypertension and blood pressure regulation where prior studies have shown a reduction in mean arterial pressure in both rodents and humans following acute administration of the AMPK activator, AICAR (Foley *et al.*, 1989, Bosselaar *et al.*, 2011). Spontaneously hypertensive rats dosed with AICAR also showed an acute drop in mean arterial pressure which was not seen in the control group of Wistar-Kyoto rats, suggesting AMPK could play a role in reducing hypertension (Ford *et al.*, 2012). Long-term administration of AICAR or resveratrol, which has been described as another activator of AMPK, again caused a reduction in mean arterial pressure in obese Zucker rats (Buhl *et al.*, 2002, Rivera *et al.*, 2009). Furthermore, short-term calorie restriction in the spontaneously hypertensive rats resulted in increased activity of AMPK which led to a reduction in blood pressure (Dolinsky *et al.*, 2010). Together, this highlights the involvement of AMPK in vascular disease and suggests that AMPK activation could play a critical role in reducing the elevated blood pressure found in both atherosclerosis and hypertension.

#### **1.6.2.1 AMPK signalling in VSM**

VSMCs are crucial in the development of hyperproliferative diseases such as atherosclerosis and restenosis as the proliferation and migration of VSMCs as well as their role in ECM production results in lesion formation. AMPK activation by AICAR has been found to inhibit human aortic VSMC proliferation induced by both PDGF and foetal calf serum (FCS) in a dose-dependent manner (Igata *et al.*, 2005). This effect was also seen in rat aortic VSMC proliferation and migration and found to be dependent on AMPK (Peyton

*et al.*, 2011). Furthermore, angiotensin II-stimulated rat VSMC proliferation was inhibited by AMPK activation using AICAR (Nagata *et al.*, 2004). OxLDL was found not to directly induce AMPK phosphorylation in rabbit femoral VSMCs but AICAR has been shown to cause a concentration-dependent reduction in oxLDL-induced macrophage proliferation (Brito *et al.*, 2009, Ishii *et al.*, 2009). In addition to its activity on individual VSMCs, AMPK has been found to have an effect on vascular reactivity affecting both endothelial and VSM function. AICAR-induced vasorelaxation in mouse aortic rings in both endothelium-intact and -denuded vessels and this was abolished in mice deficient in AMPK $\alpha$ 1 (AMPK $\alpha$ 1<sup>-/-</sup>), suggesting that AMPK $\alpha$ 1 was responsible for this action (Goirand *et al.*, 2007). In addition, mesenteric artery and aortic rings isolated from AMPK $\alpha$ 1<sup>-/-</sup> and AMPK $\alpha$ 2<sup>-/-</sup> mice produced larger contractions than their wild type controls (Wang *et al.*, 2011b). Vasorelaxation to AICAR was also enhanced in hypertensive rats compared to their normotensive controls, which was thought to be NO dependent (Ford and Rush, 2011). Little is known about the effects of individual modified lipids, which are elevated during atherosclerosis, on vascular reactivity; however, one study has found oxLDL to reduce endothelium-dependent relaxation to acetylcholine in rabbit aorta and coronary arteries (Buckley *et al.*, 1996). Together, this suggests a dysregulation of AMPK signalling occurs during CVD such as atherosclerosis and hypertension with little known to date about the impact of AMPK signalling on the effects of individual modified lipids in VSM.

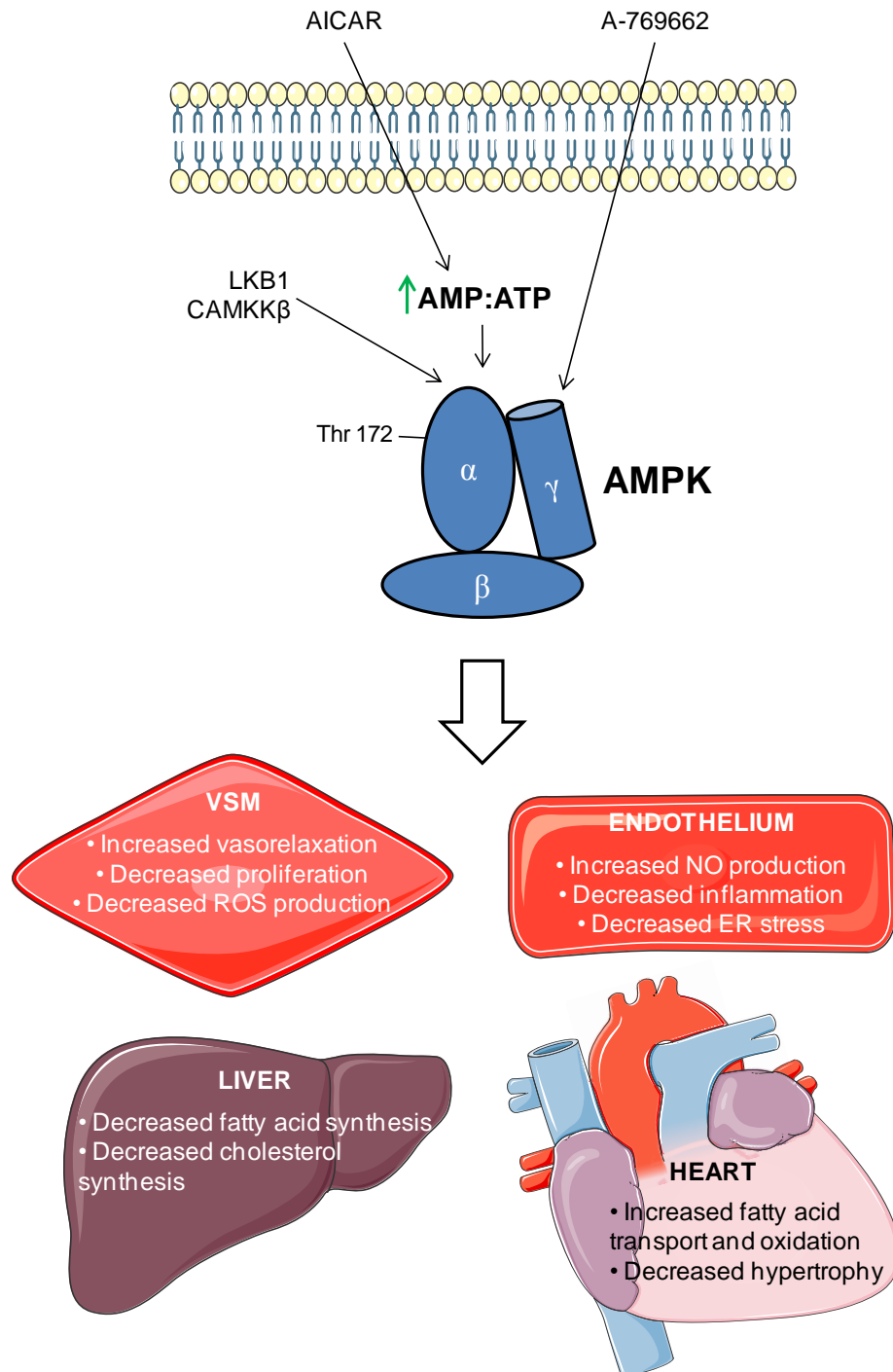


**Figure 1.5 – AMPK activation and its cardio and vasculoprotective functions.**

Endogenous and pharmacological activation of AMPK results in phosphorylation of the enzyme leading to several physiological effects in the vasculature, heart and liver which could be beneficial in CVD such as atherosclerosis, restenosis and hypertension. These effects include increased vasorelaxation in VSM, decreased inflammation and ER stress in the endothelium, decreased cholesterol synthesis in the liver and decreased hypertrophy in the heart. Adapted from Ewart and Kennedy (2012).

## 1.7 Aims of this thesis

In summary, atherosclerosis is characterised by the deposition and accumulation of modified lipids in the subendothelial space of the arterial wall as well as vascular remodelling leading to atherosclerotic plaque formation. Restenosis is a known complication of the surgical interventions used to treat atherosclerosis and results in neointimal thickening, in part by the action of VSMCs. Various physiological effects have been attributed to the action of oxLDL leading to an exacerbation of the inflammatory response. However, little is known to date about the effects of individual modified lipids including oxidised and chlorinated species, on vascular remodelling processes which are prominent in these disease phenotypes. In addition, AMPK has recently been implicated in both vascular diseases but the impact of this signalling pathway on the effects of individual modified lipids is presently unknown.

The principal research aim of this thesis was to investigate the influence of modified lipids, both chlorinated and oxidised species, in vascular injury and disease focussing primarily on their effects on VSM. This was achieved through the following experimental study aims:

- *In vitro* characterisation of the effects of modified lipids on vascular remodelling processes including VSMC proliferation, viability and migration.
- Assessment of the impact of AMPK signalling on the effects of modified lipids in VSM *in vitro*.
- *In vivo* evaluation of vascular injury in healthy and atherosclerotic mice and determination of the occurrence of modified lipids in neointima formation.
- *In vivo* characterisation of AMPK activation in healthy and atherosclerotic mice.

**CHAPTER 2**  
**GENERAL MATERIALS AND**  
**METHODS**

## Materials

### 2.1 Chemicals and Reagents

All chemicals were supplied by Sigma-Aldrich (Poole, U.K.) unless otherwise stated and were of the highest grade obtainable. Phospholipids were obtained from Avanti Polar Lipids (Alabama, U.S.A.) and all cell culture reagents were obtained from Gibco (Paisley, U.K.) unless otherwise stated. All Western blot materials were supplied by Life Technologies (Paisley, U.K.) unless otherwise stated.

## Methods

### 2.2 Lipid preparation and synthesis

All native phospholipids were purchased in powder form and aliquoted using high performance liquid chromatography (HPLC) grade methanol. The phospholipids were then dried under a steady flow of oxygen-free nitrogen gas and stored at -80 °C until reconstituted for use.

#### 2.2.1 Chlorohydrin formation

1-stearoyl-2-oleoyl-*sn*-glycero-3-phosphocholine (SOPC) and 1-stearoyl-2-linoleoyl-*sn*-glycero-3-phosphocholine (SLPC) were all prepared individually from their respective native lipids. Aliquots of the phospholipids were resuspended in equal volumes of Hanks' balanced salt solution (HBSS) at a concentration of 10 mg/ml and vortexed for 1 minute. The solution was sonicated for 15 minutes, forming lipid micelles and vortexed for a further minute producing a milky homogeneous suspension. Lipid vesicles were treated with 10-fold molar excess (per double bond) of sodium hypochlorite (NaOCl) solution at pH 6 for 15 minutes at 35 °C, forming lipid chlorohydrins. The concentration of the stock solution of NaOCl was determined spectrophotometrically at 292 nm ( $\epsilon_{292} = 350 \text{ M}^{-1} \text{ cm}^{-1}$ ). Excess hypochlorite was removed by passing the solution through a reverse phase Sep-Pak® column (Waters, Elstree, U.K.). The chlorinated phospholipids were eluted from the column in 0.5 ml of methanol and 1 ml of 1:1 methanol:chloroform and dried using oxygen-free nitrogen gas.

### **2.2.2 Measurement of stability of chlorohydrins**

Chlorohydrins were prepared as mentioned in Section 2.2.1 with the addition of 1,2-dipalmitoyl-*sn*-glycero-3-phosphocholine (DPPC) at a concentration of 10 mg/ml to the aliquots of the individual phospholipids. DPPC is a saturated phospholipid and therefore was chosen as a stable comparator for the expected breakdown of the chlorohydrins. Lipid chlorohydrins with DPPC were reconstituted in phosphate buffered saline (PBS, containing 154 mM NaCl, 100 mM Na<sub>2</sub>HPO<sub>4</sub> and 25 mM NaH<sub>2</sub>PO<sub>4</sub> at pH 7.4) with samples being incubated at 37 °C and aliquots taken at several time points including zero, 24 hours and up to 72 hours to measure the stability of the lipid chlorohydrin in relation to DPPC.

### **2.2.3 Quantification of phospholipids by ESMS**

The formation and stability of chlorohydrins was monitored using ESMS. 1 µl aliquots of the chlorohydrin sample were diluted 200 fold with 9:1 methanol:water. ESMS was performed on a LCQ-Duo mass spectrometer (ThermoFinnigan, Waltham, U.S.A.) in positive-ion mode with direct infusion of the sample. Spectra, in the range of m/z 400-1000 for SOPC and SLPC, were acquired for 2 minutes. Formation of chlorohydrins was assessed by the loss of the native phospholipid and the addition of m/z 52 or 54 (differences being due to the pattern of the chloride isotope with the addition of either <sup>35</sup>Cl or <sup>37</sup>Cl) to the native phospholipid which was usually seen in its sodiated form (an additional m/z 23 added to the value).

### **2.2.4 Alpha-chloro fatty aldehyde synthesis**

The alpha-chloro fatty aldehyde, 2-ClHDA, was synthesised and provided by Professor Andrew R. Pitt (Aston University, U.K.) following an adapted method described by Thukkani *et al.* (2002). Briefly, hexadecanol was partially oxidised to hexadecanal at -70 °C using the classical Swern oxidation method utilising pyridinium chlorochromate in oxygen-free CH<sub>2</sub>Cl<sub>2</sub> as a catalyst (Dubey *et al.*, 2008, Mancuso *et al.*, 1978). This is where an alcohol is oxidised to its corresponding carbonyl compound at low temperatures producing high yields. Hexadecanal then underwent acid methanolysis forming dimethyl acetal hexadecanal by reaction with methanol and catalytic *p*-toluenesulfonic acid. The dimethyl acetal of 2-ClHDA was then synthesised using an acetal chlorination system utilising MnO<sub>2</sub>-trimethylchlorosilane, as it has previously been shown to give a more quantitative yield for the halogenation of aldehydes than previous methods (Bellesia *et al.*, 1992). 2-ClHDA was finally produced by refluxing 1:1 trifluoroacetic

acid:dichloromethane and then purified by flash chromatography using silica and eluted with 7:3 hexane:dichloromethane to give solid 2-ClHDA (17 % overall yield). The synthesis of the compound was confirmed by analysis as follows:  $^1\text{H-NMR}$  (in  $\text{CDCl}_3$ )  $\delta$  9.47 (1H, d); 4.16 (1H, m); 1.89 (2H, m); 1.26 (24H, m); 0.88 (3H, m).  $m/z$  (ESMS) 275.2  $[\text{M-H}]^+$ . IR = 2924, 2850, 1470, 1188, 1121, 1080, 723  $\text{cm}^{-1}$ .

## **2.3 Tissue culture**

Tissue culture was performed in sterile conditions using biological safety class II vertical laminar flow cabinets. Tissue explants were incubated and cells were grown at 37 °C and maintained with 5 %  $\text{CO}_2$  and 95 % air.

### ***2.3.1 Maintenance of primary cell cultures***

The adherent cells were grown as a single layer, typically in 75  $\text{cm}^3$  culture flasks, and media was removed by aspiration and replenished every 2 days. Cells were routinely passaged when approximately 95 % confluence was reached to prevent cell cycle arrest and loss of surface contact of the cells. For passaging, cells were washed in sterile Dulbecco's PBS (Sigma-Aldrich, Poole, U.K.) and incubated with 2 ml of trypsin-ethylenediamine tetra-acetic acid (trypsin-EDTA) at 37 °C, usually for a minimum of 3 minutes. The addition of the complete media stopped the action of the trypsin-EDTA solution and allowed sub-culturing of the cell suspension. Cells were counted using a haemocytometer to ensure seeding at the correct density where appropriate.

### ***2.3.2 Rabbit aortic smooth muscle cells***

Aortae from male New Zealand white rabbits (2.5 to 3.5 kg body weight) were excised and cleaned of any connective tissue and fat. The outer and inner surface of the vessel was scraped, removing the adventitia and intima respectively, to prevent the contamination of other cell types in the culture. Aortic explants were initially cultured in 6 well plates in 1:1 Waymouth's MB 752/1 and Ham's F12 and GlutaMAX™ supplemented with 1 % (v/v) penicillin-streptomycin solution (Sigma-Aldrich, Poole, U.K.) and 10 % (v/v) FCS. Cells were checked visually for the distinctive smooth muscle cell characteristics and for the positive immunostaining of  $\alpha\text{SMA}$  (described in Section 2.3.2.1). Once the cells reached confluence, the aortic explants were removed and the cells were transferred to 75  $\text{cm}^3$  culture flasks and used between passages 3 to 8.

### **2.3.2.1 Immunostaining for $\alpha$ SMA**

Cells were seeded at 10,000 cells per well on chamberslides, incubated at 37 °C for 24 hours and then fixed with 2 % (w/v) paraformaldehyde for 10 minutes. Cells were then washed 3 times with PBS and permeabilised with 0.5 % (v/v) Triton X-100 in PBS for 15 minutes at room temperature. This was followed by 3 washes in PBS and then incubation with 10 % (v/v) heat inactivated serum for 30 minutes at 37 °C from the appropriate species that the secondary antibody was raised in which was horse in this case.  $\alpha$ SMA (Abcam, Cambridge, U.K.) was diluted 1 in 50 in 10 % (v/v) heat inactivated serum then incubated overnight at 4 °C. The following day, the cells were washed 3 times in PBS and incubated with horse anti-mouse secondary antibody (Pierce Antibodies, Thermo Scientific, Loughborough, U.K.) for 1 hour at 37 °C and washed a further 3 times in PBS. 4',6-diamidino-2-phenylindole (DAPI) was added to identify the nucleus of the cells and slides were mounted with coverslips and kept overnight in the dark at room temperature. Green fluorescence was then observed using fluorescein isothiocyanate (FITC) at a magnification of 10 x.

### **2.3.3 Measurement of cell proliferation**

Cell proliferation was measured by the incorporation of the thymidine analogue, bromodeoxyuridine (BrdU), into newly synthesised DNA during the S phase of the cell cycle (Calbiochem, Nottingham, U.K.). This assay is based on the traditional [ $^3$ H] thymidine proliferation assay with the principal difference being the replacement of [ $^3$ H] thymidine with BrdU. It is a non-radioactive compound allowing the assessment of proliferation with an enzyme-linked immunosorbent assay (ELISA) rather than scintillation counting, therefore eliminating the use of harmful radioactive substances. Cells were seeded in a 96 well plate at a density of 10,000 cells per well and quiesced in 0.1 % (v/v) FCS-containing media for 24 hours. Cells were incubated with the agonist of interest for the requisite length of time. Where appropriate, antagonists were added 30 minutes prior to incubation with agonists. The BrdU label was added to each well 24 hours prior to the end of the measurement. The assay was performed as per the manufacturer's instructions. Briefly, BrdU was incorporated into the proliferating cells. These were then fixed and partial denaturation of DNA occurred to allow the detection of the BrdU by a monoclonal antibody. Horseradish peroxidase (HRP)-conjugated goat anti-mouse binds to the antibody and facilitates the conversion of the substrate, tetramethylbenzidine (TMB) from a colourless solution to blue, which turns yellow upon the addition of the stop solution. Absorbance was measured spectrophotometrically at dual

wavelengths of 450 nm and 540 nm using a SpectraMax® M2 microplate reader (Molecular Devices, California, U.S.A.).

### **2.3.4 Assessment of cell viability**

Bioluminescent detection of cellular ATP was employed to determine cell viability as ATP is present in all metabolically active cells using a ViaLight™ Plus kit (Lonza, Basel, Switzerland). Cells were seeded in a 96 well plate at a density of 10,000 cells per well and quiesced in 0.1 % (v/v) FCS-containing media for 24 hours. Cells were incubated with the agonist of interest for the required length of time. Where appropriate, antagonists were added 30 minutes prior to incubation with agonists. The assay was performed as per the manufacturer's instructions. Briefly, the cell lysis buffer was added to release cellular ATP from the cells. Following this, ATP monitoring reagent plus was added to the lysed cells containing luciferase which catalyses the conversion of ATP and luciferin into emitted light. Luminescence was then measured using a POLARstar OPTIMA microplate reader (BMG Labtech, Germany).

### **2.3.5 Measurement of cell migration**

Cell migration was measured using a CHEMICON® QCM™ chemotaxis cell migration assay and was based on the traditional Boyden chamber method containing an 8 µm pore membrane (Millipore, Watford, U.K.). Cells were quiesced in 0.1 % (v/v) FCS-containing media for 24 hours preceding stimulation. For the pretreatment group, cells were incubated for 2 hours with each lipid separately prior to harvesting. Each lipid was added singly to the top chamber of the insert for the chronic incubation group. Cells were harvested and seeded in serum-free media into the upper chamber of the migration insert at 30,000 cells per well of a 24 well plate. 10 % (v/v) FCS-containing media was utilised as a chemotactic agent in the lower chamber to stimulate cell migration. The assay was performed as per the manufacturer's instructions. After 24 hours, the remaining cells and media present in the upper chamber were discarded and the membrane was stained. Non-migrated cells were removed from the interior side of the insert using a cotton bud before the insert was placed in the extraction buffer. An aliquot of the stained extraction buffer was assayed and absorbance was measured spectrophotometrically at 560 nm using a SpectraMax® M2 microplate reader.

## **2.4 Western blotting**

To determine the relative expression of the proteins of interest, sodium dodecyl sulphate polyacrylamide gel electrophoresis (SDS PAGE) and immunoblotting were performed using the Novex® NuPAGE® gel electrophoresis system (Life Technologies, Paisley, U.K.).

### ***2.4.1 Treatment of rabbit aortic smooth muscle cells***

Rabbit aortic smooth muscle cells were seeded in 6 well plates and grown to approximately 90 % confluence. The cells were then quiesced in 0.1 % (v/v) FCS-containing media for 24 hours. The cells were incubated with the lipids alone or an agonist or antagonist for AMPK (as indicated in the relevant results chapter) for the appropriate length of time followed by, in some cases, a 2 hour treatment with the lipids. Subsequently, the reaction was stopped by placing the 6 well plate on ice. The media was aspirated from the wells followed by the addition of ice-cold cell lysis buffer (50 mM Tris pH 7.4, 50 mM NaF, 1 mM Na<sub>4</sub>PPi, 1 mM EGTA, 1mM EDTA, 1 % (v/v) Triton X-100, 1 mM dithiothreitol (DTT), 1 % (v/v) cocktail of protease inhibitors) to each well for 5 minutes. Cell lysates were collected by scraping and stored at -80 °C for protein determination and Western blotting.

### ***2.4.2 Preparation of mouse aorta and liver***

Thoracic aortae and livers from male C57BL/6 and ApoE<sup>-/-</sup> mice, between 20 and 30 g, were excised immediately after death and cleaned of fat and connective tissue. The samples were snap frozen and stored at -80 °C until use. Aortae were pulverised in liquid nitrogen using a mortar and pestle into a fine powder and re-suspended in ice-cold cell lysis buffer while sections of liver were homogenised using a micro-rotary blade. Protein samples were transferred into ice-cold centrifuge tubes and stored at -80 °C until use.

### ***2.4.3 Quantification of protein concentration***

Protein concentrations were determined according to the Bradford method (Bradford, 1976). Cell lysates, aortae and liver samples were centrifuged at 6200 x g for 5 minutes in a Pico 17 Thermo Scientific Heraeus bench-top centrifuge (Fisher Scientific, Loughborough, U.K.). Supernatants were transferred to fresh ice-cold microcentrifuge tubes. Standard dilutions of bovine serum albumin (BSA) ranging from 0.1 mg/ml to 1

mg/ml were used to generate a standard protein curve with distilled water as a blank. Protein samples from VSMCs and aortae were diluted in distilled water at a ratio of 5:1 and 50:1 for liver samples. 10  $\mu$ l of each sample and standards were added in triplicate to a 96 well plate followed by 100  $\mu$ l of Pierce® Coomassie Plus (Bradford) assay reagent (Thermo Scientific, Loughborough, U.K.). Absorbance was read at 595 nm using a FLUOstar OPTIMA microplate reader (BMG Labtech, Germany). The mean absorbance from each sample was generated in triplicate and the protein concentration was determined by comparison with the BSA standard curve (Figure 2.1).

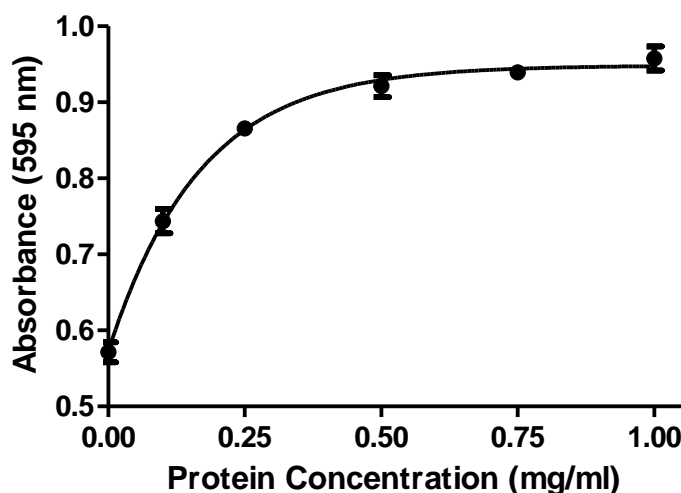


**Figure 2.1 – Representative BSA standard curve.**

#### **2.4.4 SDS PAGE**

Protein samples were mixed with 7.5  $\mu$ l of DTT and 12.5  $\mu$ l of NuPAGE® LDS sample buffer as a load dye, to a total volume of 50  $\mu$ l and heated at 70 °C for 20 minutes prior to protein loading. Samples were loaded on NuPAGE® Novex® 4-12 % Bis-Tris mini gels (1.0 mm thick, 10 or 12 wells) at 5 or 10  $\mu$ g of protein per well. 20  $\mu$ l of Novex® sharp pre-stained protein standard was added to the gel as a marker of protein size. Gels were run at 200 V for approximately 45 minutes in NuPAGE® MES SDS running buffer. After that, proteins were transferred onto a nitrocellulose membrane (pore size 0.45  $\mu$ m) at 30 V for 1 hour and 30 minutes in NuPAGE® transfer buffer supplemented with 10 % (v/v) methanol.

### **2.4.5 Immunoblotting**

After protein transfer was complete, nitrocellulose membranes were blocked for 1 hour in 5 % (w/v) dried milk powder suspended in Tris-buffered saline supplemented with 0.1 % (v/v) Tween-20 (TBST) at room temperature while shaking. Membranes were then rinsed in TBST and incubated overnight at 4 °C in primary antibody diluted in 5 % (w/v) BSA suspended in TBST. A summary of the primary and secondary antibodies used along with dilutions are presented in Table 2.1. Following this, membranes were washed in TBST and incubated for 2 hours at room temperature in HRP-conjugated secondary antibody diluted in 5 % BSA in TBST. Once complete, membranes were washed in TBST. Visualisation of protein bands was performed using a Pierce® enhanced chemiluminescence (ECL) detection kit (Thermo Scientific, Loughborough, U.K.). Membranes were incubated in 1:1 mix of ECL reagents for 60 seconds, blotted and placed in a light-sensitive cassette. Chemiluminescence of protein bands was detected with a Kodak X-Omat 2000 processor using Kodak blue-sensitive X-ray film.

### **2.4.6 Quantification of expression of protein**

The antibody-detected protein bands on the developed X-ray film were scanned into a GS-800™ Calibrated Densitometer (BioRad, Hemel Hempstead, U.K.). Densitometrical analysis of the bands was performed using Quantity One BioRad software (BioRad, Hemel Hempstead, U.K.). Housekeeping proteins, glyceraldehyde-3-phosphate dehydrogenase (GAPDH) or  $\alpha$  tubulin were used as protein loading controls therefore data were expressed as a ratio of protein of interest to the loading control or as a ratio of phosphorylated to the total amount of protein present.

## **2.5 Small vessel wire myography**

Mouse carotid arteries were excised immediately after death and cleaned of all fat and connective tissue. The intimal layer of the artery was removed by gently rubbing the interior of the vessel with a human hair to eliminate the action of the endothelium in the response. The vessels were cut into 2 mm segments and mounted on two stainless steel wires in a two-channel small vessel wire myograph (Danish Myo Technology, Aarhus, Denmark), with one of the wires connected to a force transducer and the other to an adjustable jaw (Figure 2.2). Vessels were incubated at 37 °C in Krebs-Henseleit buffer (containing: 118 mM NaCl, 4.7 mM KCl, 1.2 mM MgSO<sub>4</sub>, 25 mM NaHCO<sub>3</sub>, 1.03 mM KH<sub>2</sub>PO<sub>4</sub>, 11 mM glucose and 2.5 mM CaCl<sub>2</sub>) and gassed continuously with 95 % O<sub>2</sub> and 5

% CO<sub>2</sub>. The artery segments were equilibrated for at least 30 minutes at resting tension. A predetermined active tension of 0.25 g was then applied to the artery for a further 30 minutes (Methven *et al.*, 2009). Chart™ 5 Pro software (ADInstruments, Chalgrove, U.K.) was used to record and measure vessel responses to reagents. At the beginning of each experiment, the contractile response to 40 mM KCl was measured to establish the viability of the segments and also to sensitise the vessel before other pharmacological agents were added.

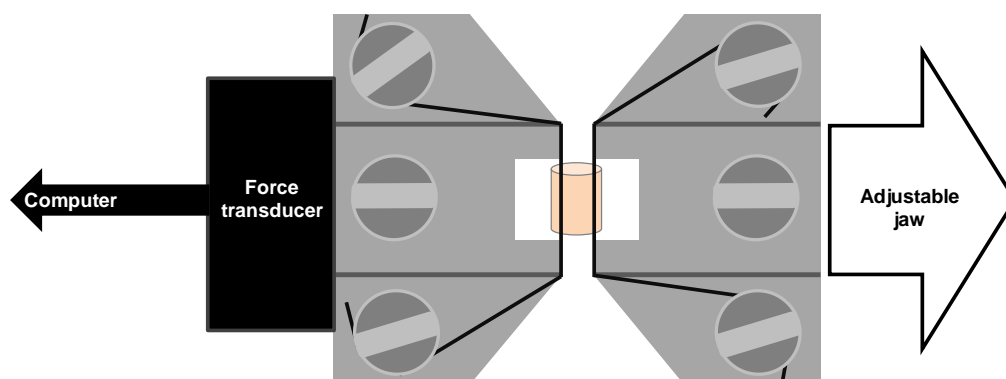


**Figure 2.2 – Representative diagram of mouse carotid artery mounted in small vessel wire myograph.**

2 mm segments of vessel were mounted on two 40 µM stainless steel wires with one connected to a force transducer and a computer to record the changes in tone of the artery. The other wire was connected to an adjustable jaw for the application of the desired amount of tension on the vessel.

### **2.5.1 Cumulative concentration-response curve**

After the vessel had been sensitised, the segments of mouse carotid arteries were incubated with 25 µM of modified lipid or vehicle (equivalent volume of Krebs' solution). Following this, the vessels were pre-constricted with the thromboxane A<sub>2</sub> receptor agonist, 9,11-dideoxy-11 $\alpha$ ,9 $\alpha$ -epoxymethanoprostaglandin F<sub>2 $\alpha$</sub>  (U46619, Sigma-Aldrich, Poole, U.K.) at a concentration of 3x10<sup>-8</sup> M, producing a submaximal contraction established from previous experiments in the laboratory. Cumulative concentration-response curves to AICAR were performed in a range of increasing concentrations from 1x10<sup>-4</sup> M to 1x10<sup>-2</sup> M at 10 minute intervals. Data were expressed as a percentage of relaxation of the U46619-induced tone of the vessel.

**Table 2.1 – Summary of antibodies and dilutions used for immunoblotting.**

<b>Protein</b>	<b>Molecular Weight</b>	<b>Host Species</b>	<b>Primary Dilution</b>	<b>Secondary Dilution</b>	<b>Source and Product Number</b>
<b>ACC</b>	280 kDa	Rabbit	1:1000	1:2000	Cell Signalling Technology #3676
<b>AMPK<math>\alpha</math></b>	62 kDa	Rabbit	1:1000	1:2000	Cell Signalling Technology #2603
<b>Caspase 3</b>	32 kDa	Rabbit	1:1000	1:1000	Abcam ab90437
<b>GAPDH</b>	37 kDa	Mouse	1:40000	1:2000	Abcam ab8245
<b>Phospho ACC</b> (Ser79)	280 kDa	Rabbit	1:1000	1:2000	Cell Signalling Technology #3661
<b>Phospho AMPK<math>\alpha</math></b> (Thr172)	62 kDa	Rabbit	1:1000	1:2000	Cell Signalling Technology #2535
<b><math>\alpha</math> tubulin</b>	50 kDa	Mouse	1:5000	1:2000	Abcam ab7291

Primary and secondary antibodies were diluted in TBST supplemented with 5 % BSA and incubated at 4 °C overnight and at room temperature for 2 hours respectively. Rabbit polyclonal and mouse monoclonal HRP-conjugated secondary antibodies were obtained from Abcam (Cambridge, U.K.).

## 2.6 Animal models

All experiments were performed in accordance with the United Kingdom Animals (Scientific Procedure) Act of 1986. All *in vivo* experimentation was performed under the project licence, 60/4114, held by Dr Simon Kennedy (University of Glasgow, U.K.) and the personal licence, 60/11726. Mice were housed at the Central Research Facility at the University of Glasgow and maintained on 12 hour cycles of light and dark and at ambient temperature. Mice were fed a standard chow diet unless otherwise stated and allowed free access to both food and water. A diagram of the *in vivo* experimental design is depicted in Figure 2.3.

### 2.6.1 C57BL/6 mice

C57BL/6 mice were utilised as a control for all experiments in this study as this strain of mouse is the genetic background for the atherosclerotic ApoE<sup>-/-</sup> mice. Male mice were age-matched in all studies and obtained from Harlan (Oxon, U.K.).

### 2.6.2 ApoE<sup>-/-</sup> mice

ApoE<sup>-/-</sup> mice are an extensively used model of atherosclerosis, as described in Section 1.2.4.1. These mice have a significant increase in plasma levels of circulating lipoproteins including LDL and VLDL leading to the development of atherosclerotic plaques which resemble the human form (Zadelaar *et al.*, 2007). ApoE<sup>-/-</sup> mice, generated from a C57BL/6 background, were obtained from Charles River (Margate, U.K.) and further bred in-house. Mice were fed on a commercially available cholesterol rich diet during the high fat feeding regime which started at 6 weeks of age for mice undergoing carotid artery injury surgery and 8 weeks for all other mice.

### 2.6.3 Mouse carotid artery injury model

Immediately prior to surgery, 8 week old male mice received an intraperitoneal (i.p.) injection of an analgesic, buprenorphine (0.1 mg/kg) and 2.5 mg of the anti-platelet drug, dipyridamole (Persantin®). Sterile saline (0.5 ml via subcutaneous injection) was also administered to prevent dehydration of the animal during surgery. All surgical procedures were performed under aseptic conditions. Carotid artery injury surgery was performed following an adapted method described by Tennant *et al.* (2008). General anaesthesia was induced by 3 % (v/v) isoflurane supplemented with oxygen (flow rate of 0.5 litres/minute)

and maintained at 1.5 % (v/v) isoflurane via a face mask throughout the procedure. The depth of anaesthesia was monitored throughout the surgery using the hind limb reflex with the other paws secured with tape. A small skin incision was made in the ventral side of the neck to expose the trachea. Blunt dissection was performed to navigate through muscle and connective tissue inferior to the trachea, exposing about 0.5 cm of the left common carotid artery. Precise dissection was used to detach the vagus nerve from the artery and two silk ligatures (size 6-0, Fine Science Tools, Heidelberg, Germany) were positioned at the proximal and distal ends of the vessel. The distal ligature was tied tightly and an arterial clip (Fine Science Tools, Heidelberg, Germany) was positioned at the most proximal end to temporarily occlude the blood flow in the vessel. A small incision was made in the artery and a piece of a modified flexible nylon wire, adapted by melting the end to create a blunt spherical tip, was inserted into the incision site and held loosely in place by tightening of the proximal ligature. Once the arterial clip was removed, the nylon wire was advanced and rotated down the carotid artery into the thoracic aorta and this was repeated several times to ensure the removal of the endothelium. Once the nylon wire was removed, the arterial clip was replaced and the proximal ligature was tied tightly and secured just below the incision site. Upon removal of the clip, the area was bathed with heparinised saline and a continuous line of subcutaneous sutures (size 6-0, Viracyl, Ethicon, Edinburgh, U.K.) was used to close the skin incision. For post-operative care, the mice received i.p. injection of buprenorphine (0.1 mg/kg) and were transferred to a heating mat and maintained at 37 °C until recovery. ApoE<sup>-/-</sup> mice were transferred from a normal chow diet to the high fat diet 2 weeks prior to the procedure and continued on the high fat diet until termination, 2 weeks after surgery. Sham-operated mice were studied as controls following the same procedure without the insertion of the nylon wire.

### **2.6.3.1 Termination of procedure**

Mice were sacrificed 14 days after the carotid artery injury surgery by i.p. injection of 200 mg/kg of sodium pentobarbital (Euthatal) to allow for tissue and blood collection. Blood was collected by cardiac puncture into K2 EDTA Microtainers® (BD Biosciences, Oxford, U.K.) and centrifuged at 1500 x g for 10 minutes to produce plasma, which was removed and stored at -80 °C until use. Carotid arteries and aortae were dissected and cleaned of any connective tissue and divided randomly into groups; either fixed for histological analysis or snap frozen in liquid nitrogen for mass spectrometry analysis. Heart, liver and spleen weight was also recorded.

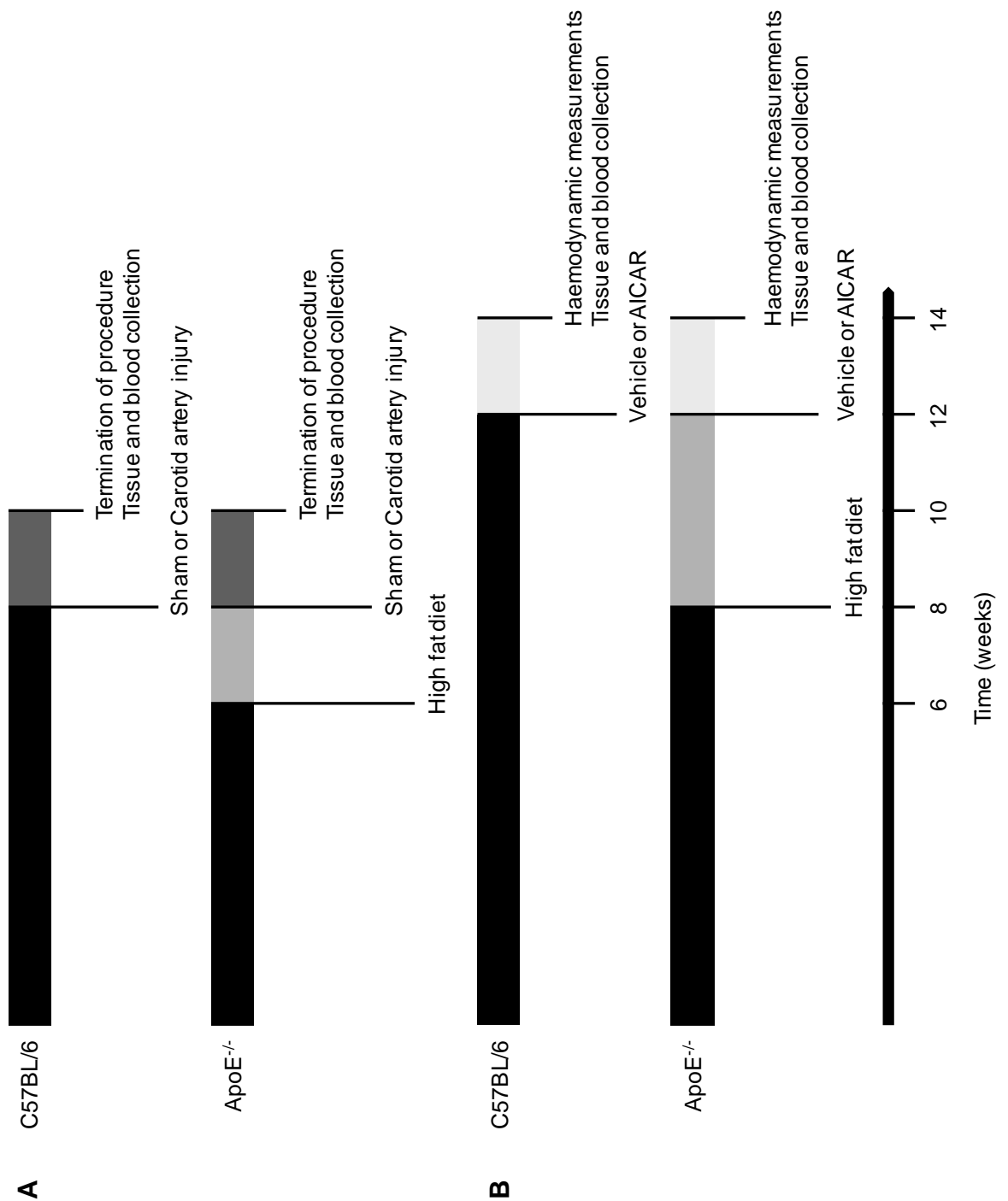


**Figure 2.3 – *In vivo* experimental design.**

For the carotid artery injury model (Section 2.6.3), C57BL/6 and ApoE<sup>-/-</sup> mice (on high fat diet at 6 weeks of age) were subjected to either sham or vascular injury of left carotid artery with the procedure terminated at 10 weeks old and tissue and blood samples collected (A). For chronic AICAR administration (Section 2.6.4), C57BL/6 and ApoE<sup>-/-</sup> mice (on high fat diet at 8 weeks of age) were injected with either vehicle or AICAR for 2 weeks followed by haemodynamic measurements after which tissue and blood samples were collected (B).

### **2.6.4 AICAR administration**

To investigate the effect of AICAR (Toronto Research Chemicals Inc., Ontario, Canada) on atherosclerosis progression and blood pressure, 10 to 12 week old C57BL/6 mice on normal chow and ApoE<sup>-/-</sup> mice fed on the high fat diet for 1 month and continued for the duration of the dosing regimen, were administered a daily i.p. injection of either saline vehicle or AICAR (400 mg/kg) for 14 days. After the completion of the 14 day period, haemodynamic measurements were performed. Mice were weighed at the beginning of the dosing regimen as well as at day 7 to adjust the dose due to potential fluctuations in body weight.

### **2.6.5 Haemodynamic measurements**

Haemodynamic measurements were performed by the cannulation of the left common carotid artery. Mice were weighed before the beginning of each experiment. General anaesthesia and isolation of the carotid artery was achieved using the same method as the mouse carotid artery injury model as described in Section 2.6.3. A polyurethane cannula (Harvard Apparatus, Boston, U.S.A.) filled with heparinised saline was inserted at the incision site, approximately 4 mm into the lumen of the carotid artery and secured in place with the proximal ligature. The cannula was connected to an Elcomatic E751A pressure transducer and MP35 data acquisition system (BIOPAC© Systems Inc., Santa Barbara, U.S.A.). Upon removal of the arterial clip and restoration of blood flow, the mean arterial blood pressure was measured.

#### **2.6.5.1 Tissue and blood collection**

Once the haemodynamic measurements were complete, the mice were sacrificed by cervical dislocation. Blood was collected via cardiac puncture and prepared as described in Section 2.6.3.1. Carotid arteries and aortae were dissected and cleaned of any connective tissue. Vessels were snap frozen in liquid nitrogen and stored at -80 °C for immunoblotting and mass spectrometry analysis. Heart, liver and spleen weight was also recorded.

### **2.6.6 Measurement of plasma MPO**

The MPO content of plasma from C57BL/6 and ApoE<sup>-/-</sup> mice was analysed using a mouse MPO ELISA kit (Hycult® Biotech Inc., Uden, Netherlands). Plasma samples, collected

from C57BL/6 and ApoE<sup>-/-</sup> mice after carotid artery injury and chronic AICAR administration, were diluted 1 in 16 in dilution buffer. This concentration was chosen after a preliminary experiment with increasing dilutions of mouse plasma. The assay was performed as per the manufacturer's instructions. The samples and a standard curve, ranging from 1.6 ng/ml to 100 ng/ml (Figure 2.4), were added to a microtiter plate coated with antibodies that recognise mouse MPO in the plasma. The bound mouse MPO binds to a biotinylated tracer antibody which in turn binds to a streptavidin-peroxidase conjugate. The conjugate then facilitates the conversion of the substrate, TMB, from a colourless to blue solution with the reaction stopped by the addition of oxalic acid. Absorbance was measured spectrophotometrically at 450 nm using a SpectraMax® M2 microplate reader.

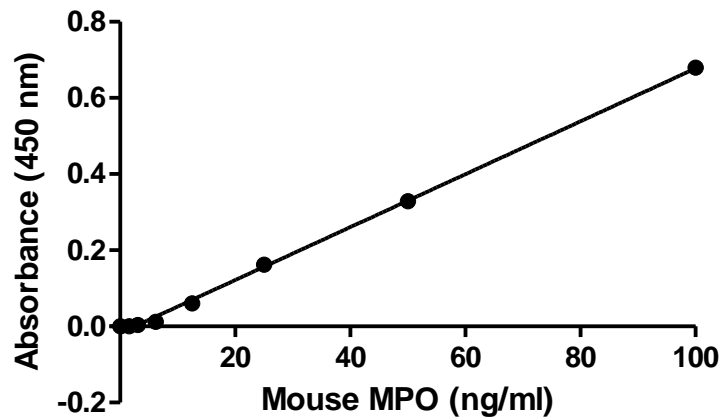


Figure 2.4 – Representative MPO standard curve.

## 2.7 Histology

### 2.7.1 Fixation

Left and right mouse carotid arteries and aortae were dissected from the cadaver from the vascular injury study, freed of any connective tissue and fixed in 10 % (v/v) neutral buffered formalin (10 % formalin, 90 % H<sub>2</sub>O, 33 mM NaH<sub>2</sub>PO<sub>4</sub>, 45 mM Na<sub>2</sub>HPO<sub>4</sub>) overnight. Tissues were processed through a gradient of alcohol solutions to HistoClear (a xylene substitute, Thermo Scientific, Loughborough, U.K.) with the terminal step into paraffin wax. This was performed in a Citadel 1000 tissue processor (Thermo Shandon, Runcorn, U.K.) in the following sequence:

**Table 2.2 – Sequence for processing samples for histological analysis.**

Solution	Length of incubation of sample
70 % ethanol	15 minutes
85 % ethanol	15 minutes
90 % ethanol	25 minutes
95 % ethanol	25 minutes
100 % ethanol	15 minutes
100 % ethanol	15 minutes
100 % ethanol	15 minutes
HistoClear	30 minutes
HistoClear	30 minutes
Paraffin wax	30 minutes
Paraffin wax	30 minutes

Samples were positioned and held vertically to embed the vessels in the correct orientation in the paraffin wax for sectioning using a Shandon Histocenter 3 embedding centre (Fisher Scientific, Loughborough, U.K.). Paraffin blocks were cut into 4 µm slices to expose the transverse sections of the embedded arteries using a Leica Finesse 325 Microtome (Fisher Scientific, Loughborough, U.K.).

### **2.7.2 Haematoxylin and eosin staining**

Haematoxylin and eosin (H&E) stain the nucleus and cytoplasm of cells respectively and was used to investigate neointima formation in the vascular injury study. Paraffin was removed from the cut sections and rehydrated through an alcohol gradient of 100 %, 90 % and 70 % ethanol for 5 minutes each and washed in deionised water for a further 5 minutes. Sections were then stained with haematoxylin for 4 minutes and washed in deionised water before being placed in acid alcohol (1 % (v/v) HCl in ethanol) for 30 seconds. Slides were washed in deionised water for 1 minute, placed in eosin for 2 minutes before a further 5 minute wash in deionised water. Sections were then dehydrated by incubation in 70 %, 90 % and 100 % ethanol followed by 10 minutes in HistoClear. Finally, cover slips were fixed using DPX mounting medium (VWR BDH Prolabo, Leicestershire, U.K.). Nuclei appeared blue/purple whereas cytoplasm was stained pink.

### **2.7.3 Immunohistochemistry**

Paraffin was removed from the cut sections and rehydrated through an alcohol gradient of 100 %, 90 % and 70 % ethanol for 5 minutes each and washed in running water. Heat-induced antigen retrieval was then performed with the sections incubated in 10 mM citric acid at pH 6.0 at 95-100 °C for 10 minutes and allowed to cool to room temperature. Carotid artery sections were washed in running water for 10 minutes and then endogenous peroxidase activity was blocked by the incubation of 3 % (v/v) H<sub>2</sub>O<sub>2</sub> in methanol for 20 minutes. Following this, sections were washed in running water for 10 minutes and incubated with 2.5 % normal horse blocking serum for all non-specific binding in a humidified chamber for 1 hour at room temperature. The arterial sections were then incubated with the primary antibody diluted in 1 % (w/v) BSA in PBS (Sigma Aldrich, Poole, U.K.) in a humidified chamber. A summary of the primary antibodies used along with dilutions and lengths of incubations are found in Table 2.3. A blank and negative control was carried out for each experiment using 1 % BSA in PBS and rabbit IgG antibody diluted in 1 % BSA in PBS respectively. Following this, sections were washed twice in PBS for 10 minutes and incubated with ImmPRESS™ anti-rabbit Ig antibody (Vector Laboratories, Peterborough, U.K.) for 1 hour at room temperature in a humidified chamber with the exception of sections stained for phosphorylated and total AMPK. These sections were incubated with a biotinylated secondary antibody followed by treatment with streptavidin-peroxidase solution using the Histostain®-Plus Bulk kit (Life Technologies, Paisley, U.K.), both for 10 minutes at room temperature to amplify the signal. All sections

were next washed twice in PBS for 10 minutes each. DAB chromagen solution (3,3-diaminobenzidine and hydrogen peroxidase solution, Vector Laboratories, Peterborough, U.K.) was utilised for immunoperoxidase staining with the solution incubated with the sections until a dark brown staining was evident. This was typically between 2 and 5 minutes and the reaction was stopped by washing the sections in water. Sections were then counterstained with haematoxylin to visualise the nucleus of the cells by incubation for 4 minutes followed by washing in warm water for 5 minutes to “blue” the nuclei. Finally, the sections were dehydrated by incubation in 70 %, 90 % and 100 % ethanol followed by 10 minutes in HistoClear. Cover slips were then fixed using DPX mounting medium. Staining was visualised using a light microscope and positive immunostaining was seen as a brown/dark brown and nuclei appearing blue/purple. Sections were photographed using QCapture Pro 6.0 software and analysed with Image-Pro® Analyzer 7.0 software (Media Cybernetics, Marlow, U.K.).

**Table 2.3 – Summary of antibodies, dilutions and length of incubations used for immunohistochemistry.**

<b>Protein</b>	<b>Dilution and Length of Incubation</b>	<b>Source and Product Number</b>
<b>Active caspase 3</b>	1 in 50 for 2 hours at room temperature	Abcam ab2302
<b>αSMA</b>	1 in 200 for 2 hours at room temperature	Abcam ab5694
<b>AMPKα</b>	1 in 100 overnight at 4 °C	Abcam ab131512
<b>Ki67</b>	1 in 100 for 2 hours at room temperature	Abcam ab15580
<b>Phospho AMPKα</b> (Thr172)	1 in 100 overnight at 4 °C	Cell Signalling Technology #2535

All primary antibodies were diluted in 1 % (w/v) BSA in PBS.

## 2.8 Detection of lipids in murine arteries

### 2.8.1 Lipid extraction from mouse carotid arteries and aortae

The lipid content of mouse carotid arteries and aortae from both the vascular injury and chronic AMPK activation studies were investigated using a modified version of the Bligh-Dyer procedure, previously used for cell extractions (Spickett *et al.*, 2001). Equal volumes of solvents and aqueous solutions were used for lipid extraction. Vessels were incubated in 1.5 ml Ultra High Recovery microcentrifuge tubes (Starlab, Milton Keynes, U.K.) in methanol containing 100 µg/ml of butylated hydroxytoluene (BHT), which is used as an antioxidant. Tissue samples were vortexed for 30 seconds and sonicated in a water bath for 15 minutes. Chloroform was then added to the sample and vortexed for 30 seconds and left overnight in the fridge for the lipids to extract. An aqueous layer of 0.88 % (w/v) KCl in water was added and vortexed for a further 30 seconds before incubation in the fridge for 20 minutes. The sample was then centrifuged at 13800 x g for 1 minute, separating the solvents and KCl into separate layers. The chloroform layer was removed using a Hamilton syringe into a fresh microcentrifuge tube and particular care was taken to avoid removal of any of the aqueous layer. The samples were then dried under a steady flow of oxygen-free nitrogen gas and stored at -80 °C until use.

### 2.8.2 Quantification of lipids by ESMS

Dried lipid extracts were reconstituted in 100 µl of 20 % (v/v) chloroform in methanol and vortexed for 1 minute. The samples were then diluted 1 in 10 in methanol which allowed the samples to be further diluted for analysis using ESMS in either positive- or negative-ion mode performed on an QTRAP® 5500 mass spectrometer (Figure 2.5, AB SCIEX, Warrington, U.K.). For analysis using positive-ion mode with direct infusion, samples were diluted 1 in 100 for aortae, 1 in 50 for left injured carotids and 1 in 25 for right carotids with 1 % (v/v) aqueous formic acid in methanol, giving a final dilution of the lipid extracts of 1 in 1000, 1 in 500 and 1 in 250 respectively. Spectra, in the range of m/z 300-1000, were acquired for 2 minutes. Precursor ion scanning was performed for m/z 184.1 for PCs and SMs and m/z 369.1 for cholesterol and cholesteryl esters, as well as neutral ion loss for 141.1 Da for PEs. For analysis using negative-ion mode with direct infusion, samples were diluted 1 in 10 for aortae, 1 in 5 for left injured carotids and 1 in 2.5 for right carotids with 10 % (v/v) 5 mM ammonium acetate in methanol, giving a final dilution of the lipid extracts of 1 in 100, 1 in 50 and 1 in 25 respectively. Spectra in the range of m/z 300-1000 were acquired for 4 minutes. Precursor ion scanning was performed for m/z

241.0 for PIs and neutral loss scan for 87.0 Da for PSs. Collision energy of 45 eV was used for all scans except for precursor ion scanning for  $m/z$  369.1 where 30 eV was used. Ion intensities for each  $m/z$  value were normalised by dividing the value by the obtained total ion count value, giving a percentage using PeakView® software (AB SCIEX, Warrington, U.K.). Ion intensities were evaluated by comparing the percentage  $m/z$  values from one sample group with the percentage  $m/z$  values from a different sample group.



**Figure 2.5 – Photograph of QTRAP® 5500 mass spectrometer.**

## 2.9 Statistical analysis

All results are expressed as mean  $\pm$  standard error of the mean (SEM) where  $n$  represents the number of experiments performed. Data were analysed with GraphPad Prism 5.0 software (California, U.S.A.) using either a paired or unpaired Student's  $t$  test, one-way analysis of variance (ANOVA) followed by a Dunnett's or Newman-Keuls' post hoc test or two-way ANOVA followed by Bonferroni's post hoc test as appropriate and described in the respective methods of each chapter. In all cases, a  $p$  value of less than 0.05 was considered statistically significant.

**CHAPTER 3**

**THE INFLUENCE OF MODIFIED  
LIPIDS ON VSMCs**

### 3.1 Introduction

VSMCs situated in the medial layer of vessels are in a quiescent phenotypic state, producing SM MHC and  $\alpha$ SMA; both are involved in contractile function (Owens *et al.*, 2004, Doran *et al.*, 2008). VSMCs can then switch into a synthetic state where they have a higher rate of proliferation and produce more scavenger receptors, allowing the uncontrolled uptake of lipids and therefore formation of foam cells (Owens *et al.*, 2004, Campbell and Campbell, 1994). Phenotypic switching of VSMCs is critical in the development of atherosclerosis and also restenosis, as both processes are characterised by a thickening of the arterial wall. This highlights the importance of VSMCs in arterial disease progression, while the modification of LDL and formation of oxidised phospholipids also contributes significantly to the pathophysiology of atherosclerosis (Witztum and Steinberg, 1991). These oxidised phospholipids, such as oxPAPC and its constituent POVPC, have been found to decrease SM MHC and  $\alpha$ SMA leading to an increase in the expression of pro-inflammatory genes encoding chemokines such as MCP-1 thereby inducing the phenotypic switching process of VSMCs and enhancing the inflammatory state (Pidkovka *et al.*, 2007).

Oxidised phospholipids PGPC and POVPC, are the predominant truncated products formed from the autoxidation of PAPC and mimic the biological effects of mmLDL and hence could be critical markers of atherosclerotic progression (Watson *et al.*, 1995, Watson *et al.*, 1997). However, conflicting results have been observed in relation to VSMCs, with a biphasic response involving a proliferative effect at low concentrations and apoptosis predominating at higher concentrations (Auge *et al.*, 2002, Fruhwirth *et al.*, 2006, Johnstone *et al.*, 2009). Oxidised phospholipids have also demonstrated other pro-inflammatory effects in human aortic endothelial cells with incubation of oxPAPC inducing expression of MKP-1, which leads to the production of MCP-1 and chemotaxis of monocytes (Reddy *et al.*, 2001). In addition, oxPAPC induced monocyte adhesion and inflammation in atherosclerotic mice *in vivo* (Furnkranz *et al.*, 2005).

Production of oxidised lipids and modification of LDL is thought to occur by a number of ways including by the action of metals and the phagocytic enzyme, MPO. Attention has focused on MPO's ability to produce chlorinated species at physiological and pathological conditions *in vivo* as it catalyses the production of HOCl from H<sub>2</sub>O<sub>2</sub> and chloride anions (Schultz and Kaminker, 1962). There is growing evidence of the involvement of MPO and HOCl in atherosclerosis with the active form of the enzyme being found in human

atherosclerotic plaques as well as HOCl-modified LDL (Daugherty *et al.*, 1994, Hazell *et al.*, 1996). Wildtype mice overexpressing human MPO in macrophages were produced using the Visna virus promoter and then repopulated in bone marrow of lethally irradiated LDLr<sup>-/-</sup> mice. These hypercholesterolaemic mice expressing human MPO have also been found to promote atherosclerotic progression (McMillen *et al.*, 2005). HOCl can be added across the unsaturated bonds of phospholipids by electrophilic attack forming lipid chlorohydrins (Winterbourn *et al.*, 1992). Phospholipid chlorohydrins have demonstrated toxicity in myeloid cells and endothelial cells, thought to be due to their high polarity which leads to disruption of the membrane (Dever *et al.*, 2003, Vissers *et al.*, 2001, Carr *et al.*, 1997). Pro-inflammatory effects have also been observed with chlorohydrins inducing leukocyte adhesion in ApoE<sup>-/-</sup> mice, primarily through the upregulation of P-selectin (Dever *et al.*, 2008). Alpha-chloro fatty aldehydes are another class of chlorinated species produced by the action of MPO, formed by the addition of HOCl across the vinyl ether bond of plasmalogens (Albert *et al.*, 2001). Activation of neutrophils results in the production of 2-ClHDA which has been found to be a natural inhibitor of endothelial NO biosynthesis as well as accumulating during MI (Thukkani *et al.*, 2002, Marsche *et al.*, 2004, Thukkani *et al.*, 2005). Unlike chlorohydrins, there is evidence of alpha-chloro fatty aldehydes in human atherosclerotic plaques with potential proatherogenic properties through inducing P-selectin expression in primary HCAECs (Thukkani *et al.*, 2003b). However, considering the mounting evidence of biological effects of modified lipids, little is known about the actions of different classes of modified lipids on VSMC proliferation, viability and migration which are all important remodelling processes in the development of atherosclerosis and also restenosis.

### **3.1.1 Aims**

The aims investigated in this chapter were:

- To determine the stability of phospholipid chlorohydrins over a 72 hour period.
- To determine the effect of either short- or long-term modified lipid incubation on VSMC proliferation, viability and migration.
- To elucidate the mechanism of cell death induced by modified lipids.

## **3.2 Methods**

### ***3.2.1 Lipid preparation and analysis***

SOPC and SLPC were modified to form lipid chlorohydrins as detailed in Section 2.2.1. Native phospholipids were incubated with HBSS to form lipid micelles and chlorinated with excess HOCl. DPPC was added to each of the native phospholipids to assess the stability of each chlorohydrin. Excess HOCl was removed using a reverse phase Sep-Pak® column and dried under nitrogen. Lipid chlorohydrins were reconstituted in PBS with chlorohydrin formation and stability analysed by ESMS over a 72 hour period. 2-CIHDA was synthesised by Professor Andrew R. Pitt (Aston University, U.K.) and oxidised phospholipids were purchased from Avanti Polar Lipids. For cell experiments, all lipids were reconstituted in culture medium and added to the cells at increasing concentrations.

### ***3.2.2 VSMC proliferation***

Immunostaining for  $\alpha$ SMA was first performed to characterise the origin of the primary cell culture as described in Section 2.3.2.1. VSMC proliferation was then assessed by determining the incorporation of BrdU into newly synthesised DNA using an ELISA kit (as detailed in Section 2.3.3). For pretreatment experiments, cells were incubated with 1-100  $\mu$ M of each lipid for 2 or 6 hours prior to stimulation with 10 % FCS and the addition of BrdU for 24 hours at 37 °C. For assessing the effect of chronic incubation, cells were stimulated with 10 % FCS and the addition of BrdU along with 1 to 100  $\mu$ M of each lipid for 24 hours.

### ***3.2.3 VSMC viability***

Cell viability was measured by the bioluminescent detection of cellular ATP as it is present in all metabolically active cells (described in Section 2.3.4). For pretreatment experiments, cells were incubated with 1-100  $\mu$ M of each lipid for 2 or 6 hours prior to stimulation with 10 % FCS for 24 hours at 37 °C. For assessing the effect of chronic incubation, cells were stimulated with 10 % FCS along with 1-100  $\mu$ M of each lipid for 24 hours.

### ***3.2.4 Western blotting***

Expression of caspase 3 was measured by Western blot analysis as detailed in Section 2.4. VSMCs were seeded in 6 well plates and grown to 80 % confluency before quiescing in

0.1 % FCS for 24 hours. Following exposure to each lipid (1-100  $\mu\text{M}$ ) for 2 hours, VSMC lysates were prepared. Protein estimation analysis from these lysates was carried out and protein was added at 10  $\mu\text{g}$  per well. Immunoblotting was performed with antibodies against caspase 3 and  $\alpha$  tubulin (all antibody dilutions found in Table 2.1) which was used as a loading control followed by densitometrical analysis of the detected protein bands.

### 3.2.5 VSMC migration

Cell migration was measured using a QCM chemotaxis cell migration assay which is based on the Boyden chamber method containing an 8  $\mu\text{m}$  pore membrane (as described in Section 2.3.5). For the acute incubation, cells were pretreated in quiescing medium with each lipid (1-100  $\mu\text{M}$  for chlorinated lipids and 1-25  $\mu\text{M}$  for oxidised phospholipids) prior to harvesting. Lipid (1-100  $\mu\text{M}$ ) was added to the top chamber of the insert for chronic incubation.

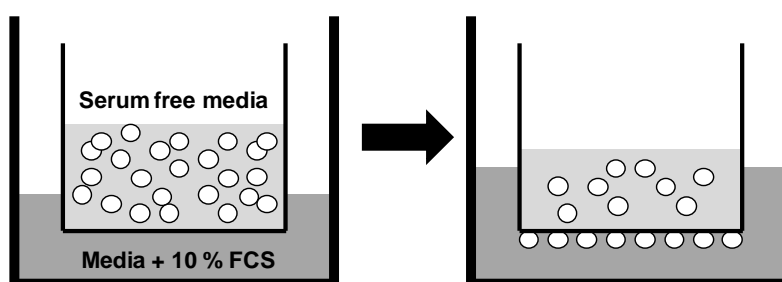


**Figure 3.1 – Illustration of chemotactic cell migration assay.**

Cells were seeded in serum-free media in the top of the insert (with or without lipid) with media supplemented with 10 % (v/v) FCS in the lower chamber acting as a chemotactic agent. Cells migrated through the porous membrane and adhered to the underside where they were stained and cell migration was measured colourimetrically.

### 3.2.6 Statistical analysis

All results are displayed as mean  $\pm$  SEM and n represents the number of independent experiments performed. Data were analysed using a two-way ANOVA for the control BrdU experiments, a one-way ANOVA followed by Dunnett's post hoc test for all proliferation, viability and migration experiments and a one-way ANOVA followed by Newman-Keuls' post hoc test for caspase 3 expression.

### 3.3 Results

#### 3.3.1 *Detection and assessment of the stability of phospholipid chlorohydrins*

The conversion of native phospholipids to their respective chlorohydrins was observed using ESMS in positive-ion mode with an increase in the  $m/z$  of 52 for the mono-chlorohydrins and 104 for bis-chlorohydrins. Phospholipid chlorohydrins were reconstituted in PBS to assess stability over a 72 hour time period with samples taken at 7, 24, 48 and 72 hours. Representative spectra from the initial sample time point are shown in Figure 3.2. Treatment of native SOPC ( $m/z$  788) with HOCl resulted in complete conversion to the mono-chlorohydrin, identified by the peak at  $m/z$  862 due to the addition of a sodium ( $\text{Na}^+$ ) ion. In contrast, DPPC ( $m/z$  734) was unaffected by incubation with HOCl with a peak seen at about  $m/z$  756, again in its sodiated form. A smaller additional peak was observed at  $m/z$  864 representing the chlorine isotope distribution pattern with the addition of  $^{37}\text{Cl}$  as chlorine exists as a mixture in a ratio of 3:1 of  $^{35}\text{Cl}$  to  $^{37}\text{Cl}$ . Treatment of SLPC ( $m/z$  786) resulted primarily in the conversion to the bis-chlorohydrin, observed at around  $m/z$  912 (plus  $\text{Na}^+$  ion). Furthermore, a peak was observed at about  $m/z$  916 indicating the addition of  $^{37}\text{Cl}$  rather than  $^{35}\text{Cl}$ . DPPC was again unaffected by the electrophilic attack with a peak observed at about  $m/z$  756. A further peak was seen at about  $m/z$  894 due to the loss of water from the chlorohydrin product, corresponding to the loss of  $m/z$  18. The stability of the chlorohydrin products was measured as a percentage of the stable DPPC peak. SOPC chlorohydrins (SOPC ClOH) remained stable over the initial 24 hour period and remained consistently larger than the DPPC peak. The peaks began to reduce steadily after this time point down to about 130 % of the DPPC peak after 72 hours. SLPC chlorohydrins (SLPC ClOH) followed a similar trend to the stability of SOPC ClOH but the amount of chlorohydrin product was reduced. Due to the complete conversion to the mono-chlorohydrin, SOPC ClOH was selected for subsequent experiments with 24 hours incubation.

#### 3.3.2 *Effect of pretreatment of modified lipids on VSMC proliferation and viability*

Immunostaining for  $\alpha\text{SMA}$  was performed to confirm the origin of the primary cell culture. Strong green fluorescence indicates positive staining for  $\alpha\text{SMA}$  and therefore VSMCs (Figure 3.3). Increasing concentrations of FCS were used to test the efficiency of the BrdU proliferation assay; 10 % FCS induced the largest rate of proliferation and was

therefore employed for all subsequent experiments (Figure 3.4). The influence of modified lipids (both chlorinated and oxidised) on VSMC proliferation and viability was then investigated. Acute effects were monitored after 2 hour incubation of the modified lipids in quiescing medium after which the cells were stimulated with 10 % FCS for 24 hours (with the addition of BrdU in the proliferation experiments).

Pretreatment of 2 hours with both chlorinated lipids, SOPC ClOH (Figure 3.5) and 2-ClHDA (Figure 3.6), had no effect on either VSMC proliferation or viability. In contrast, incubation with oxidised lipids, PGPC (Figure 3.7) and POVPC (Figure 3.8), caused a significant reduction in VSMC proliferation and viability with only  $17.6 \pm 6.5$  % and  $64.1 \pm 8.5$  % of viable cells remaining at 50  $\mu$ M of lipid compared to the 10 % FCS control respectively. The mechanism of cell death was investigated by assessing activation of caspase 3, an extensively used marker of programmed cell death or apoptosis. Caspase 3 is produced as an inactive pro-enzyme and is processed by upstream proteases such as caspase 8 and self proteolysis to its active form; therefore a reduction in the level of caspase 3 would infer activation. Cells were also photographed to assess the morphological changes in the VSMCs after 2 hours incubation with the modified lipids. Chlorinated lipids had no effect on either morphological changes or caspase 3 levels in VSMCs after a 2 hour treatment (Figure 3.9). In contrast, morphological changes were initially seen at 25  $\mu$ M PGPC and 50  $\mu$ M POVPC with cells appearing granular and the formation of vesicles suggesting apoptotic bodies had formed (Figure 3.10). This was increased at the higher concentrations of both of the oxidised lipids with almost complete obliteration of all cells at 100  $\mu$ M PGPC. Caspase 3 levels were reduced with increasing concentrations of both PGPC and POVPC; however a reduction in the expression of the protein loading control,  $\alpha$  tubulin, was also observed at the higher concentrations (50 and 100  $\mu$ M). These concentrations were therefore discounted from the analysis and no overall differences were observed. A longer period of 6 hours incubation in quiescing medium was utilised for modified lipids, where viable cells were still present after the 2 hour treatment to ensure all effects were witnessed (Figure 3.11). 6 hour treatment with SOPC ClOH caused a concentration-dependent reduction in VSMC viability with  $54.1 \pm 6.1$  % of viable cells at 100  $\mu$ M, whereas no effect was witnessed with 2-ClHDA incubation. POVPC caused a dramatic reduction in VSMC viability (similar to the 2 hour incubation with the other oxidised lipid, PGPC) with  $35.5 \pm 4.9$  % of viable cells at 25  $\mu$ M POVPC. Incubation with increasing concentrations of HOCl, which was used to chlorinate the phospholipids, had no effect on VSMC proliferation after either 1 hour or 2 hours treatment (Figure 3.12).

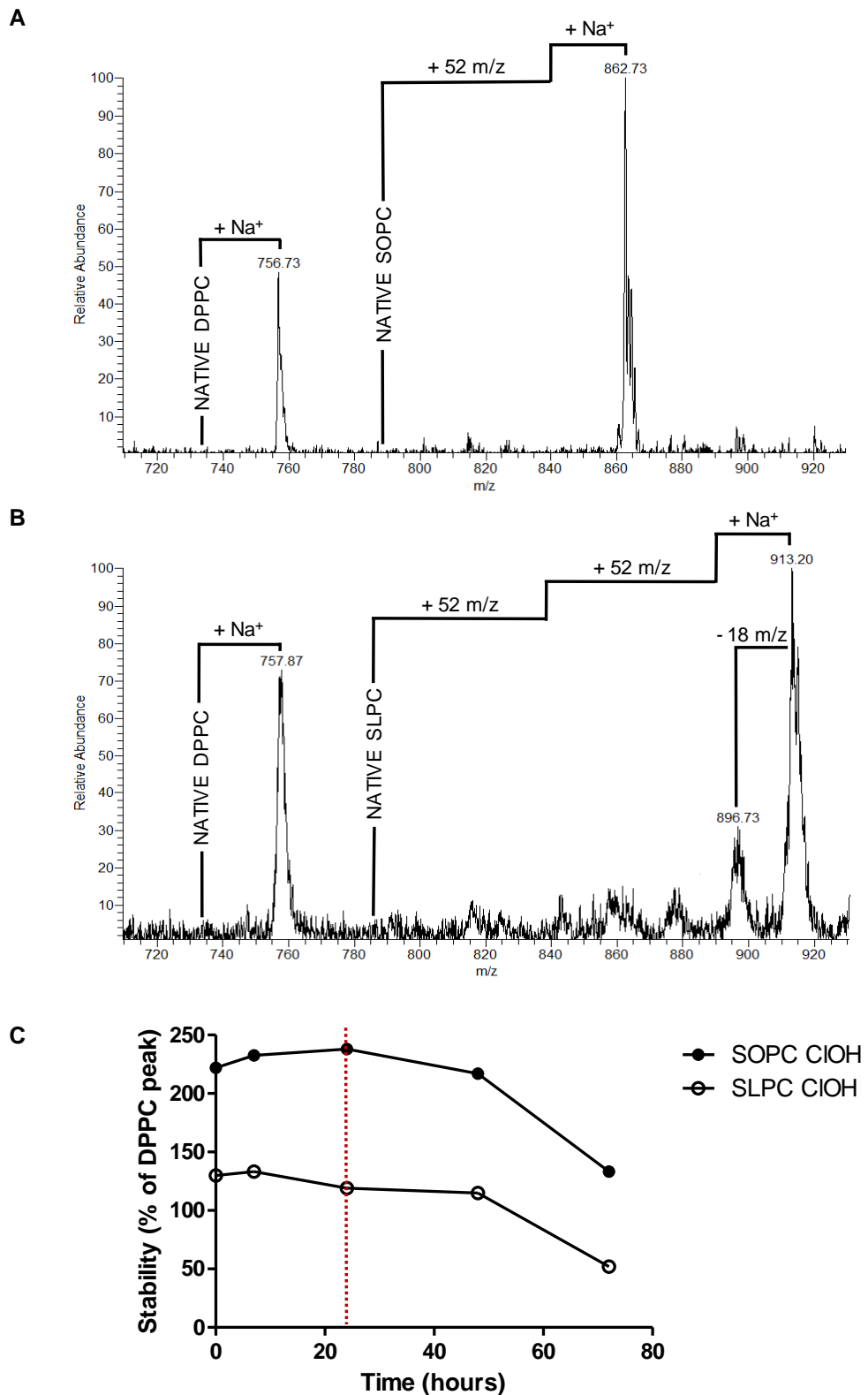


**Figure 3.2 – Stability of SOPC and SLPC ClOH over 72 hour period.**

Native SOPC and SLPC were chlorinated to their respective chlorohydrins and stability was measured as a percentage of the stable phospholipid, DPPC using positive-ionisation ESMS (C). Red dashed line indicates 24 hours which was the length of incubation used for all subsequent cell experiments. Spectra shown for SOPC (A) and SLPC (B) are representative of first sample collection at time zero.

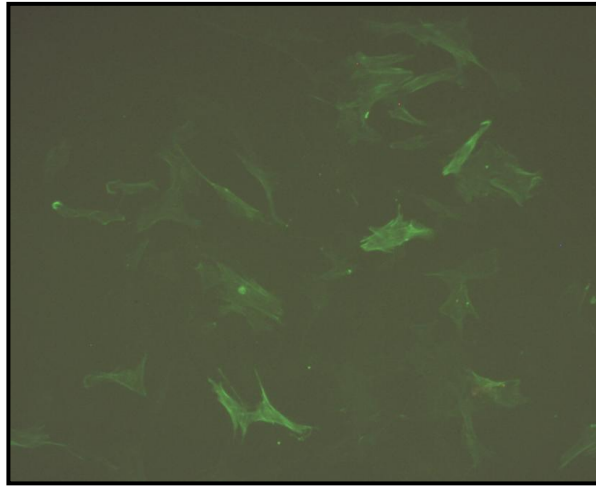


**Figure 3.3 – Immunostaining of primary cell culture for  $\alpha$ SMA.**

To confirm the origin of the primary cell culture, cells were fixed and permeabilised before incubation overnight with the primary antibody for  $\alpha$ SMA. Secondary antibody was then added and DAPI was also used to localise the nucleus of the cells. Green fluorescence was visualised using FITC at 10 x objective highlighting the presence of rabbit aortic VSMCs.

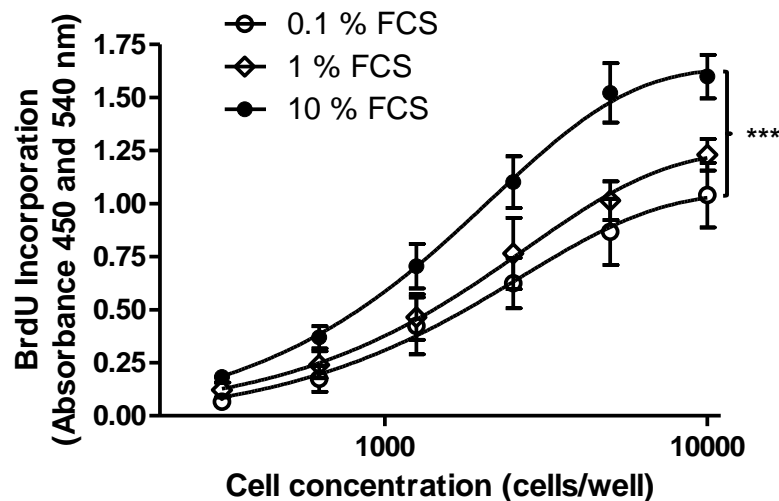


**Figure 3.4 – Effect of increasing concentrations of FCS on BrdU incorporation in proliferating VSMCs in culture.**

To test the efficiency of the non-radioactive proliferation assay, an increasing number of VSMCs were incubated with increasing concentrations of FCS for 24 hours with the addition of BrdU. \*\*\* $p < 0.001$  vs 0.1 % FCS,  $n = 3$  and performed in triplicate.

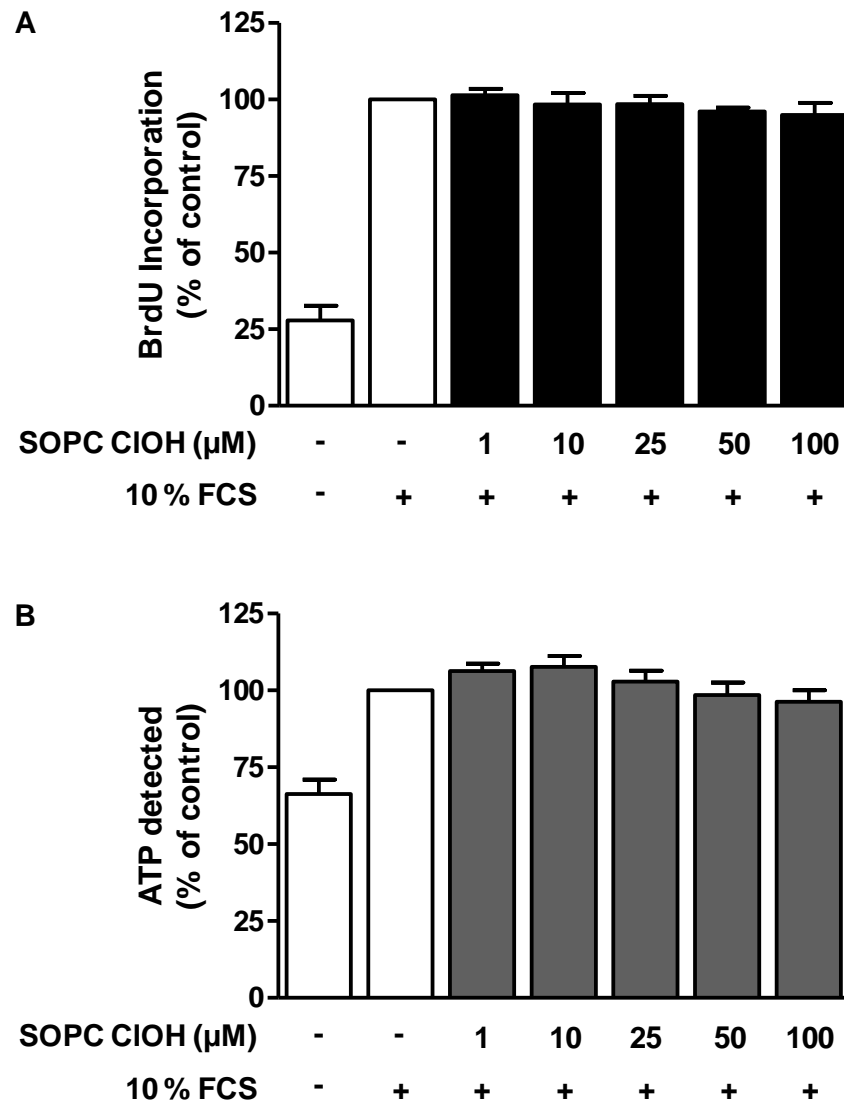


**Figure 3.5 – Effect of 2 hour pretreatment of SOPC ClOH on VSMC proliferation and viability.**

BrdU incorporation (A) and detection of ATP (B) were utilised to measure VSMC proliferation and viability respectively. VSMCs were incubated for 2 hours with increasing concentrations of SOPC ClOH in quiescing media and then stimulated with 10 % FCS for 24 hours with the addition of BrdU in proliferation measurements.  $n = 6$  and performed in triplicate.

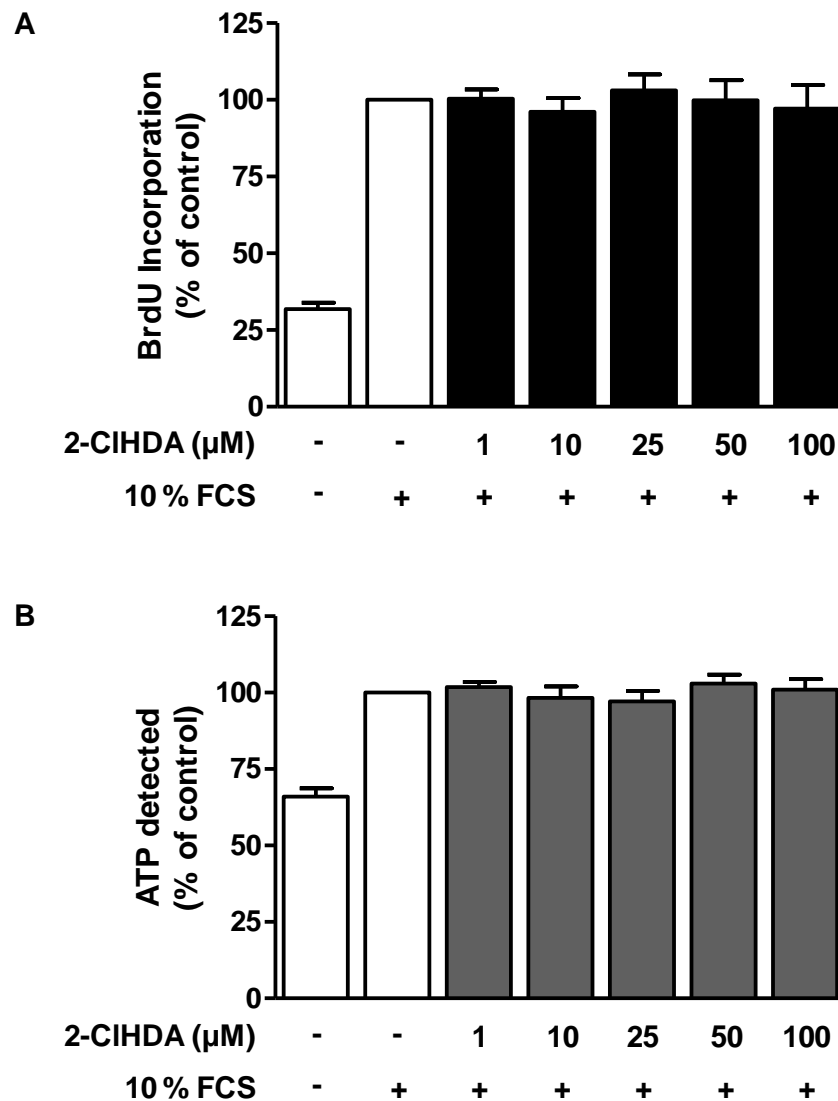


**Figure 3.6 – Effect of 2 hour pretreatment with 2-CIHDA on VSMC proliferation and viability.**

BrdU incorporation (A) and detection of ATP (B) were utilised to measure VSMC proliferation and viability respectively. VSMCs were incubated for 2 hours with increasing concentrations of 2-CIHDA in quiescing media and then stimulated with 10 % FCS for 24 hours with the addition of BrdU in proliferation measurements.  $n = 6$  and performed in triplicate.

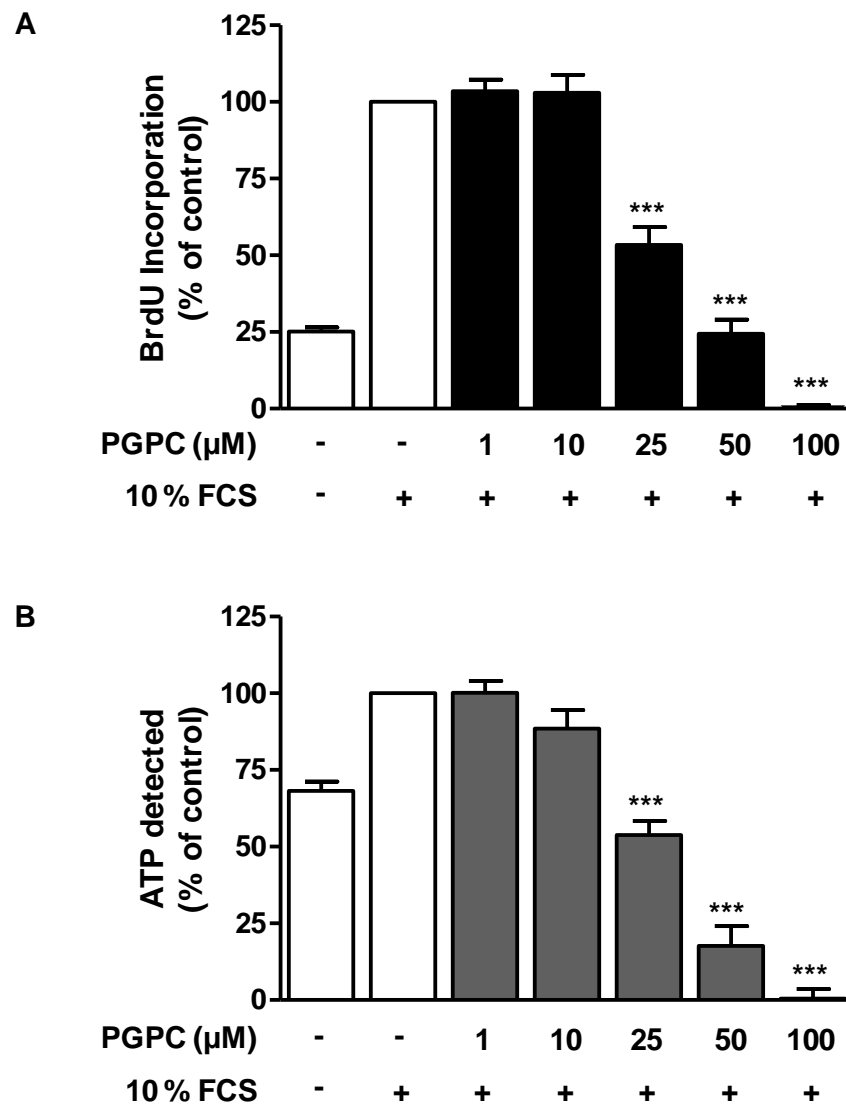


**Figure 3.7 – Effect of 2 hour pretreatment with PGPC on VSMC proliferation and viability.**

BrdU incorporation (A) and detection of ATP (B) were utilised to measure VSMC proliferation and viability respectively. VSMCs were incubated for 2 hours with increasing concentrations of PGPC in quiescing media and then stimulated with 10 % FCS for 24 hours and the addition of BrdU in proliferation measurements. \*\*\* $p < 0.001$  vs 10 % FCS control,  $n = 6$  and performed in triplicate.

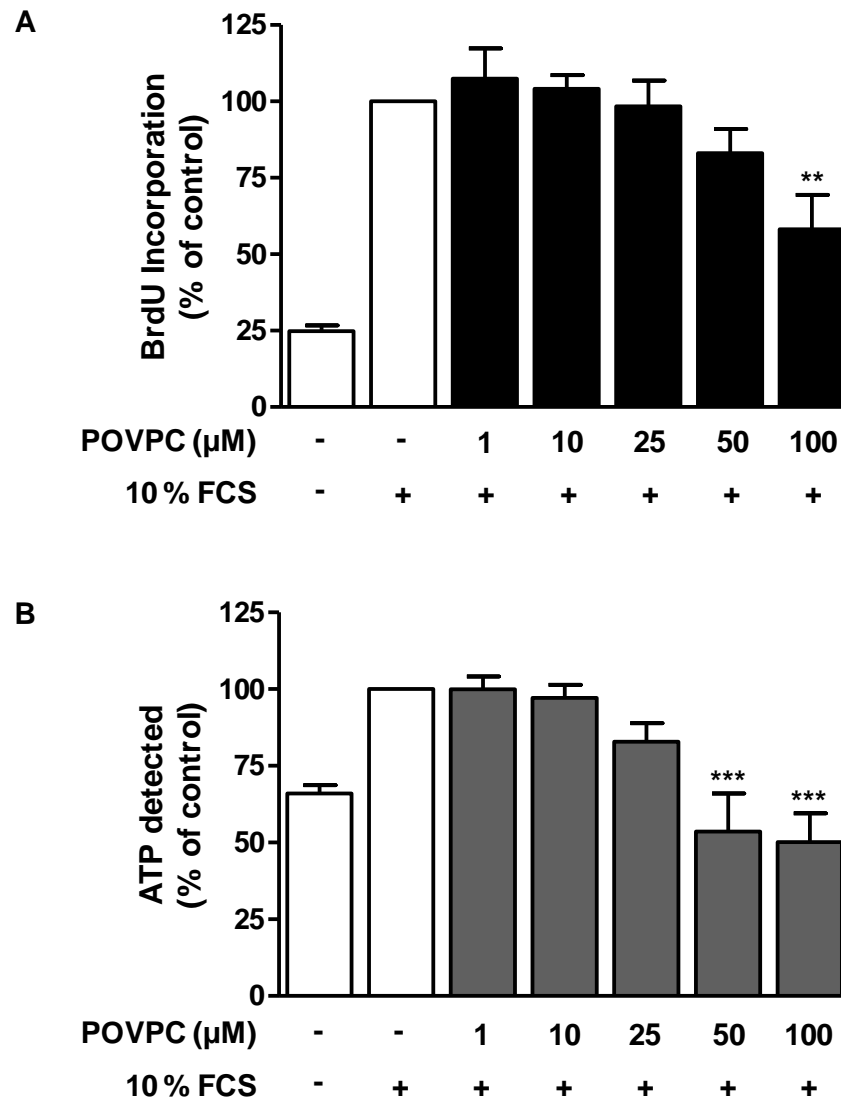


**Figure 3.8 – Effect of 2 hour pretreatment with POVPC on VSMC proliferation and viability.**

BrdU incorporation (A) and detection of ATP (B) were utilised to measure VSMC proliferation and viability respectively. VSMCs were incubated for 2 hours with increasing concentrations of POVPC in quiescing media and then stimulated with 10 % FCS for 24 hours with the addition of BrdU in proliferation measurements. \*\* $p < 0.01$  and \*\*\* $p < 0.001$  vs 10 % FCS control,  $n = 6$  and performed in triplicate.

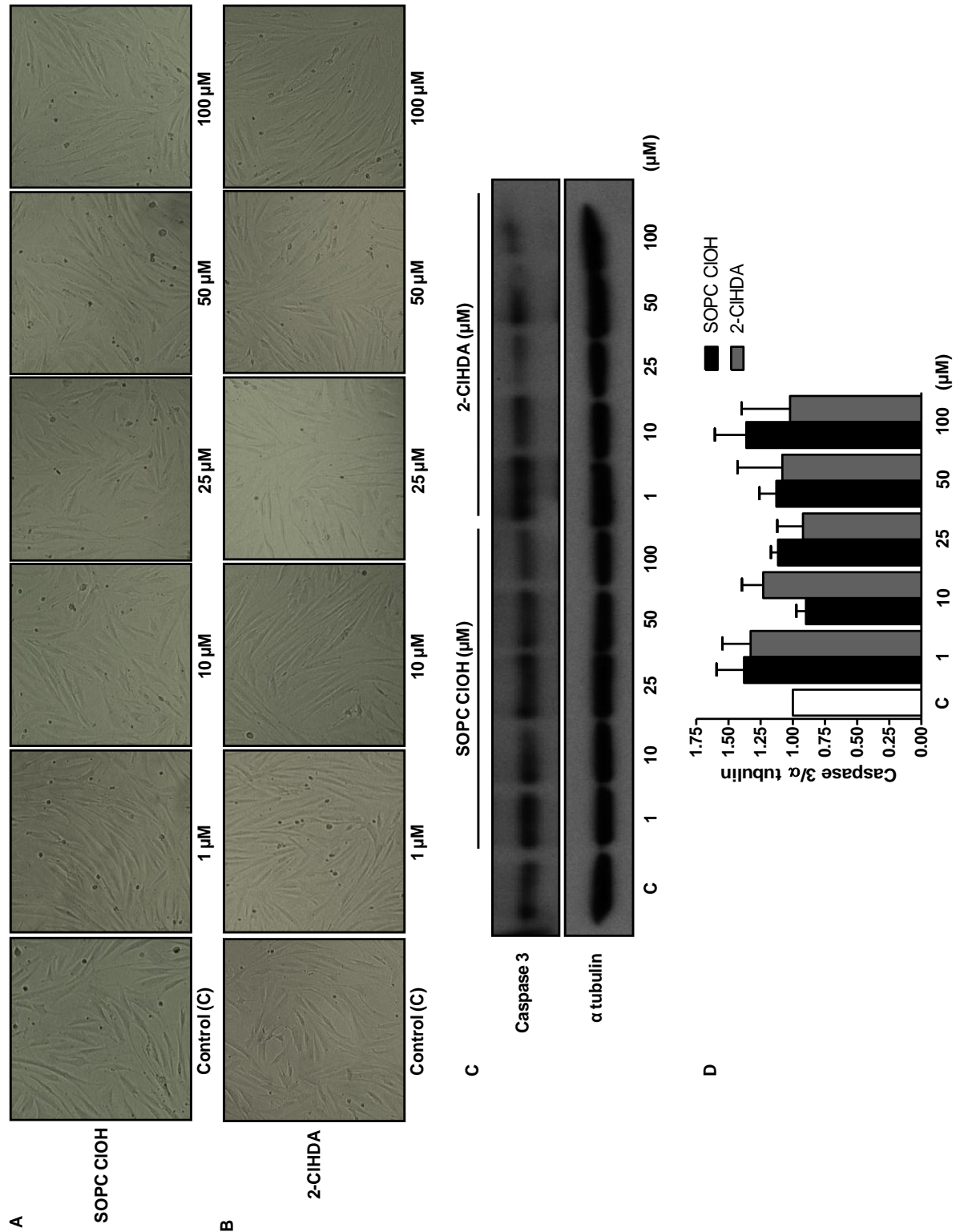


**Figure 3.9 – Effect of 2 hour pretreatment of chlorinated lipids on VSMC morphological changes and caspase 3 expression.**

VSMCs were photographed at 20 x magnification to visualise morphological changes after the cells were treated with SOPC ClOH (A) and 2-ClHDA (B) for 2 hours. Caspase 3 expression (a marker of apoptosis) was investigated after 2 hours incubation with each chlorinated lipid and the graph is expressed as the fold change of caspase 3 divided by α tubulin to adjust for protein loading (D). Blots shown are representative (C). n = 3.

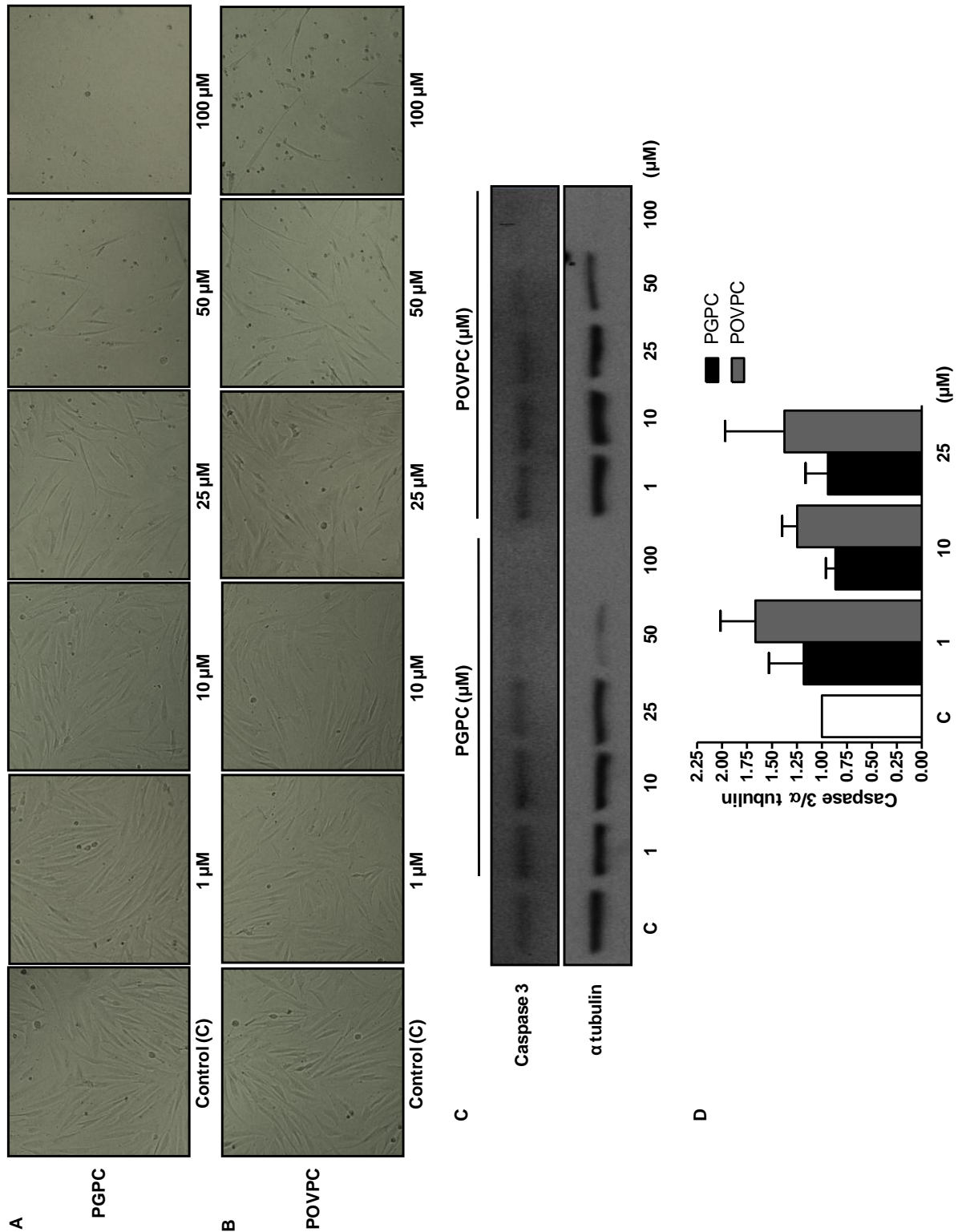


**Figure 3.10 – Effect of 2 hour pretreatment of oxidised lipids on VSMC morphological changes and caspase 3 expression.**

VSMCs were photographed at 20 x magnification to visualise morphological changes after the cells were treated with PGPC (A) and POVPC (B) for 2 hours. Caspase 3 expression (a marker of apoptosis) was investigated after 2 hours incubation with each oxidised lipid and the graph is expressed as the fold change of caspase 3 divided by  $\alpha$  tubulin to adjust for protein loading (D). Blots shown are representative (C).  $n = 3$ .

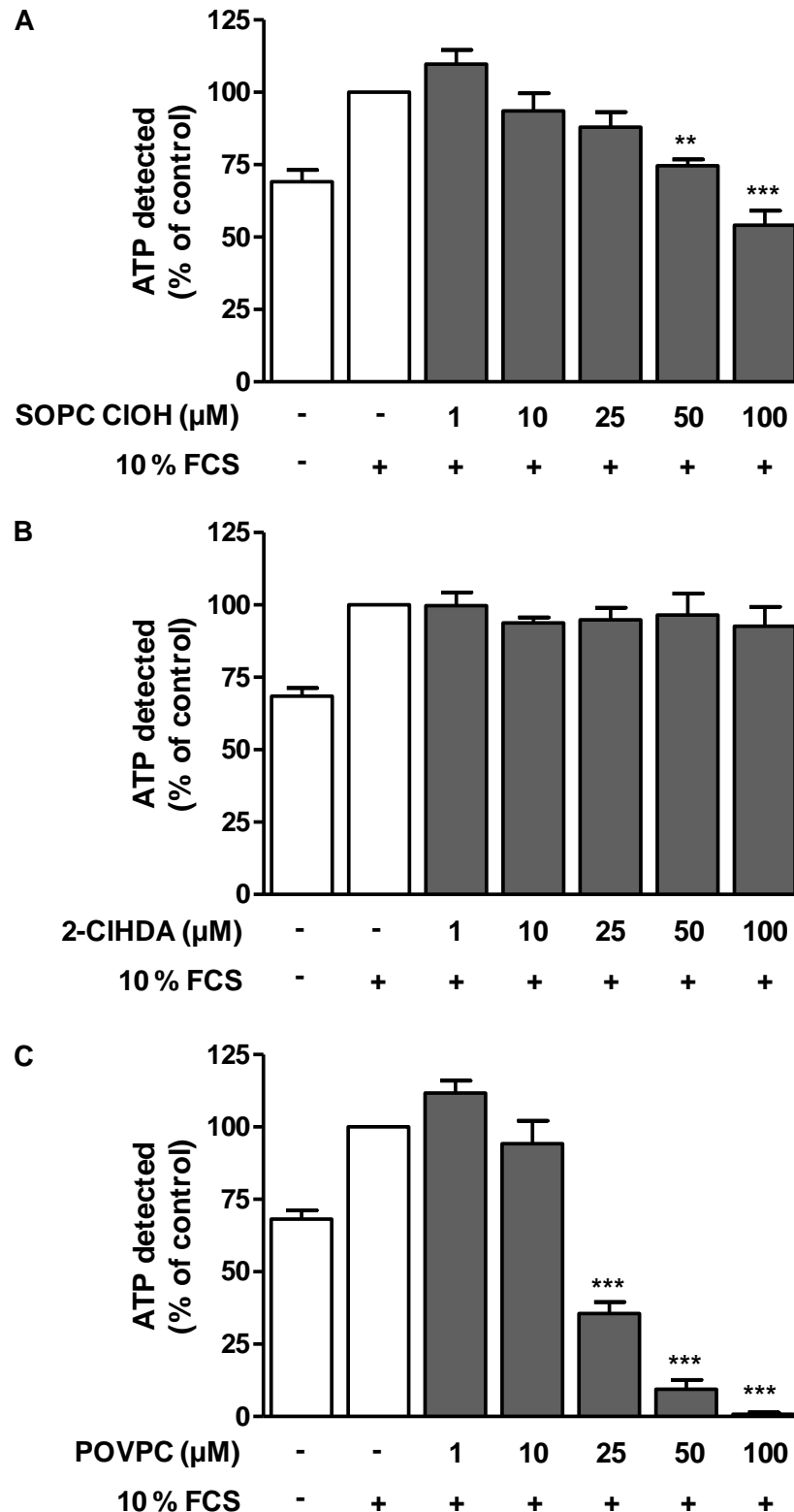


**Figure 3.11 – Effect of 6 hour pretreatment with chlorinated lipids and selected oxidised phospholipid on VSMC viability.**

Increasing concentrations of SPOC ClOH (A), 2-ClHDA (B) and POVPC (C) were incubated for 6 hours in quiescing medium followed by stimulation with 10 % FCS for 24 hours after which detection of ATP was used to measure VSMC viability. \*\* $p < 0.01$  and \*\*\* $p < 0.001$  vs 10 % FCS control,  $n = 3$  and performed in triplicate.

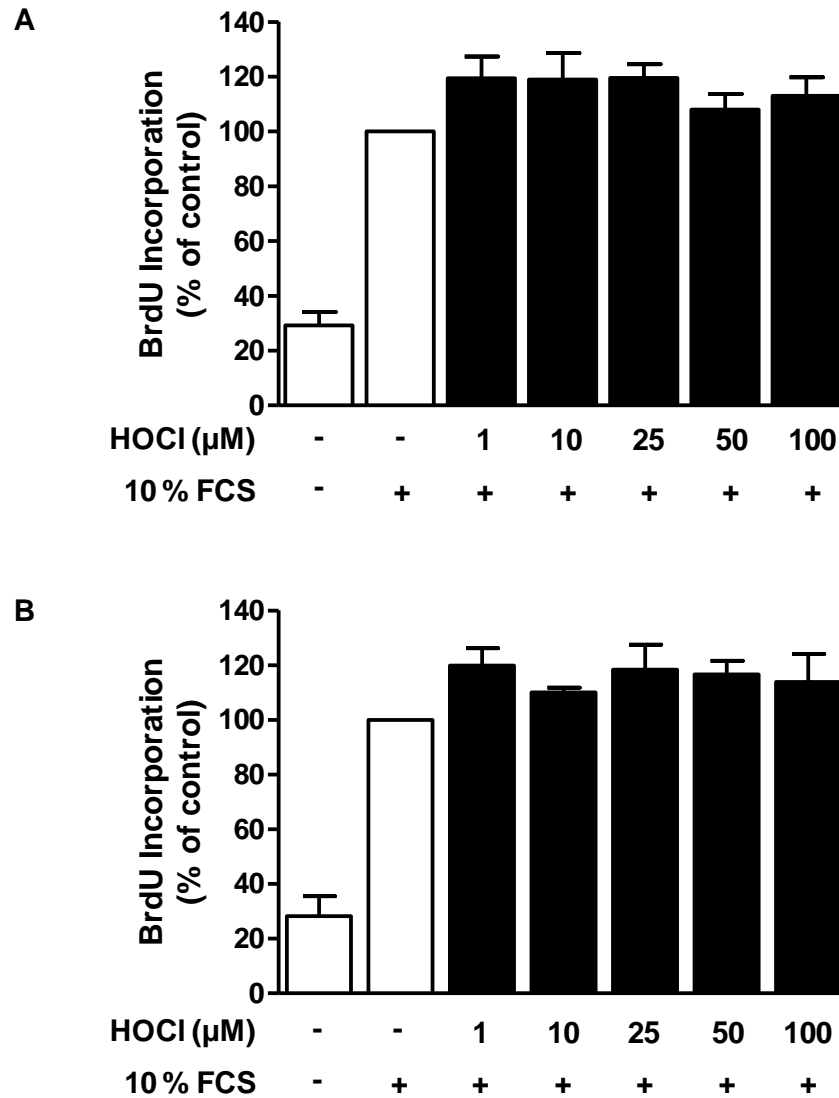


**Figure 3.12 – Effect of HOCl incubation on VSMC proliferation.**

Cells were treated with increasing concentrations of HOCl for either 1 hour (A) or 2 hours (B) then stimulated with 10 % FCS and incubated with BrdU for 24 hours, VSMC proliferation was then measured by the amount of BrdU incorporation.  $n = 4$  and performed in triplicate.

### **3.3.3 Effect of chronic incubation of modified lipids on VSMC proliferation and viability**

The chronic effects of the modified lipids were investigated with the lipids incubated with VSMCs for 24 hours along with stimulation with 10 % FCS (and the addition of BrdU in proliferation experiments).

Chlorinated lipids, either SOPC ClOH (Figure 3.13) or 2-ClHDA (Figure 3.14), incubated for 24 hours had no effect on VSMC proliferation or viability. Chronic treatment with PGPC caused an increase in VSMC proliferation and viability which was in stark contrast to the effects observed with 2 hour pretreatment, with  $155.8 \pm 12.6$  % of viable cells present at 50  $\mu$ M PGPC compared to 10 % FCS control (Figure 3.15). Similarly, the effect of 2 hour incubation was reversed for POVPC as chronic treatment had no effect on VSMC proliferation or viability compared to 10 % FCS control (Figure 3.16).

### **3.3.4 Effect of modified lipids on VSMC migration**

The effect of modified lipids on VSMC migration was also investigated as it is another process critical in vascular remodelling. VSMCs were either pretreated with modified lipid for 2 hours and then migration was assessed in the presence of the chemoattractant, 10 % FCS or VSMCs were incubated with modified lipids during the migration process for 24 hours.

Pretreatment of 2 hours with chlorinated lipids had no effect on FCS-induced VSMC migration (Figure 3.17). The higher concentrations of oxidised phospholipids (50 and 100  $\mu$ M) were discounted due to the high levels of cell death observed in proliferation and viability experiments. No effect was seen after 2 hours incubation of oxidised lipids prior to FCS-induced VSMC migration (Figure 3.18). Chlorinated lipids incubated with VSMCs in the top chamber for 24 hours had no effect on FCS-induced VSMC migration; however an apparent increase was observed at the highest concentrations of SOPC ClOH but this was not significant (Figure 3.19). 24 hour incubation with oxidised phospholipids caused a marked reduction in FCS-induced VSMC migration at the highest concentration with  $48.4 \pm 7.1$  % and  $73.3 \pm 4.4$  % of migrated cells at 100  $\mu$ M PGPC and POVPC respectively (Figure 3.20). A greater effect was again observed with PGPC which was in agreement with the proliferation and viability measurements.

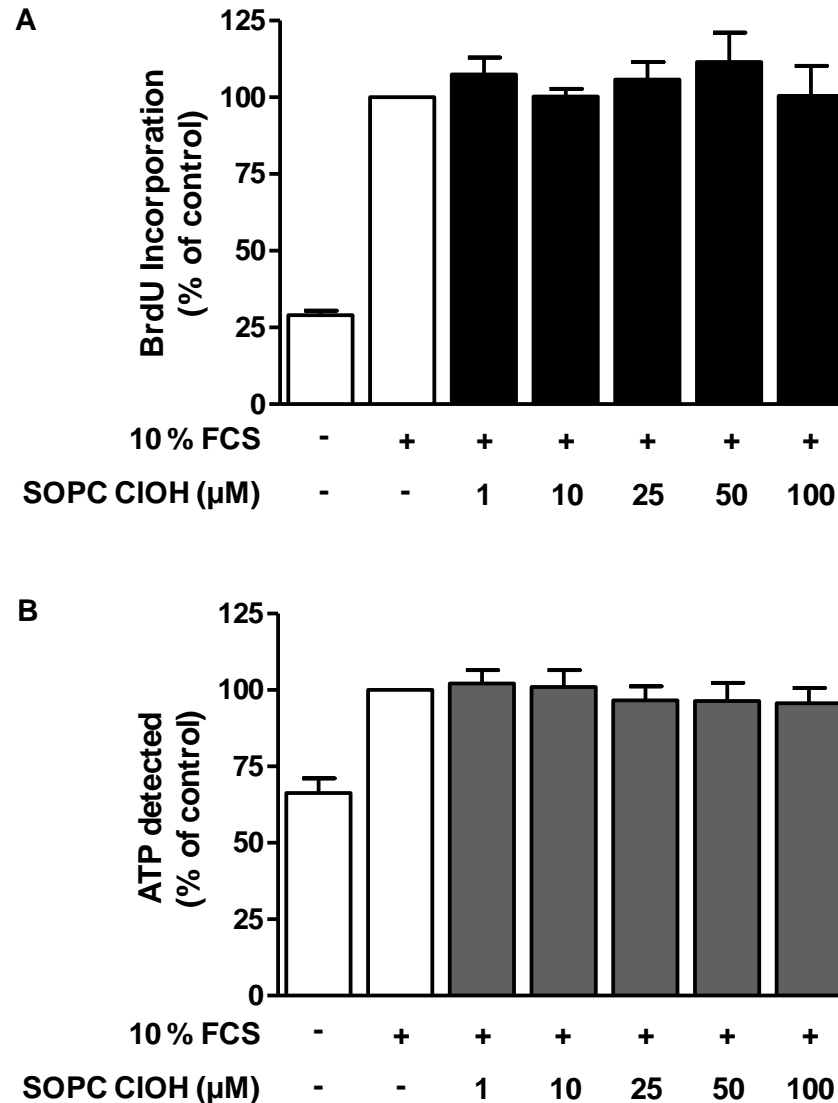


**Figure 3.13 – Effect of chronic treatment of SOPC ClOH on VSMC proliferation and viability.**

BrdU incorporation (A) and detection of ATP (B) were utilised to measure VSMC proliferation and viability respectively. Increasing concentrations of SOPC ClOH were incubated while VSMCs were stimulated with 10 % FCS for 24 hours with addition of BrdU in proliferation measurements.  $n = 4-6$  and performed in triplicate.

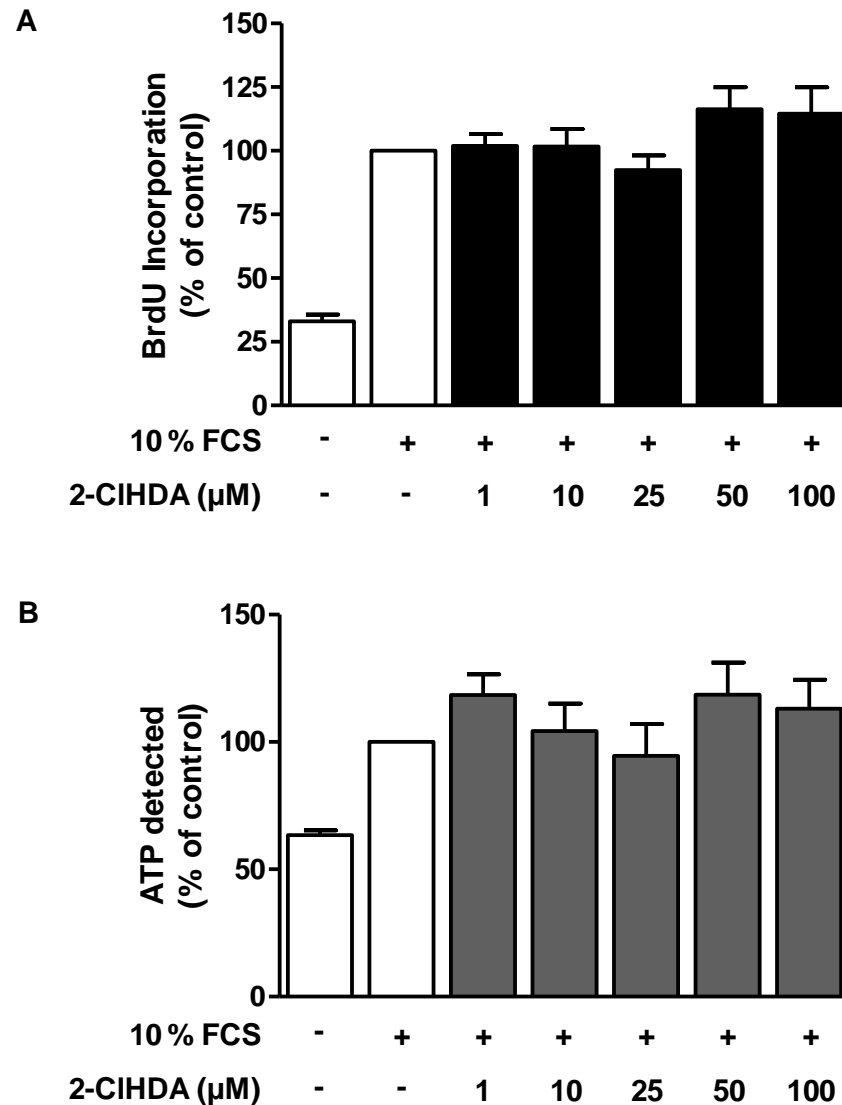


**Figure 3.14 – Effect of chronic treatment of 2-CIHDA on VSMC proliferation and viability.**

BrdU incorporation (A) and detection of ATP (B) were utilised to measure VSMC proliferation and viability respectively. Increasing concentrations of 2-CIHDA were incubated while VSMCs were stimulated with 10 % FCS for 24 hours with the addition of BrdU in proliferation measurements.  $n = 6$  and performed in triplicate.

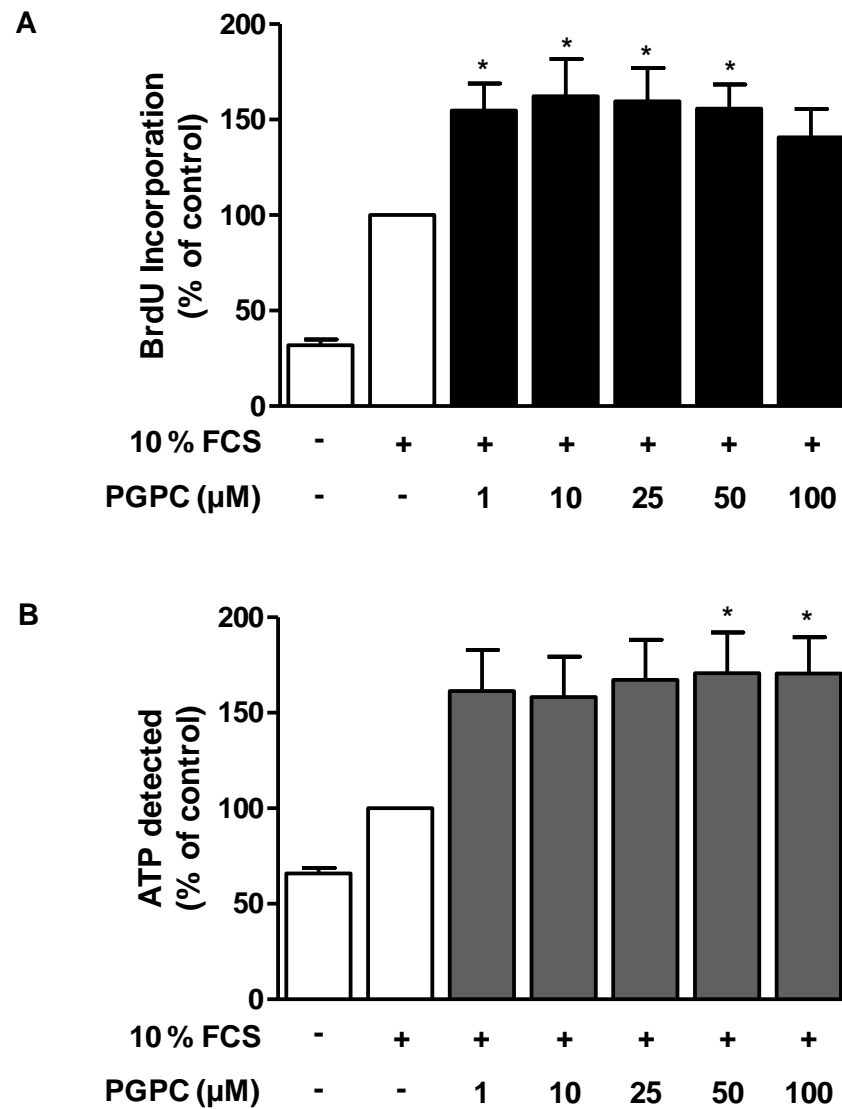


**Figure 3.15 – Effect of chronic treatment of PGPC on VSMC proliferation and viability.**

BrdU incorporation (A) and detection of ATP (B) were utilised to measure VSMC proliferation and viability respectively. Increasing concentrations of PGPC were incubated while VSMCs were stimulated with 10 % FCS for 24 hours with the addition of BrdU in proliferation measurements. \* $p < 0.05$  vs 10 % FCS control,  $n = 6$  and performed in triplicate.

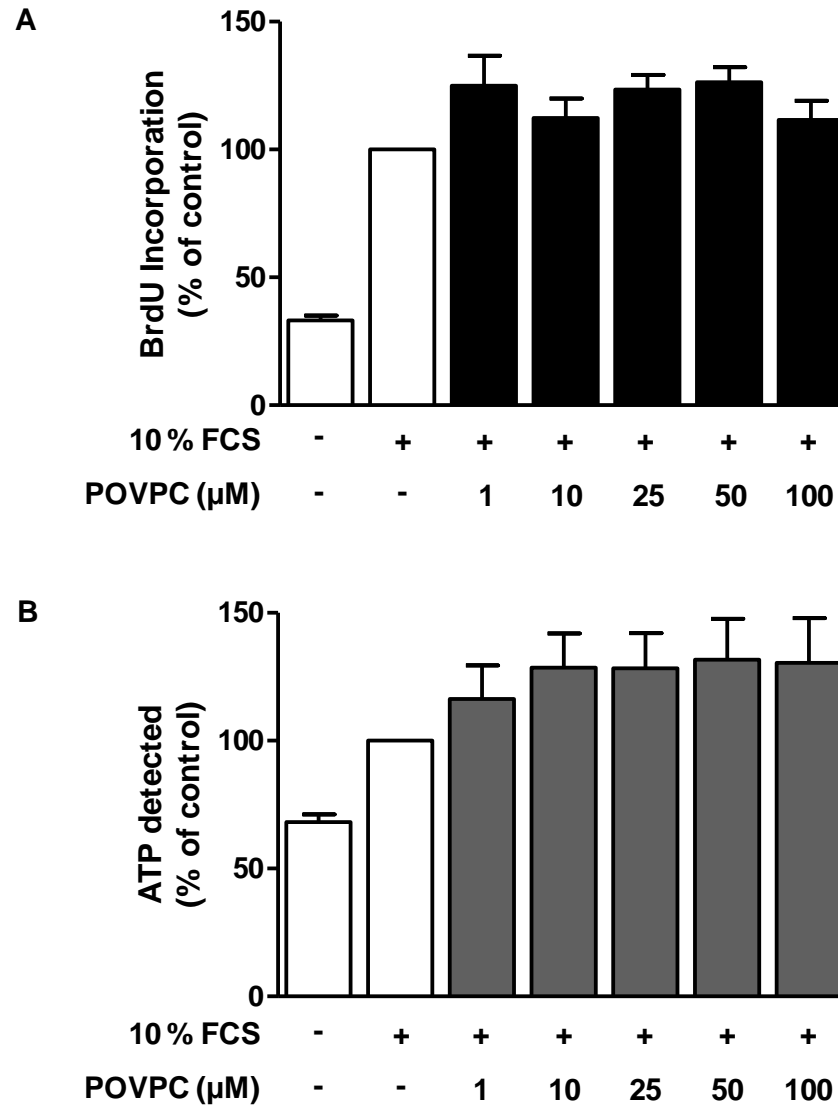


**Figure 3.16 – Effect of chronic treatment of POVPC on VSMC proliferation and viability.**

BrdU incorporation (A) and detection of ATP (B) were utilised to measure VSMC proliferation and viability respectively. Increasing concentrations of POVPC were incubated while VSMCs were stimulated with 10 % FCS for 24 hours with the addition of BrdU in proliferation measurements.  $n = 6$  and performed in triplicate.

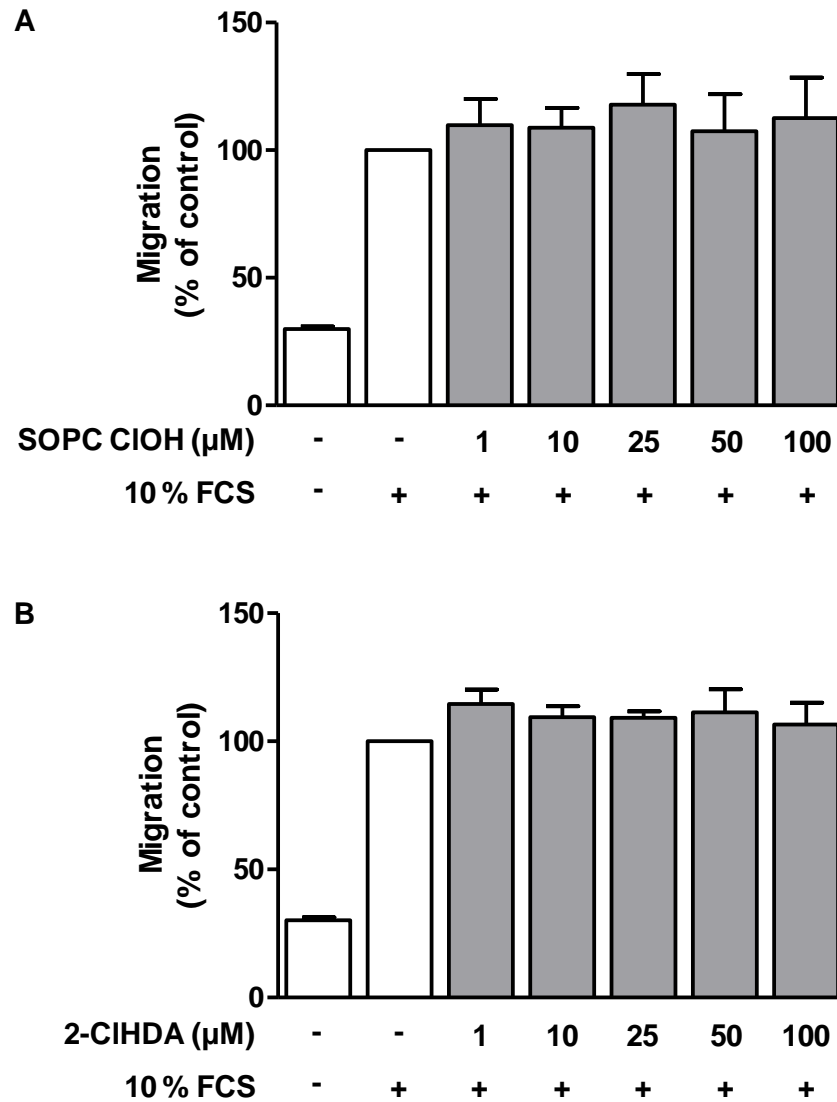


**Figure 3.17 – Effect of prior incubation of chlorinated lipids on FCS-induced VSMC migration.**

Cells incubated with increasing concentrations of SOPC ClOH (A) or 2-ClHDA (B) for 2 hours and then harvested to assess VSMC migration in the presence of the chemoattractant, 10 % FCS, in the bottom chamber of the assay.  $n = 4$ .

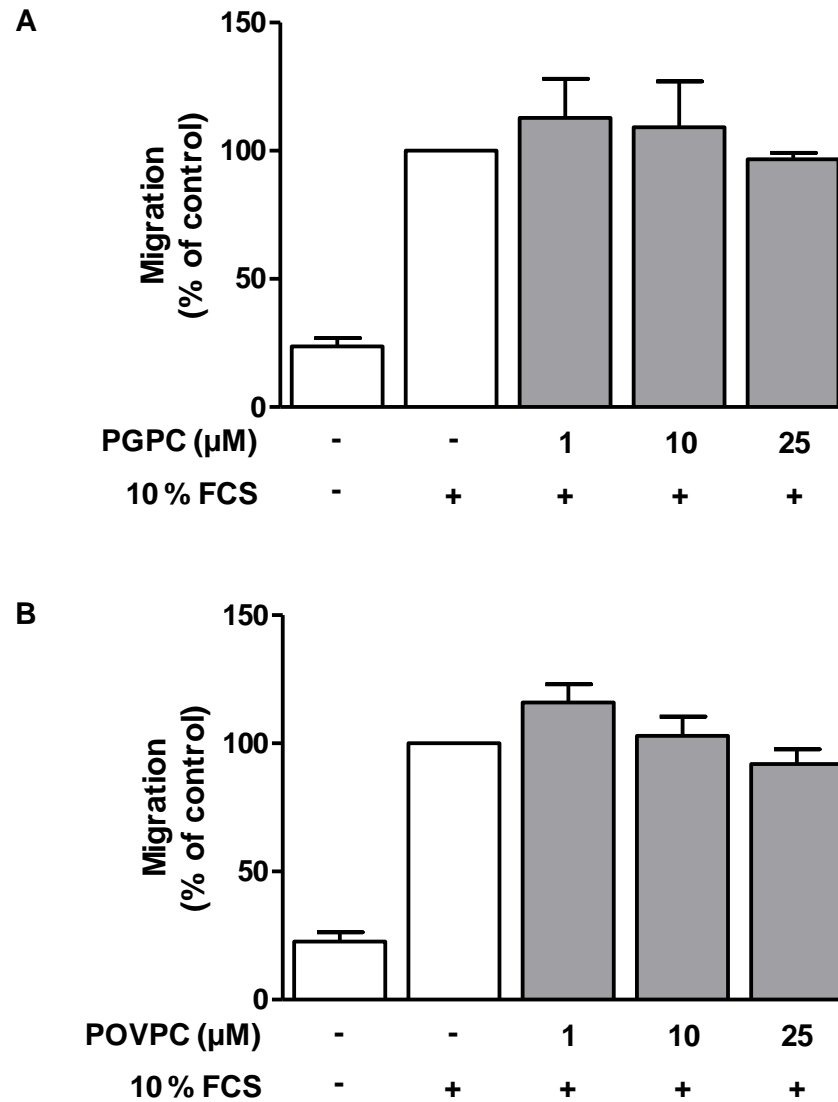


**Figure 3.18 – Effect of prior incubation of oxidised lipids on FCS-induced VSMC migration.**

Cells incubated with increasing concentrations of PGPC (A) or POVPC (B) for 2 hours and then harvested to assess VSMC migration in the presence of the chemoattractant, 10 % FCS, in the bottom chamber of the assay.  $n = 4-5$ .

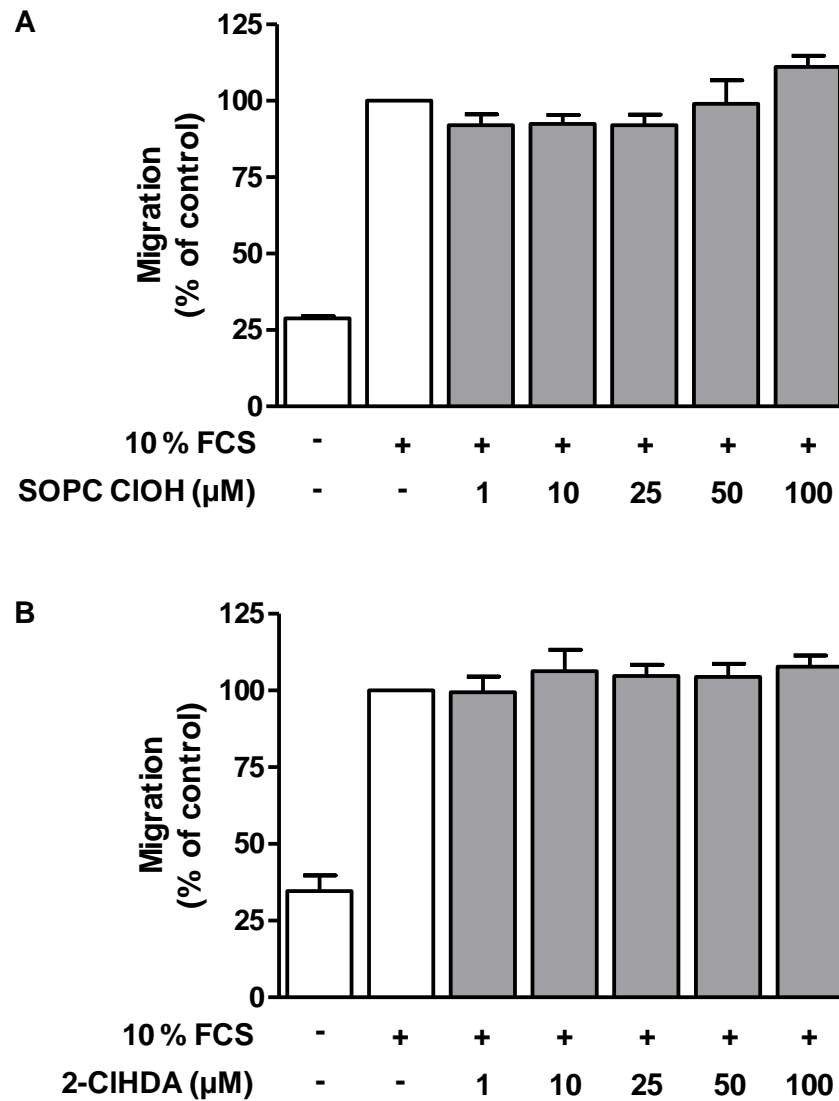


**Figure 3.19 – Effect of incubation of chlorinated lipids during FCS-induced VSMC migration.**

Cells were incubated with increasing concentrations of chlorinated lipids, SOPC ClOH (A) or 2-ClHDA (B), in the top chamber for 24 hours during the migration process induced by the chemoattractant, 10 % FCS, in the bottom chamber of the assay.  $n = 4$ .

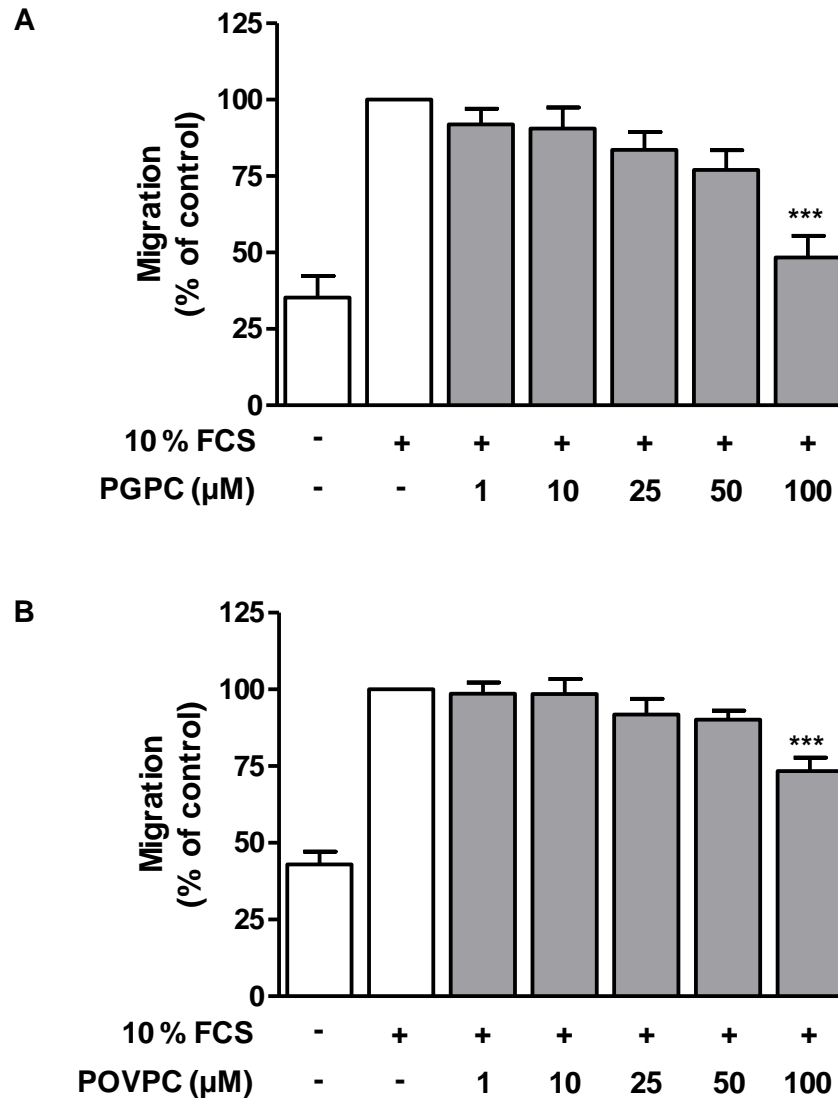


**Figure 3.20 – Effect of incubation of oxidised lipids during FCS-induced VSMC migration.**

Cells were incubated with increasing concentrations of oxidised lipids, PGPC (A) or POVPC (B), in the top chamber for 24 hours during the migration process induced by the chemoattractant, 10 % FCS, in the bottom chamber of the assay. \*\*\* $p < 0.001$  vs 10 % FCS control,  $n = 4$ .

### 3.4 Discussion

The results provided in this study show for the first time the effects of chlorinated lipids on VSMC remodelling processes and highlight the differences between chlorinated and oxidised lipid species. Chlorinated lipids had no effect on VSMC proliferation, viability or migration while oxidised phospholipids caused a concentration-dependent reduction in all of these remodelling processes.

The identification of native phospholipids and their respective chlorohydrins using ESMS in positive-ion mode has been used for a number of years to successfully detect both modified lipids in LDL molecules as well as isolated chlorohydrin preparations (Jerlich *et al.*, 2000, Carr *et al.*, 1996). The addition of standard molecules such as DPPC can be used as an indicator of signal intensity as well as the potential breakdown of chlorohydrins and makes relative quantification of peaks possible (Arnhold *et al.*, 2001). SOPC was selected as an example of the effects of phospholipid chlorohydrins as it is a significant component of LDL and less likely to hydrolyse to its respective lysolipids than other unsaturated species (Dever *et al.*, 2008). Complete conversion to its mono-chlorohydrin was observed with stability over 24 hours which was the longest period of incubation used in cell experiments. This is in agreement with previous studies as SOPC has only one unsaturated bond and therefore one site for chlorination, leading to increased stability in comparison with other phospholipids with multiple adjacent unsaturated bonds (Arnhold *et al.*, 2001, Arnhold *et al.*, 2002). Additionally, a significant reduction in cellular ATP in myeloid cell lines, both monocytes and neutrophils, was observed with SOPC ClOH at a lower concentration (25  $\mu\text{M}$ ) compared with 1-stearoyl-2-arachidonoyl-*sn*-glycero-3-phosphocholine (SAPC) and SLPC ClOH where higher concentrations (50 and 100  $\mu\text{M}$  respectively) were needed to elicit the same response (Dever *et al.*, 2003).

The levels of modified lipids found in pathophysiological conditions have proved hard to quantify with the large number of different structures present and the limited availability of suitable standards. In areas of inflammation such as rheumatoid arthritis, the presence of  $\text{OCl}^-$ , the anion present in  $\text{HOCl}$ , has been found to reach concentrations of up to 300  $\mu\text{M}$ , due to the presence of neutrophils releasing MPO (Katrantzis *et al.*, 1991). The levels of oxidised phospholipids have mainly been measured using mass spectrometry coupled to HPLC for both human and animal samples. In human atherosclerotic plaque samples, POVPC was found between 20 to 40  $\mu\text{g}$  per gram of tissue with slightly higher levels, of between 40 to 100  $\mu\text{g}$  per gram of tissue, being reported in rabbit aorta for POVPC and

PGPC (Ravandi *et al.*, 2004, Watson *et al.*, 1997, Subbanagounder *et al.*, 2000). This suggests that modified lipids are present within in the micromolar range and these concentrations of lipids were utilised for all *in vitro* experiments in this study.

Within this concentration range, the chlorinated lipids used were found to have little to no effect on VSMC proliferation, viability or migration after both incubation times. The only exception was SOPC ClOH which caused a significant reduction in cellular ATP at the highest concentration after 6 hours treatment in quiescing medium. The majority of work published previously has observed toxicity with incubation of chlorohydrins thought to be via disruption of the membrane due to their high polarity (Carr *et al.*, 1997). However, necrotic cell death has also been reported in HUVECs with incubation of halohydrins and an increase in caspase 3 levels suggesting apoptosis has been observed in myeloid cells (Dever *et al.*, 2006, Vissers *et al.*, 2001). Together, this would suggest chlorohydrins could have an effect on intracellular mechanisms rather than just physical disruption of the membrane. This is also highlighted in the time-dependent effects observed with SOPC ClOH incubation (Dever *et al.*, 2003). The lack of cytotoxicity described in this study may be due to the different cell type used, as VSMCs were more resistant to the effects of chlorohydrins than myeloid and endothelial cells. There could also be an effect due to species differences as rabbit VSMCs were used for all *in vitro* experiments and human cells were utilised in the majority of other studies. In contrast to chlorohydrins, very little is known about the actions of alpha-chloro fatty aldehydes as the few studies conducted focussed primarily on endothelial cells. 2-ClHDA was found to inhibit endothelial NO biosynthesis and induce expression of COX-2 in endothelial cells (Marsche *et al.*, 2004, Messner *et al.*, 2008a). 2-ClHDA was thought to be an exciting prospect with the identification of this class of chlorinated lipids in atherosclerotic lesions *in vivo*; however, no effects were observed on the vascular remodelling processes examined in this study.

The direct action of HOCl incubation on VSMCs was also investigated as very low concentrations, in the nanomolar range, have been shown to induce apoptosis in HUVECs (Vissers *et al.*, 1999). Incubation with HOCl in the same concentration range as the modified lipids had no effect on VSMC proliferation after either 1 hour or 2 hours treatment. In contrast, a study investigating a newly identified haem-containing peroxidase, VPO1, reported enhanced VSMC proliferation after 1 hour incubation with 20  $\mu\text{M}$  HOCl (Shi *et al.*, 2011). VPO1 is thought to catalyse the production of HOCl from  $\text{H}_2\text{O}_2$  and chloride similar to the action of MPO (Cheng *et al.*, 2008).

In stark contrast to the effects observed with the chlorinated lipids, oxidised phospholipids caused a dramatic concentration-dependent reduction in VSMC proliferation and viability after 2 hours incubation. The investigation into the mechanism of cell death induced by the oxidised phospholipids proved inconclusive in this study. There was a substantial amount of non-specific binding of the antibodies producing “dirty” blots which was probably due to the antibody used being raised in the same species as the origin of the VSMCs. However, the cell death observed in this study is in agreement with other results after the incubation of oxidised phospholipids. Modified lipids have been found to induce apoptotic signalling pathways by the activation of SMase and, in particular, the acid form of the enzyme which is known to be involved in the earlier stages of apoptosis (Loidl *et al.*, 2003). This leads to the formation of ceramide, a hydrolysis product of SM, which in turn causes the phosphorylation of MAPK and caspase 3 signalling (Loidl *et al.*, 2004). Effects have also been seen *in vivo* with LDLr<sup>-/-</sup> mice crossed with mice deficient in programmed cell death-1 receptor exhibiting a large increase in atherosclerotic plaque size and a change in composition of the lesion containing more macrophages than the LDLr<sup>-/-</sup> control mice (Bu *et al.*, 2011). A biphasic response of oxidised phospholipids has been previously reported with proliferation occurring at low concentration and apoptosis predominating at high concentrations (Auge *et al.*, 2002, Johnstone *et al.*, 2009). The results of this study do not seem to follow this trend; however, with the chronic incubation of oxidised phospholipids in the presence of the growth supplement, FCS, the predominant cell death was abolished and an increase in proliferation was observed. This would suggest that the presence of serum phospholipases causes a breakdown of the detrimental effects of oxidised phospholipids and, in turn, produces a proliferative product. This is in partial agreement with a previous study; however, the antiproliferative nature of the lipids was still seen with the oxidised phospholipid treatment in the presence of FCS (Fruhirth *et al.*, 2006).

Little is known about the effects of modified lipids on VSMC migration, which is another important process in vascular remodelling and central to the restenotic phenotype. POVPC and PGPC have been found to induce VSMC migration and increase the expression of type VIII collagen, important in the composition of ECM in atherosclerotic plaques (Cherepanova *et al.*, 2009). In this study, pretreatment for 2 hours with PGPC and POVPC appeared to have no lasting effects on VSMCs and therefore there was no effect on the FCS-induced migration. However, when VSMC migration was stimulated in the presence of the oxidised phospholipids, a concentration-dependent decrease was observed. The effect seen was markedly less than in the proliferation and viability experiments,

suggesting the migration of VSMCs could be occurring faster than the detrimental action of the oxidised phospholipids. This is consistent with the initial activation of MAPK, occurring within 15 minutes, which is one of the proposed mechanisms of VSMC migration, leading to movement of VSMCs by the action of PDGF, and therefore could be occurring before the effect of the oxidised phospholipids (Nelson *et al.*, 1998).

The greater effect of the oxidised phospholipids, in all cellular experiments and in both treatment conditions, was seen with PGPC rather than POVPC, despite the fact that the latter had previously been suggested to be the more potent of the two truncated oxidation products of PAPC (Fruhworth *et al.*, 2006, Loidl *et al.*, 2003). Hermetter's group have consistently found POVPC to be more apoptogenic than PGPC, which is thought to be due to its aldehyde moiety compared with the carboxylic acid functional group found on PGPC. Using fluorescently labelled analogues of PGPC and POVPC, the phospholipids were found to localise in separate compartments of the VSMCs with PGPC located in lysosomes while POVPC formed covalent adducts with the plasma membrane (Moumtzi *et al.*, 2007). However, recently this group have reported a higher toxicity with PGPC in cultured macrophages believed to be due to more efficient membrane blebbing in apoptotic cells (Stemmer *et al.*, 2012). As oxLDL is very heterogeneous in its composition, it is useful to characterise its effects by using individual lipids in order to attribute the effects seen to each component.

Previous studies have found apoptosis to peak at about 24 hours after vascular injury while proliferation occurs later in the process, at around 4 days after injury (Yang *et al.*, 2006, Matter *et al.*, 2006). This correlates with the oxidised phospholipid data described in this study, where VSMC death was induced after a short incubation time of only 2 hours. Modified lipids could also be involved in the latter proliferative stages of vascular injury leading to the formation of neointima; however, this would be difficult to measure *in vitro*. Longer incubations with modified lipids would not be possible in quiescing medium, and incubating VSMCs with medium containing growth supplements such as FCS along with modified lipids would lead to the breakdown of these lipids by serum phospholipases (Fruhworth *et al.*, 2006). This is a key limitation of the *in vitro* VSMC model as effects of longer incubations in quiescing medium with modified lipids could not be attributed solely to the lipids because, in absence of growth supplements, the cells would likely induce programmed cell death processes due to the lack of available nutrients. The different classes of modified lipids may also have different durations of action and be involved in different cell processes for example; the oxidised phospholipids could participate in the

primary effects seen while chlorinated lipids could be involved in the later stages. PGPC could be involved in the early cell death as it induces substantial death after 2 hours in the *in vitro* experiments. This effect could be followed by the action of POVPC as the level of cell death observed was significantly increased after 6 hours incubation compared to 2 hours. SOPC CIOH and other chlorohydrins may be involved in the last stage of cell death, as a significant reduction in cell death was witnessed after 6 hours treatment at the higher concentrations. This would suggest a cumulative effect of the modified lipids inducing cell death which is one of the first processes seen after vascular injury and in the formation of neointima. *In vivo* analysis of injured or atherosclerotic vessels could provide a better insight into the actions of these different classes of modified lipids on important cellular processes involved in vascular remodelling.

### 3.5 Conclusions

In summary, both chlorinated species, chlorohydrins and alpha-chloro fatty aldehydes, had little to no effect on rabbit VSMC proliferation, viability or migration except that SOPC CIOH induced a concentration-dependent depletion of cellular ATP after a prolonged incubation of 6 hours. In contrast, the truncated oxidation products of PAPC, PGPC and POVPC, caused a large concentration-dependent reduction in VSMC proliferation, migration and cellular ATP with the greater effect seen with PGPC. The effects reported were further enhanced by a longer treatment time with POVPC, which is thought to operate through apoptotic signalling pathways. This is the first study to investigate the effects of chlorinated lipids on VSMC processes; these processes being essential in vascular remodelling. This study also highlights the divergent effects of different classes of modified lipids which are all known components of modified LDL and therefore critical in atherosclerosis progression.

**CHAPTER 4**

**THE IMPACT OF AMPK  
SIGNALLING ON THE EFFECTS OF  
MODIFIED LIPIDS IN VSM**

## 4.1 Introduction

AMPK is a key regulator of energy homeostasis and is commonly referred to as a cellular “fuel gauge” (Hardie and Carling, 1997). It is a highly conserved heterotrimeric complex consisting of a catalytic  $\alpha$  subunit and two regulatory subunits;  $\beta$  and  $\gamma$ , with each having two or more isoforms that are expressed in different cell and tissue types (Davies *et al.*, 1994, Stapleton *et al.*, 1994). Activation of AMPK occurs via phosphorylation of the threonine residue at position 172 in the activation loop of the catalytic  $\alpha$  domain (Hawley *et al.*, 1996). AMPK can only become activated when the regulatory subunits undergo conformational change to expose the catalytic site. The regulatory  $\gamma$  subunits contain areas termed “Bateman domains” with the capacity to bind one molecule of either AMP or ATP (Bateman, 1997, Cheung *et al.*, 2000, Scott *et al.*, 2004). In well energised cells, ATP is bound to AMPK, which keeps it in an inactive locked state. In situations where there is a depletion of ATP and an elevation of AMP, such as during periods of cellular stress, hypoxia or glucose deprivation, AMP displaces ATP leading to the phosphorylation of AMPK at the threonine residue. Furthermore, AMPK activity can be modulated by pharmacological agents such as AICAR which mimics the action of AMP. AICAR is transported into the cell via the adenosine transporter where it is phosphorylated to form the AMP analogue, ZMP (Merrill *et al.*, 1997). Another agent, A-769662 is an extremely potent AMPK activator which directly stimulates AMPK by mimicking the effects of AMP as well as inhibiting enzyme de-phosphorylation (Göransson *et al.*, 2007). AMPK signalling directly regulates a number of enzymes involved in energy consumption within the cell. AMPK can correct the energy imbalance by inhibiting ATP-consuming events such as fatty acid and cholesterol biosynthesis by directly phosphorylating the enzymes responsible: ACC and HMG-CoA reductase respectively, leading to the inhibition of enzyme activity.

AMPK has been implicated in CVD including atherosclerosis where AMPK activation has found to be beneficial in altering the inflammatory response as it reduces leukocyte adhesion to human aortic endothelial cells and alleviates atherosclerosis in ApoE<sup>-/-</sup> mice *in vivo* (Ewart *et al.*, 2008, Li *et al.*, 2010a). VSMCs are also critical in the progression of atherosclerosis with AMPK activation by AICAR found to inhibit human and rat aortic VSMC proliferation and migration, induced by both FCS and PDGF (Igata *et al.*, 2005, Peyton *et al.*, 2011). Angiotensin II-stimulated rat VSMC proliferation was also inhibited when AMPK is activated by AICAR (Nagata *et al.*, 2004). Furthermore, AMPK activation reduces oxLDL-induced macrophage proliferation and oxLDL-induced ER stress *in vivo*

(Ishii *et al.*, 2009, Dong *et al.*, 2010). Chlorinated and oxidised lipids are critical in the progression of atherosclerosis and previously shown to induce apoptosis in both vascular and myeloid cells (Vissers *et al.*, 2001, Dever *et al.*, 2003, Fruhwirth *et al.*, 2006, Johnstone *et al.*, 2009). Whereas, AMPK activation has been found to exert anti-apoptotic effects in a number of cell types including endothelial cells (Ido *et al.*, 2002, Kim *et al.*, 2008, Liu *et al.*, 2010). To date nothing is known about how AMPK signalling could modulate the effects of the individual chlorinated and oxidised lipids used in this thesis within VSMCs. Understanding these pathways better may improve the understanding of how these modified lipids are important in the progression of atherosclerosis.

Furthermore, AMPK has been found to have an effect on vascular reactivity affecting both endothelial and VSM function. AICAR induced vasorelaxation in mouse aortic rings, both in endothelium-intact and -denuded vessels, and was abolished in AMPK $\alpha$ 1<sup>-/-</sup> mice suggesting AMPK $\alpha$ 1 in VSM was responsible for this action (Goirand *et al.*, 2007). Vasorelaxation to AICAR was also enhanced in spontaneously hypertensive rats compared to their normotensive controls and this effect was thought to be NO-dependent (Ford and Rush, 2011). Due to the vascular remodelling which occurs as a result of atherosclerosis, the relaxant properties of VSM may be impaired. OxLDL has been found to reduce endothelium-dependent relaxation to acetylcholine in rabbit aorta and coronary arteries by affecting the vasodilator function (Simon *et al.*, 1990, Buckley *et al.*, 1996). Together, this suggests there could be a dysregulation of AMPK signalling in vascular disease with little known to date about the influence of AMPK in modulating the effects of modified lipids in VSM.

### **4.1.1 Aims**

The aims investigated in this chapter were:

- To examine the effect of AMPK activation or inhibition on VSMC proliferation, viability and protein expression.
- To investigate the interaction of AMPK signalling and modified lipids on VSMC proliferation, viability and protein expression.
- To determine the effect of modified lipid incubation on AICAR-induced relaxation in VSM.

## 4.2 Methods

### 4.2.1 Smooth muscle proliferation

A schematic diagram displaying the experimental protocol for all VSMCs experiments is shown in Figure 4.1. Cell proliferation was assessed by determining the incorporation of BrdU into newly synthesised DNA using an ELISA kit (as detailed in Section 2.3.3). In control experiments, the AMPK activator, 6,7-dihydro-4-hydroxy-3-(2'-hydroxy[1,1'-biphenyl]-4-yl)-6-oxo-thieno[2,3-*b*]pyridine-5-carbonitrile (A-769662, Tocris Bioscience, Bristol, U.K.) or the AMPK inhibitor, 6-[4-(2-piperidin-1-yl-ethoxy)-phenyl]-3-pyridin-4-yl-pyrazolo[1,5-*a*]-pyrimidine (Compound C, Sigma Aldrich, Poole, U.K.) were incubated separately for 45 and 30 minutes respectively prior to stimulation with 10 % FCS and the addition of BrdU for 24 hours at 37 °C. VSMCs were also pretreated with A-769662 and Compound C followed by incubation with modified lipids in the range of 1 to 100 µM for 2 hours prior to stimulation with 10 % FCS and the addition of BrdU for 24 hours at 37 °C.

### 4.2.2 Smooth muscle viability

Cell viability was measured by the bioluminescent detection of cellular ATP (described in Section 2.3.4). Similar to proliferation experiments, A-769662 and Compound C were incubated for 45 and 30 minutes respectively prior to stimulation with 10 % FCS for 24 hours at 37 °C. VSMCs were pretreated with A-769662 and Compound C (45 and 30 minutes respectively) followed by incubation with modified lipids in the range of 1 to 100 µM for 2 hours prior to stimulation with 10 % FCS for 24 hours at 37 °C.

### 4.2.3 Western blotting

Expression of AMPK $\alpha$  and ACC was measured by Western blot analysis as detailed in Section 2.4. VSMCs were seeded in 6 well plates and grown to 80 % confluency before quiescing in 0.1 % FCS for 24 hours. Cells were incubated with A-769662, Compound C or 25 µM of the modified lipids for 45 minutes, 30 minutes or 2 hours respectively. Cells were also pretreated with A-769662 or Compound C prior to the incubation of modified lipids for 2 hours. Following exposure to the different reagents, VSMC lysates were prepared and protein estimation analysis was carried out with the addition of 10 µg of protein per well. Immunoblotting was then performed with antibodies against AMPK $\alpha$ , ACC and the loading control, GAPDH (all antibody dilutions found in Table 2.1) then densitometrical analysis was performed.

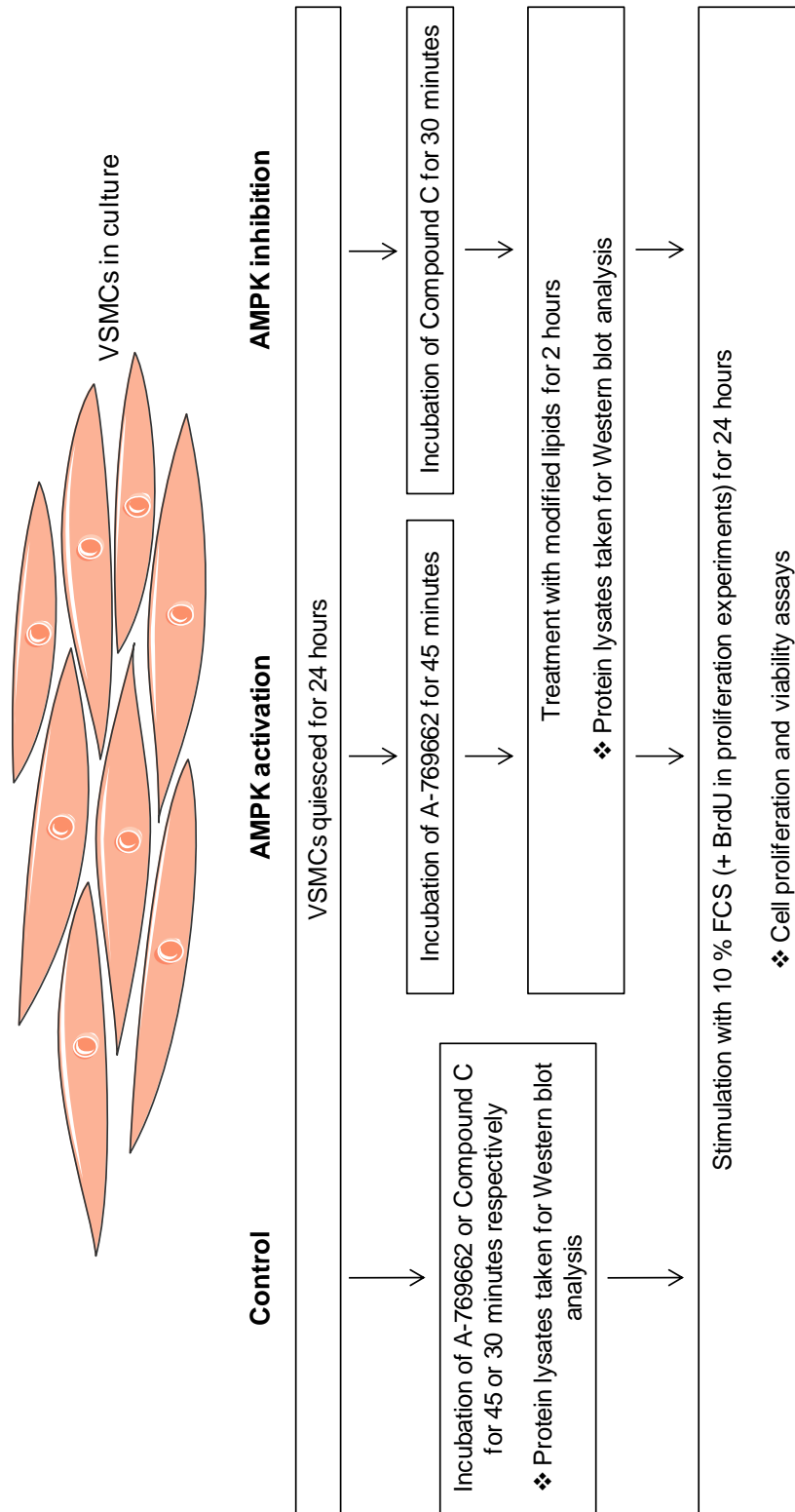


**Figure 4.1 – Schematic diagram of *in vitro* VSMC experiments for AMPK activation or inhibition prior to modified lipid incubation.**

Rabbit aortic VSMCs were treated with AMPK activator, A-769662 or AMPK inhibitor, Compound C for 45 or 30 minutes respectively, followed by the modified lipid treatment for 2 hours in quiescing medium. Bullet point represents point at which the experiment was performed.

#### 4.2.4 Small vessel wire myography

Mouse carotid arteries were cut into 2 mm segments and mounted on two 40  $\mu\text{m}$  diameter wires in a small artery wire myograph as detailed in Section 2.5. Arterial rings were maintained in Krebs' solution at 37 °C and gassed continuously with 95 %  $\text{O}_2$  and 5 %  $\text{CO}_2$ . Following a 30 minute equilibration period, the vessels were set to a predetermined optimal tension of 0.25 g. Viability of arterial segments was measured with 40 mM KCl. Following this, the vessels were washed and incubated with either 25  $\mu\text{M}$  of the modified lipid or vehicle for 30 minutes and then pre-constricted with U46619 for a further 30 minutes. A cumulative concentration-response curve to AICAR was then performed at a concentration range from  $1 \times 10^{-4}$  M to  $1 \times 10^{-2}$  M at 10 minute intervals (Figure 4.2).

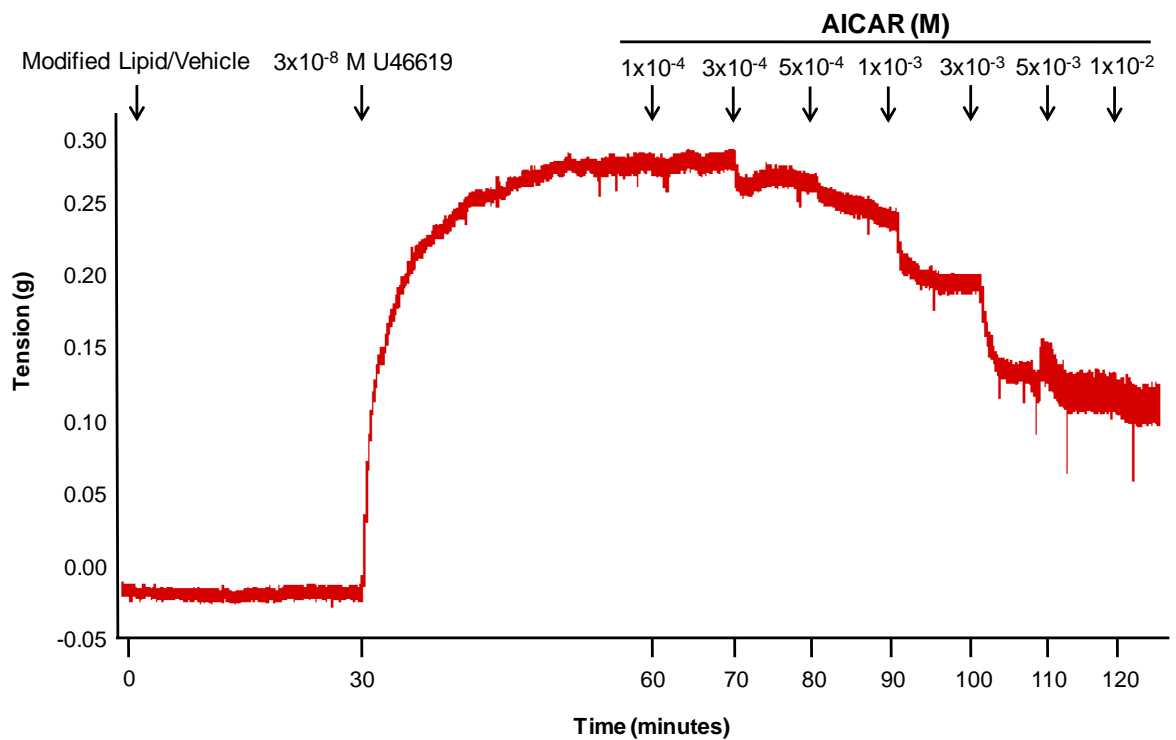


**Figure 4.2 – Representative myography recording for AICAR-induced relaxation.**

Mouse carotid arteries were incubated either in the presence or absence of modified lipids at 25  $\mu\text{M}$  for 30 minutes. The vessels were then contracted to U46619 for a further 30 minutes. AMPK activator, AICAR, was then added at 10 minute intervals at increasing concentrations from  $1 \times 10^{-4}$  to  $1 \times 10^{-2}$  M.

### **4.2.5 Statistical analysis**

All results are presented as mean  $\pm$  SEM and n represents the number of independent experiments performed. Data were analysed using a one-way ANOVA followed by either a Dunnett's post hoc test for control experiments or a Newman-Keuls' post hoc test for Western blotting analysis, a two-way ANOVA for comparison of AMPK treatment and modified lipids with modified lipids alone and for comparison of the cumulative concentration response curves to AICAR, and a paired Student's t-test for the U46619 contraction.

## 4.3 Results

### 4.3.1 Effect of AMPK activation or inhibition in VSMCs

The effects of AMPK activator, A-769662 and inhibitor, Compound C on VSMC proliferation and viability were investigated in VSMCs by incubating for 45 and 30 minutes respectively (Figure 4.3). Vehicle treatment (1 % (v/v) DMSO) in quiescing medium had no effect on either VSMC proliferation or viability. AMPK activation with A-769662 for 45 minutes prior to stimulation with 10 % FCS had no effect on either VSMC proliferation or viability. However, Compound C alone caused an inhibition of proliferation at 40  $\mu$ M with only  $16.4 \pm 7.2$  % proliferating cells but had no effect on viability with  $81.2 \pm 9.2$  % of viable cells present. In contrast, at 100  $\mu$ M, Compound C appeared to have toxic effects with only  $0.9 \pm 0.9$  % of proliferating cells and  $3.0 \pm 1.2$  % of viable cells present.

The effects of 10  $\mu$ M of AMPK activator, A-769662 and inhibitor, Compound C on expression of phosphorylated and total AMPK $\alpha$  and its downstream target, ACC by immunoblotting were next investigated. Inhibition of AMPK with Compound C was also investigated by treatment for 30 minutes prior to the AMPK activators, A-769662 or AICAR. Graphs are expressed as the fold change of the phosphorylated form of the enzyme over the total amount giving an indication of activity of either enzyme (Figure 4.4). Phosphorylation of ACC causes enzyme inhibition, thus limiting the pathway to fatty acid synthesis. Vehicle treatment (1 % DMSO) in quiescing medium had no effect on either AMPK $\alpha$  or ACC phosphorylation in VSMCs. There was also no effect on AMPK $\alpha$  observed after incubation with any of the AMPK activators or the inhibitor. In contrast, changes in relative expression of ACC were seen following incubations with A-769662 and in the presence of Compound C. A-769662 caused about a 2-fold increase in the ratio of ACC compared to the control while Compound C pretreatment did not affect this increase. AMPK inhibition by Compound C alone had no effect on the relative ACC expression but significantly reduced the relative ratio of ACC in comparison to the phosphorylation induced by A-769662. Similarly, AMPK inhibition prior to AMPK activation by AICAR caused a significant reduction in the relative ACC expression compared to the same conditions with A-769662. The concentration selected for all subsequent VSMC experiments was 10  $\mu$ M for both agents as A-769662 and Compound C induced an activation or inhibition of AMPK respectively but had no effect alone on VSMC proliferation and viability at this concentration.

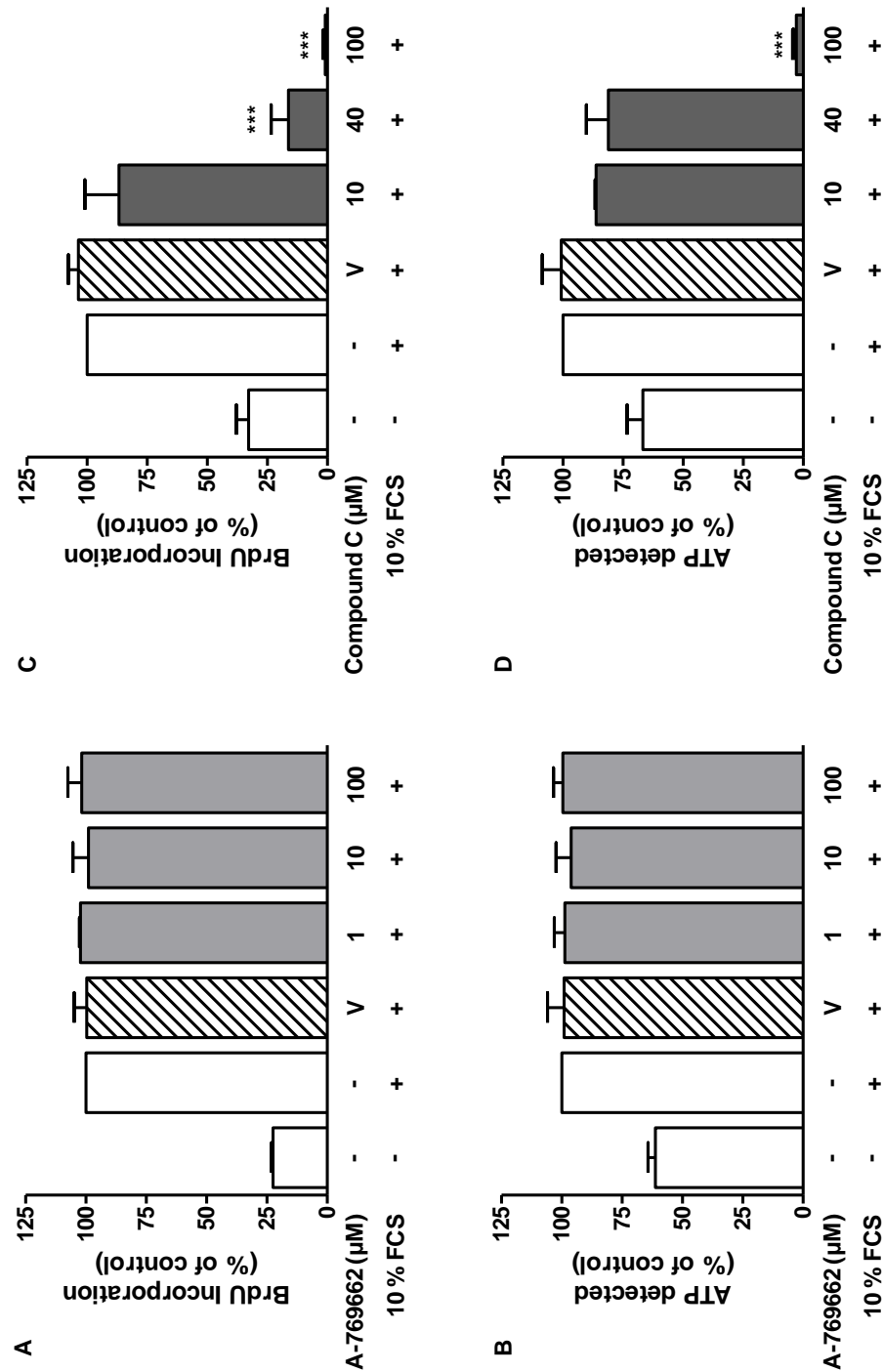


**Figure 4.3 – Effect of AMPK activation or inhibition on VSMC proliferation and viability.**

BrdU incorporation (A and C) and detection of ATP (B and D) were utilised to measure VSMC proliferation and viability respectively. Increasing concentrations of AMPK activator, A-769662 (A and B) and inhibitor, Compound C (B and D) were incubated for 45 and 30 minutes respectively and then stimulated with 10 % FCS for 24 hours. V = vehicle (1 % DMSO in quiescing medium). \*\*\*p<0.001 vs 10 % FCS control, n = 3 and performed in triplicate.

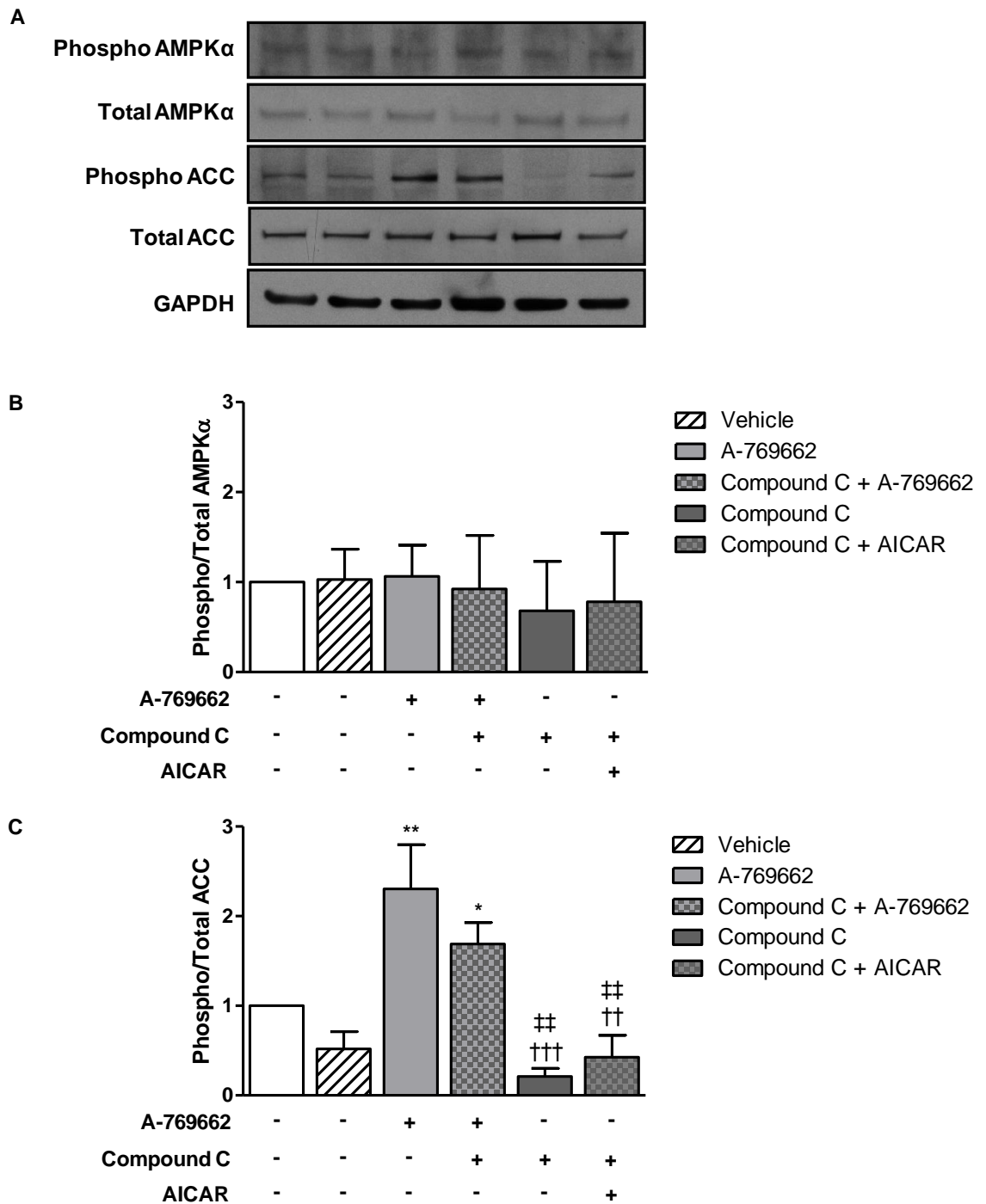


**Figure 4.4 – Effect of AMPK activators and inhibitors on AMPK $\alpha$  and ACC expression in VSMCs.**

VSMCs were incubated with vehicle of 1 % DMSO, AMPK activator, A-769662 (10  $\mu$ M) or AMPK inhibitor, Compound C (10  $\mu$ M) for 45 and 30 minutes respectively. Compound C was also incubated for 30 minutes prior to incubation with AMPK activators, A-769662 or AICAR. Graphs are expressed as the fold change of the phosphorylated form of each enzyme divided by the total amount of AMPK $\alpha$  (B) and ACC (C) to measure the activation of the enzyme. Blots shown are representative (A). \* $p$ <0.05 and \*\* $p$ <0.01 vs control, †† $p$ <0.01 and ††† $p$ <0.001 vs A-769662, †† $p$ <0.01 vs Compound C + A-769662,  $n$  = 3.

### **4.3.2 Effect of AMPK activation or inhibition prior to modified lipid treatment on VSMC proliferation and viability**

To determine if AMPK activation or inhibition prior to incubation of modified lipids could modulate the effects witnessed in VSMCs in Chapter 3, the effect of activation of AMPK by A-769662 or inhibition with Compound C prior to modified lipid treatment was investigated. In all experiments, a concentration of 25  $\mu$ M was selected for each of the modified lipids as it caused biological effects whilst retaining cell viability (described fully in Chapter 3). The effects of the full range of concentrations of both chlorinated and oxidised lipids after AMPK activation or inhibition are presented in Table 4.1 and 4.2 respectively.

At 25  $\mu$ M, the chlorinated lipids, SOPC ClOH and 2-ClHDA, alone had no effect on either VSMC proliferation or viability. With AMPK activated prior to chlorinated lipid treatment, there was a significant increase in VSMC proliferation with SOPC ClOH showing  $139.9 \pm 17.2$  % of proliferating cells compared to  $98.5 \pm 2.7$  % with SOPC ClOH alone (Figure 4.5). However, SOPC ClOH treatment had no effect on cell viability while 2-ClHDA had no consequence on either viability or proliferation. Oxidised phospholipids, PGPC and POVPC, caused a concentration-dependent reduction in VSMC proliferation and viability although at 25  $\mu$ M POVPC, there was not a significant decrease. When AMPK was activated prior to 2 hour treatment with PGPC, there was no significant difference on VSMC proliferation or viability compared to the lipid alone (Figure 4.6). In contrast, AMPK activation prior to POVPC incubation caused a significant reduction in both VSMC proliferation and viability with  $52.8 \pm 7.8$  % of viable cells present compared with  $83.0 \pm 6.0$  % of viable cells with 25  $\mu$ M of the lipid alone. Thus, AMPK activation increased the susceptibility of VSMCs to POVPC-induced inhibition of proliferation while prior AMPK activation stimulated SOPC ClOH-induced proliferation in VSMCs.

When AMPK was inhibited prior to chlorinated lipid treatment, there was no effect on VSMC proliferation but a significant increase was observed in VSMC viability after 2-ClHDA treatment compared with incubation of the lipid alone (Figure 4.7). When AMPK was inhibited prior to oxidised phospholipid treatment, there was no further effect seen with PGPC incubation but a further significant reduction with POVPC incubation in both VSMC proliferation and viability with  $56.5 \pm 9.4$  % of proliferating cells, compared with  $83.0 \pm 6.0$  % with POVPC alone, was seen (Figure 4.8).

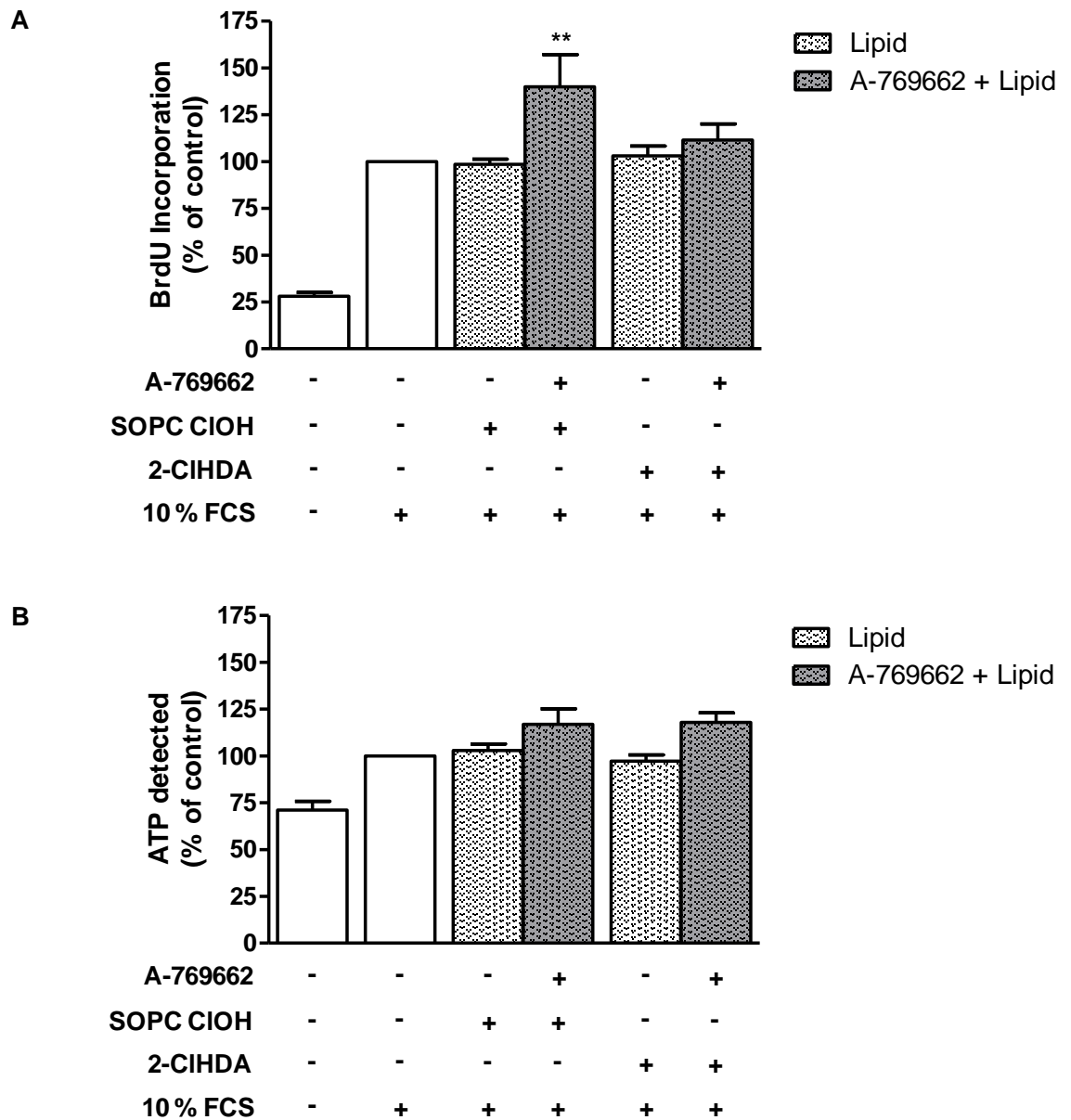


**Figure 4.5 – Effect of AMPK activation prior to 2 hour chlorinated lipid treatment on VSMC proliferation and viability.**

BrdU incorporation (A) and detection of ATP (B) were utilised to measure VSMC proliferation and viability respectively. VSMCs were incubated for 45 minutes with AMPK activator, A-769662 prior to 2 hours treatment with 25  $\mu$ M SIPC ClOH or 2-ClHDA in quiescing media and then stimulated with 10 % FCS for 24 hours with the addition of BrdU in proliferation measurements. \*\* $p < 0.01$  vs SIPC ClOH alone,  $n = 4-6$  and performed in triplicate.

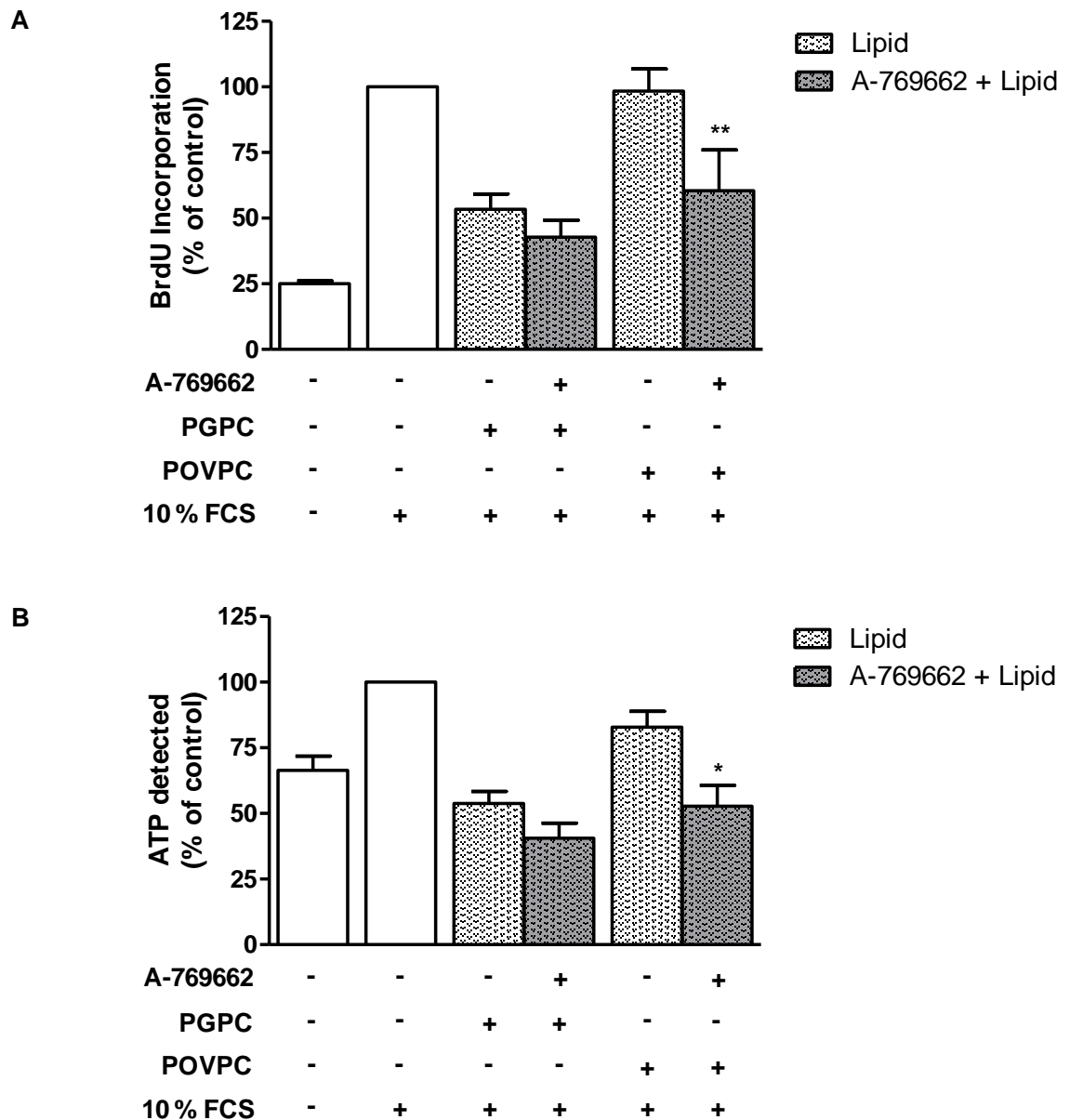


**Figure 4.6 – Effect of AMPK activation prior to 2 hour oxidised phospholipid treatment on VSMC proliferation and viability.**

BrdU incorporation (A) and detection of ATP (B) were utilised to measure VSMC proliferation and viability respectively. VSMCs were incubated for 45 minutes with AMPK activator, A-769662 prior to 2 hours treatment with 25  $\mu$ M PGPC or POVPC in quiescing media and then stimulated with 10 % FCS for 24 hours with the addition of BrdU in proliferation measurements. \* $p < 0.05$  and \*\* $p < 0.01$  vs POVPC alone,  $n = 4-6$  and performed in triplicate.

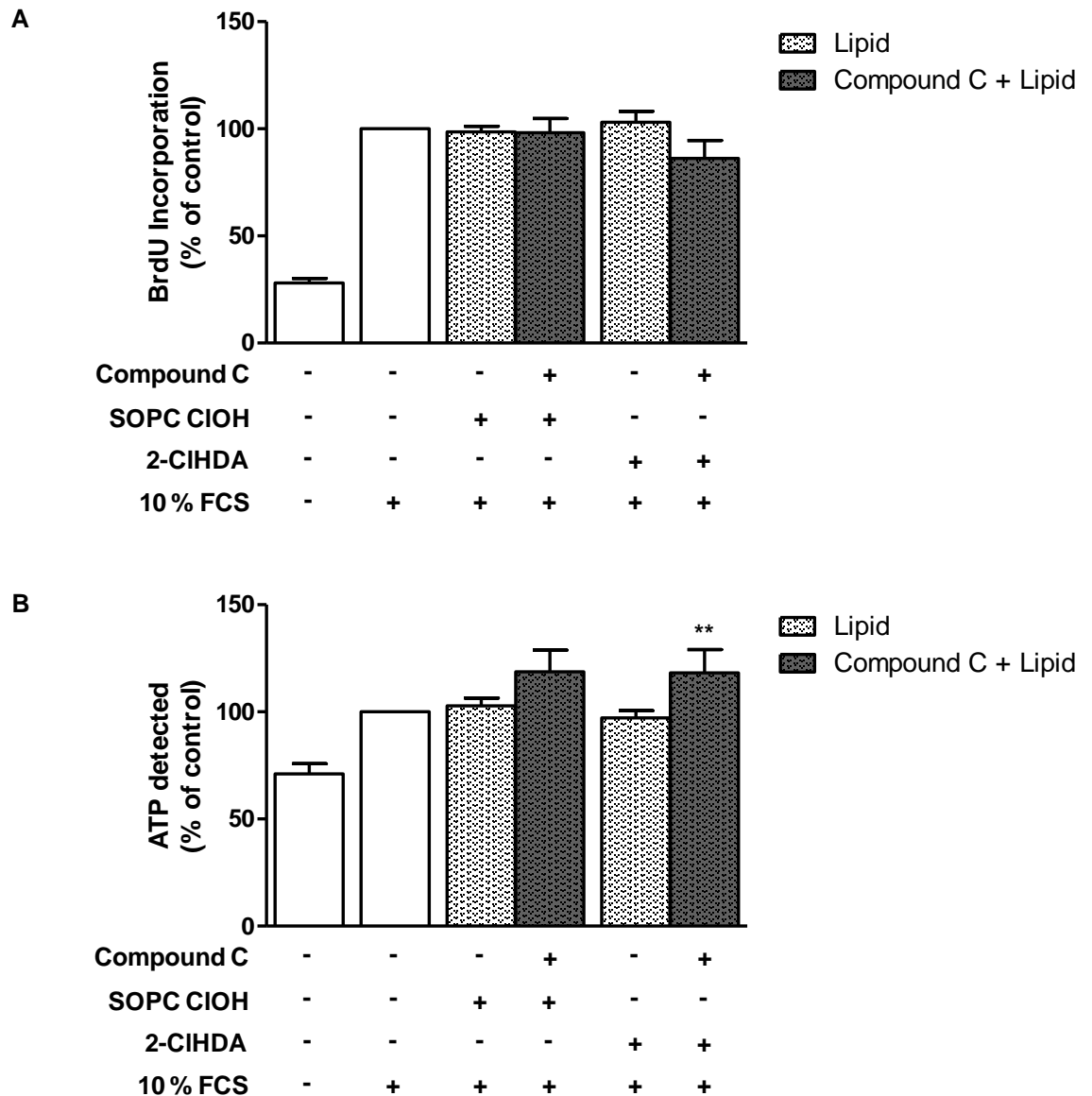


**Figure 4.7 – Effect of AMPK inhibition prior to 2 hour chlorinated lipid treatment on VSMC proliferation and viability.**

BrdU incorporation (A) and detection of ATP (B) were utilised to measure VSMC proliferation and viability respectively. VSMCs were incubated for 30 minutes with AMPK inhibitor, Compound C prior to 2 hours treatment with 25  $\mu$ M SOPC ClOH or 2-ClHDA in quiescing media and then stimulated with 10 % FCS for 24 hours with the addition of BrdU in proliferation measurements.  $n = 3-6$  and performed in triplicate.

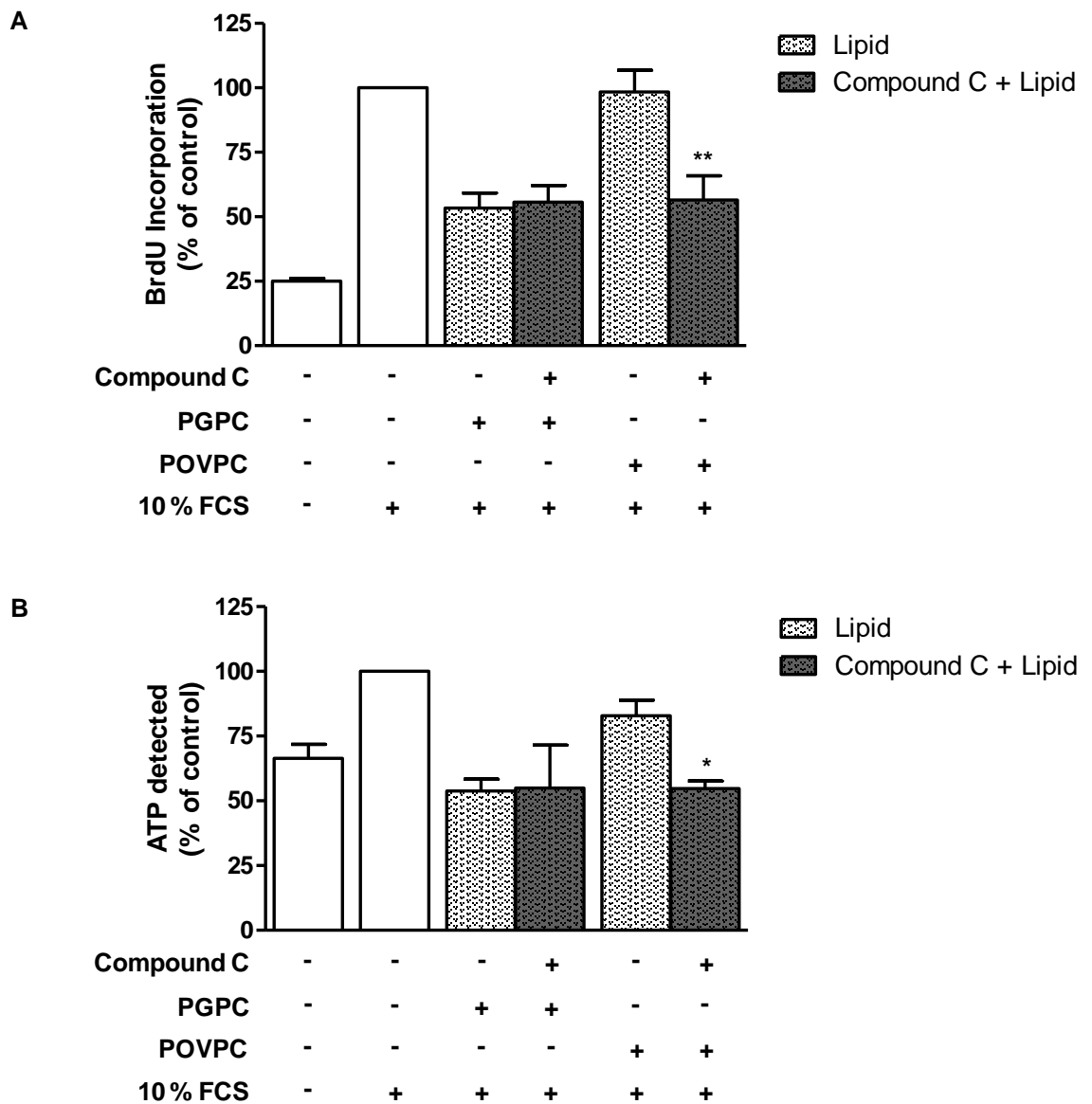


**Figure 4.8 – Effect of AMPK inhibition prior to 2 hour oxidised phospholipid treatment on VSMC proliferation and viability.**

BrdU incorporation (A) and detection of ATP (B) were utilised to measure VSMC proliferation and viability respectively. VSMCs were incubated for 30 minutes with AMPK inhibitor, Compound C prior to 2 hours treatment with 25  $\mu$ M PGPC or POVPC in quiescing media and then stimulated with 10 % FCS for 24 hours with the addition of BrdU in proliferation measurements. \* $p < 0.05$  and \*\* $p < 0.01$  vs POVPC alone,  $n = 3-6$  and performed in triplicate.

**Table 4.1 – Percentage of proliferating or viable VSMCs after AMPK activation or inhibition prior to 2 hour incubation with increasing concentrations of chlorinated lipids.**

Treatment	Assay type	Chlorinated Lipid Concentration ( $\mu\text{M}$ )				
		1	10	25	50	100
<b>SOPC ClOH</b>	<b>BrdU</b>	101.4 $\pm$ 2.1	98.4 $\pm$ 3.8	<b>98.5 <math>\pm</math> 2.7</b>	96.1 $\pm$ 1.3	95.0 $\pm$ 4.0
	<b>ATP</b>	106.3 $\pm$ 2.4	107.7 $\pm$ 3.5	<b>102.9 <math>\pm</math> 3.6</b>	98.5 $\pm$ 4.1	96.3 $\pm$ .7
<b>A-769662 + SOPC ClOH</b>	<b>BrdU</b>	142.1 $\pm$ 11.1**	141.5 $\pm$ 14.6***	<b>139.9 <math>\pm</math> 17.2**</b>	140.7 $\pm$ 16.2***	116.4 $\pm$ 9.5
	<b>ATP</b>	120.2 $\pm$ 12.1	120.6 $\pm$ 9.0	<b>116.9 <math>\pm</math> 8.3</b>	114.0 $\pm$ 13.5	101.5 $\pm$ 15.5
<b>Compound C + SOPC ClOH</b>	<b>BrdU</b>	109.0 $\pm$ 17.5	117.4 $\pm$ 8.4	<b>98.2 <math>\pm</math> 6.6</b>	132.4 $\pm$ 24.9	109.9 $\pm$ 17.1
	<b>ATP</b>	112.1 $\pm$ 10.3	117.1 $\pm$ 10.9	<b>118.7 <math>\pm</math> 10.2</b>	112.0 $\pm$ 14.2	114.2 $\pm$ 10.1
<b>2-CIHDA</b>	<b>BrdU</b>	100.4 $\pm$ 2.9	96.1 $\pm$ 4.4	<b>103.0 <math>\pm</math> 5.2</b>	99.8 $\pm$ 6.6	97.1 $\pm$ 7.7
	<b>ATP</b>	101.8 $\pm$ 1.7	98.3 $\pm$ 3.8	<b>97.1 <math>\pm</math> 3.4</b>	103.0 $\pm$ 2.9	101.0 $\pm$ 3.4
<b>A-769662 + 2-CIHDA</b>	<b>BrdU</b>	105.1 $\pm$ 10.1	110.5 $\pm$ 7.8	<b>111.6 <math>\pm</math> 8.6</b>	117.3 $\pm$ 14.2	85.9 $\pm$ 15.5
	<b>ATP</b>	108.6 $\pm$ 4.0	118.4 $\pm$ 3.4 <sup>††</sup>	<b>117.9 <math>\pm</math> 5.2<sup>††</sup></b>	112.6 $\pm$ 5.0	113.1 $\pm$ 6.7
<b>Compound C + 2-CIHDA</b>	<b>BrdU</b>	99.3 $\pm$ 2.6	89.0 $\pm$ 1.8	<b>86.2 <math>\pm</math> 8.3</b>	83.7 $\pm$ 13.1	93.3 $\pm$ 22.3
	<b>ATP</b>	110.5 $\pm$ 8.5	110.1 $\pm$ 4.7	<b>118.2 <math>\pm</math> 10.9</b>	118.3 $\pm$ 8.3	114.4 $\pm$ 8.9

All values are a percentage of 10 % FCS control. \*\*p<0.01 and \*\*\*p<0.001 vs SOPC alone, <sup>††</sup>p<0.01 vs 2-CIHDA alone, n = 3-6 and performed in triplicate.

**Table 4.2 – Percentage of proliferating or viable VSMCs after AMPK activation or inhibition prior to 2 hour incubation with increasing concentrations of oxidised phospholipids.**

Treatment	Assay type	Oxidised Phospholipid Concentration ( $\mu\text{M}$ )				
		1	10	25	50	100
<b>PGPC</b>	<b>BrdU</b>	103.5 $\pm$ 3.8	103.0 $\pm$ 5.9	<b>53.4 <math>\pm</math> 5.8</b>	24.4 $\pm$ 4.6	0.2 $\pm$ 1.0
	<b>ATP</b>	100.2 $\pm$ 3.8	88.5 $\pm$ 6.1	<b>53.8 <math>\pm</math> 4.7</b>	17.6 $\pm$ 6.5	0.5 $\pm$ 3.1
<b>A-769662 + PGPC</b>	<b>BrdU</b>	115.5 $\pm$ 10.2	88.5 $\pm$ 11.8	<b>42.8 <math>\pm</math> 6.4</b>	14.0 $\pm$ 4.6	-0.24 $\pm$ 0.4
	<b>ATP</b>	104.6 $\pm$ 2.4	86.8 $\pm$ 8.2	<b>46.5 <math>\pm</math> 5.7</b>	10.5 $\pm$ 1.6	0.7 $\pm$ 0.2
<b>Compound C + PGPC</b>	<b>BrdU</b>	97.0 $\pm$ 4.2	82.3 $\pm$ 12.3	<b>55.7 <math>\pm</math> 6.4</b>	27.6 $\pm$ 5.1	2.5 $\pm$ 2.0
	<b>ATP</b>	99.7 $\pm$ 9.8	90.3 $\pm$ 13.6	<b>54.9 <math>\pm</math> 16.6</b>	15.3 $\pm$ 8.9	2.3 $\pm$ 1.2
<b>POVPC</b>	<b>BrdU</b>	107.5 $\pm$ 9.9	104.1 $\pm$ 4.5	<b>98.4 <math>\pm</math> 8.3</b>	83.0 $\pm$ 7.9	58.2 $\pm$ 11.3
	<b>ATP</b>	99.9 $\pm$ 4.1	97.1 $\pm$ 4.3	<b>83.0 <math>\pm</math> 6.0</b>	64.1 $\pm$ 8.5	39.7 $\pm$ 10.5
<b>A-769662 + POVPC</b>	<b>BrdU</b>	112.9 $\pm$ 7.9	100.3 $\pm$ 14.0	<b>60.5 <math>\pm</math> 15.5**</b>	36.0 $\pm$ 16.3***	7.7 $\pm$ 4.5***
	<b>ATP</b>	111.7 $\pm$ 6.9	102.8 $\pm$ 10.1	<b>52.8 <math>\pm</math> 7.8</b>	23.8 $\pm$ 7.2	7.6 $\pm$ 3.3
<b>Compound C + POVPC</b>	<b>BrdU</b>	97.7 $\pm$ 9.7	83.9 $\pm$ 4.5	<b>56.5 <math>\pm</math> 9.4</b>	27.9 $\pm$ 3.0	9.4 $\pm$ 2.5
	<b>ATP</b>	100.5 $\pm$ 4.6	84.9 $\pm$ 4.2	<b>54.7 <math>\pm</math> 3.0**</b>	27.1 $\pm$ 5.4***	7.6 $\pm$ 3.5**

All values are a percentage of 10 % FCS control. \*\*p<0.01 and \*\*\*p<0.001 vs POVPC alone, n = 3-6 and performed in triplicate.

### ***4.3.3 Effect of AMPK activation or inhibition prior to modified lipid incubation on AMPK $\alpha$ and ACC expression***

To investigate the effects of modified lipids on the relative protein expression of AMPK $\alpha$  and its downstream target, ACC, AMPK was activated with A-769662 for 45 minutes or inhibited with Compound C for 30 minutes in VSMCs, followed by 2 hours treatment with each of the modified lipids then Western blotting was performed. Each of the graphs are expressed as the fold change of the phosphorylated form over the total amount of the enzyme.

There was no effect on the relative expression of AMPK $\alpha$  under any conditions with any incubation of either class of modified lipids. In contrast, A-769662, in the presence and absence of SOPC CIOH, caused a trend towards an increase in the ratio of ACC but this was not significant (Figure 4.9). SOPC CIOH alone had no effect but there was a significant reduction in the ratio of ACC with AMPK inhibition followed by incubation with SOPC CIOH compared with VSMCs treated in the same way with A-769662. Similar to SOPC CIOH, A-769662, in the presence and absence of 2-CIHDA, again caused a trend towards an increase in the relative expression of ACC but this was not significant (Figure 4.10). 2-CIHDA had no effect on ACC expression alone which was similar for Compound C alone or with the inhibitor prior to 2-CIHDA incubation.

There was an apparent 2-fold increase in the relative ratio of ACC expression in VSMCs with A-769662 treatment and a significant 2.5-fold increase with A-769662 treatment followed by PGPC incubation; this was significant compared to the untreated control (Figure 4.11). PGPC incubation alone had no effect on the relative ratio of phosphorylated to total ACC expression which was similar for Compound C alone or with the inhibitor prior to PGPC incubation. A-769662, in the presence or absence of POVPC, caused an increase in the ratio of ACC expression; this was only significant for the combination of the activator and oxidised phospholipid (Figure 4.12). Similar to the rest of modified lipids, POVPC alone had no effect on the relative ACC expression as did Compound C and the inhibitor followed by POVPC.

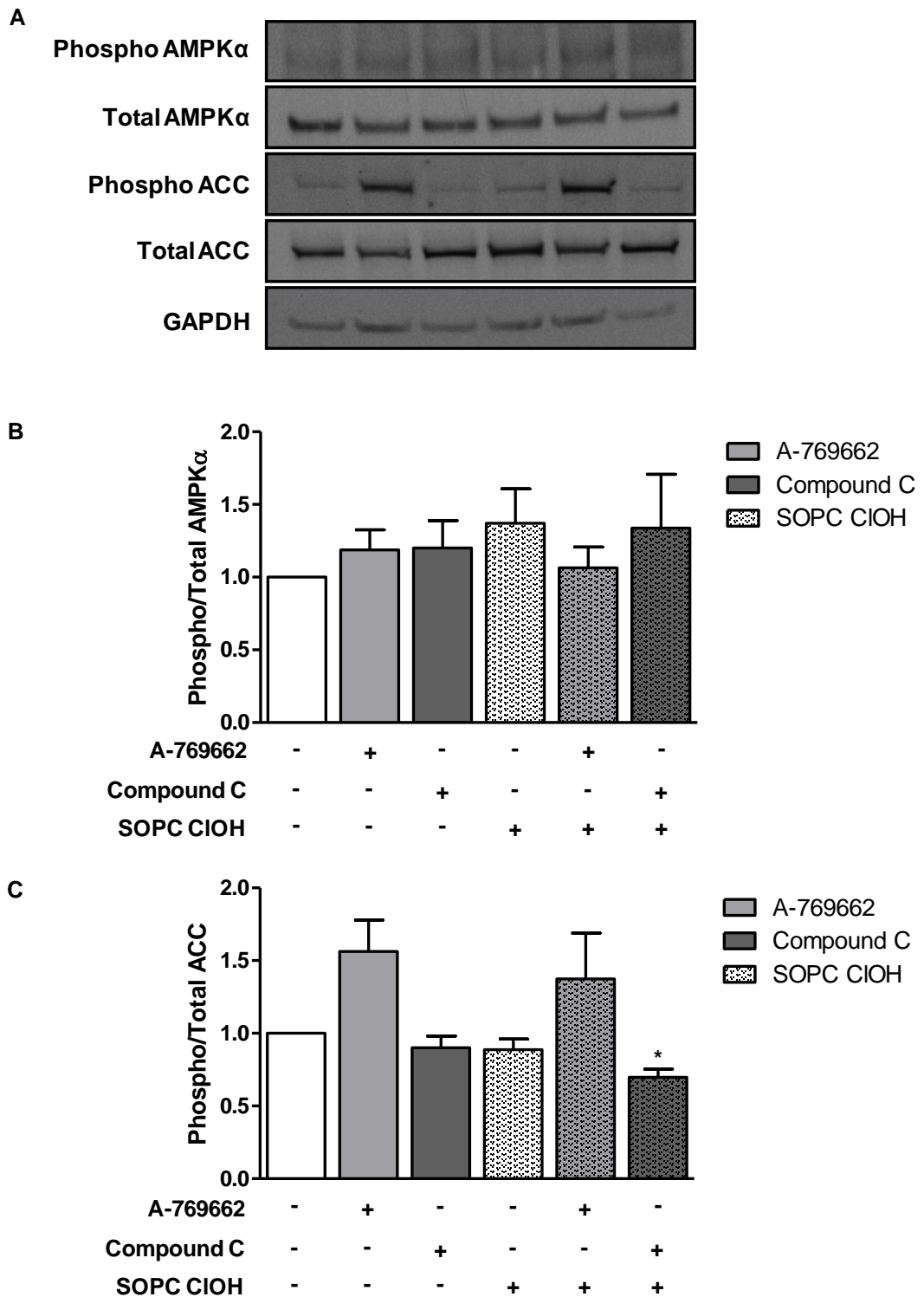


**Figure 4.9 – Effect of AMPK activation and inhibition prior to 2 hour SOPC CIOH incubation on AMPK $\alpha$  and ACC expression.**

VSMCs were incubated with A-769662 or Compound C alone or prior to 25  $\mu$ M SOPC CIOH treatment for 2 hours in quiescing medium after which the cells were lysed and immunoblotting was performed. Graphs are expressed as the fold change of the phosphorylated form of each enzyme divided by the total amount of AMPK $\alpha$  (B) and ACC (C) to measure the activation of the enzyme. Blots shown are representative (A). \* $p < 0.05$  vs A769662 + SOPC CIOH,  $n = 3$ .

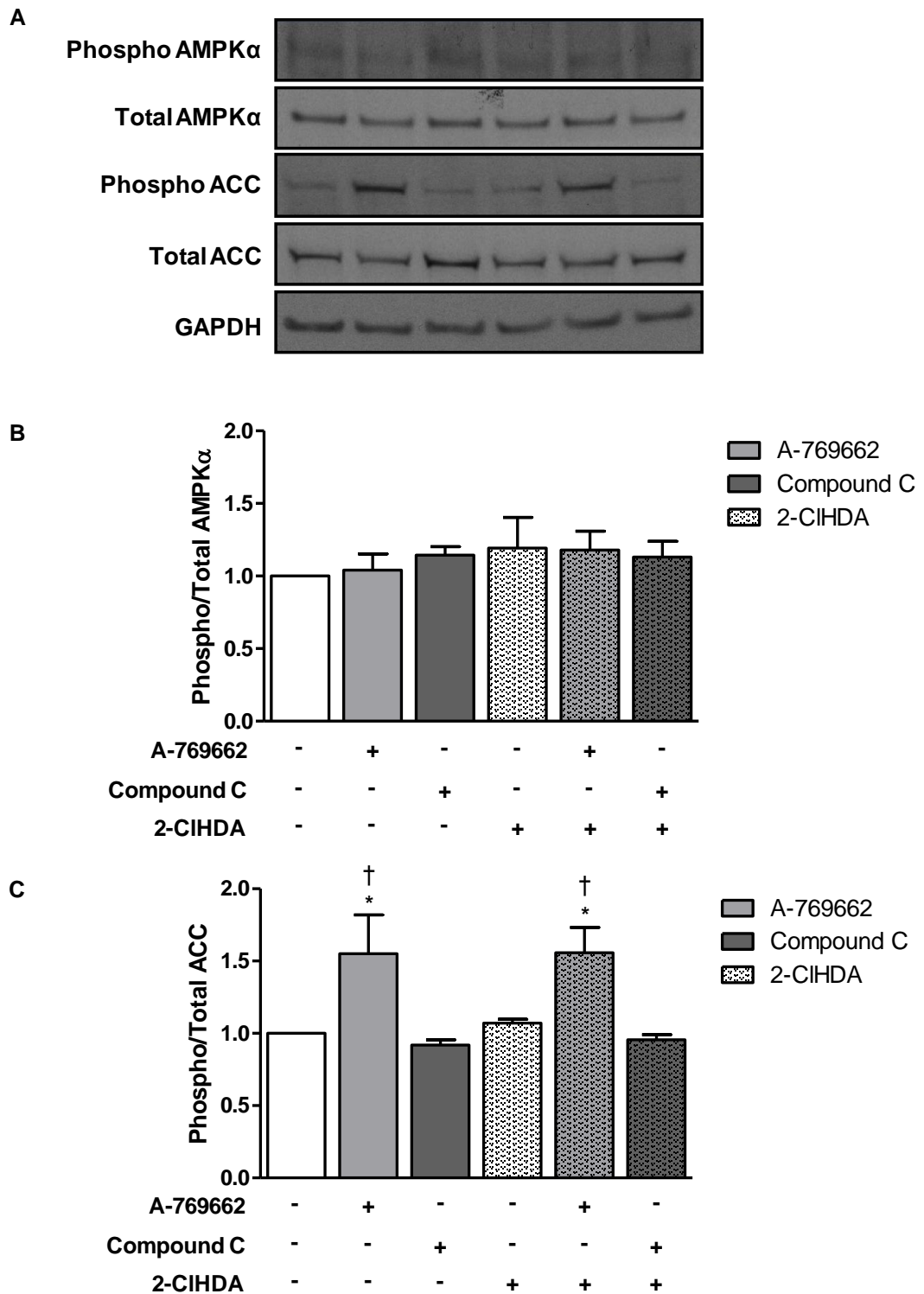


**Figure 4.10 – Effect of AMPK activation and inhibition prior to 2 hour 2-CIHDA incubation on AMPK $\alpha$  and ACC expression.**

VSMCs were incubated with A-769662 or Compound C alone or prior to 25  $\mu$ M 2-CIHDA treatment for 2 hours in quiescing medium after which the cells were lysed and immunoblotting was performed. Graphs are expressed as the fold change of the phosphorylated form of each enzyme divided by the total amount of AMPK $\alpha$  (B) and ACC (C) to measure the activation of the enzyme. Blots shown are representative (A). \* $p$ <0.05 vs Compound C alone, <sup>†</sup> $p$ <0.05 vs Compound C + 2-CIHDA,  $n = 3$ .

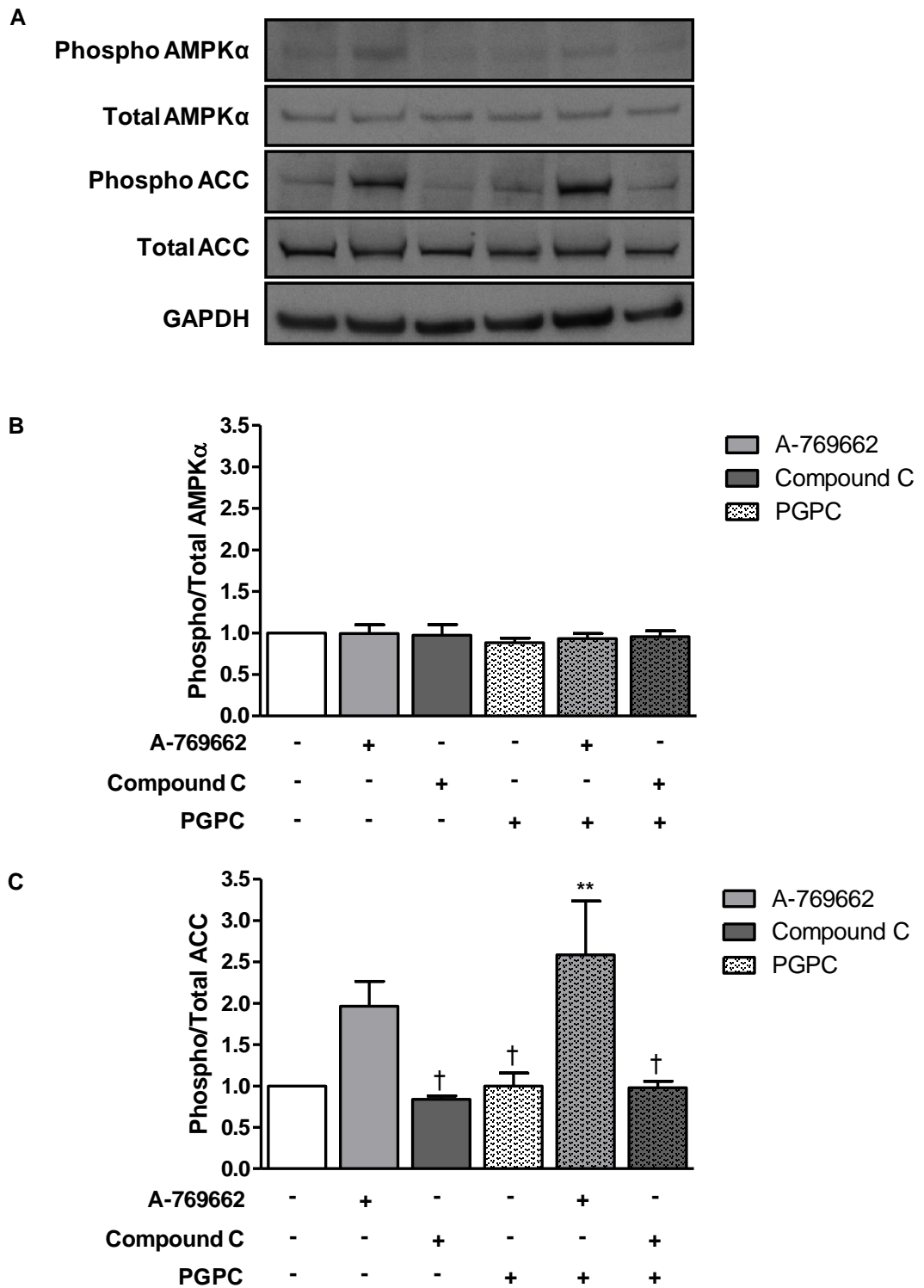


**Figure 4.11 – Effect of AMPK activation and inhibition prior to 2 hour PGPC incubation on AMPK $\alpha$  and ACC expression.**

VSMCs were incubated with A-769662 or Compound C alone or prior to 25  $\mu$ M PGPC treatment for 2 hours in quiescing medium after which the cells were lysed and immunoblotting was performed. Graphs are expressed as the fold change of the phosphorylated form of each enzyme divided by the total amount of AMPK $\alpha$  (B) and ACC (C) to measure the activation of the enzyme. Blots shown are representative (A). \*\* $p < 0.01$  vs control, <sup>†</sup> $p < 0.05$  vs A-769662 + PGPC,  $n = 3$ .

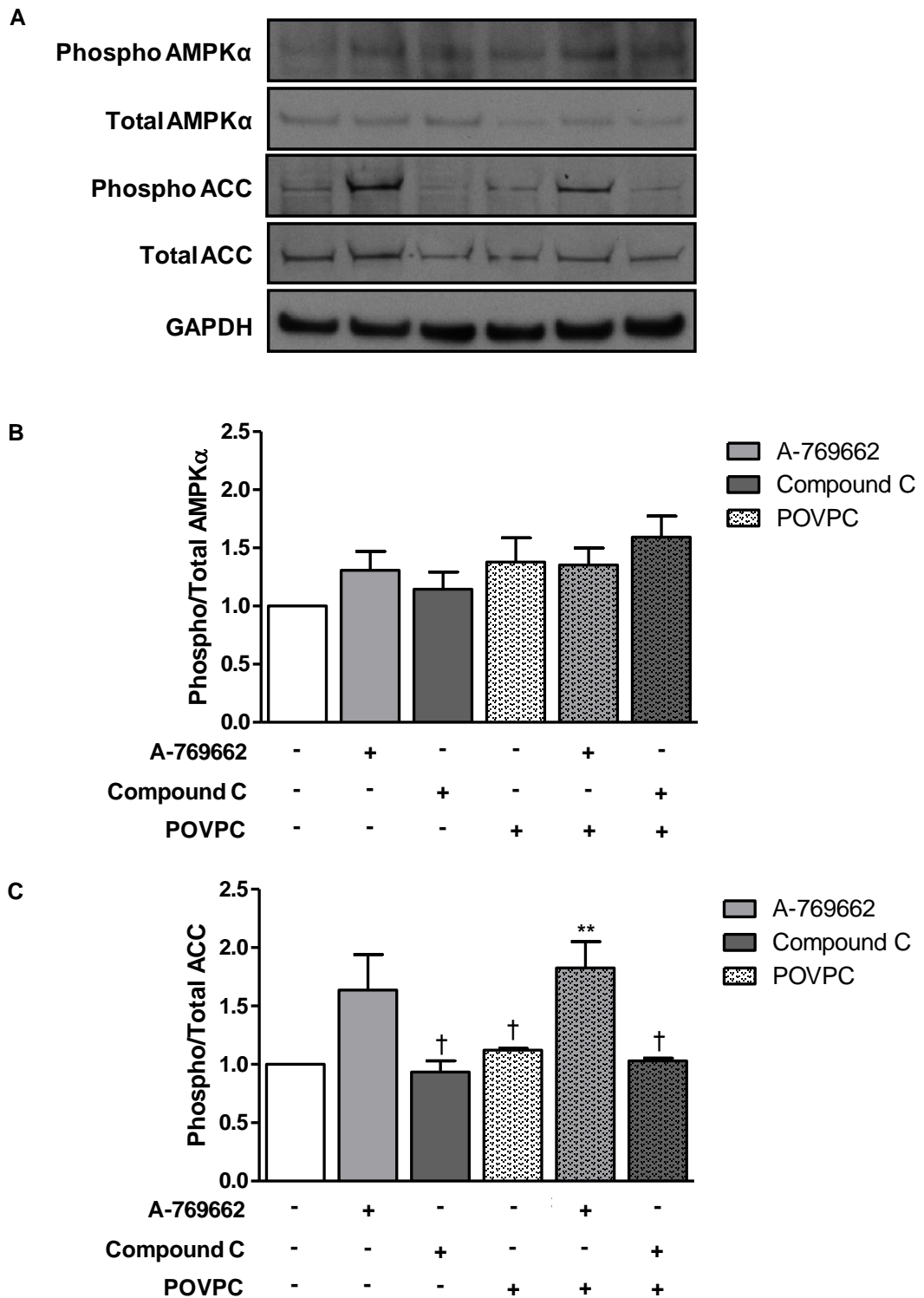


**Figure 4.12 – Effect of AMPK activation and inhibition prior to 2 hour POVPC incubation on AMPK $\alpha$  and ACC expression.**

VSMCs were incubated with A-769662 or Compound C alone or prior to 25  $\mu$ M POVPC treatment for 2 hours in quiescing medium after which the cells were lysed and immunoblotting was performed. Graphs are expressed as the fold change of the phosphorylated form of each enzyme divided by the total amount of AMPK $\alpha$  (B) and ACC (C) to measure the activation of the enzyme. Blots shown are representative (A). \*\* $p < 0.01$  vs control, † $p < 0.05$  vs A-769662 + POVPC,  $n = 3$ .

#### **4.3.4 Effect of modified lipid incubation of AICAR-induced relaxation**

To determine if incubation of modified lipids altered vascular reactivity, the effect of modified lipid treatment on the AICAR-induced relaxation in mouse carotid arteries was assessed. Firstly, the effect of modified lipid treatment on U46619-induced contraction was investigated in the vessels (Figure 4.13). As with the *in vitro* VSMC experiments, chlorinated lipids, SOPC ClOH and 2-ClHDA, had no effect on the contraction to the thromboxane A<sub>2</sub> receptor agonist, U46619, in the arterial rings. Similar to the chlorinated lipids, POVPC treatment had no effect on the U46619-induced contraction but PGPC caused a significant reduction in contraction from  $0.22 \pm 0.04$  g to  $0.07 \pm 0.01$  g. Vasorelaxation was induced with increasing concentrations of the AMPK activator, AICAR (Figure 4.14). Neither chlorinated lipid had any effect on the AICAR-induced relaxation. In contrast, both oxidised phospholipids caused a concentration-dependent decrease in the relaxation to AICAR with PGPC abolishing almost all of the relaxation observed.

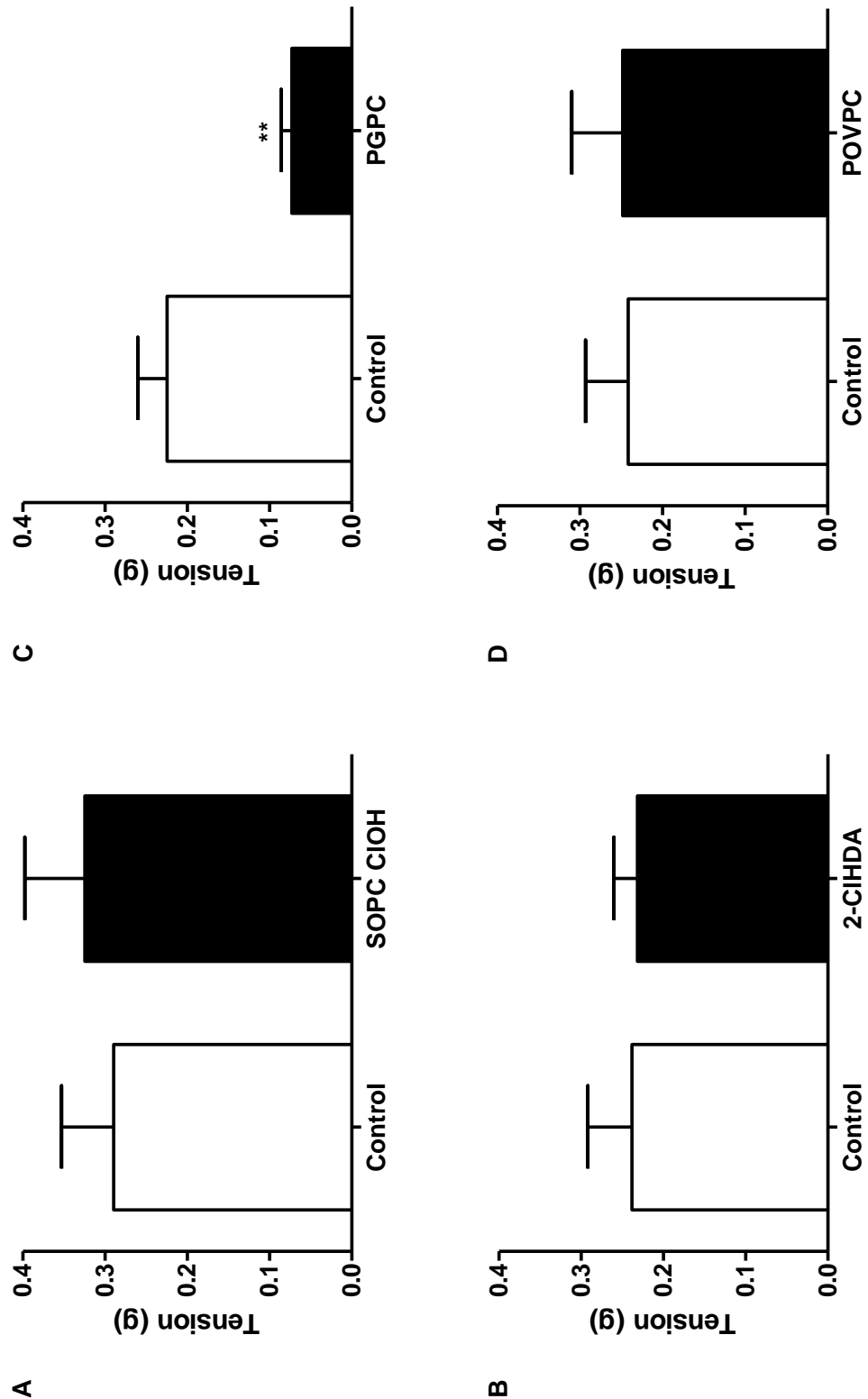


**Figure 4.13 – Effect of modified lipid incubation on U46619-induced contraction in mouse carotid arteries.**

25  $\mu$ M SOPC ClOH (A), 2-CIHDA (B), PGPC (C) and POVPC (D) were incubated for 30 minutes prior to U46619-induced contraction in mouse carotid arteries performed using small vessel wire myography. \*\* $p < 0.01$  vs control,  $n = 5-6$ .

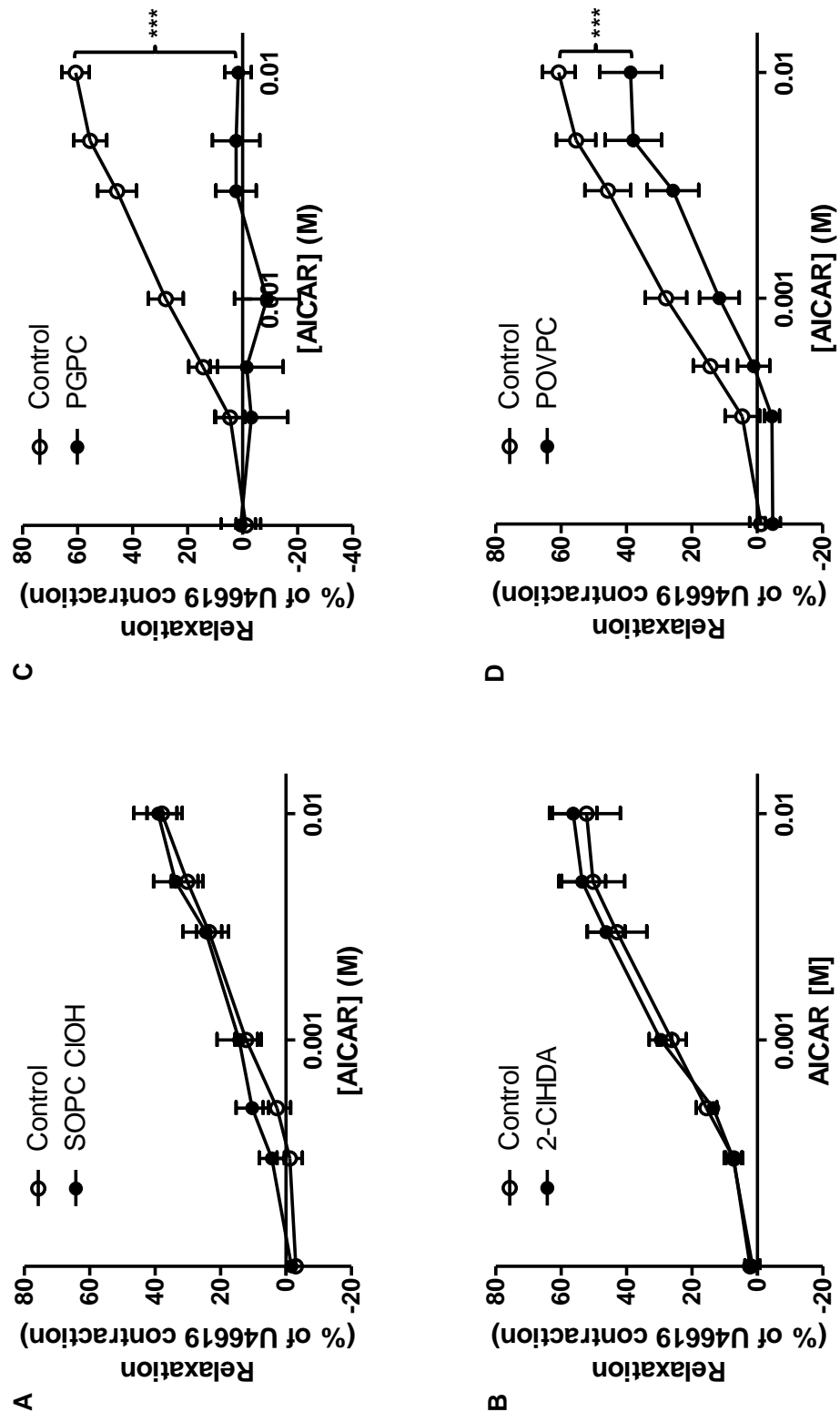


**Figure 4.14 – Effect of modified lipid incubation on AICAR-induced relaxation in mouse carotid arteries.**

Concentration-response curves to AICAR were produced by small vessel wire myography with 25  $\mu$ M SOPC ClOH (A), 2-ClHDA (B), PGPC (C) and POVPC (D) incubated for 30 minutes prior to U46619-induced contraction and relaxation to AICAR. \*\*\* $p < 0.001$  vs control,  $n = 5-6$ .

## 4.4 Discussion

This study revealed for the first time the effects of AMPK signalling on the actions of individual modified lipids in VSM and on vascular reactivity with AICAR-induced relaxation in arterial rings. Activation of AMPK prior to SOPC CIOH incubation resulted in increased VSMC proliferation while POVPC was found to reduce VSMC proliferation and cellular ATP under the same conditions. Oxidised phospholipids also reduced AICAR-mediated vasorelaxation in mouse carotid arteries.

The impact of AMPK signalling in CVD and in particular atherosclerosis is a relatively new concept with an increasing amount of research in the last ten years focussing on this area. To confirm the presence and to investigate AMPK signalling in rabbit aortic VSM, Western blot analysis was utilised to measure phosphorylation of the threonine residue at position 172. Also analysed by this technique was its downstream target, ACC which is deactivated by AMPK by the phosphorylation of the serine residue at position 79. Measurement of ACC phosphorylation provides further evidence of targeted AMPK activation as AICAR and A-769662 are not known to have any non-specific effects that could involve the activation of ACC at this phosphorylation site. No effects were observed in the phosphorylation status of AMPK $\alpha$  with any of the AMPK activators or inhibitors in this experimental protocol. In contrast, the AMPK activator, A-769662 increased the phosphorylation status of ACC by 2-fold while the AMPK inhibitor, Compound C had no effect. This could result from the subsequent dephosphorylation of AMPK after activation of its downstream signalling pathway resulting in an observed change in phosphorylation of ACC and not AMPK as the activity of AMPK has been found to reduce 45 minutes after stimulation (Morrow *et al.*, 2003). Furthermore, inhibition of AMPK by Compound C had no effect on A-769662-induced phosphorylation of AMPK $\alpha$ . This is consistent with a previous study in rat skeletal muscle cells which suggested that A-769662 abrogated the effect of Compound C (Benziane *et al.*, 2009). Compound C alters the conformation of the activation loop of AMPK preventing activation by this route; however, A-769662 activates AMPK both allosterically and by inhibiting its dephosphorylation therefore AMPK can still be phosphorylated in the presence of Compound C (Handa *et al.*, 2011). This would suggest that the length of experimental protocol was sufficient to stimulate AMPK signalling and highlights AMPK stimulation by the activator, A-769662.

In contrast to the effects observed on phosphorylation, incubation with the potent activator, A-769662 had no effect on the proliferation or viability of rabbit aortic VSMCs. This is in

contrast with previous studies where AMPK activation caused a concentration- and time-dependent decrease in VSMC proliferation with AICAR (Igata *et al.*, 2005). This could be due to the different mechanisms by which the activators induce phosphorylation of AMPK as well as the different experimental protocols utilised. In this study, AMPK was activated when VSMCs were in a quiescent state for 45 minutes and then stimulated with 10 % FCS medium for 24 hours while in the study by Igata *et al.* (2005), VSMCs were stimulated with either PDGF or FCS in the presence of AICAR for 4 days. This suggests that the AMPK-mediated inhibition of VSMC proliferation is potentially dependent on the phenotypic state of the VSMCs where AMPK activation only inhibits growth in proliferating VSMCs and therefore has no lasting effects in quiescent cells. In contrast, AMPK inhibition by Compound C caused cytostatic actions at 40  $\mu\text{M}$  and cytotoxic effects at 100  $\mu\text{M}$  in VSMCs. Compound C is a cell-permeable potent agent which inhibits AMPK by competitively displacing ATP (Zhou *et al.*, 2001). It is found to block AMPK activity with an  $\text{IC}_{50}$  value in the range of 0.1 to 0.2  $\mu\text{M}$  (Bain *et al.*, 2007) and previous studies have found Compound C to inhibit proliferation of non-vascular cells including preadipocytes and glioma cells (Nam *et al.*, 2008, Vucicevic *et al.*, 2009). Compound C has also recently been shown to inhibit VSMC proliferation and migration by an AMPK-independent mechanism resulting in the inhibition of cell cycle progression in VSMCs (Peyton *et al.*, 2011). Similar to the action of AICAR, VSMCs were primarily arrested in the G0/G1 phase of the cell cycle after Compound C treatment and this was linked to altered expression and phosphorylation of various cell cycle regulatory proteins such as cyclin A and D1 (Peyton *et al.*, 2011). Peyton *et al.* (2011) also found Compound C to be cytostatic in VSMCs using a concentration range up to 10  $\mu\text{M}$ . Apoptosis has also been observed in other cell types at similar concentrations suggesting cell-specific effects of Compound C (Jin *et al.*, 2009, Jang *et al.*, 2010). In this study, Compound C was cytostatic at 40  $\mu\text{M}$  and cytotoxic at 100  $\mu\text{M}$  suggesting a switch from cytostatic to cytotoxic effects of Compound C at higher concentrations in VSMCs thus, 10  $\mu\text{M}$  was selected for all subsequent VSMC experiments in this study.

AMPK signalling has previously been implicated in modulating the effects of modified lipids with activation of AMPK found to suppress oxLDL-induced macrophage proliferation and lessen the atherosclerotic burden in high fat fed ApoE<sup>-/-</sup> mice (Ishii *et al.*, 2009, Li *et al.*, 2010a). In addition, AMPK activation has been found to exert anti-apoptotic effects in a number of cell types including endothelial cells (Ido *et al.*, 2002, Kim *et al.*, 2008, Liu *et al.*, 2010). The impact of AMPK signalling on modulating the effects of individual modified lipids in VSMCs witnessed in Chapter 3 was subsequently

investigated in this study. VSMCs stimulated with A-769662 prior to SOPC CIOH incubation caused a significant increase in proliferation, not mirrored in viability, and no effects were observed with 2-ClHDA on remodelling processes. This suggests that AMPK activation prior to SOPC CIOH treatment results in the stimulation of proliferation pathways which SOPC CIOH cannot trigger alone. AMPK activation prior to oxidised phospholipid treatment had no effect on PGPC-induced cell death but a greater effect was observed after POVPC treatment suggesting AMPK activation prior to POVPC incubation results in enhanced stimulation of cell death pathways than POVPC alone. This could be a protective measure to clear damaged or dying cells, resulting from the action of oxidised phospholipids, faster via AMPK signalling. Similar to the action of oxLDL, all of the individual modified lipids were found not to cause phosphorylation of AMPK $\alpha$  directly (Brito *et al.*, 2009). The study also found incubation of oxLDL and resveratrol together resulted in no AMPK activation suggesting oxLDL prevented the resveratrol-induced activation of AMPK (Brito *et al.*, 2009). This was not the case with the individual modified lipids used in this study. In contrast, AMPK signalling has previously been found to be influential in atherosclerosis and lipid accumulation with activation reducing oxLDL-induced macrophage proliferation and foam cell formation (Ishii *et al.*, 2009, Li *et al.*, 2010a).

In addition to the effects observed with modulation of AMPK in VSMCs, AICAR-mediated AMPK activation resulted in a concentration-dependent relaxation of precontracted denuded mouse carotid arteries. As the murine arterial segments were denuded of endothelium, the effects witnessed are likely caused by the activation of AMPK in VSM. AICAR concentrations used were within a range previously shown to activate AMPK in various tissues and induce AMPK phosphorylation (Morrow *et al.*, 2003, Nagata *et al.*, 2003). AMPK-induced relaxation has previously been shown in mouse aortic rings where almost complete relaxation was observed at  $3 \times 10^{-3}$  M AICAR after precontraction to phenylephrine (Goirand *et al.*, 2007). However, relaxation induced by AICAR was only about 60 % of the U46619 contraction in this study. This could be due to different vascular beds and contracting agents used as well as the differences in the administration of AICAR. In this study, AICAR was added to the myograph bath at 10 minutes intervals producing a cumulative concentration-response curve whereas in the study by Goirand *et al.* (2007), the response to AICAR was allowed to plateau before the next concentration was added thus their study protocol was significantly longer. This is important as AICAR has previously been shown to increase the amount of phosphorylated AMPK in a time-dependent manner in rabbit and human aortic VSMCs (Igata *et al.*, 2005),

suggesting if AICAR has longer to act then more AMPK is phosphorylated and this could account for the total relaxation of the aortic rings seen by Goirand *et al.* (2007).

Due to the presence of lesions and accumulation of VSMC proliferation in the arterial wall, atherosclerotic vessels are not as susceptible to relaxation in comparison to healthy controls (Freiman *et al.*, 1986, Shimokawa and Vanhoutte, 1989). Atherosclerosis significantly reduces the relaxing capacity of arteries with impairment to both endothelium-dependent and -independent actions in arteries isolated from ApoE<sup>-/-</sup> mice (Crauwels *et al.*, 2003, d'Uscio *et al.*, 2001). These effects could be partly due to the increased concentrations of modified lipids in the vascular wall as oxLDL has been found to inhibit endothelial-dependent relaxation in pig and rabbit coronary arteries (Simon *et al.*, 1990, Buckley *et al.*, 1996). However, the contribution of individual modified lipids has not previously been investigated in relation to vascular reactivity. Chlorinated lipids had no effect on U46619-induced contraction or on AICAR-induced relaxation of mouse carotid arteries. In contrast, oxidised phospholipids caused a significant reduction in AICAR-relaxation with PGPC almost abolishing all the relaxation observed. PGPC was also found to significantly reduce the U46619-mediated contraction while POVPC had no effect. This could be due to toxicity or a loss of viability of the VSM after oxidised lipids incubation. Oxidised phospholipids have also previously been implicated in cellular calcium handling with low concentrations of PGPC and POVPC evoking increases in intracellular Ca<sup>2+</sup> via transient receptor potential proteins which make up cationic channels in human embryonic kidney cells (Al-Shawaf *et al.*, 2010). This could potentially explain the differences in relaxation which were observed after incubation with oxidised phospholipids. Similar to the effects witnessed in VSMCs in Chapter 3, PGPC had a greater impact on AICAR-induced relaxation compared to POVPC.

Although the mechanism of AICAR-induced relaxation is presently unknown, this study suggests that the action is not dependent on the endothelium. This is in further agreement with previously published work by Goirand *et al.* (2007), where to confirm their observations from endothelium intact and denuded vessels, rings of aorta were incubated with a NOS inhibitor and no significant change in the response to AICAR was seen. These findings indicate that AICAR-mediated AMPK activation results in relaxation by a direct action on VSM. Arterial relaxation can occur by alteration of the calcium handling machinery in VSMCs with hypoxia, known to activate AMPK, found to alter the phosphorylation/dephosphorylation cascade of SM MLC as well as interfering with Ca<sup>2+</sup> homeostasis by altering the regulation of potassium channels (Wardle *et al.*, 2006, Thorne

*et al.*, 2004). Vascular remodelling including VSMC proliferation and migration and the reduced ability to alter vascular tone in the presence of oxidised phospholipids can lead to poor blood pressure regulation and therefore hypertension. Since AMPK activation has been shown to have vasorelaxant effects on VSM, which is impaired in the presence of these modified lipids, it has emerged as a potential target for the treatment of atherosclerosis and hypertension.

## 4.5 Conclusions

In summary, AMPK activation by A-769662 had no effect on VSMC proliferation or viability whereas Compound C, which inhibits AMPK activity, caused cytostatic and cytotoxic effects in VSMCs at increasing concentrations. Although the modified lipids used were found not to cause phosphorylation of AMPK $\alpha$  or its downstream target ACC directly, SOPC ClOH induced VSMC proliferation after AMPK was stimulated. POVPC was found to reduce VSMC proliferation and cellular ATP under the same conditions. In addition to the effects on VSMCs, oxidised phospholipids reduced AICAR mediated vasorelaxation in mouse carotid arteries with the greater effect seen using PGPC. This is the first study to investigate AMPK signalling on the effects of individual modified lipids in VSM as well as utilising the more potent AMPK activator, A-769662. This study also highlights the differing effects of modified lipid classes on vascular reactivity which is critical in atherosclerotic progression and the elevated blood pressures found in hypertension.

**CHAPTER 5**

**THE OCCURRENCE OF MODIFIED  
LIPIDS IN NEOINTIMA FORMATION  
IN MICE**

## 5.1 Introduction

As atherosclerosis develops, advanced complex plaques are formed that protrude into the lumen of the vessel and can result in complete occlusion of the affected artery. PCI is commonly utilised to alleviate the angina pain which is a consequence of the reduced lumen and restore blood flow through the atherosclerotic vessel. PTCA is used for revascularisation by controlled inflation of a balloon to dilate the vessel either alone or in combination with deployment of a stent to provide a rigid scaffold; resulting in a widening of the lumen (Gruntzig *et al.*, 1979, Sigwart *et al.*, 1987). The major limitation affecting the long-term success of all forms of PCI is restenosis, which is thought to be an exaggerated form of wound healing after vascular injury. Restenosis is characterised by a recurrence of luminal narrowing resulting from neointimal hyperplasia and rapid vascular remodelling of the treated vessel. The formation of neointima occurs by excessive VSMC proliferation and migration as well as the production of large amounts of ECM.

The pathophysiology of restenosis involves a complex cascade of events. The initial consequence of PCI is stretch of the entire artery and endothelial denudation. Mechanical injury results in compression and damage to the atherosclerotic plaque and exposure of the pro-thrombogenic core to circulating blood. This leads to recruitment of inflammatory cells by the expression of adhesion molecules on activated platelets and thrombus formation caused by the deposition of fibrin (Libby and Simon, 2001, Inoue and Node, 2009). These pro-inflammatory responses are sustained for several weeks following injury of the vessel (Libby *et al.*, 1992). Balloon-injured vessels show a significant increase in leukocyte adhesion 24 hours after injury in rabbit subclavian arteries, as well as up-regulation of adhesion molecules such as P-selectin and VCAM-1 (Kennedy *et al.*, 2000). There is also evidence of sustained inflammation with inflammatory cells remaining in close proximity to the stent struts in rabbit iliac arteries up to 28 days after placement (Kennedy *et al.*, 2004, Coats *et al.*, 2008). In addition, increased leukocyte adhesion has been demonstrated *ex vivo* up to 28 days following surgery in a mouse wire injury model (Tennant *et al.*, 2008). The importance of circulating inflammatory cells was demonstrated in neutropaenic rabbits which had a significantly reduced extent of neointima formation after 28 days (Miller *et al.*, 2001). Stent deployment also results in neutrophil activation which is associated with neointimal thickening (Inoue *et al.*, 2006).

Disruption of the atherosclerotic plaque during PCI results in the exposure of the modified lipid-containing core to circulating blood and the other components of the lesion. The

presence of extravasated leukocytes such as neutrophils within the lesion could lead to an increase in the production of modified lipids such as chlorinated and oxidised species in the neointima by the action of the MPO system. Arterial segments from ApoE<sup>-/-</sup> mice treated *in vitro* with a phospholipid chlorohydrin formed by MPO, displayed an increase in leukocyte adhesion in a concentration-dependent manner as well as an increase in P-selectin expression (Dever *et al.*, 2008). VSMC proliferation was also evident 24 hours after the topical application of oxidised phospholipid, POVPC to mouse carotid arteries *in vivo* (Johnstone *et al.*, 2009). Furthermore, an increase in the presence of MPO and HOCl-modified proteins was found to correlate with an increase in the intima-to-media ratio in human iliac arteries (Hazell *et al.*, 2001). HOCl was also found to mediate neointimal hyperplasia in a time- and dose-dependent manner, initially causing apoptosis followed by vascular proliferation in a rat model of balloon injury (Yang *et al.*, 2006). The total plasma cholesterol level in ApoE<sup>-/-</sup> mice was also found to be markedly elevated after carotid balloon injury which was in parallel with neointima formation (Matter *et al.*, 2006).

In addition, AMPK, an enzyme involved in cellular energy homeostasis, has been implicated in vascular disease. In the previous chapter, AMPK signalling was found to alter the effects of modified lipids on vascular remodelling processes. In addition, mice deficient in AMPK $\alpha$ 2 had a dramatic increase in the formation of neointima after wire injury of the carotid artery compared to wild type controls and a reduction in AMPK activity also led to an increase in neointima development after arterial injury (Song *et al.*, 2011, Yu *et al.*, 2012). Taken together, this suggests that inflammation in the vessel following injury may induce lipid modification which drives the proliferative response. One possible mechanism for this response is via alterations in VSM AMPK signalling and to date this link between modified lipids and AMPK has not been investigated in an *in vivo* model of vascular injury.

### **5.1.1 Aims**

The aims investigated in this chapter were:

- To determine the extent of neointima formation after carotid artery injury in mice.
- To investigate the occurrence of modified lipids in neointima formation in C57BL/6 and ApoE<sup>-/-</sup> mice.
- To assess the role of AMPK in neointima formation.

## 5.2 Methods

### 5.2.1 Carotid artery injury

Male C57BL/6 mice on normal chow and male ApoE<sup>-/-</sup> mice at 8 to 10 weeks of age (weighing between 21 and 30 g) were fed on a high fat diet for 2 weeks prior to the vascular injury surgery. ApoE<sup>-/-</sup> mice were continued on the high fat diet throughout the study period and all mice were weighed at the start of the procedure, at day 7 and at the end of the procedure. Vascular injury was performed by isolation of the left common carotid artery and insertion of a modified flexible nylon wire as outlined in Section 2.6.3. Sham operated animals followed the same procedure without the insertion of the flexible nylon wire into the carotid artery. At the end of the procedure, mice were sacrificed by an i.p. injection of 200 mg/kg of sodium pentobarbital (Euthatal). Blood was collected by cardiac puncture into EDTA-coated tubes and centrifuged at 1500 x g for 10 minutes to produce plasma. Heart, liver and spleen weights were also recorded at time of death.

### 5.2.2 MPO assay

The MPO content of the plasma from sham-operated and injured C57BL/6 and ApoE<sup>-/-</sup> mice was analysed using a mouse MPO ELISA kit as described in Section 2.6.6. Samples were diluted 1 in 16 in dilution buffer and the assay was performed as per the manufacturer's instructions. Absorbance was measured spectrophotometrically at 450 nm.

### 5.2.3 Histology

Carotid artery and aorta sections were processed, cut and stained as detailed in Section 2.7. Vessels from the sham-operated and injured animals were excised immediately after death and placed in neutral buffered formalin overnight. Arteries were processed through a gradient of alcohols to HistoClear and embedded vertically in paraffin wax before being cut into 4 µm sections. H&E staining was performed to assess the extent of neointima formation. Immunohistochemistry was utilised to investigate the composition of the neointima with antibodies against αSMA, Ki67 (a proliferation marker), active caspase 3 (an indicator of apoptosis) as well as phosphorylated and total AMPKα. Sections were analysed using Image-Pro® software and the intima-media thickness was measured to assess neointima formation after H&E staining. The pixel density of positive DAB staining was calculated as a percentage of the neointimal area for quantification of the immunohistochemistry.

### **5.2.4 Detection of lipids in carotid arteries**

Lipids were extracted and analysed from the left and right carotid arteries of sham-operated and injured C57BL/6 and ApoE<sup>-/-</sup> mice as described in Section 2.8. Vessels were incubated in equal volumes of methanol containing the antioxidant BHT, chloroform and an aqueous solution to extract lipids then dried under a steady flow of oxygen-free nitrogen gas. Dried lipid extracts were reconstituted and further diluted in methanol. For analysis using positive-ion mode, samples were diluted 1 in 50 for left injured carotids and 1 in 25 for right carotids with 1 % aqueous formic acid in methanol and scans performed for PCs and SMs, PEs, cholesterol and cholesteryl esters. Spectra, in the range of m/z 300-1000, were acquired for 2 minutes. For analysis using negative-ion mode, samples were diluted 1 in 5 for left injured carotids and 1 in 2.5 for right carotids with 10 % 5 mM ammonium acetate in methanol and scans performed for PIs and PSs. Spectra in the range of m/z 300-1000 were acquired for 4 minutes. Samples were analysed by identifying consistent differences between spectra from different sample groups.

### **5.2.5 Statistical analysis**

All results are displayed as mean  $\pm$  SEM and n represents the number of mice used for each experiment. Data were analysed using a one-way ANOVA followed by a Newman-Keuls' post hoc test for analysis of spectra and two-way ANOVA followed by Bonferroni's post hoc test for all other measurements taken.

## 5.3 Results

### 5.3.1 Extent of neointima formation in C57BL/6 and ApoE<sup>-/-</sup> mice after vascular injury

Histological analysis of H&E stained sections was performed to assess the extent of neointimal growth in C57BL/6 and ApoE<sup>-/-</sup> mice after the carotid artery injury procedure (Figure 5.1). The contralateral right carotid artery was cut and stained as an uninjured control. There was no significant difference in neointima formation observed between C57BL/6 sham-operated and injured carotid arteries. However, there was a substantial increase in neointimal growth in injured vessels of ApoE<sup>-/-</sup> mice compared to their sham-operated counterparts. In addition, there was a significant increase in the intima to media ratio in injured ApoE<sup>-/-</sup> arteries compared to their C57BL/6 counterparts. There was no difference in the circumference and therefore size of the carotid arteries which was calculated by measuring the EEL of the vessels (Figure 5.2). In contrast, there was no evident injury in aorta of either strain or no atherosclerotic plaques were observed in the ApoE<sup>-/-</sup> mice (Figure 5.3). Body weight was monitored throughout the study and no differences were found between strains or between sham-operated and injured mice (Table 5.1). No differences in the whole heart weight were observed between C57BL/6 and ApoE<sup>-/-</sup> mice, while liver weight was reduced in ApoE<sup>-/-</sup> mice that underwent the vascular injury procedure compared to injured C57BL/6 mice. There was also a marked increase in spleen weight in the injured group of ApoE<sup>-/-</sup> mice in relation to their C57BL/6 injured controls.

**Table 5.1 – Body and organ weight measurements of C57BL/6 and ApoE<sup>-/-</sup> mice before and 14 days after carotid artery injury procedure.**

	C57BL/6		ApoE <sup>-/-</sup>	
	Sham	Injured	Sham	Injured
<b>Start weight (g)</b>	25.4 ± 0.9	25.6 ± 0.8	23.9 ± 0.6	24.4 ± 0.5
<b>Final weight (g)</b>	25.8 ± 1.0	26.1 ± 0.7	25.4 ± 0.8	24.5 ± 0.5
<b>Heart/Body weight (%)</b>	0.49 ± 0.02	0.48 ± 0.02	0.48 ± 0.02	0.47 ± 0.02
<b>Liver/Body weight (%)</b>	5.26 ± 0.25	5.74 ± 0.10	4.99 ± 0.20	5.18 ± 0.10 <sup>‡</sup>
<b>Spleen/Body weight (%)</b>	0.37 ± 0.03	0.31 ± 0.01	0.42 ± 0.03	0.40 ± 0.02 <sup>##</sup>

Organ weight was taken as a percentage of the body weight. <sup>‡</sup>p<0.05 and <sup>##</sup>p<0.01 vs C57BL/6 injured, n = 6-10.

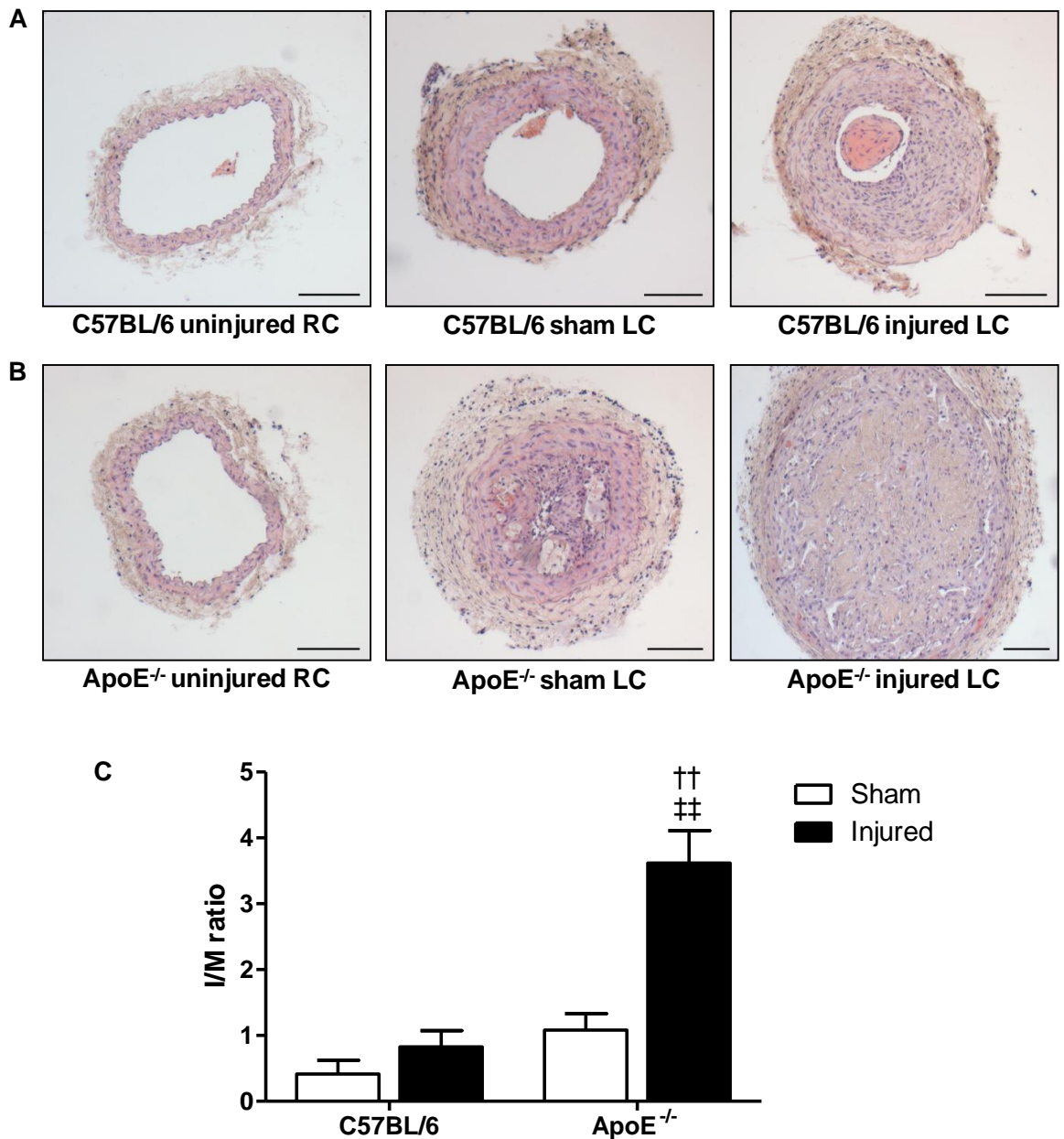


**Figure 5.1 – Neointimal growth in the carotid arteries of C57BL/6 and ApoE<sup>-/-</sup> mice after sham-operated and carotid artery injury procedure.**

Representative histological sections of the left and right common carotid arteries (LC and RC respectively) from sham-operated and injured C57BL/6 (A) and ApoE<sup>-/-</sup> mice (B) using H&E staining. Nuclei appear blue/purple whereas cytoplasm is stained pink. Neointimal growth in left carotid arteries after vascular injury was assessed as a ratio of intima to media thickness (C). Scale bar = 100  $\mu$ m, magnification x 10. <sup>††</sup>p<0.01 vs C57BL/6 injured, <sup>††</sup>p<0.01 vs ApoE<sup>-/-</sup> sham, n = 3-4.

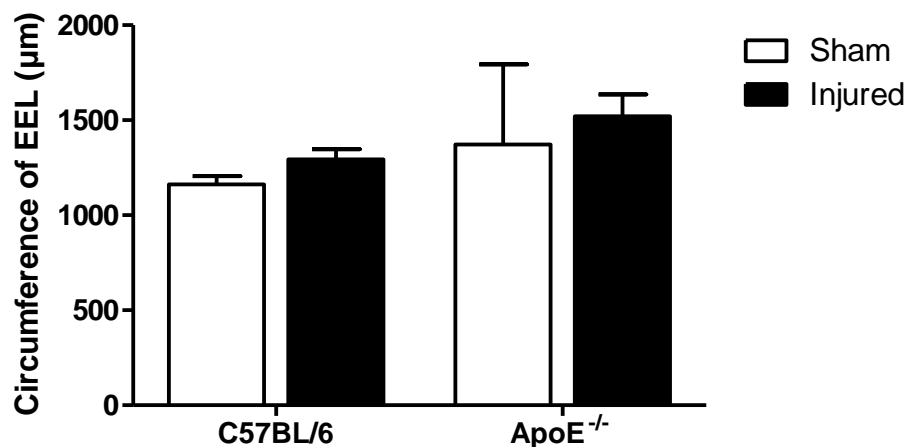


**Figure 5.2 – Circumference of carotid arteries of sham-operated and injured C57BL/6 and ApoE<sup>-/-</sup> mice.**

The EEL was measured to calculate the circumference and therefore size of the carotid artery sections in sham-operated and injured C57BL/6 and ApoE<sup>-/-</sup> mice. n = 3-4.

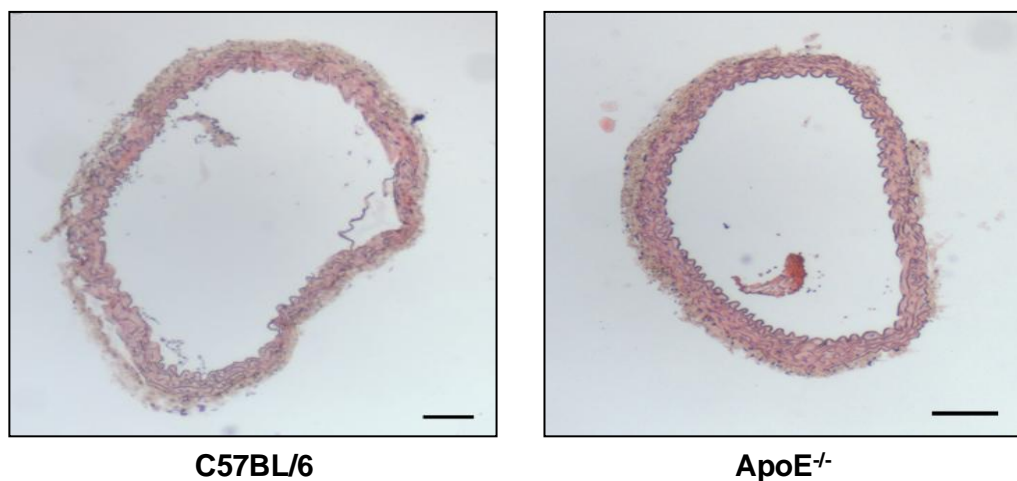


**Figure 5.3 – Aortic sections from C57BL/6 and ApoE<sup>-/-</sup> mice after carotid artery injury.**

Representative histological sections of aorta from injured C57BL/6 and ApoE<sup>-/-</sup> mice using H&E staining. Nuclei appear blue/purple whereas cytoplasm is stained pink. Scale bar = 250 µm, magnification x 4.

### **5.3.2 Structural composition of neointima in C57BL/6 and ApoE<sup>-/-</sup> mice after vascular injury**

Due to the differences observed in neointimal growth between C57BL/6 and ApoE<sup>-/-</sup> mice, the composition of the lesions in sham-operated and injured left common carotid arteries was investigated by immunohistochemistry. The contribution of VSMCs was assessed by the presence of  $\alpha$ SMA in the neointimal area (Figure 5.4). No significant differences were observed between the sections of carotid arteries from mice in each treatment group; however, a trend towards an increase in  $\alpha$ SMA was seen in sham-operated ApoE<sup>-/-</sup> mice compared to their C57BL/6 counterparts. The effect of vascular injury on remodelling processes was also assessed by expression of the proliferative marker, Ki67 and the activity of the apoptosis marker, caspase 3. There were no significant differences in the number of Ki67-positive cells in the neointima in either strain of mice or in the treatment groups (Figure 5.5). Furthermore, there was minimal caspase 3 activity in the sham-operated or injured carotid arteries in either strain of mice 14 days after procedure (Figure 5.6).

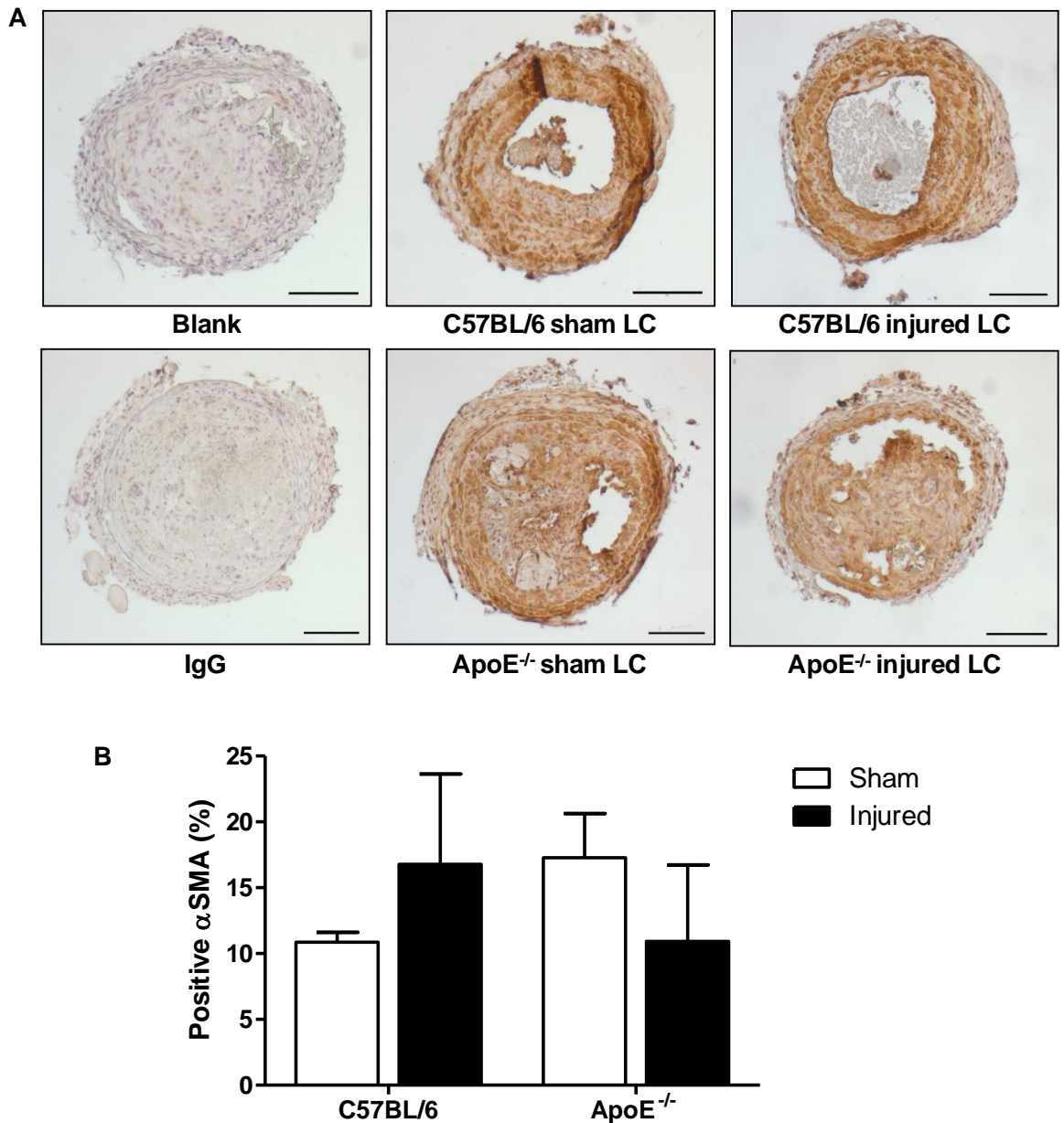


**Figure 5.4 –  $\alpha$ SMA staining in left carotid arteries of sham-operated and injured C57BL/6 and ApoE<sup>-/-</sup> mice.**

Representative histological sections of left common carotid arteries (LC) from sham-operated and injured C57BL/6 and ApoE<sup>-/-</sup> mice stained with anti- $\alpha$ SMA and counterstained with haematoxylin (A). Positive immunoreactivity for  $\alpha$ SMA was measured as a percentage of positive staining divided by the neointimal area (B). Scale bar = 100  $\mu$ m, magnification x 10. n = 3.

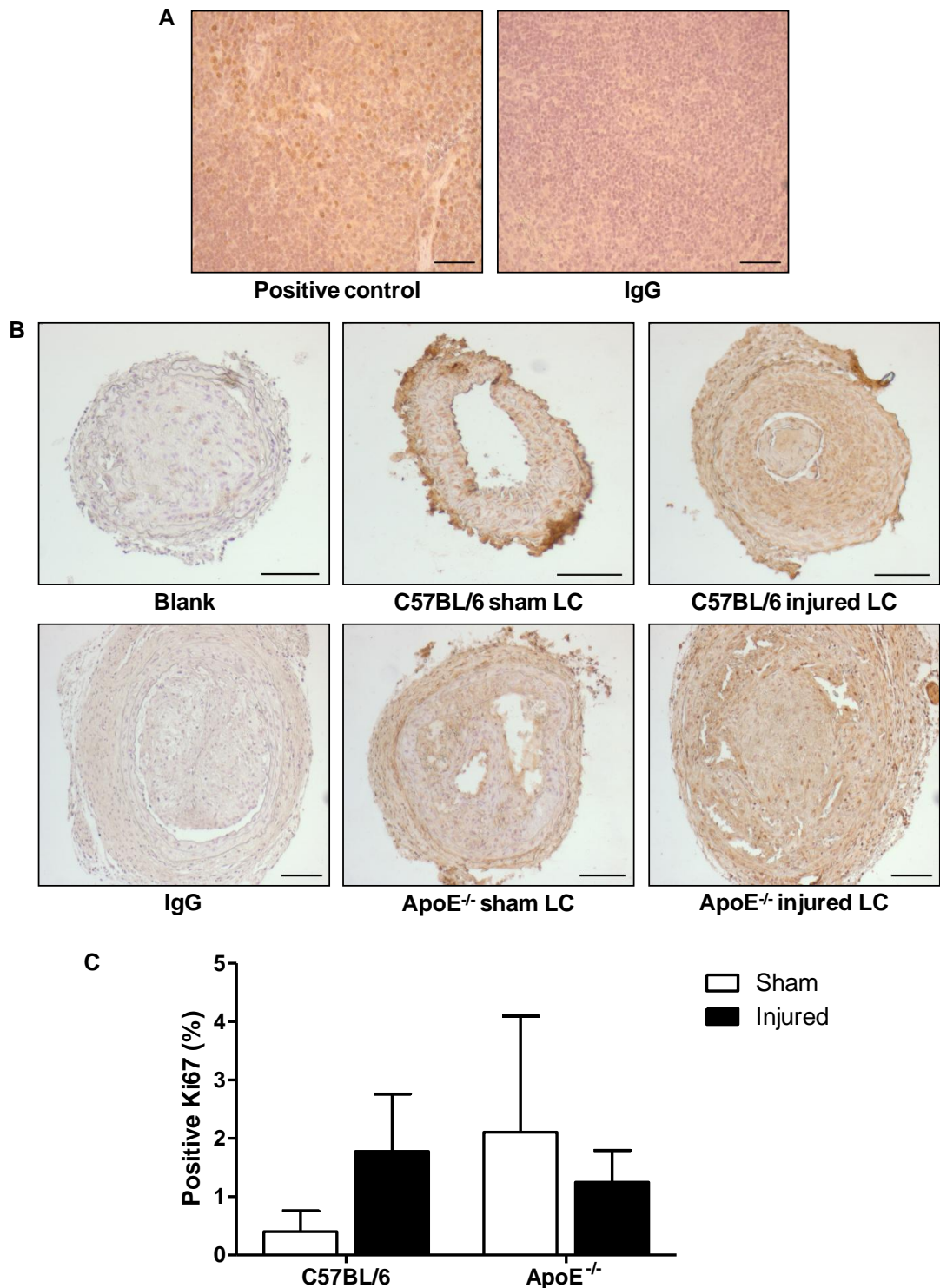


**Figure 5.5 – Ki67 staining in left carotid arteries of sham-operated and injured C57BL/6 and ApoE<sup>-/-</sup> mice.**

C57BL/6 mouse spleen was utilised as a positive control for the anti-Ki67 antibody (A). Scale bar = 50  $\mu$ m, magnification x 20. Representative histological sections of left common carotid arteries (LC) from sham-operated and injured C57BL/6 and ApoE<sup>-/-</sup> mice stained with anti-Ki67 and counterstained with haematoxylin (B). Scale bar = 100  $\mu$ m, magnification x 10. Positive immunoreactivity for Ki67 was measured as a percentage of positive staining divided by the neointimal area (C). n = 3.

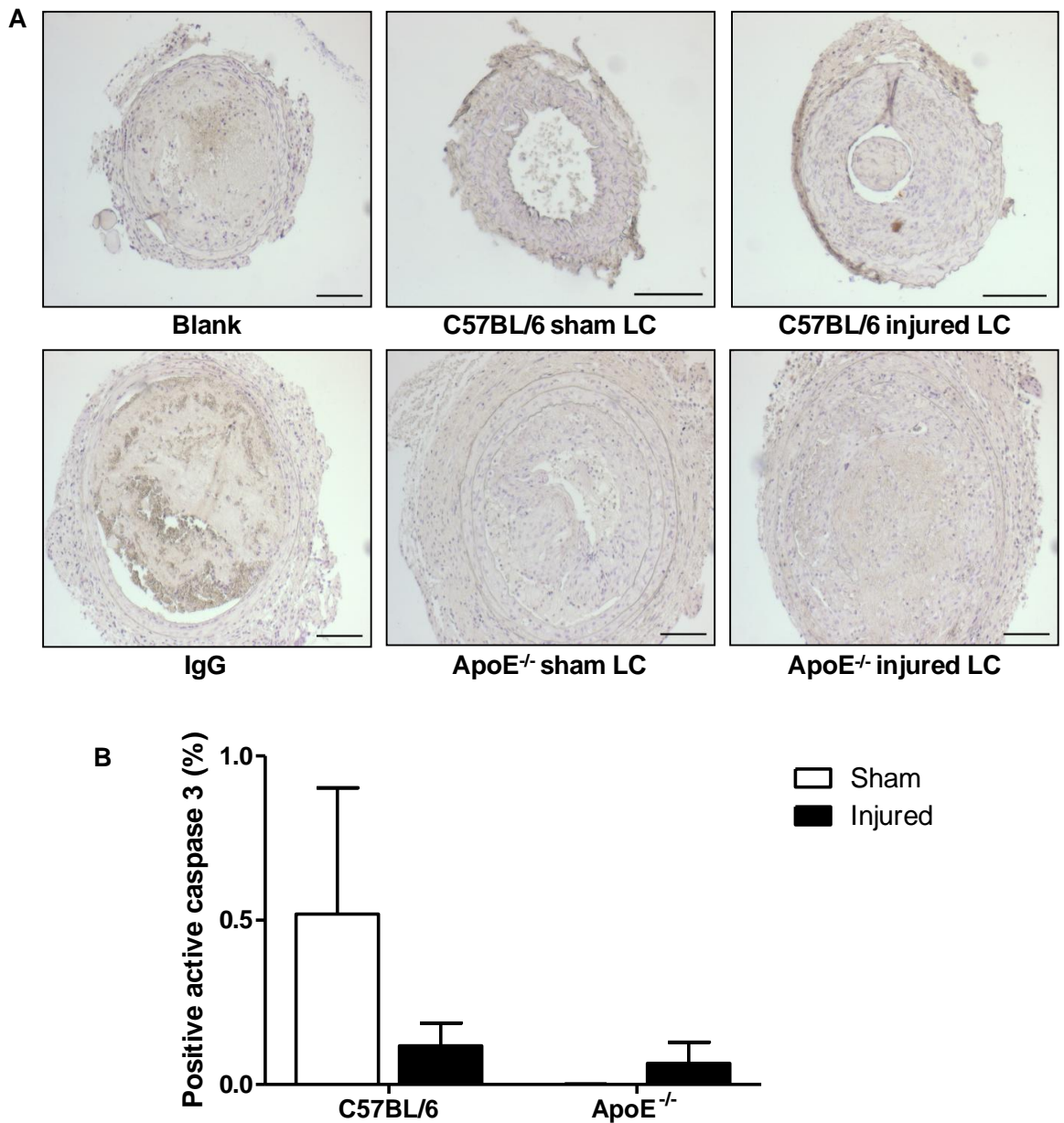


**Figure 5.6 – Active caspase 3 staining in left carotid arteries from sham-operated and injured C57BL/6 and ApoE<sup>-/-</sup> mice.**

Representative histological sections of left common carotid arteries (LC) from sham-operated and injured C57BL/6 and ApoE<sup>-/-</sup> mice stained with anti-active caspase 3 and counterstained with haematoxylin (A). Positive immunoreactivity for active caspase 3 was measured as a percentage of positive staining divided by the neointimal area (B). Scale bar = 100  $\mu$ m, magnification x 10. n = 3.

### **5.3.3 Occurrence of modified lipids in neointima formation after vascular injury**

The influence of vascular injury on the MPO content of plasma from healthy C57BL/6 mice and ApoE<sup>-/-</sup> mice fed on high fat diet for 1 month was investigated. A dramatic increase in MPO levels in sham-operated ApoE<sup>-/-</sup> mice compared to their C57BL/6 counterparts was observed from  $267.7 \pm 18.0$  ng/ml to  $865.7 \pm 117.2$  ng/ml (Figure 5.7). This increase was mirrored in the injured mice with the MPO content of plasma at  $934.3 \pm 74.5$  ng/ml in ApoE<sup>-/-</sup> mice compared to  $219.7 \pm 21.0$  ng/ml in C57BL/6 mice.

The distribution of several classes of phospholipids, present at various proportions in LDL particles including PCs, PEs, PSs and PIs as well as cholesterol and cholesteryl esters in uninjured right and injured left common carotid arteries were studied using ESMS. The differences between the two strains of mice were investigated as well as the effect of carotid artery injury. The percentage relative abundances of the signals detected from all phospholipid species in the left and right carotid arteries are displayed in Table 5.2 and 5.3 respectively.

Precursor ion scanning of m/z 184.1 in positive-ion mode is selective for SMs and PCs, the most abundant phospholipid in mammals, but showed no difference in distribution within individual samples in each group (Figure 5.8). Lysolipids were present in all samples at m/z 496.7 (16:0) and 524.7 (18:0) with significantly higher proportions relative to other signals found in ApoE<sup>-/-</sup> mice, especially in the sham-operated mice. There was an apparent reduction in lysolipids present in the uninjured right carotid arteries compared to the left. Furthermore, there was an elevation in the relative levels of PCs, m/z 758.9 (16:0/18:2) and 786.9 (18:0/18:2) in the left carotid arteries of both sham-operated and injured ApoE<sup>-/-</sup> mice which were reduced in the right carotid arteries to percentage values more similar to the C57BL/6 mice. There also appears to be a trend towards an increase in m/z 810.9 (18:0/20:4) in relation to other signals in uninjured right carotid arteries of C57BL/6 mice compared to their injured counterparts. In addition, relative levels of SM, m/z 787.9 (22:0) were significantly increased in the left carotid arteries of ApoE<sup>-/-</sup> mice with a similar trend observed in the lipid extracts from the contralateral right arteries. The spectra were then expanded between m/z 550 and 700 to display any changes in chain-shortened PCs, which are breakdown products of phospholipid oxidation, as they could be masked by the high signal of native PCs and long-chain products (Figure 5.9). Repeating signals were observed in the spectra at m/z 564, 592, 620, 648 and 676 at different

intensities within the groups suggesting a polyethylene contaminant as the peaks are separated by 28 Da and were, therefore, discounted from the analysis (Jaber and Wilkins, 2005). No detectable changes were observed in the formation of chain-shortened PCs in any of the sample groups.

Neutral loss scans for 141.1 and 87 Da were performed to detect changes in PE and PS expression respectively (Figure 5.10 and Figure 5.11). PEs and PSs were found at a much lower concentration than PCs and there was high signal to noise ratio in spectra in both left and right carotid artery samples. Precursor ion scanning for  $m/z$  241 in positive-ion mode is selective for PIs and found no significant changes across the groups (Figure 5.12). Although there were no significant changes across groups in the left carotid arteries of either strain of mice, there appeared to be an increase in relative intensity of the PI,  $m/z$  885.9 (18:0/20:4) in comparison with the uninjured right arteries. In addition to the several classes of phospholipids, precursor ion scanning for  $m/z$  369.1 was performed to detect cholesterol and cholesteryl esters present in the aortae (Figure 5.13). The major product ion for each treatment group was  $m/z$  369.6, indicating the dehydration product of protonated cholesterol. No detectable changes were observed in the formation of cholesteryl esters in any of the sample groups.

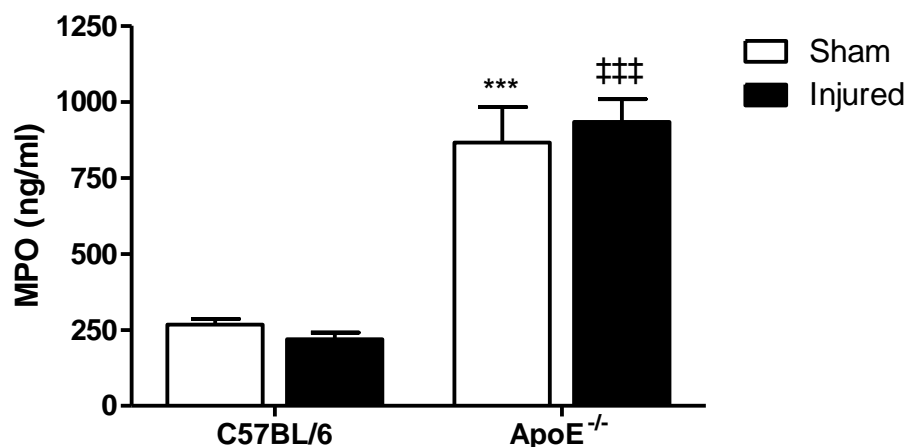


**Figure 5.7 – Effect of carotid artery injury on MPO plasma content of C57BL/6 and ApoE<sup>-/-</sup> mice.**

Blood samples were taken from each mouse at sacrifice by cardiac puncture into EDTA-coated tubes. Blood was centrifuged at 1500 x g for 10 minutes to produce plasma. The MPO content of mouse plasma was measured by an ELISA and absorbance read spectrophotometrically at 450 nm. \*\*\*p<0.001 vs C57BL/6 sham, ###p<0.001 vs C57BL/6 injured, n = 6.

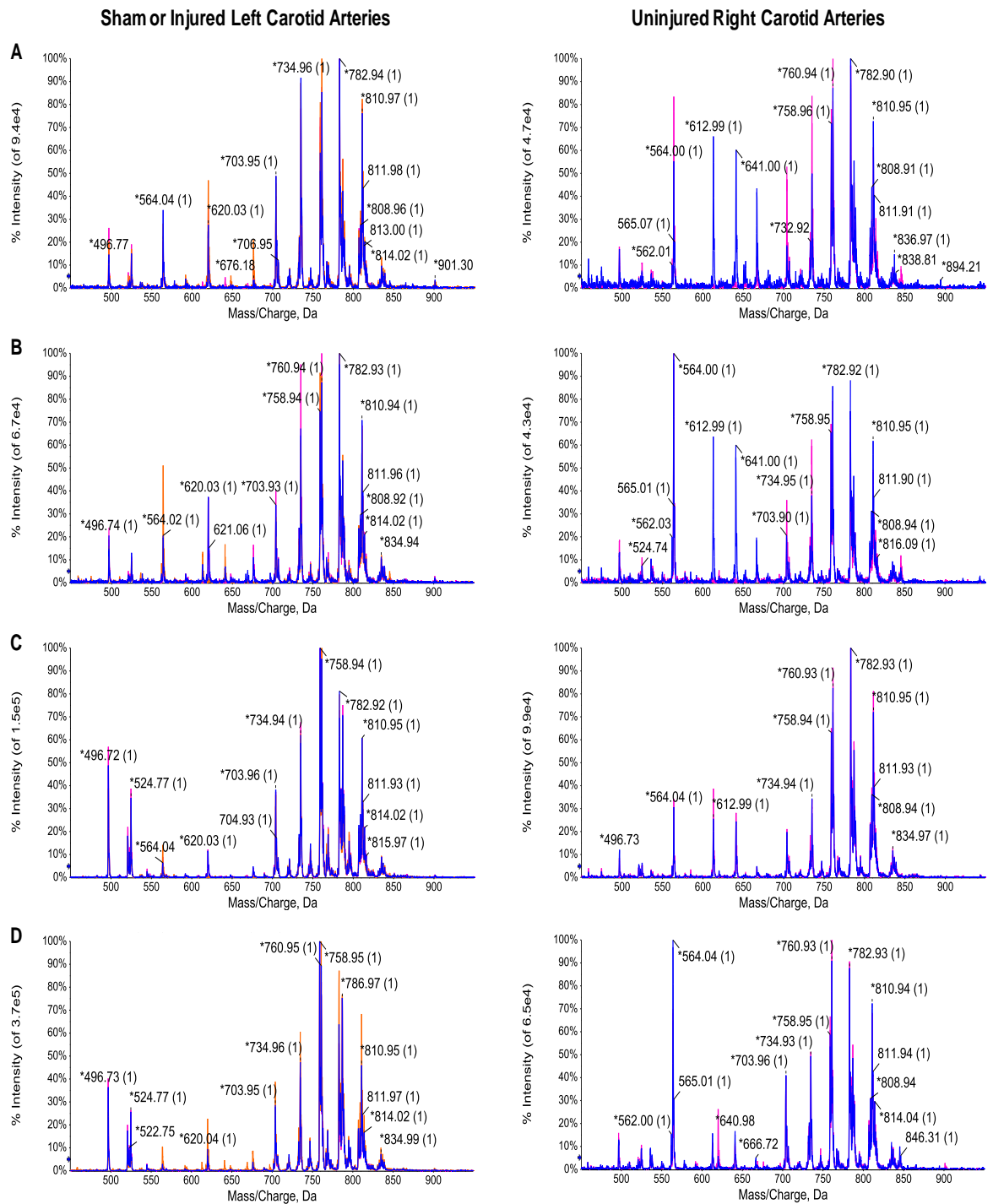


**Figure 5.8 – Detection of PCs and SMs from left and right carotid arteries of sham-operated and injured C57BL/6 and ApoE<sup>-/-</sup> mice.**

Precursor ion scanning for m/z 184.1 by positive-ionisation ESMS was performed to identify PCs and SMs present in left and right common carotid arteries from C57BL/6 sham-operated (A), C57BL/6 injured (B), ApoE<sup>-/-</sup> sham-operated (C) and ApoE<sup>-/-</sup> injured mice (D). Individual spectra were overlaid to highlight any potential differences in distributions within and between groups. n = 2-3.

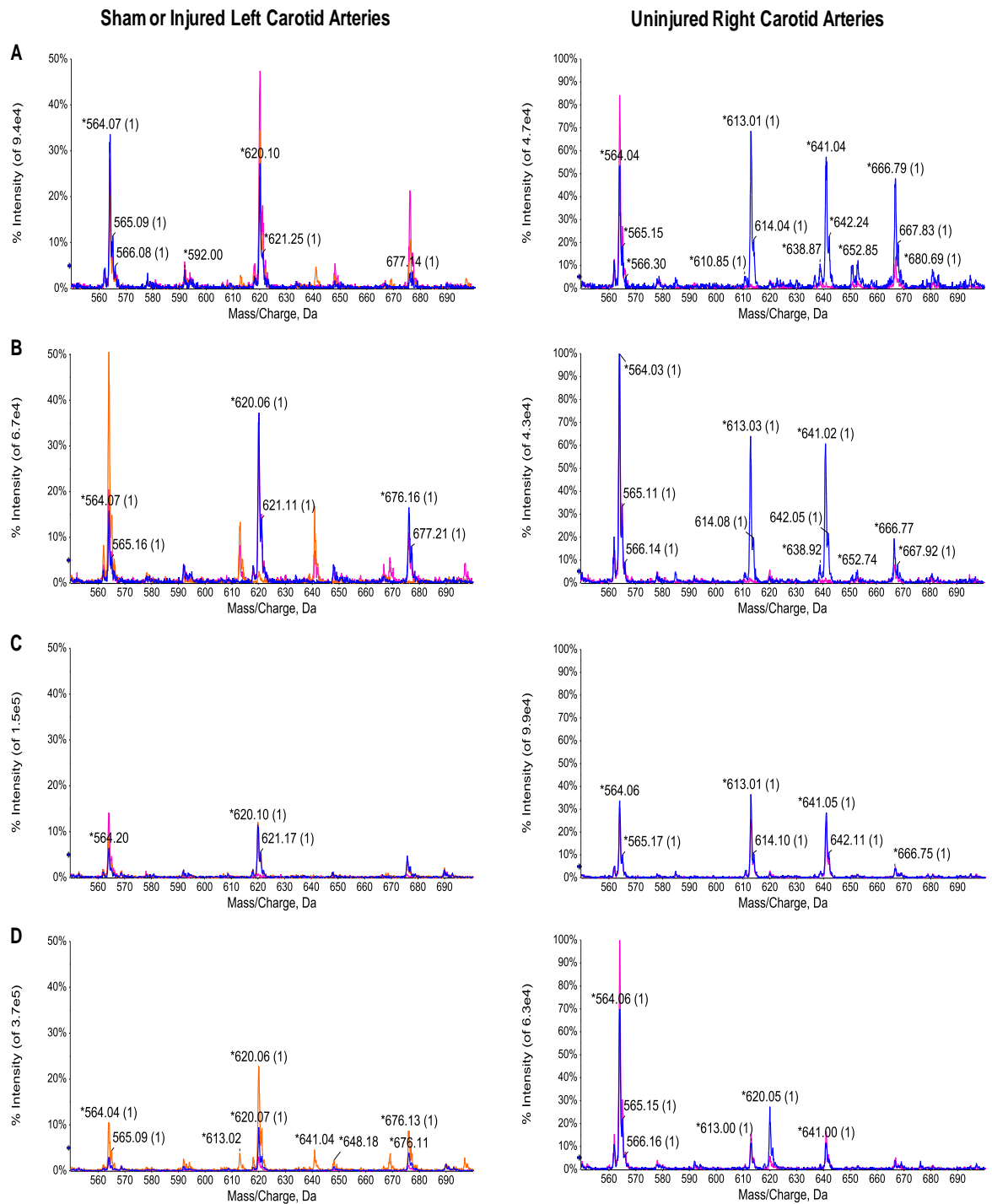


**Figure 5.9 – Detection of chain-shortened PCs from left and right carotid arteries of sham-operated and injured C57BL/6 and ApoE<sup>-/-</sup> mice.**

Precursor ion scanning for m/z 184.1 by positive-ionisation ESMS was performed to identify PCs present in left and right carotid arteries from C57BL/6 sham-operated (A), C57BL/6 injured (B), ApoE<sup>-/-</sup> sham-operated (C) and ApoE<sup>-/-</sup> injured mice (D). Individual spectra were expanded between m/z 550 and 700 to focus on chain-shortened PCs and overlaid to highlight any potential differences in distributions within and between groups. n = 2-3.

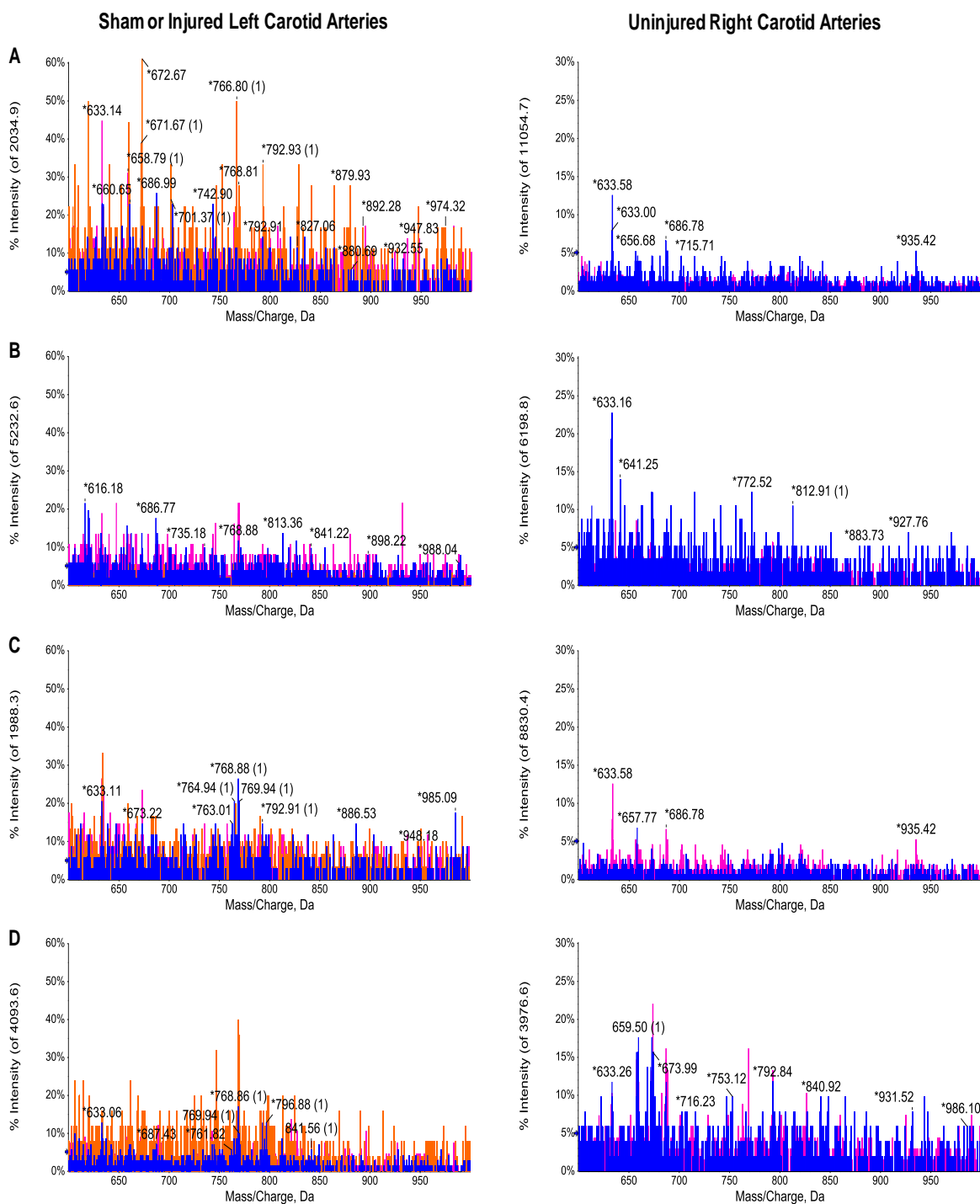


**Figure 5.10 – Detection of PEs from left and right carotid arteries of sham-operated and injured C57BL/6 and ApoE<sup>-/-</sup> mice.**

Neutral loss of 141.1 Da by positive-ionisation ESMS was performed to identify PEs present in left and right common carotid arteries from C57BL/6 sham-operated (A), C57BL/6 injured (B), ApoE<sup>-/-</sup> sham-operated (C) and ApoE<sup>-/-</sup> injured mice (D). Individual spectra were overlaid to highlight any differences in distributions within and between groups. n = 2-3.

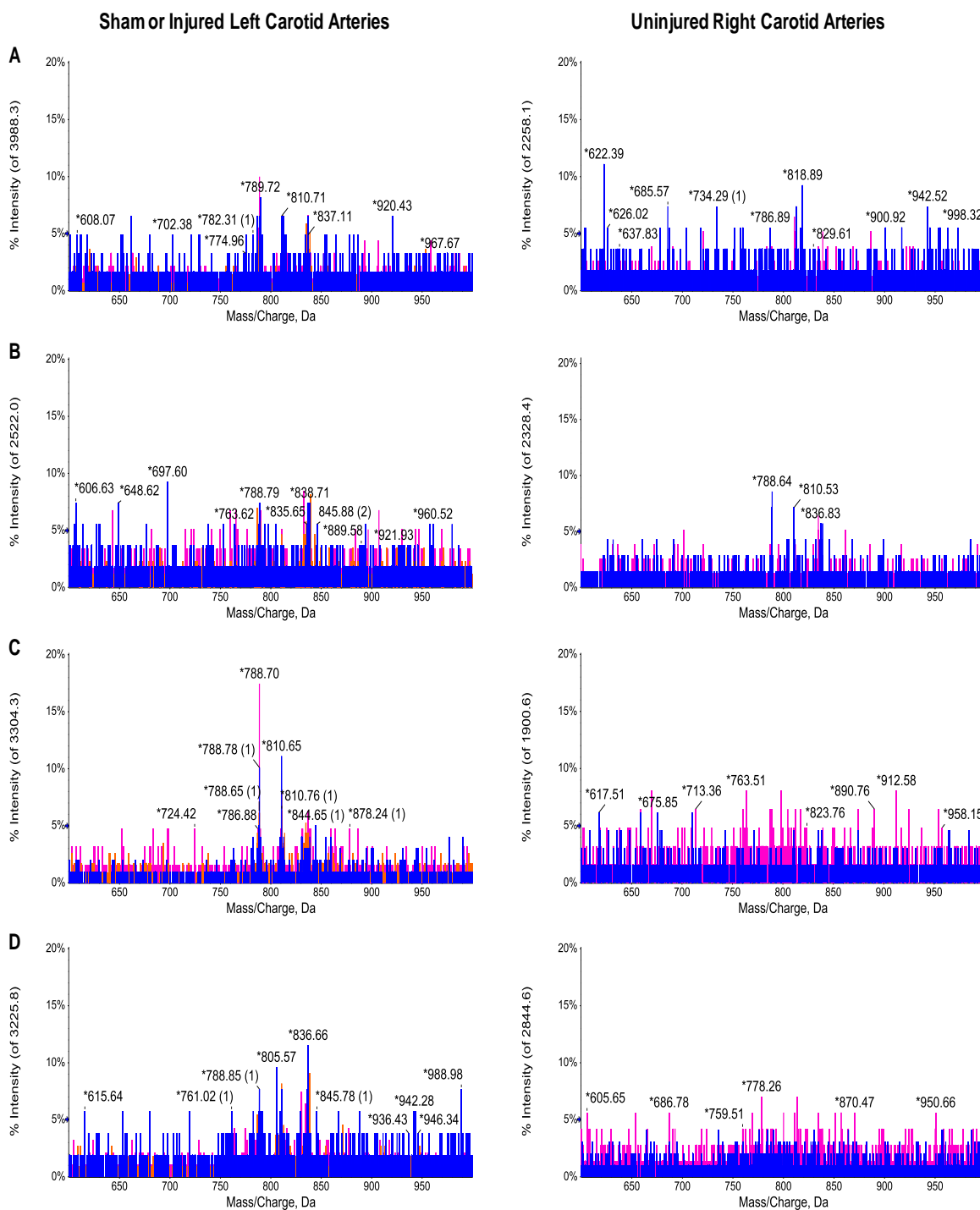


**Figure 5.11 – Detection of PSs from left and right carotid arteries of sham-operated and injured C57BL/6 and ApoE<sup>-/-</sup> mice.**

Neutral loss of 87 Da by negative-ionisation ESMS was performed to identify PSs present in left and right common carotid arteries from C57BL/6 sham-operated (A), C57BL/6 injured (B), ApoE<sup>-/-</sup> sham-operated (C) and ApoE<sup>-/-</sup> injured mice (D). Individual spectra were overlaid to highlight any differences in distributions within and between groups. n = 2-3.

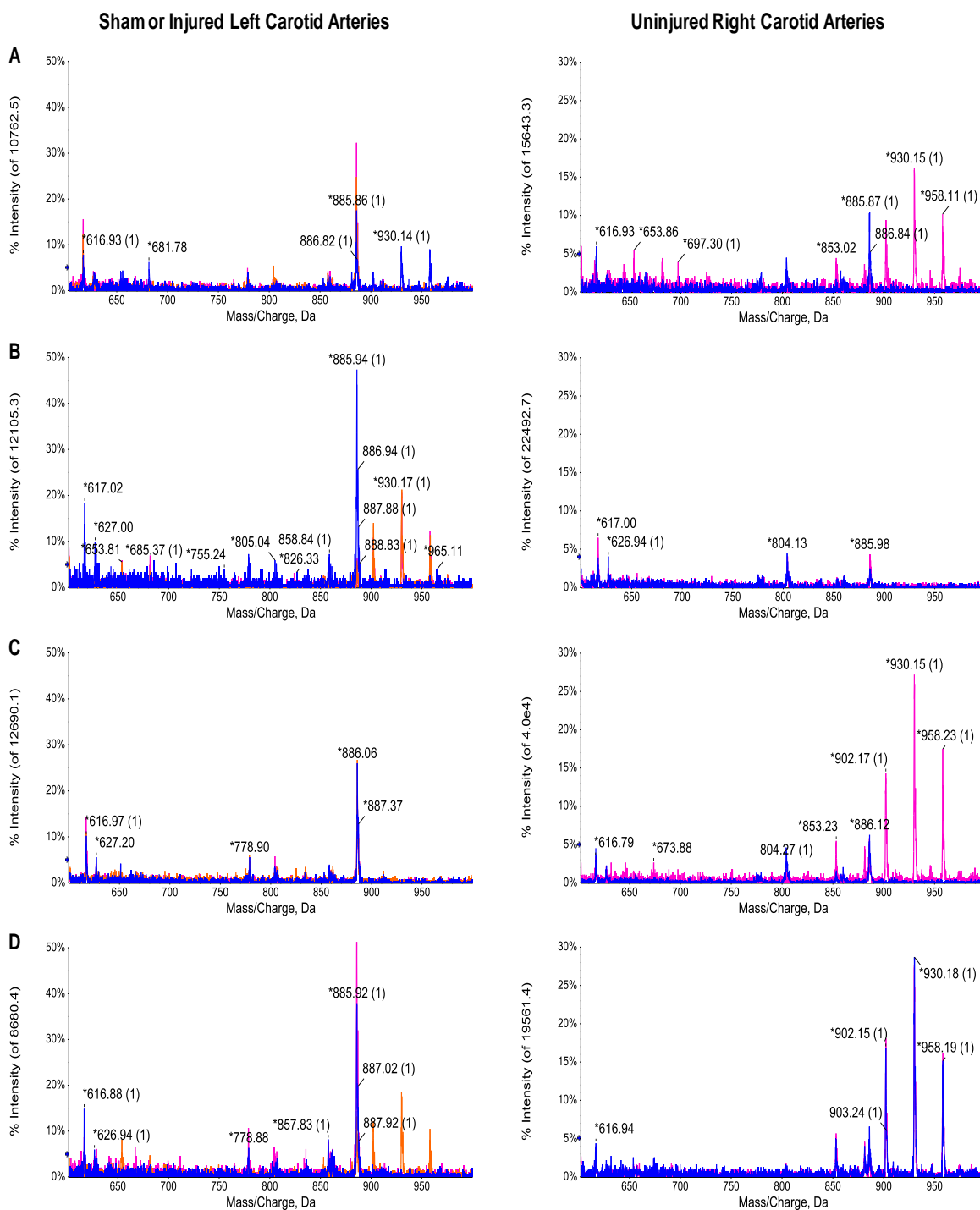


**Figure 5.12 – Detection of PIs from left and right carotid arteries of sham-operated and injured C57BL/6 and ApoE<sup>-/-</sup> mice.**

Precursor ion scanning of  $m/z$  241 by negative-ionisation ESMS was performed to identify PIs present in left and right common carotid arteries from C57BL/6 sham-operated (A), C57BL/6 injured (B), ApoE<sup>-/-</sup> sham-operated (C) and ApoE<sup>-/-</sup> injured mice (D). Individual spectra were overlaid to highlight any differences in distributions within and between groups.  $n = 2-3$ .

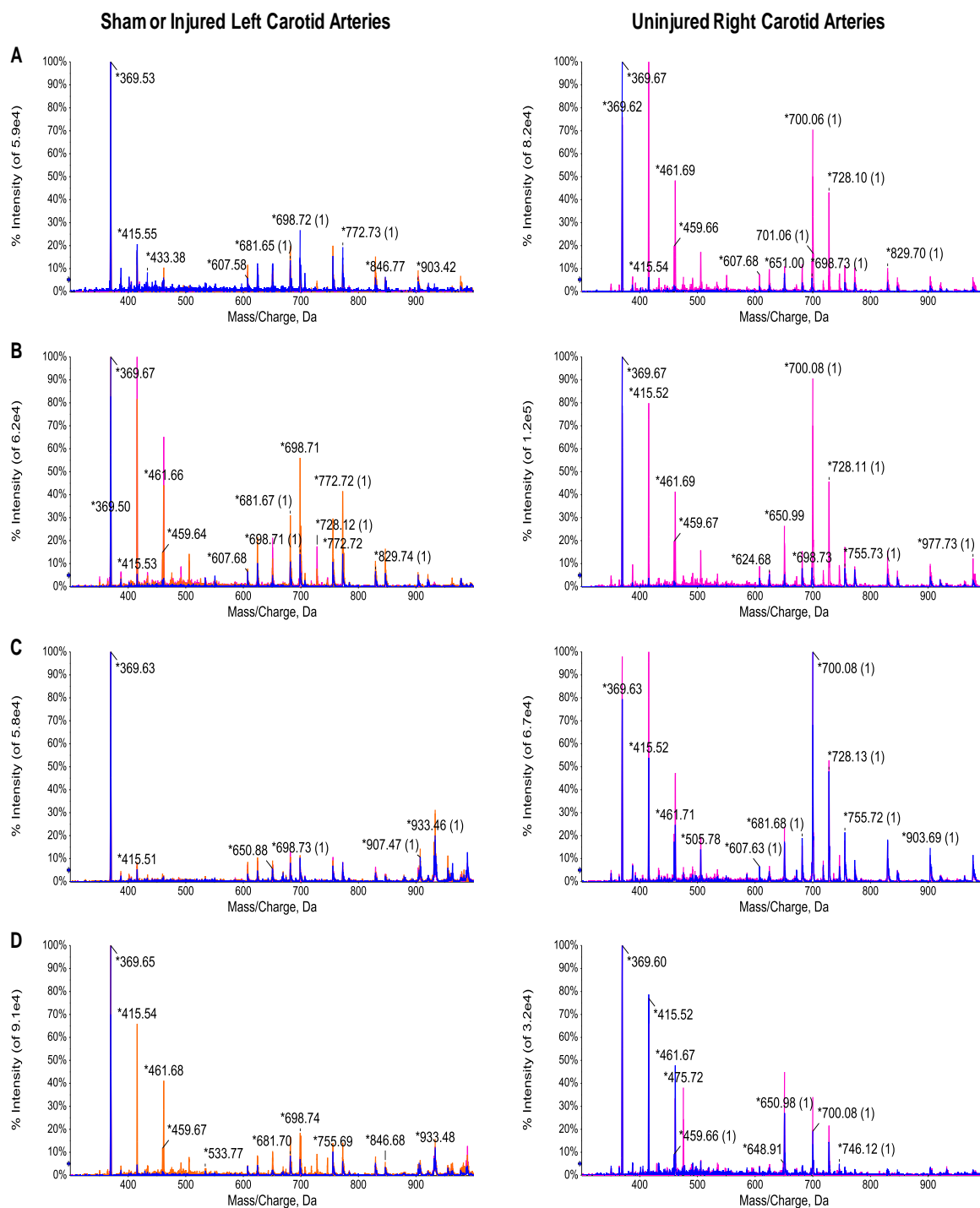


**Figure 5.13 – Detection of cholesterol and cholesteryl esters from left and right carotid arteries of sham-operated and injured C57BL/6 and ApoE<sup>-/-</sup> mice.**

Precursor ion scanning of m/z 369.1 by positive-ionisation ESMS was performed to identify cholesterol and cholesteryl esters present in left and right common carotid arteries from C57BL/6 sham-operated (A), C57BL/6 injured (B), ApoE<sup>-/-</sup> sham-operated (C) and ApoE<sup>-/-</sup> injured mice (D). Individual spectra were overlaid to highlight any differences in distributions within and between groups. n = 2-3.

**Table 5.2 – Relative abundances of detected phospholipid species in left common carotid arteries of sham-operated and injured C57BL/6 and ApoE<sup>-/-</sup> mice.**

m/z (H)	PL class	Major species	Relative abundance of ions (% of base peak)			
			C57BL/6 sham	C57BL/6 injured	ApoE <sup>-/-</sup> sham	ApoE <sup>-/-</sup> injured
496.7	LPC	16:0	20.8 ± 3.4	21.0 ± 3.1	50.5 ± 3.3 <sup>***</sup>	35.5 ± 3.4 <sup>†‡</sup>
524.7	LPC	18:0	16.8 ± 1.3	11.0 ± 1.2	34.0 ± 1.0 <sup>***</sup>	22.3 ± 1.7 <sup>†††,‡‡‡</sup>
703.9	SM	16:0	46.1 ± 3.0	34.8 ± 4.1	38.1 ± 1.4	31.3 ± 5.6
732.9	PC	16:0/16:1	17.2 ± 1.5	18.7 ± 1.4	13.9 ± 0.9	11.5 ± 2.8
734.9	PC	16:0/16:0	83.0 ± 4.7	73.5 ± 13.5	62.2 ± 3.0	52.0 ± 6.4
<b>758.9</b>	<b>PC</b>	<b>16:0/18:2</b>	<b>72.1 ± 7.1</b>	<b>84.6 ± 4.6</b>	<b>100 ± 0.0<sup>**</sup></b>	<b>100 ± 0.0</b>
760.9	PC	16:0/18:1	71.0 ± 5.1	71.4 ± 6.4	74.8 ± 5.0	68.8 ± 8.0
768.8	PE	18:0/20:4	22.4 ± 5.3	11.7 ± 6.6	19.7 ± 4.0	20.5 ± 9.9
782.9	PC	16:0/20:4	100 ± 0.0	99.5 ± 0.5	81.5 ± 5.5	75.4 ± 11.3
784.9	PC	18:0/18:3	26.6 ± 1.6	26.8 ± 0.6	27.0 ± 0.4	25.0 ± 3.1
<b>786.9</b>	<b>PC</b>	<b>18:0/18:2</b>	<b>41.4 ± 4.7</b>	<b>40.1 ± 1.0</b>	<b>60.8 ± 2.3<sup>**</sup></b>	<b>65.3 ± 1.6<sup>‡‡</sup></b>
<b>787.9</b>	<b>SM</b>	<b>22:0</b>	<b>12.8 ± 0.9</b>	<b>16.1 ± 1.01</b>	<b>22.2 ± 1.7<sup>**</sup></b>	<b>23.7 ± 0.7<sup>‡‡</sup></b>
806.9	PC	16:0/22:6	24.7 ± 1.3	24.5 ± 0.4	22.1 ± 1.5	20.1 ± 2.3
810.9	PC	18:0/20:4	69.1 ± 2.2	59.5 ± 3.1	52.0 ± 3.6	45.6 ± 9.6
813.0	SM	24:1	9.7 ± 0.5	10.1 ± 0.6	8.4 ± 1.4	7.1 ± 1.8
834.9	PC	18:0/22:6	10.0 ± 1.2	10.6 ± 0.2	7.8 ± 0.5	6.7 ± 1.2
885.9	PI	18:0/20:4	23.6 ± 3.9	19.3 ± 13.8	23.9 ± 2.7	33.5 ± 11.1

Relative abundances for each m/z value (protonated adduct ions) were calculated as a percentage of the largest peak in the individual spectra. Significant differences in distribution of ions are highlighted in bold. PL = phospholipid, LPC = lysophosphatidylcholine, ND = not detected. <sup>\*\*\*</sup>p<0.001 vs C57BL/6 sham, <sup>†</sup>p<0.05 and <sup>‡‡‡</sup>p<0.001 vs C57BL/6 injured, <sup>†</sup>p<0.05 and <sup>†††</sup>p<0.01 vs ApoE<sup>-/-</sup> sham, n = 3.

**Table 5.3 – Relative abundances of detected phospholipid species in right common carotid arteries of sham-operated and injured C57BL/6 and ApoE<sup>-/-</sup> mice.**

m/z (H)	PL class	Major species	Relative abundance of ions (% of base peak)			
			C57BL/6 sham	C57BL/6 injured	ApoE <sup>-/-</sup> sham	ApoE <sup>-/-</sup> injured
496.7	LPC	16:0	17.5 ± 0.9	16.5 ± 2.9	10.7 ± 1.3	15.4 ± 2.1
524.7	LPC	18:0	8.4 ± 2.4	8.3 ± 2.1	5.1 ± 0.4	10.8 ± 0.0
703.9	SM	16:0	36.1 ± 18.7	28.0 ± 8.1	19.9 ± 1.8	43.0 ± 1.8
732.9	PC	16:0/16:1	17.4 ± 0.5	15.7 ± 1.3	11.3 ± 3.0	16.7 ± 0.2
734.9	PC	16:0/16:0	60.3 ± 17.2	46.0 ± 13.4	29.5 ± 0.3	49.1 ± 1.3
758.9	PC	16:0/18:2	76.4 ± 4.1	68.0 ± 2.5	63.1 ± 0.8	66.8 ± 5.2
760.9	PC	16:0/18:1	75.6 ± 4.8	65.0 ± 2.8	67.4 ± 3.7	77.2 ± 6.5
782.9	PC	16:0/20:4	100 ± 0.0	81.9 ± 7.1	100 ± 0.0	95.2 ± 4.9
784.9	PC	18:0/18:3	28.1 ± 2.3	27.2 ± 0.0	31.3 ± 3.4	31.2 ± 1.6
786.9	PC	18:0/18:2	39.4 ± 6.3	31.7 ± 2.5	43.4 ± 4.3	39.5 ± 1.7
787.9	SM	22:0	11.5 ± 1.1	11.7 ± 0.3	16.1 ± 0.3	20.8 ± 0.5
806.9	PC	16:0/22:6	24.5 ± 1.4	16.4 ± 2.2	23.0 ± 0.1	21.7 ± 2.2
810.9	PC	18:0/20:4	56.7 ± 1.6	44.8 ± 5.1	63.6 ± 4.2	60.0 ± 0.8
813.0	SM	24:1	12.2 ± 0.1	10.9 ± 1.3	10.5 ± 1.8	11.5 ± 1.1
834.9	PC	18:0/22:6	7.6 ± 0.3	7.3 ± 0.3	10.4 ± 0.5	9.8 ± 0.8
885.9	PI	18:0/20:4	4.6 ± 4.6	3.3 ± 0.9	5.0 ± 0.5	2.6 ± 2.6

Relative abundances for each m/z value (protonated adduct ions) were calculated as a percentage of the largest peak in the individual spectra. PL = phospholipid, LPC = lysophosphatidylcholine, ND = not detected. n = 2.

### **5.3.4 Role of AMPK in neointima formation**

AMPK, involved in energy homeostasis, has been recently implicated in restenosis and therefore its expression in sham-operated and injured carotid arteries from the two mouse strains was studied. The total amount of AMPK $\alpha$  was found to be elevated in injured carotid arteries in both strains but there was only a significant increase in sham-operated ApoE<sup>-/-</sup> mice compared to their C57BL/6 counterparts (Figure 5.14). In addition, there was minimal phosphorylated AMPK $\alpha$  present in the sham-operated or injured carotid arteries in either strain of mice 14 days after procedure. However, there was a trend towards an increase in phosphorylation in the ApoE<sup>-/-</sup> mice compared to the C57BL/6 mice (Figure 5.15).

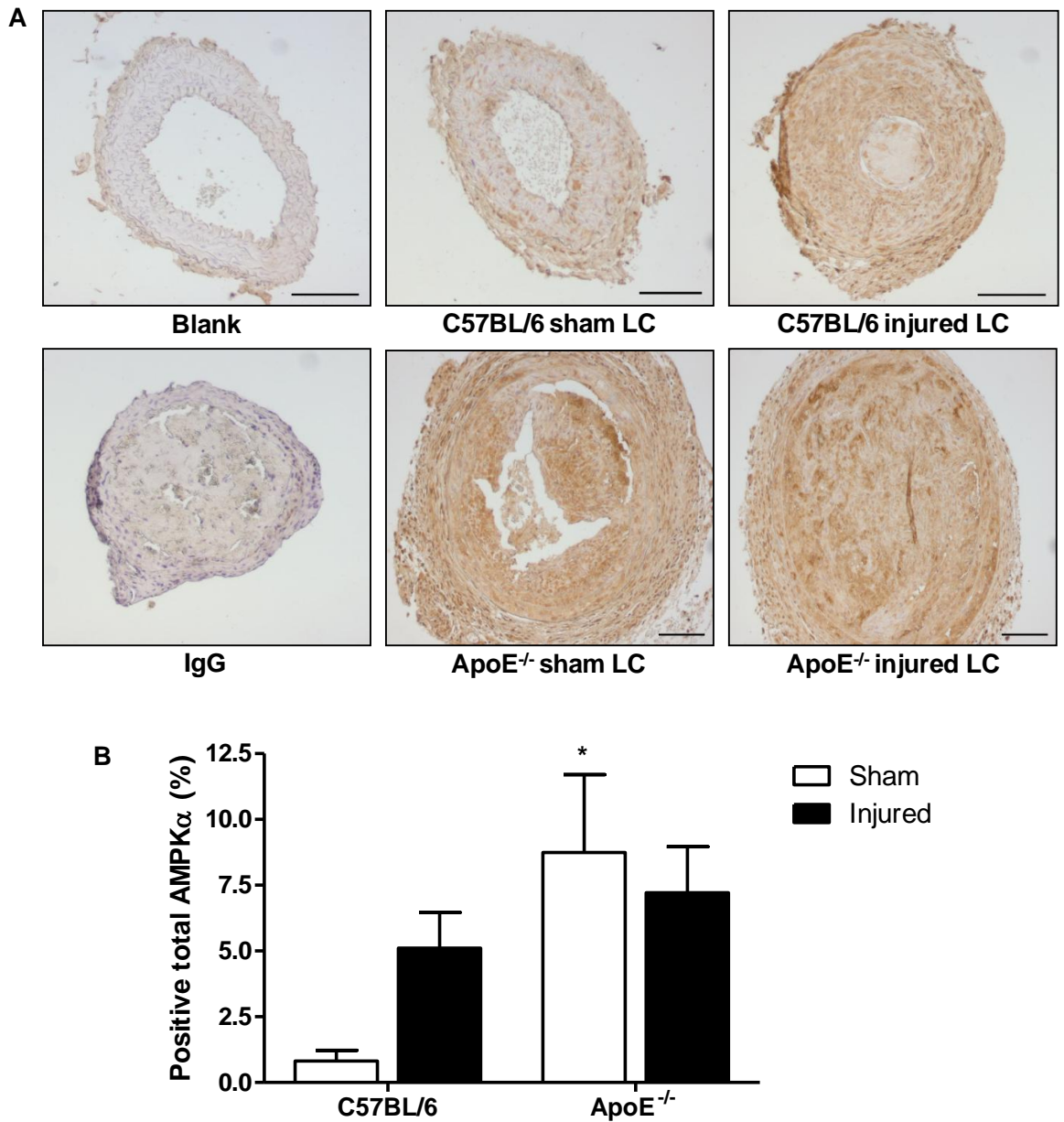


**Figure 5.14 – Total AMPK $\alpha$  staining in left carotid arteries from sham-operated and injured C57BL/6 and ApoE<sup>-/-</sup> mice.**

Representative histological sections of left common carotid arteries (LC) from sham-operated and injured C57BL/6 and ApoE<sup>-/-</sup> mice stained with anti-total AMPK $\alpha$  and counterstained with haematoxylin (A). Positive immunoreactivity for total AMPK $\alpha$  was measured as a percentage of positive staining divided by the neointimal area (B). Scale bar = 100  $\mu$ m, magnification x 10. n = 3-4.

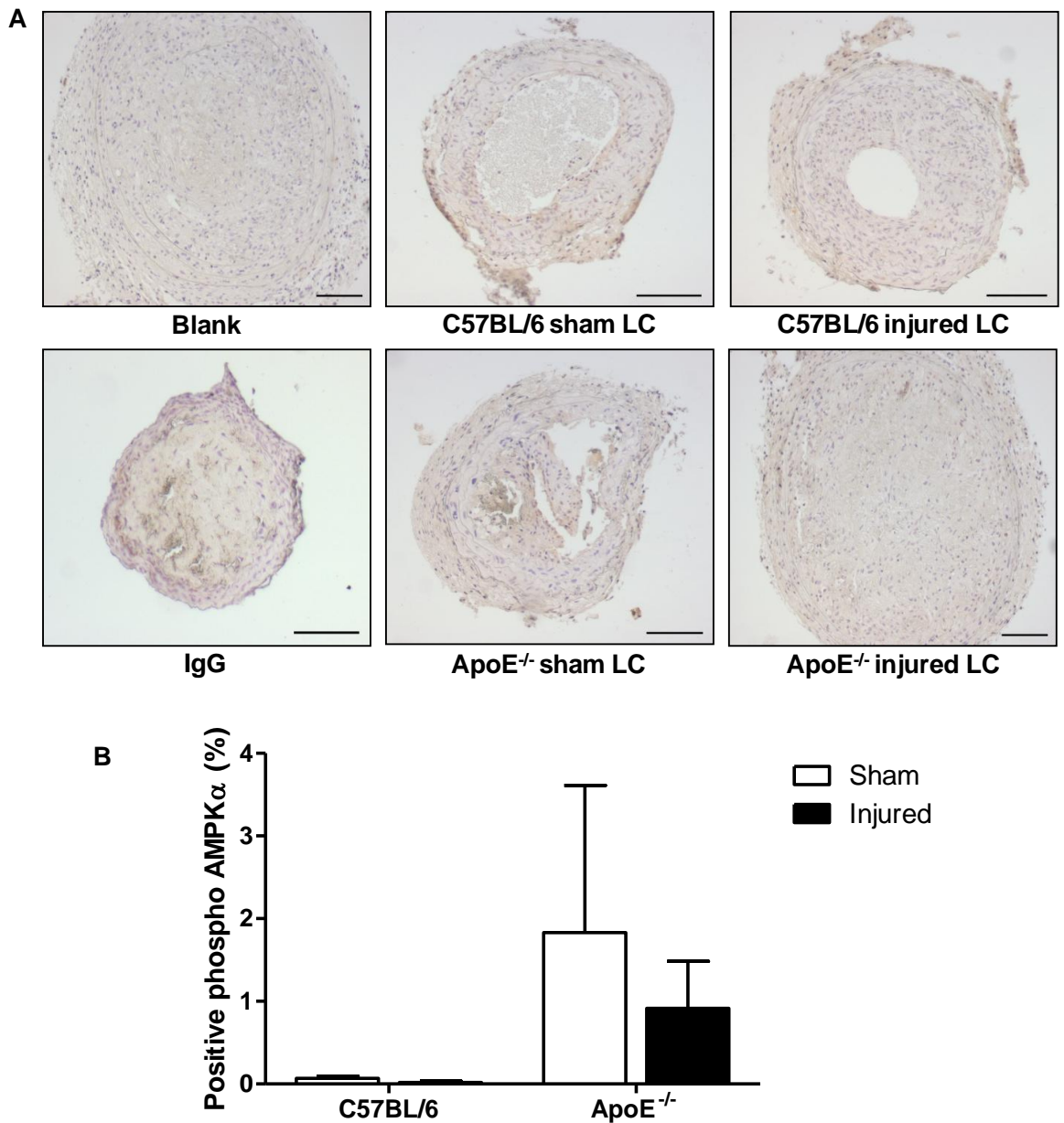


**Figure 5.15 – Phosphorylated AMPK $\alpha$  staining in left carotid arteries from sham-operated and injured C57BL/6 and ApoE<sup>-/-</sup> mice.**

Representative histological sections of left common carotid arteries (LC) from sham-operated and injured C57BL/6 and ApoE<sup>-/-</sup> mice stained with anti-phosphorylated AMPK $\alpha$  and counterstained with haematoxylin (A). Positive immunoreactivity for phosphorylated AMPK $\alpha$  was measured as a percentage of positive staining divided by the neointimal area (B). Scale bar = 100  $\mu$ m, magnification x 10. n = 3-4.

## 5.4 Discussion

The present study characterises for the first time the phospholipid molecular species present in the carotid arteries of C57BL/6 and ApoE<sup>-/-</sup> mice after carotid artery injury. Increased neointima formation was observed in injured ApoE<sup>-/-</sup> mice compared with sham-operated controls and healthy C57BL/6 mice treated in the same way. Plasma MPO and LPCs were also found to be elevated in ApoE<sup>-/-</sup> mice and vascular injury altered the relative proportions of several PCs present in the arterial wall of ApoE<sup>-/-</sup> mice compared with C57BL/6 mice. Total AMPK expression was also increased in sham-operated ApoE<sup>-/-</sup> mice compared to their C57BL/6 counterparts.

After PCI and mechanical injury to the arterial wall, neointima formation occurs mainly by the proliferation and migration of VSMCs leading to a narrowing of the previously stenotic vessel. In this study, the left common carotid artery was injured by insertion of a flexible nylon wire several times to cause endothelial denudation and then subsequently ligated. The same procedure was performed for the sham-operated mice without the insertion of the nylon wire. This means there was mechanical injury to the carotid artery due to removal of the endothelium as well as stretching of the vessel. The blood flow was also disrupted in this study due to ligation of the artery which has been utilised by many other studies and could induce unrelated compensatory mechanisms (Kumar and Lindner, 1997, Godin *et al.*, 2000, Kawasaki *et al.*, 2001). However, vascular lesions in humans can develop at sites where haemodynamics are altered and are often associated with low shear stress (Ku *et al.*, 1985). In this study, neointima formation was dramatically increased in injured ApoE<sup>-/-</sup> mice compared to their sham-operated controls, while no significant differences were observed in healthy C57BL/6 mice treated in the same way. This observation has previously been seen following both wire and balloon injuries in ApoE<sup>-/-</sup> mice (Zhu *et al.*, 2000, Grassia *et al.*, 2009, Matter *et al.*, 2006). In addition, overexpression of human apoE3 transgene in mice resulted in a reduction in neointimal formation (Zhu *et al.*, 2000). This suggests that there is an increased susceptibility for neointima formation in mice deficient in apoE compared to healthy controls. ApoE has previously been shown to exhibit cytostatic effects causing the inhibition of PDGF-induced VSMC proliferation and migration by growth arrest in the G0 phase of the cell cycle (Ishigami *et al.*, 1998). LDL receptor-related protein (LRP) has also been implicated in the enhanced rate of VSMC proliferation and migration found in atherosclerosis, as apoE was unable to inhibit PDGF-induced VSMC migration in VSMCs deficient in LRP (Swertfeger *et al.*, 2002). Together, this suggests that PDGF signalling is altered in ApoE<sup>-/-</sup> mice which

may explain the significant increase in neointimal growth observed in injured carotid arteries of ApoE<sup>-/-</sup> mice compared to their C57BL/6 controls. As the flexible nylon wire was extended to the aortic arch and aorta, H&E staining was performed to examine any damage in this region. No differences in the morphology of the aorta in either strain of mouse were seen or any atherosclerotic plaque formation in the ApoE<sup>-/-</sup> mice. This could be due to the length of time the mice were on the high fat diet; however the first signs of disease have previously been reported at 6 to 8 weeks without the high fat diet to accelerate the progression (Nakashima *et al.*, 1994, Coleman *et al.*, 2006). The high levels of circulating cholesterol-containing lipoproteins could be deposited in the denuded area of the injured carotid artery as disruption of the endothelium is critical in the initiation of atherosclerotic plaque and foam cell formation.

The structural composition of the neointima was investigated in both C57BL/6 mice and ApoE<sup>-/-</sup> mice by immunohistochemistry. No change in Ki67 or active caspase 3 expression was observed in the strain of mouse or in sham-operated or injured vessels. This could be due to the small sample size available or the 14 day time point studied. Many studies investigating neointima formation have looked at different time points post-operation. Apoptosis was found to be elevated 1 hour and 1 day after balloon distension injury in ApoE<sup>-/-</sup> mice while proliferation was increased 7 and 28 days post injury (Matter *et al.*, 2006). An increase in VSMC apoptosis via a caspase 3 dependent mechanism was also upregulated 24 hours after procedure in balloon injured New Zealand white rabbits (Spiguel *et al.*, 2010). In contrast, cell proliferation was found to peak approximately 4 days prior to the peak in apoptosis after angioplasty in atherosclerotic rabbits (Durand *et al.*, 2002). There was also evidence of apoptosis in patients undergoing either directional atherectomy for primary atherosclerotic lesions or recurrent arterial narrowing but it was typically limited to less than 2 % of cells in the specimen (Isner *et al.*, 1995). This study is in agreement, as minimal caspase 3 activity was detected 14 days after the vascular injury procedure. In contrast, an increase in proliferation was still evident in these studies 14 days after surgery. In the present study, it must be remembered that the carotid arteries were injured as well as ligated causing a change in the haemodynamics of the vessel. This in turn may have led to a faster response as mechanisms were occurring to compensate for both the change in vessel diameter as well as the removal of endothelium causing complete occlusion in a number of vessels. In addition to markers of the remodelling processes, there was no change in  $\alpha$ SMA between different strains of mice, between sham-operated or injured vessels with  $\alpha$ SMA accounting for between 10 and 15 % of the neointimal area. Proliferation and migration of VSMCs is one of the hallmarks of restenosis resulting in

intimal thickening with both non-dividing and proliferating VSMCs contributing to the neointima (Clowes and Schwartz, 1985). Quiescent VSMCs are normally maintained in a nonproliferative phase but become activated after mechanical injury to the arterial wall. There is a decrease in VSMC differentiation markers in intimal VSMCs 7 days after injury; this returns to normal levels by day 14 (Regan *et al.*, 2000). This phenotypic modulation of VSMCs after injury results in the increased propensity of these cells to proliferate and migrate resulting in neointima formation. Although, there was no difference between strains of mice in the extent of  $\alpha$ SMA present or proliferative index at day 14, the neointimal growth was greater in the injured ApoE<sup>-/-</sup> mice suggesting that proliferation occurred at an earlier time point.

In addition to the effects of vascular injury on VSMC remodelling processes, the lipid involvement in neointima formation in injured carotid arteries was investigated. The enhanced inflammatory state after vascular injury results in recruitment of inflammatory cells such as neutrophils which could lead to an increase in the production of reactive oxidants and therefore modified lipids in the neointima by the action of the MPO system. The plasma MPO content was found to be elevated in ApoE<sup>-/-</sup> mice compared to C57BL/6 mice controls. Incubation of MPO and its product, HOCl in a temporarily isolated carotid artery was found to induce neointima hyperplasia in a rat model (Yang *et al.*, 2006). In addition, HOCl-induced apoptosis, in both the intima and medial layers, was followed by a proliferative response (Yang *et al.*, 2006). In this study, only the plasma MPO was measured and therefore the levels in the neointima could be greater due to the infiltration of inflammatory cells at the site of injury leading to the secretion of MPO. The levels of MPO have been shown to be elevated in human atherosclerotic plaques and therefore a similar effect could be found in restenotic lesions (Daugherty *et al.*, 1994). It would be beneficial to measure the levels of circulating neutrophils in C57BL/6 and ApoE<sup>-/-</sup> mice to establish if this accounts for the elevation in plasma MPO.

MPO is a known route for producing modified lipids *in vivo*; both chlorinated and oxidised species. The distribution of several classes of phospholipids, including the main phospholipids present in LDL particles such as PCs, PEs, PSs and PIs as well as cholesterol and cholesteryl esters was assessed in uninjured right and injured left common carotid arteries. ESMS was utilised to detect different classes of modified lipids as precursor ion and neutral loss scanning allows the detection of certain types of phospholipids or oxidised products but does not specify individual species (Spickett *et al.*, 2011). Analysis of the injured and uninjured carotid arteries identified PCs, LPCs, SMs and PIs as well as

cholesterol present within the samples. There were increased relative levels of lysolipids at  $m/z$  496.7 and 524.7 in ApoE<sup>-/-</sup> mice compared to the contralateral right carotid arteries and the C57BL/6 control mice. Lysolipids have previously been found to be elevated in the intima and inner media of the atherosclerotic aorta of squirrel monkeys (Portman and Alexander, 1969). Chlorohydrins of polyunsaturated phospholipids have been reported to break down readily to lysolipids (Arnhold *et al.*, 2002). Lysophosphatidylcholine has also been shown to stimulate expression of MCP-1 in rat aortic VSMCs as well as induce pro-inflammatory cytokine production and recruitment of monocytes (Rong *et al.*, 2002, Olofsson *et al.*, 2008). This could therefore lead to an exacerbated inflammatory response which in turn could increase the production of modified lipids within the atherosclerotic plaque as well as at the site of injury. Phospholipid chlorohydrins have yet to be observed in diseased vessels *in vivo* while lysophosphatidylcholine-chlorohydrins have been detected in human atherosclerotic plaques with a 60-fold increase in human tissue compared to control (Messner *et al.*, 2008b). The precursor ion scan for  $m/z$  184.1 displayed roughly similar distribution of PCs and SMs between groups and contralateral carotid arteries; however, an increase in relative abundance of  $m/z$  758.9 and 786.9 was observed in left carotid arteries of ApoE<sup>-/-</sup> mice compared to injured C57BL/6 carotid arteries. These peaks likely corresponds to the protonated adducts of PCs, 16:0/18:2 and 18:0/18:2 respectively. A trend towards an increase in  $m/z$  810.9 in relation to other signals was also observed in the uninjured right carotid arteries of ApoE<sup>-/-</sup> mice compared to their injured counterparts, corresponding to the protonated adduct of PC 18:0/20:4. This suggests that injured carotid arteries are enriched with linoleoyl-containing PCs. These unsaturated phospholipids could then undergo modification by MPO leading to an increase in modified lipids present at the site of injury. There was also a relative increase in  $m/z$  787.9 in left carotid arteries of ApoE<sup>-/-</sup> mice, which likely corresponds to the protonated adduct of SM 22:0. Elevated levels of plasma SM have previously been shown to be a risk factor in CAD which is often associated with atherosclerosis (Jiang *et al.*, 2000). Chain-shortened PCs were not detected which could be due to low concentrations compared to their native phospholipids within these samples or they may be metabolised or detoxified *in vivo* (Spickett *et al.*, 2011). Separation of oxidation products by coupling liquid chromatography to ESMS could provide more insight into their presence and role in neointima formation.

Similarly to PCs and SMs, the distribution and proportions of PEs, PSs and PIs were also investigated. There was a low signal to noise ratio in the spectra of PEs and PSs, suggesting that these phospholipids were present at low levels within both injured and

uninjured arteries; therefore it was not possible to obtain sufficiently adequate data to determine whether differences occurred between these groups. There was an apparent relative increase in  $m/z$  885.9 in injured vessels compared to their uninjured controls, corresponding to the protonated adduct of PI 18:0/20:4. This suggests that increased levels of PIs are associated with lesion formation. Moreover, precursor scanning of  $m/z$  369.1 was utilised for detection of cholesterol and cholesteryl esters present in carotid arteries of C57BL/6 and ApoE<sup>-/-</sup> mice. The protonated dehydration product of cholesterol,  $m/z$  369.6, was consistently the largest peak in all samples. Together, this highlights a difference in proportion of several phospholipids present in carotid arteries of ApoE<sup>-/-</sup> mice after the vascular injury procedure compared to the uninjured contralateral artery and the healthy mice controls. In addition, the detection of chlorinated lipids in the vessels was not performed due to time constraints. The high levels of plasma MPO in ApoE<sup>-/-</sup> mice would suggest an increase in the presence of HOCl-modified lipids in the vessels and further analysis of these samples would give a more complete indication of the occurrence of modified lipid species in the vascular wall.

A limitation of the present study is the lack of internal or external standards in the ESMS analysis of the injured and uninjured carotid arteries. Standards are commonly used as quantification of levels within samples by the addition of a lipid at a known concentration. Saturated lipids can also be used as a “base peak” in spectra for example  $m/z$  734 (PC 16:0/16:0), for comparison of peak intensities with signals from mono- and polyunsaturated lipids. However, in these spectra  $m/z$  734.9 was found to vary between samples and therefore not suitable for this role. This could reflect the oxidation of polyunsaturated lipids such as  $m/z$  758.9 and 782.9, therefore their intensity is reduced and the levels of saturated lipids (such as  $m/z$  734.9) appear to fluctuate. In contrast, there would be further limitations in using standards in these samples as the sizes of the arteries varied and were not weighed before lipid extraction, thus the lipid concentrations cannot be calculated. The amount of lipid is likely to vary within the artery therefore, while standards may indicate the absolute concentration, all lipids should fluctuate depending on the total lipid content extracted. Comparisons were made instead between the relative intensities of the lipids present in these samples, which allow information about changes in the lipid profile in the different strains and in response to treatments. It should also be noted that ESMS is not a quantitative technique in itself, due to the different ionisation efficiencies of lipid classes, therefore PC levels cannot be directly compared with PEs or PSs, *etc.* There is also further variation within the PC class as short chains ionise better than long chains. However, all these differences should be the same between samples, thus

it is valid to look for changes in relative intensities and patterns between samples in this study.

In addition to the modified lipids present in the neointima, AMPK has recently been implicated in vascular disease as it has been shown to suppress VSMC proliferation (Nagata *et al.*, 2004, Igata *et al.*, 2005, Peyton *et al.*, 2011). In the previous chapter, AMPK signalling was found to alter the effect of modified lipids on vascular remodelling processes. In this study, total AMPK $\alpha$  was found to be significantly increased in neointimal growth in sham-operated ApoE<sup>-/-</sup> mice compared to their C57BL/6 counterparts. This could be due to an increase in cell number within the neointima formation resulting in an increase in AMPK present. Minimal phosphorylated AMPK $\alpha$  was detected in the neointimal sections; however, there was a trend towards an increase in the ApoE<sup>-/-</sup> mice. Deletion of the AMPK $\alpha$ 2 subunit in mice has been shown to cause an increase in neointima formation and VSMCs derived from aorta of AMPK $\alpha$ 2<sup>-/-</sup> mice were found to exhibit increased proliferation rate compared to wild type and AMPK $\alpha$ 1<sup>-/-</sup> mice (Song *et al.*, 2011). In addition, decreased AMPK activity in VSMCs has been associated with receptor for advanced glycation endproducts (RAGE) ligand-induced signalling to promote neointima formation in mice (Yu *et al.*, 2012). Together, this suggests a protective role of AMPK in neointima formation and the elevation of total AMPK in neointima observed in this study could be a compensatory mechanism to combat the neointimal growth.

## 5.5 Conclusions

In summary, increased neointima formation was observed in injured ApoE<sup>-/-</sup> mice compared to C57BL/6 mice and sham-operated controls, while there was no change in  $\alpha$ SMA, Ki67 or active caspase 3 expression in any treatment groups 14 days after surgery. Plasma MPO content was elevated and altered phospholipid levels in ApoE<sup>-/-</sup> mice were observed with a large increase in the formation of lysolipids. Total AMPK $\alpha$  expression was also increased in ApoE<sup>-/-</sup> mice compared to their C57BL/6 counterparts. This is the first study to investigate the effects of carotid artery injury on the lipid profile in neointima formation in C57BL/6 and ApoE<sup>-/-</sup> mice. However, further analysis is required to confirm these differences and to investigate the formation of oxidised species within the vasculature after injury. This study also examined a role of AMPK in vascular injury in ApoE<sup>-/-</sup> mice and highlights its actions in vascular disease.

**CHAPTER 6**

**THE EFFECT OF AMPK  
ACTIVATION IN HEALTHY AND  
ATHEROSCLEROTIC MICE**

## 6.1 Introduction

Atherosclerosis and hypertension are closely related but separate cardiovascular disorders which combined lead to high risk of CAD and MI. Previous clinical trials have shown a strong correlation between hypertension and the risk of developing atherosclerosis highlighted by the predominance of atherosclerotic plaques in areas of the vasculature subjected to high pressures (Kannel *et al.*, 1986, Alexander, 1995). LDL from hypertensive patients is also more vulnerable to oxidation *in vitro* than LDL isolated from normotensive patients (Maggi *et al.*, 1993). In animal models, angiotensin II-induced hypertension increased lesional area in the thoracic aorta of ApoE<sup>-/-</sup> mice fed a high fat diet compared to their counterparts on normal chow diet (Weiss *et al.*, 2001). Both atherosclerosis and hypertension have been shown to enhance oxidative stress within the arterial wall, leading to an exacerbated phenotype that can accelerate atherosclerotic progression (Alexander, 1995).

ApoE<sup>-/-</sup> mice develop spontaneous hypercholesterolaemia and atherosclerosis, with the first signs of disease occurring at 6 to 8 weeks of age. These include monocyte adhesion, disruption of the subendothelial elastic lamina and initial foam cell formation which is accelerated further by high fat feeding (Nakashima *et al.*, 1994, Coleman *et al.*, 2006). Some studies have shown ApoE<sup>-/-</sup> mice to exhibit similar blood pressure recordings to control mice (Gervais *et al.*, 2003, Hartley *et al.*, 2000). However, continuous blood pressure measurements over a 24 hour period revealed ApoE<sup>-/-</sup> mice to have elevated systolic and diastolic pressures as well as heart rate and an elimination of circadian cycles compared to C57BL/6 control mice (Pelat *et al.*, 2003). The majority of studies examining mean arterial pressure have been in older atherosclerotic mice and little is known about the effect of short-term high fat feeding on these haemodynamic measurements.

AMPK regulates cellular energy homeostasis and responds to changes in the AMP to ATP ratio. Under states of stress, it is activated by a depletion of ATP or an elevation of AMP concentration. In atherosclerosis, activation of AMPK by AICAR, a known activator of AMPK, has been shown to reduce ER stress and inhibit macrophage proliferation, both induced by high levels of circulating oxLDL (Dong *et al.*, 2010, Ishii *et al.*, 2009). OxLDL also caused a 40-fold increase in expression of serine/threonine protein phosphatase 2A in human monocytes, the enzyme responsible for inactivating AMPK (Kang *et al.*, 2006). In addition, AMPK has been implicated in reverse cholesterol transport, as activation increased protein levels of ABCG1 and ABCA1, which resulted in

cholesterol efflux from foam cells derived from macrophages and reduced plaque formation in ApoE<sup>-/-</sup> mice (Li *et al.*, 2010a, Li *et al.*, 2010b). AMPK has also been associated with neutrophils, which are the primary source of MPO, a phagocytic enzyme involved in one of the mechanisms by which LDL can become modified (Alba *et al.*, 2004). AMPK activation attenuated neutrophil activity and metformin, an anti-diabetic drug known to activate AMPK, decreased MPO levels in lung tissue (Zhao *et al.*, 2008, Tsoyi *et al.*, 2011). Therapeutic agents such as statins, extensively used in the treatment of atherosclerosis due to their effects on lipid lowering, have also been shown to partially mediate their effects through the action of AMPK, reviewed in Ewart and Kennedy (2011). Incubation with atorvastatin increased phosphorylation of AMPK and its downstream target ACC, both *in vitro* and *in vivo* (Sun *et al.*, 2006). Together, this highlights the emerging evidence for the importance of functional AMPK signalling to prevent lipid accumulation and the development of atherosclerosis.

The activation of AMPK has also been associated with blood pressure regulation where prior studies have shown a reduction in mean arterial pressure in both rodents and humans, following acute administration of the AMPK activator, AICAR (Foley *et al.*, 1989, Bosselaar *et al.*, 2011). Furthermore, spontaneously hypertensive rats dosed with AICAR showed an acute drop in blood pressure which was not seen in the control group of Wistar-Kyoto rats suggesting AMPK could play a role in reducing hypertension (Ford *et al.*, 2012). Long-term administration of AICAR or resveratrol, which has been described as another activator of AMPK, also reduced mean arterial pressure in obese Zucker rats (Buhl *et al.*, 2002, Rivera *et al.*, 2009). This suggests that AMPK activation could play a critical role in the reduction of blood pressure in both atherosclerosis and hypertension. However, to date there is no information available on the effect of chronic AMPK activation on blood pressure regulation and lipid profile in atherosclerotic mice and how this would also affect the activity of AMPK and its downstream targets in health and early atherosclerosis.

### **6.1.1 Aims**

The aims investigated in this chapter were:

- To determine the effect of short-term high fat feeding on blood pressure and AMPK expression in ApoE<sup>-/-</sup> mice.
- To examine the effect of chronic AMPK activation on blood pressure, protein expression and MPO content in healthy and atherosclerotic mice.

## 6.2 Methods

### 6.2.1 Chronic AICAR administration

Male C57BL/6 mice on normal chow and male ApoE<sup>-/-</sup> mice fed on a high fat diet for 1 month prior (10 to 12 weeks of age, weighing between 20 and 31 g) were administered a daily i.p. injection of either saline (vehicle) or AICAR at 400 mg/kg for 14 days. ApoE<sup>-/-</sup> mice were continued on the high fat diet throughout the dosing period. Mice were weighed at the start of the dosing regimen, at day 7 to adjust the AICAR dose due to potential weight fluctuations and at the end of the study period.

### 6.2.2 Haemodynamic measurements

Haemodynamic measurements were performed by cannulation of the left common carotid artery as outlined in Section 2.6.5. A representative arterial blood pressure trace is shown in Figure 6.1. At the end of the procedure, mice were sacrificed by cervical dislocation and following this, blood was collected by cardiac puncture into EDTA-coated tubes and centrifuged at 1500 x g for 10 minutes to produce plasma. Heart, liver and spleen weights were also recorded at time of death and snap frozen for future use.

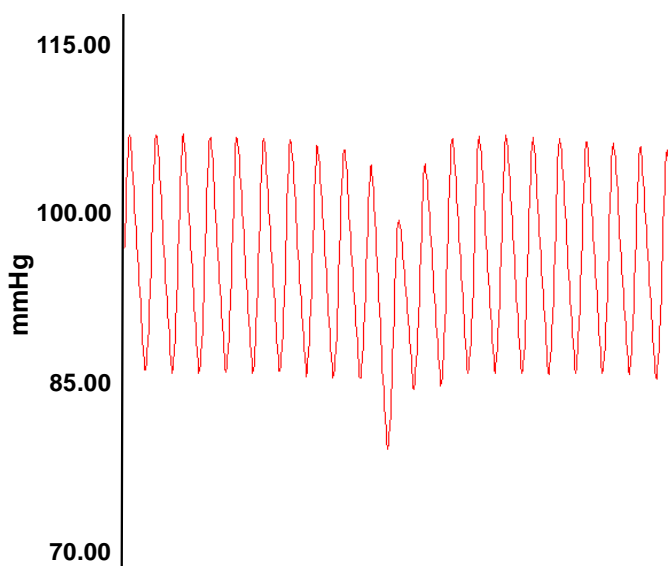


**Figure 6.1 – Representative arterial blood pressure trace from cannulation of the left common carotid artery.**

A four second recording in a vehicle-treated C57BL/6 mouse. Systolic and diastolic pressures were measured by taking an average of three individual peaks or troughs respectively. Heart rate was measured by dividing the time the trace takes to complete ten consecutive waves by 600 (as measured in beats per minute (bpm)).

### **6.2.3 Western blotting**

Expression of ACC and AMPK $\alpha$  were measured by Western blot analysis as detailed in Section 2.4. Thoracic aortae and liver from male C57BL/6 and ApoE<sup>-/-</sup> mice that had been administered with either vehicle or AICAR for 14 days, were excised immediately after death. Protein estimation analysis from lysates was carried out and protein was added at 5  $\mu$ g for aorta and 10  $\mu$ g for liver samples per well. Immunoblotting was performed with antibodies against phosphorylated and total ACC and AMPK $\alpha$  as well as GAPDH which was used as a loading control (all antibody dilutions found in Table 2.1). Densitometrical analysis was then performed.

### **6.2.4 MPO assay**

MPO content of the plasma from vehicle- and AICAR-treated C57BL/6 and ApoE<sup>-/-</sup> mice was analysed using a mouse MPO ELISA kit as described in Section 2.6.6. Samples were diluted 1 in 16 in dilution buffer and the assay was performed as per the manufacturer's instructions. Absorbance was measured spectrophotometrically at 450 nm.

### **6.2.5 Detection of lipids in aortae by ESMS**

Lipids were extracted from aortae of chronically treated C57BL/6 and ApoE<sup>-/-</sup> mice with either vehicle or AICAR and analysed as described in Section 2.8. Vessels were incubated in equal volumes of methanol containing BHT, chloroform and an aqueous solution to extract lipids then dried under a steady flow of oxygen-free nitrogen gas. Dried lipid extracts were reconstituted and further diluted in methanol. For analysis using positive-ion mode, aortic samples were diluted 1 in 100 with 1 % aqueous formic acid in methanol and scans performed for PCs and SMs, PEs, cholesterol and cholesteryl esters. For analysis using negative-ion mode, aortic samples were diluted 1 in 10 with 10 % 5 mM ammonium acetate in methanol and scans performed for PIs and PSs. Aortic samples were analysed by identifying consistent differences between spectra from different sample groups.

### **6.2.6 Statistical analysis**

All results are displayed as mean  $\pm$  SEM and n represents the number of mice used. Data were analysed using an unpaired Student's t test for the body weight measurements, one-way ANOVA followed by Newman-Keuls' post hoc test for analysis of spectra and two-way ANOVA followed by Bonferroni's post hoc test for all other measurements.

## 6.3 Results

### 6.3.1 Effect of chronic AICAR administration on blood pressure and weight in healthy and atherosclerotic mice

Values for all weights and haemodynamic measurements are summarised in Table 6.1 as mean  $\pm$  SEM.

For each haemodynamic measurement, a histogram (A in each graph) and scatter dot plot (B in each graph) is shown to highlight the mean values as well as the distribution of the data. Mean arterial pressure was significantly increased in the vehicle-treated ApoE<sup>-/-</sup> mice compared to their age-matched C57BL/6 controls from  $94.1 \pm 1.5$  mmHg to  $112.2 \pm 1.5$  mmHg (Figure 6.2). AICAR treatment had no effect on mean arterial pressure in C57BL/6 mice but lowered the value almost to the baseline ( $98.5 \pm 1.8$  mmHg) in the ApoE<sup>-/-</sup> mice. A similar trend was observed with the diastolic pressure in both C57BL/6 and ApoE<sup>-/-</sup> mice (Figure 6.3). The vehicle-treated ApoE<sup>-/-</sup> group had a significantly elevated systolic pressure of  $115.3 \pm 1.6$  mmHg compared to their C57BL/6 counterparts ( $105.1 \pm 1.3$  mmHg) whereas administration of AICAR had no effect in either strain of mouse (Figure 6.4). Vehicle-treated ApoE<sup>-/-</sup> mice had a reduced pulse pressure of  $5.3 \pm 0.5$  mmHg compared to their C57BL/6 controls ( $18.3 \pm 0.9$  mmHg; Figure 6.5). Furthermore, AICAR treatment had no effect on C57BL/6 mice but increased the pulse pressure of ApoE<sup>-/-</sup> mice to  $24.4 \pm 1.5$  mmHg, similar to healthy C57BL/6 mice levels. Heart rate was also increased in ApoE<sup>-/-</sup> mice dosed with the saline vehicle compared to their C57BL/6 controls from  $317.7 \pm 13.9$  bpm to  $410.7 \pm 15.1$  bpm (Figure 6.6). AICAR administration had no effect on heart rate in either strain of mouse.

Body weight was monitored throughout the dosing regimen to allow for the adjustment of the AICAR dose as required (Figure 6.7). ApoE<sup>-/-</sup> mice had increased body weights compared to their age-matched C57BL/6 controls at the beginning of the experimental protocol. This was maintained during the study and at the final body weight measurement. The percentage change in body weight at the midpoint of the investigation (day 7) and at the end, in relation to their start weights, was also investigated to take into account the differing start weights of the mice. C57BL/6 mice consistently gained weight over the 14 day period, with AICAR treatment having no effect compared to the vehicle-treated mice. In contrast, both groups of ApoE<sup>-/-</sup> mice lost weight over the study period with a significant percentage loss in ApoE<sup>-/-</sup> mice treated with AICAR between the midpoint and final weight measurements.

Organ weights were also measured as a percentage of the final body weight for each mouse (Figure 6.8). No differences in the whole heart weight were observed between C57BL/6 and ApoE<sup>-/-</sup> mice. Furthermore, chronic AICAR treatment had no effect on whole heart weight in either strain of mouse. Liver weight was reduced in ApoE<sup>-/-</sup> mice compared to C57BL/6 mice whereas administration of AICAR increased liver weights in both strains of mice compared to their saline-treated controls. There was also a marked increase in spleen weight in both ApoE<sup>-/-</sup> groups in relation to their C57BL/6 controls which was unaffected by AICAR treatment.

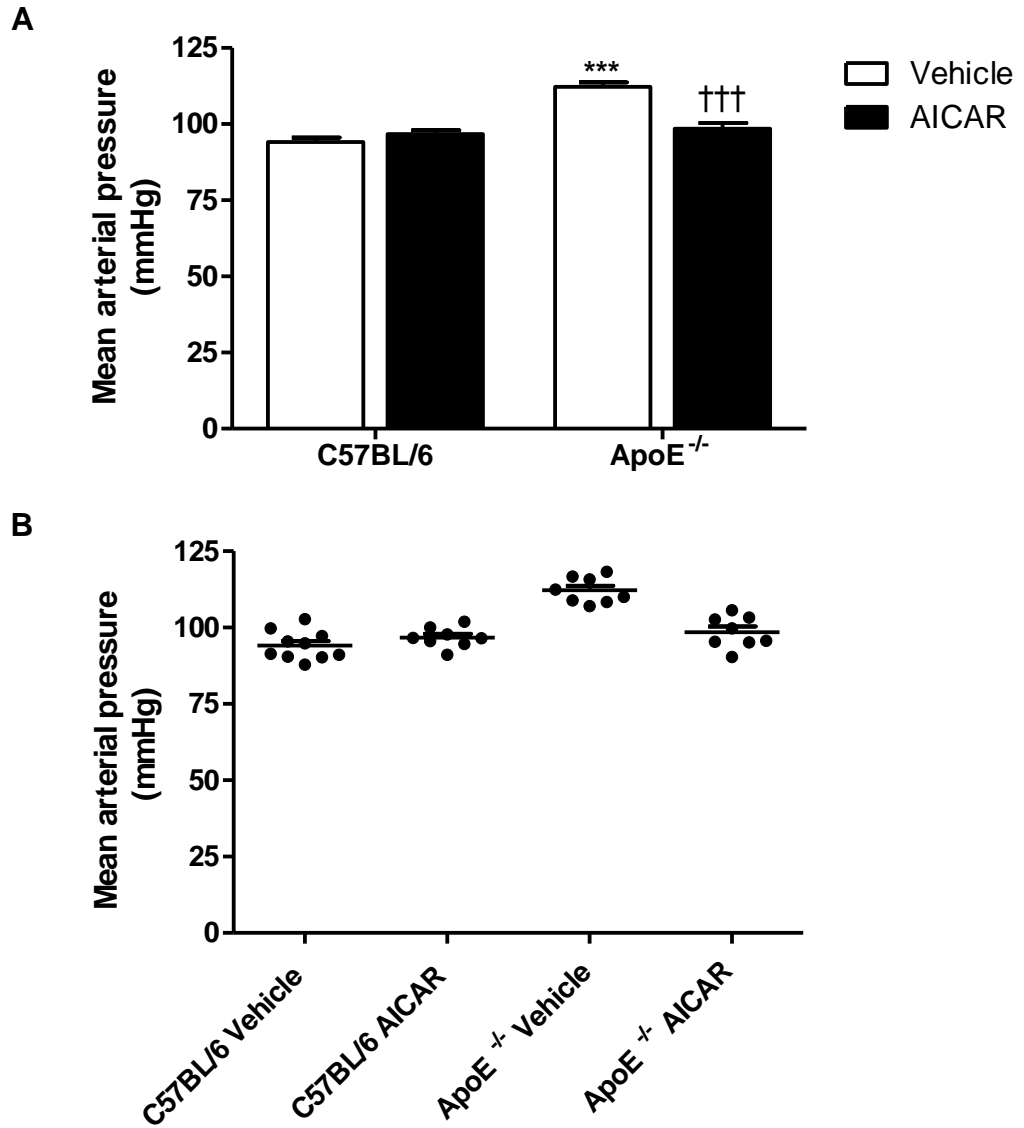


**Figure 6.2 – Effect of AICAR dosing on mean arterial pressure of C57BL/6 and ApoE<sup>-/-</sup> mice.**

Mean arterial pressure was measured by cannulation of the left common carotid artery.

\*\*\*p<0.001 vs C57BL/6 vehicle, †††p<0.001 vs ApoE<sup>-/-</sup> vehicle, n = 6-10.

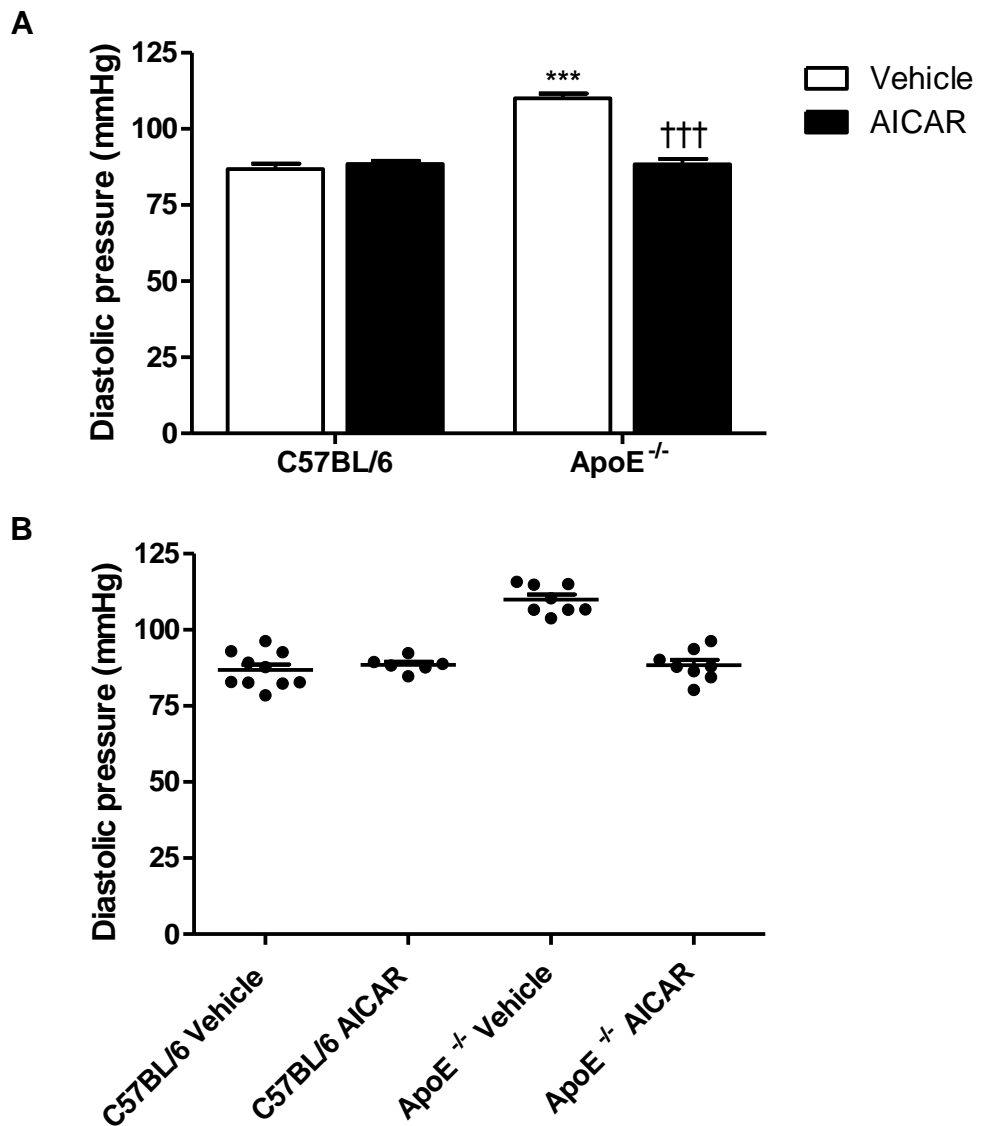


**Figure 6.3 – Effect of AICAR dosing on diastolic pressure of C57BL/6 and ApoE<sup>-/-</sup> mice.**

Mean diastolic pressure was calculated from the arterial blood pressure traces by taking an average of three troughs from three separate waves. \*\*\* $p < 0.001$  vs C57BL/6 vehicle, ††† $p < 0.001$  vs ApoE<sup>-/-</sup> vehicle,  $n = 6-10$ .

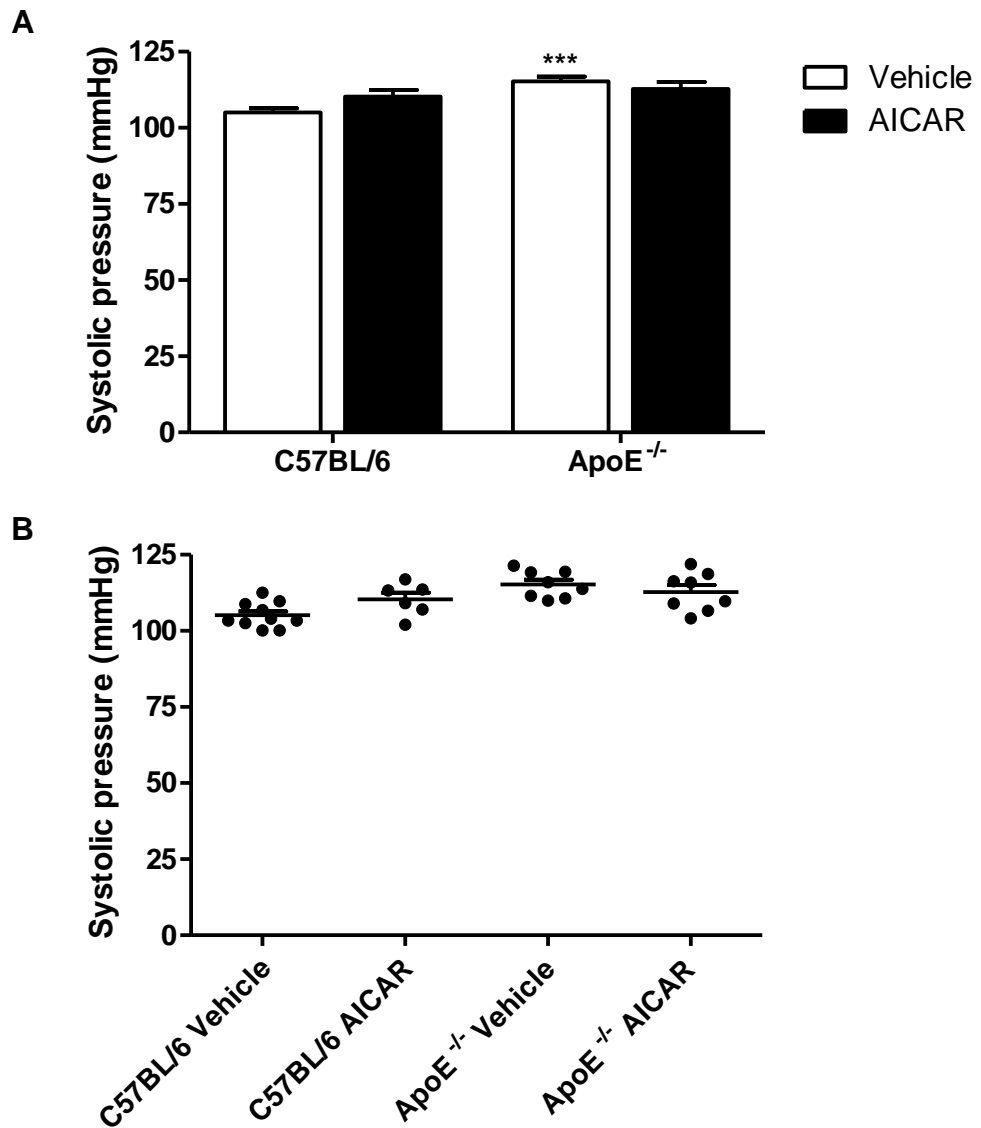


**Figure 6.4 – Effect of AICAR dosing on systolic pressure of C57BL/6 and ApoE<sup>-/-</sup> mice.**

Mean diastolic pressure was calculated from the arterial blood pressure traces by taking an average of three peaks from three separate waves. \*\*\* $p < 0.001$  vs C57BL/6 vehicle,  $n = 6-10$ .

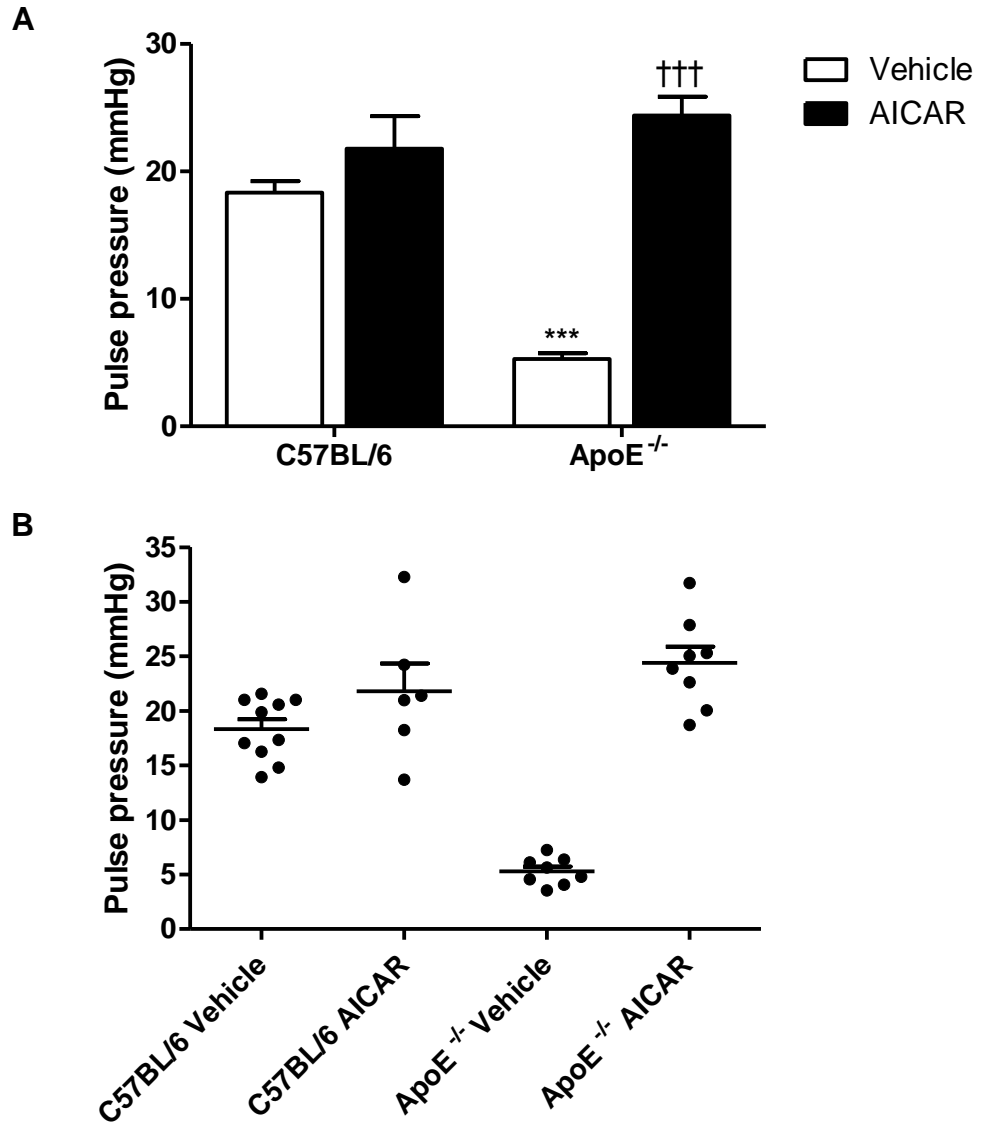


**Figure 6.5 – Effect of AICAR dosing on pulse pressure of C57BL/6 and ApoE<sup>-/-</sup> mice.** Mean pulse pressure was calculated by subtracting the mean diastolic from the mean systolic pressure in each animal. \*\*\* $p < 0.001$  vs C57BL/6 vehicle, ††† $p < 0.001$  vs ApoE<sup>-/-</sup> vehicle,  $n = 6-10$ .

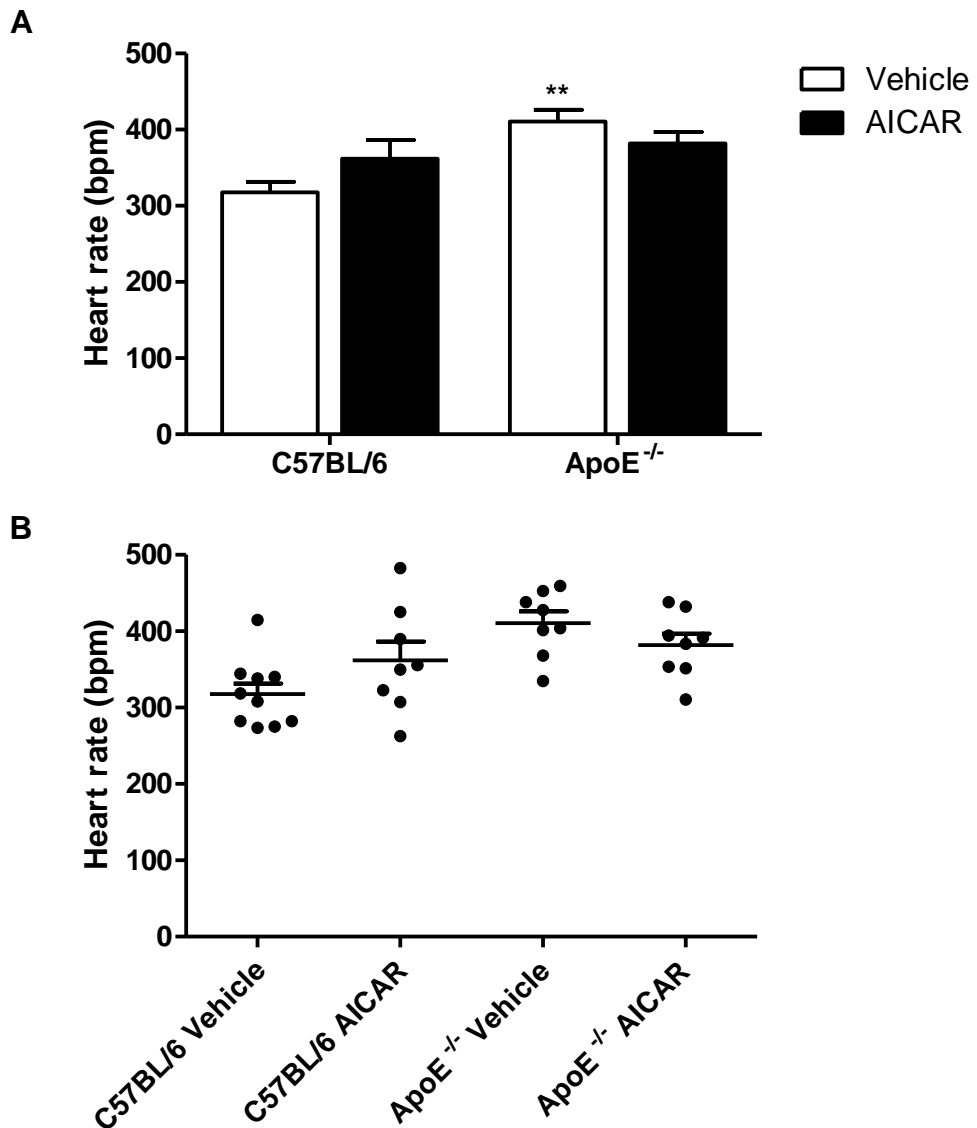


**Figure 6.6 – Effect of AICAR dosing on heart rate of healthy and atherosclerotic mice.**

Heart rate was measured by dividing the time the arterial blood pressure trace takes to complete ten consecutive waves by 600 (as measured in bpm). \*\* $p < 0.01$  vs C57BL/6 vehicle,  $n = 7-10$ .

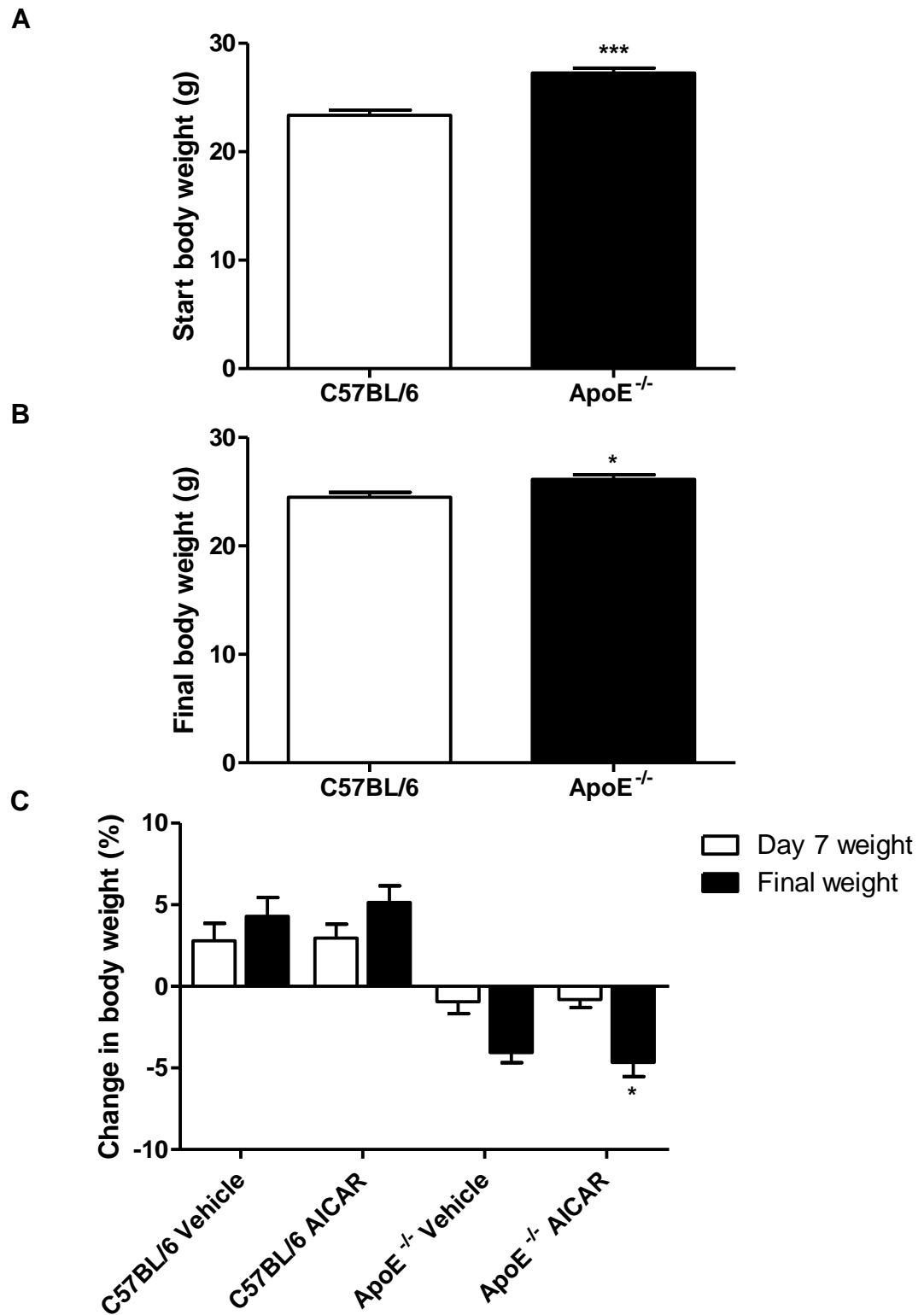


**Figure 6.7 – Effect of 14 day dosing regimen on body weight of C57BL/6 and ApoE<sup>-/-</sup> mice.**

The weight of each mouse was recorded at the beginning (A), midpoint (day 7) and at the end of the procedure (B). \* $p < 0.05$  and \*\*\* $p < 0.001$  vs C57BL/6,  $n = 18-20$ . The percentage change in body weights from start to day 7 and to final weight were also measured (C). \* $p < 0.05$  vs ApoE<sup>-/-</sup> AICAR day 7 weight,  $n = 9-10$ .

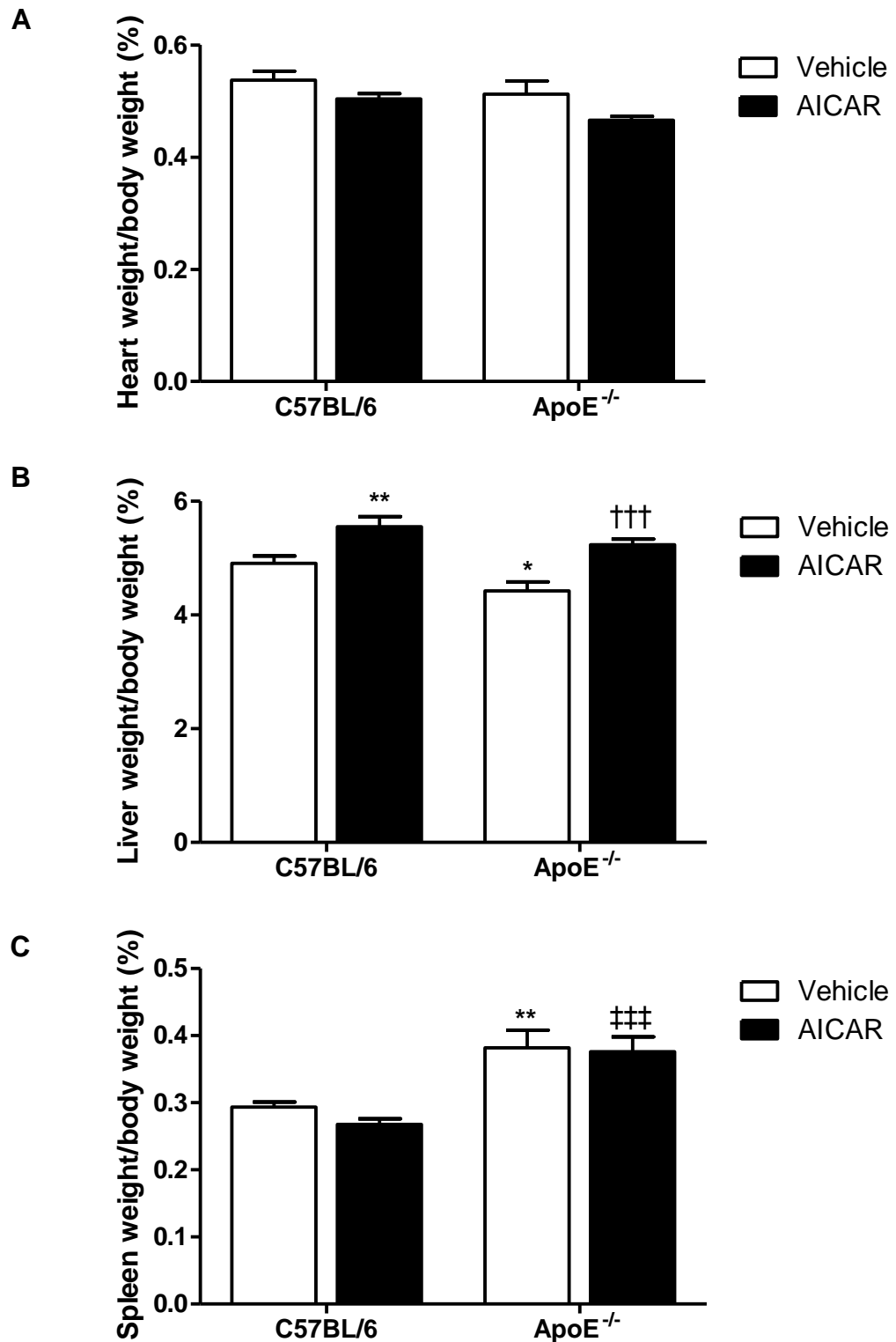


**Figure 6.8 – Effect of AICAR dosing on organ weight of C57BL/6 and ApoE<sup>-/-</sup> mice.** Heart (A), liver (B) and spleen (C) weights were calculated as a percentage of the final body weight of the mice. \* $p < 0.05$  and \*\* $p < 0.01$  vs C57BL/6 vehicle, †† $p < 0.001$  vs C57BL/6 AICAR, ††† $p < 0.001$  vs ApoE<sup>-/-</sup> vehicle,  $n = 9-10$ .

**Table 6.1 – Weight and haemodynamic measurements of C57BL/6 and ApoE<sup>-/-</sup> mice before and after 14 days of AICAR administration.**

	C57BL/6		ApoE <sup>-/-</sup>	
	Vehicle	AICAR	Vehicle	AICAR
<b>Start weight (g)</b>	25.0 ± 0.5	21.7 ± 0.4 <sup>***</sup>	28.0 ± 0.6 <sup>***</sup>	26.5 ± 0.6 <sup>†††</sup>
<b>Final weight (g)</b>	26.1 ± 0.3	22.9 ± 0.4 <sup>***</sup>	26.9 ± 0.6	25.3 ± 0.5 <sup>†,††</sup>
<b>Heart /Body weight (%)</b>	0.54 ± 0.02	0.50 ± 0.01	0.51 ± 0.02	0.47 ± 0.01
<b>Liver/Body weight (%)</b>	4.91 ± 0.13	5.55 ± 0.18 <sup>**</sup>	4.42 ± 0.16 <sup>*</sup>	5.24 ± 0.10 <sup>†††</sup>
<b>Spleen/Body weight (%)</b>	0.29 ± 0.01	0.27 ± 0.01	0.38 ± 0.03 <sup>**</sup>	0.38 ± 0.02 <sup>†††</sup>
<b>MAP (mmHg)</b>	94.1 ± 1.5	96.8 ± 1.2	112.2 ± 1.5 <sup>***</sup>	98.5 ± 1.8 <sup>†††</sup>
<b>DAP (mmHg)</b>	86.8 ± 1.8	88.5 ± 1.0	110.0 ± 1.7 <sup>***</sup>	88.4 ± 1.8 <sup>†††</sup>
<b>SAP (mmHg)</b>	105.1 ± 1.3	110.3 ± 2.2	115.3 ± 1.6 <sup>***</sup>	112.8 ± 2.2
<b>PP (mmHg)</b>	18.3 ± 0.9	21.8 ± 2.6	5.3 ± 0.5 <sup>***</sup>	24.4 ± 1.5 <sup>†††</sup>
<b>HR (bpm)</b>	317.7 ± 13.9	344.7 ± 20.2	410.7 ± 15.1 <sup>**</sup>	381.9 ± 15.1

Organ weight was taken as a percentage of the body weight. Mean arterial pressure (MAP), diastolic arterial pressure (DAP), systolic arterial pressure (SAP), pulse pressure (PP) and heart rate (HR) were calculated from the trace from the cannula inserted in the left common carotid artery of C57BL/6 and ApoE<sup>-/-</sup> mice. Data are expressed as mean ± SEM. \*p<0.05, \*\*p<0.01 and \*\*\*p<0.001 vs C57BL/6 vehicle, ††p<0.01 and †††p<0.001 vs C57BL/6 AICAR, †p<0.05 and †††p<0.001 vs ApoE<sup>-/-</sup> vehicle, n = 6-10.

### **6.3.2 Effect of chronic AICAR treatment on expression of AMPK $\alpha$ and ACC in mouse aorta and liver**

The expression of phosphorylated and total AMPK $\alpha$  and its downstream target, ACC, were investigated in both mouse aortae and liver to assess the influence of chronic AMPK activation with AICAR on this pathway. Phosphorylated and total levels of each protein were divided by the density of the GAPDH band to adjust for protein loading. Phosphorylated levels of AMPK $\alpha$  and ACC were also divided by the total values of each protein to measure the activation of these enzymes.

Phosphorylated AMPK $\alpha$  levels in aortae were elevated in C57BL/6 mice dosed with AICAR and reduced in ApoE<sup>-/-</sup> mice treated in the same way (Figure 6.9). There was no effect on the amount of total AMPK $\alpha$  in C57BL/6 mice but a reduction was seen in ApoE<sup>-/-</sup> mice administered AICAR. In contrast, the ratio of phosphorylated to total AMPK $\alpha$  was significantly higher in aortae of C57BL/6 mice treated with AICAR while no effect was seen in ApoE<sup>-/-</sup> mice. Similarly to AMPK $\alpha$ , phosphorylated ACC was increased in aortae of C57BL/6 mice treated with AICAR for 14 days compared to their vehicle-treated controls (Figure 6.10). In comparison with their C57BL/6 counterparts, there was a trend towards a reduction in the amount of phosphorylated ACC in vehicle-treated ApoE<sup>-/-</sup> mice and a significant decrease of phosphorylated ACC present in aortae of ApoE<sup>-/-</sup> mice treated with AICAR. A similar effect was observed with total ACC in the aortae with increased levels in C57BL/6 mice dosed with AICAR and a significant reduction in vehicle-treated and AICAR-dosed ApoE<sup>-/-</sup> mice. Administration of AICAR had no effect on the phosphorylated to total ACC ratio in either strain of mouse but was significantly elevated in atherosclerotic ApoE<sup>-/-</sup> mice compared to their healthy C57BL/6 controls.

No differences were observed in phosphorylated AMPK $\alpha$  levels in the liver across any of the groups (Figure 6.11). However, there was a significant reduction in total AMPK $\alpha$  expression in ApoE<sup>-/-</sup> mice liver in both vehicle- and AICAR-treated groups in relation to their C57BL/6 controls. There was a large elevation in the phosphorylated to total AMPK $\alpha$  ratio in ApoE<sup>-/-</sup> mice livers compared their C57BL/6 counterparts and a slight decrease in ApoE<sup>-/-</sup> mice treated with AICAR compared to their vehicle-treated controls. Reduced levels of phosphorylated ACC were seen in ApoE<sup>-/-</sup> mice compared to their healthy C57BL/6 controls with AICAR administration had no effect (Figure 6.12). A similar trend was seen for total ACC but this did not reach significance. No differences were observed in the phosphorylated to total ACC ratio across any of the groups.

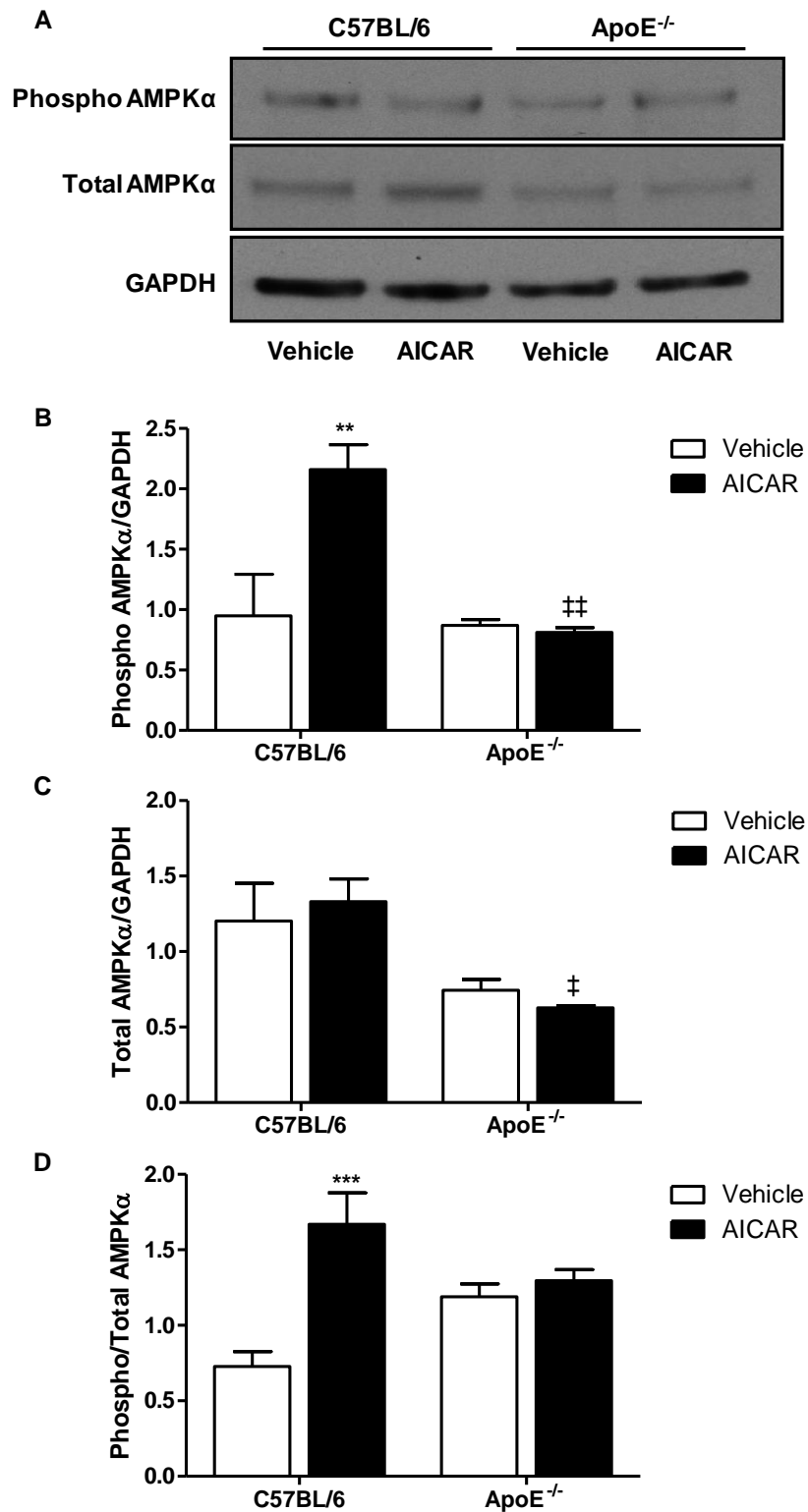


**Figure 6.9 – Effect of AICAR dosing on phosphorylated and total AMPK $\alpha$  expression in aortae of C57BL/6 and ApoE<sup>-/-</sup> mice.**

Phosphorylated (B) and total (C) AMPK $\alpha$  were divided by GAPDH to adjust for protein loading to measure the amount of each form of the protein present and phosphorylated was divided by total AMPK $\alpha$  to measure the activation of the enzyme (D). Blots shown are representative (A). \*\*p < 0.01 and \*\*\*p < 0.001 vs C57BL/6 vehicle, ‡p < 0.05 and ‡‡p < 0.01 vs C57BL/6 AICAR, n = 4.

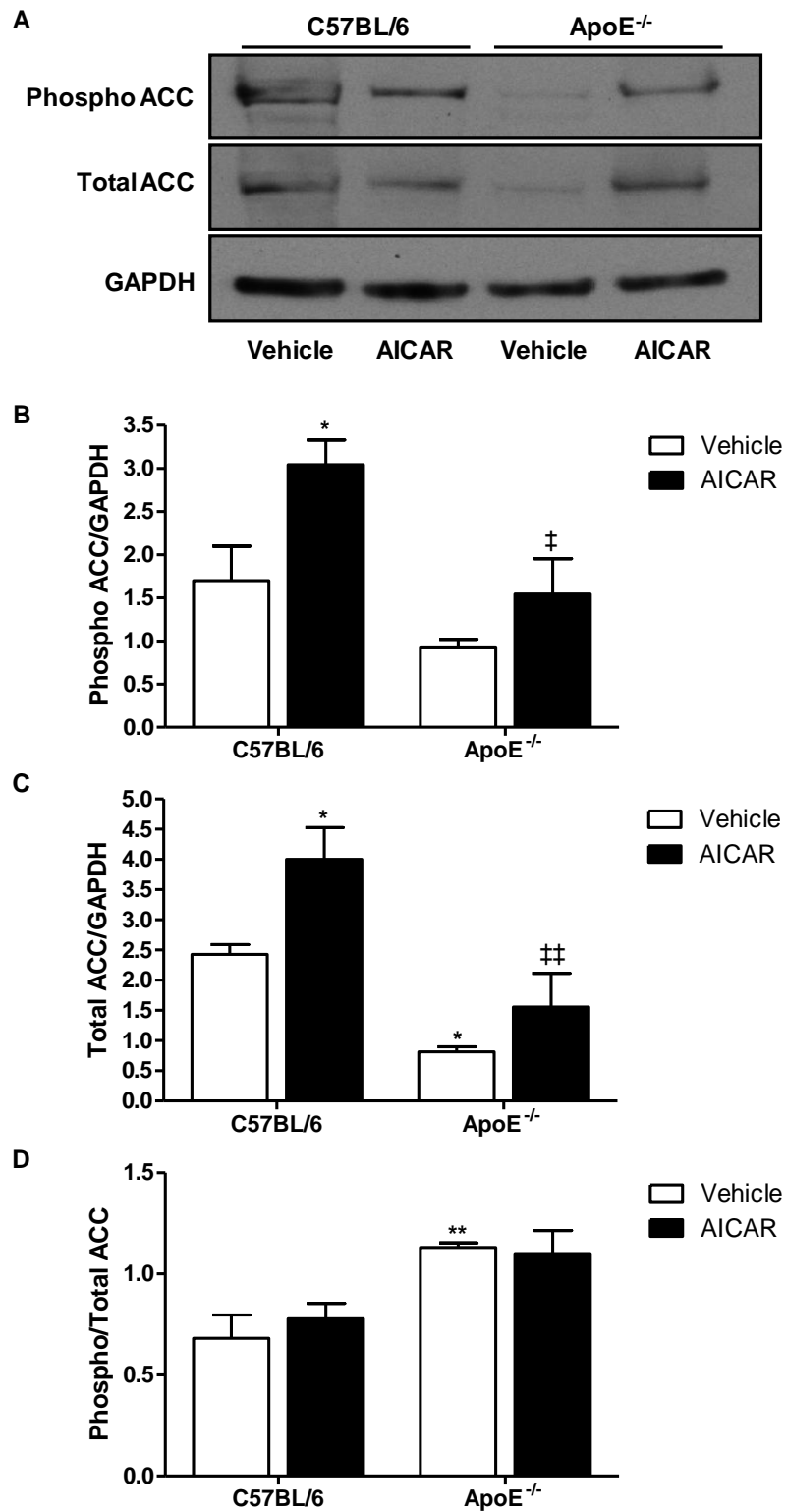


**Figure 6.10 – Effect of AICAR dosing on phosphorylated and total ACC expression in aortae of C57BL/6 and ApoE<sup>-/-</sup> mice.**

Phosphorylated (B) and total (C) ACC were divided by GAPDH to adjust for protein loading to measure the amount of each form of the protein present and phosphorylated was divided by total ACC to measure the activation of the enzyme (D). Blots shown are representative (A). \* $p < 0.05$  and \*\* $p < 0.01$  vs C57BL/6 vehicle, ‡ $p < 0.05$  and ## $p < 0.01$  vs C57BL/6 AICAR,  $n = 4$ .

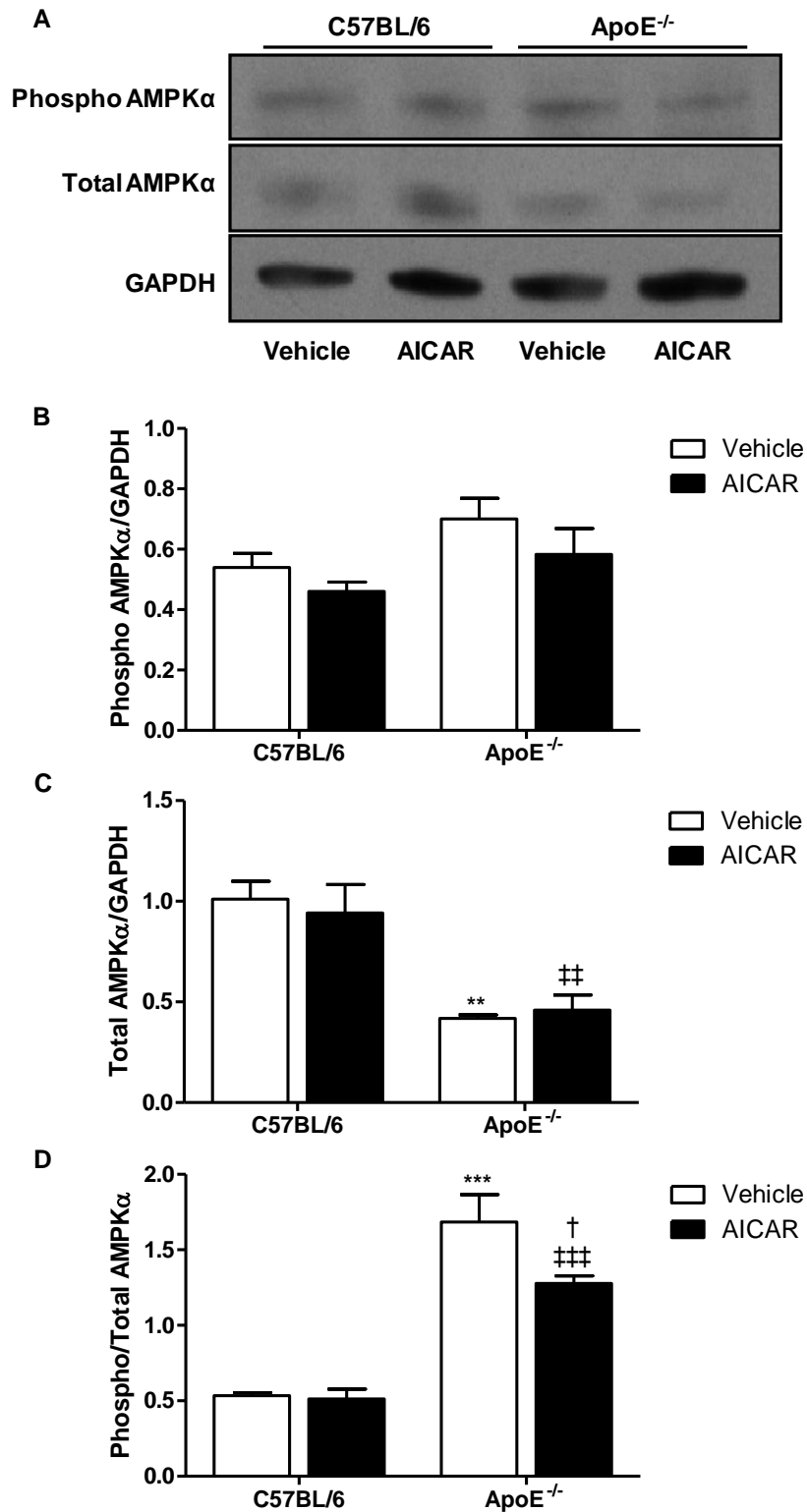


**Figure 6.11 – Effect of AICAR dosing on phosphorylated and total AMPK $\alpha$  expression in liver of C57BL/6 and ApoE<sup>-/-</sup> mice.**

Phosphorylated (B) and total (C) AMPK $\alpha$  were divided by GAPDH to adjust for protein loading to measure the amount of each form of the protein present and phosphorylated was divided by total AMPK $\alpha$  to measure the activation of the enzyme (D). Blots shown are representative (A). \*\*p < 0.01 and \*\*\*p < 0.001 vs C57BL/6 vehicle, ‡p < 0.01 and ‡‡‡p < 0.001 vs C57BL/6 AICAR, †p < 0.05 vs ApoE<sup>-/-</sup> vehicle, n = 4.

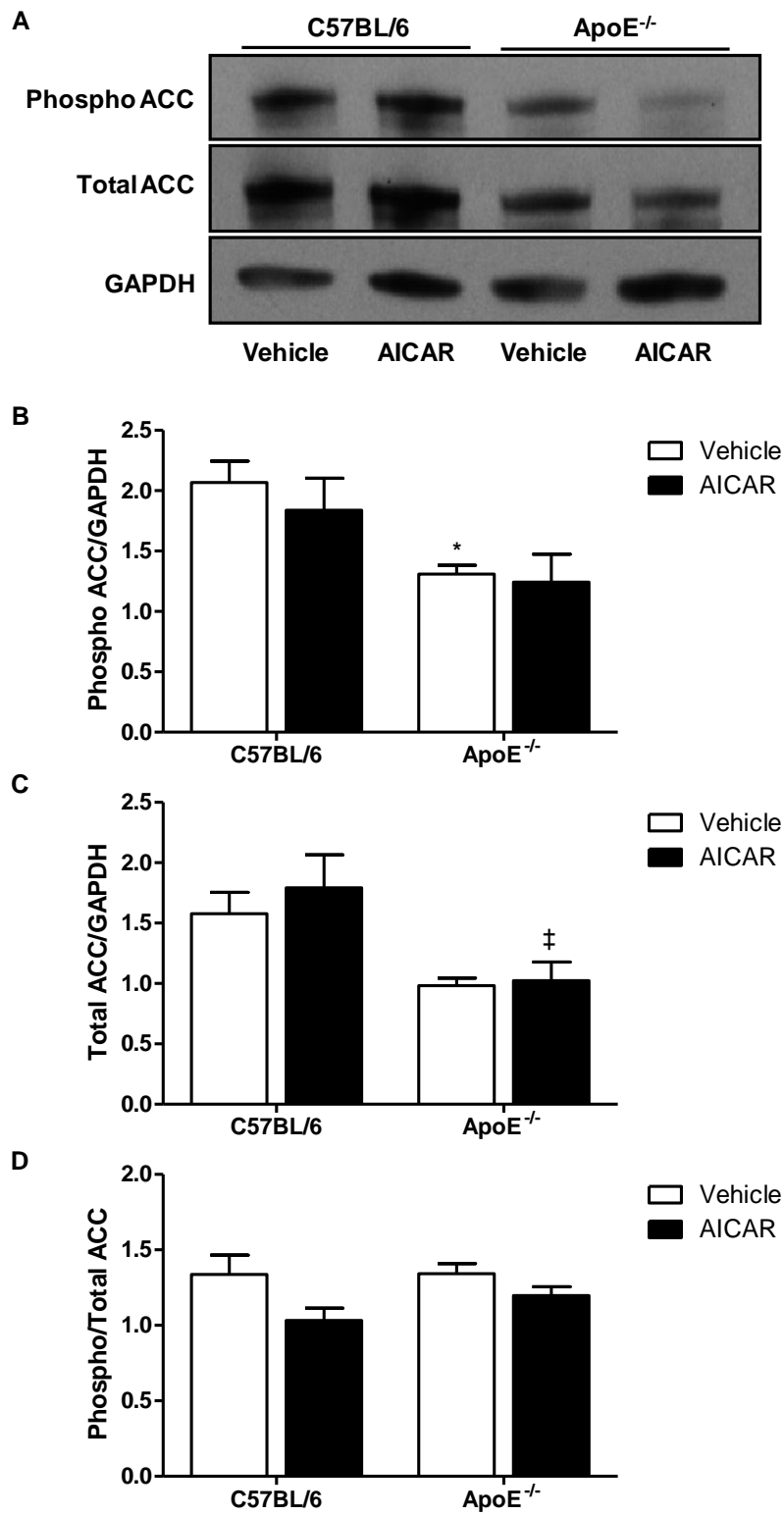


**Figure 6.12 – Effect of AICAR dosing on phosphorylated and total ACC expression in liver of C57BL/6 and ApoE<sup>-/-</sup> mice.**

Phosphorylated (B) and total (C) ACC were divided by GAPDH to adjust for protein loading to measure the amount of each form of the protein present and phosphorylated was divided by total ACC to measure the activation of the enzyme (D). Blots shown are representative (A). \* $p < 0.05$  vs C57BL/6 vehicle, ‡ $p < 0.05$  vs C57BL/6 AICAR,  $n = 4$ .

### **6.3.3 Effect of AICAR administration on modified lipids in healthy and atherosclerotic mice**

The influence of chronic AICAR treatment on the MPO content of plasma from healthy C57BL/6 mice and ApoE<sup>-/-</sup> mice fed on high fat diet for 6 weeks was investigated (Figure 6.13). A dramatic increase in MPO levels in ApoE<sup>-/-</sup> mice compared to their C57BL/6 controls was observed from  $151.9 \pm 17.9$  ng/ml to  $598.2 \pm 55.0$  ng/ml. AICAR treatment had no effect on C57BL/6 mice but significantly increased MPO in the plasma of ApoE<sup>-/-</sup> mice to  $762.7 \pm 71.1$  ng/ml.

The distribution of several classes of phospholipids, present at various proportions in LDL particles including PCs, PEs, PSs and PIs as well as cholesterol and cholesteryl esters, in aortae were observed by ESMS. The differences between vehicle-treated C57BL/6 and ApoE<sup>-/-</sup> mice were investigated and the effect of chronic AMPK activation. The percentage relative abundances of the signals detected from all phospholipid species are displayed in Table 6.2.

Precursor ion scanning of m/z 184.1 in positive-ion mode is selective for SMs and PCs, the most abundant phospholipid in mammals, and exhibited similar distribution within individual samples in each group (Figure 6.14). Peaks at m/z 496.7 (16:0) and 524.7 (18:0) were consistently seen in all groups indicating the presence of lysolipids. All treatment groups displayed roughly similar distribution of ions with the most abundant product ion occurring at m/z 782.9 (16:0/20:4); however, there were some notable changes in PC and SM expression between strains of mice and AICAR administration groups. The only difference observed in AICAR-treated mice was a reduction in intensity of m/z 732.9 (16:0/16:1) relative to other signals in ApoE<sup>-/-</sup> mice. In vehicle-treated ApoE<sup>-/-</sup> mice compared to their C57BL/6 counterparts, there was also a relative elevation in m/z 810.9 (18:0/20:4). The only differences observed in SM expression were a relative increase in m/z 787.9 (22:0) in AICAR-treated ApoE<sup>-/-</sup> mice compared to their vehicle-treated counterparts and C57BL/6 mice treated in the same way. The spectra were then expanded between m/z 550 and 700 to display any changes in chain-shortened PCs as they could be masked by the high signal of native PCs and long-chain products (Figure 6.15). Repeating signals were observed in the spectra at m/z 564, 592, 620, 648 and 676 at different intensities within the groups (highest in one of the samples from the AICAR-treated ApoE<sup>-/-</sup> group) suggesting a polyethylene contaminant as the peaks are separated by 28 Da and were, therefore, discounted from the analysis (Jaber and Wilkins, 2005). No detectable

changes were observed in the formation of chain-shortened PCs in any of the sample groups.

A neutral loss scan for 141.1 Da in positive-ion mode was performed to detect changes in PE expression in murine aortae (Figure 6.16). PEs were found at a much lower concentration than PCs but there was an increase in relative intensity of  $m/z$  768.8 (18:0/20:4) in ApoE<sup>-/-</sup> mice after chronic activation in comparison to their saline-treated controls and C57BL/6 mice treated in the same way. In addition,  $m/z$  760.9 was only detectable in vehicle-treated C57BL/6 mice. Similar to PEs, the concentration of PSs, detected by a neutral loss scan of 87 Da in negative-ion mode, in the aortic samples was relatively low and no significant differences were observed within or between the treatment groups (Figure 6.17). Precursor ion scanning for  $m/z$  241 in positive-ion mode is selective for PIs and a trend towards a reduction in  $m/z$  885.9 (18:0/20:4) relative to other signals was observed in both AICAR-treated mice compared to their vehicle-treated controls (Figure 6.18). In addition to the several classes of phospholipids, precursor ion scanning for  $m/z$  369.1 was performed to detect cholesterol and cholesteryl esters present in the aortae (Figure 6.19). The major product ion for each treatment group was  $m/z$  369.6, indicating the dehydration product of protonated cholesterol, with no detectable changes in the formation of cholesteryl esters in any of the sample groups.

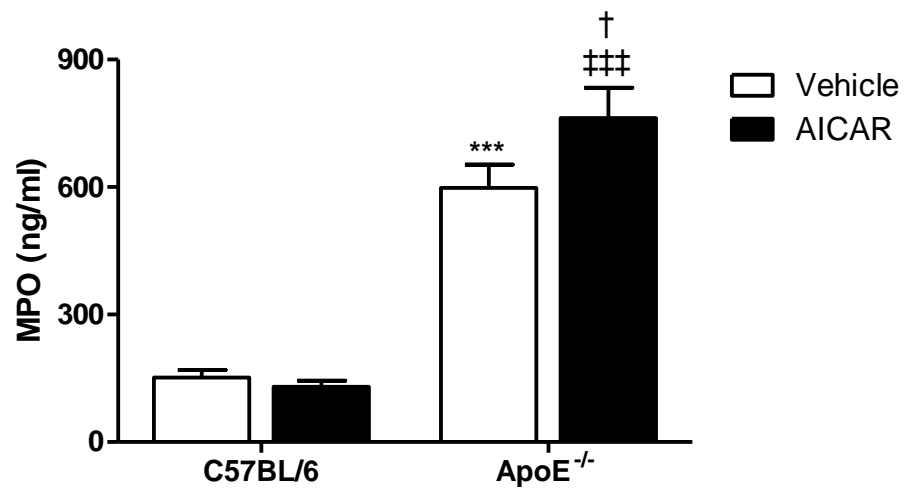


**Figure 6.13 – Effect of AICAR treatment on MPO content of C57BL/6 and ApoE<sup>-/-</sup> mouse plasma.**

Blood samples were taken from each mouse at sacrifice by cardiac puncture into EDTA-coated tubes. Blood was centrifuged at 1500 x g for 10 minutes to produce plasma. The MPO content of mouse plasma was measured by an ELISA and absorbance read spectrophotometrically at 450 nm. \*\*\*p<0.001 vs C57BL/6 vehicle, ###p<0.001 vs C57BL/6 AICAR, †p<0.05 vs ApoE<sup>-/-</sup> vehicle, n = 8-9.

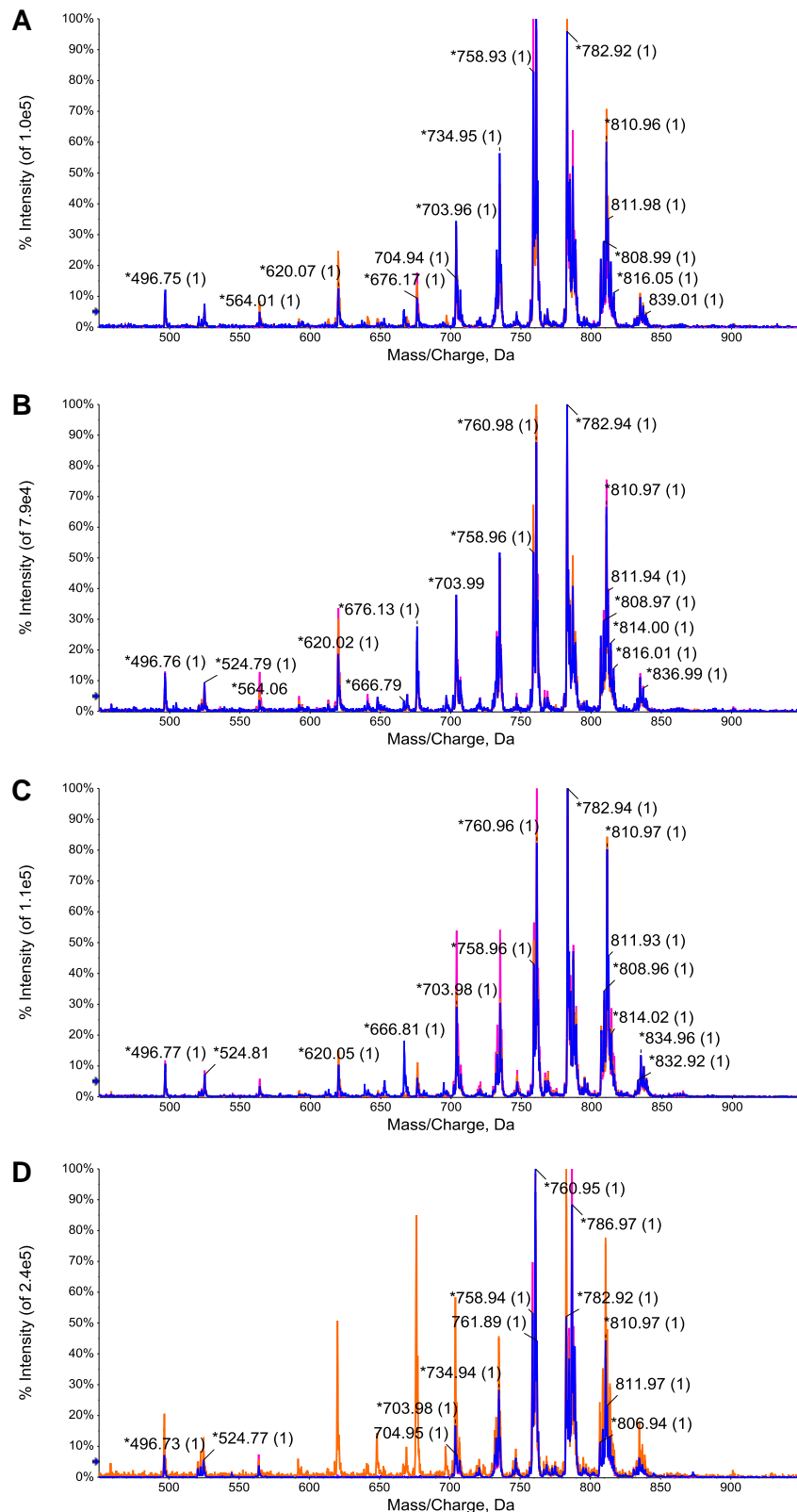


**Figure 6.14 – Detection of PCs and SMs from aortae of vehicle- and AICAR-treated C57BL/6 and ApoE<sup>-/-</sup> mice.**

Precursor ion scanning for m/z 184.1 by positive-ionisation ESMS was performed to identify PCs and SMs present in aortae from C57BL/6 vehicle- (A) and AICAR-treated mice (B) and ApoE<sup>-/-</sup> vehicle- (C) and AICAR-treated mice (D). Individual spectra were overlaid to highlight any potential differences in distributions within and between groups. n = 3.

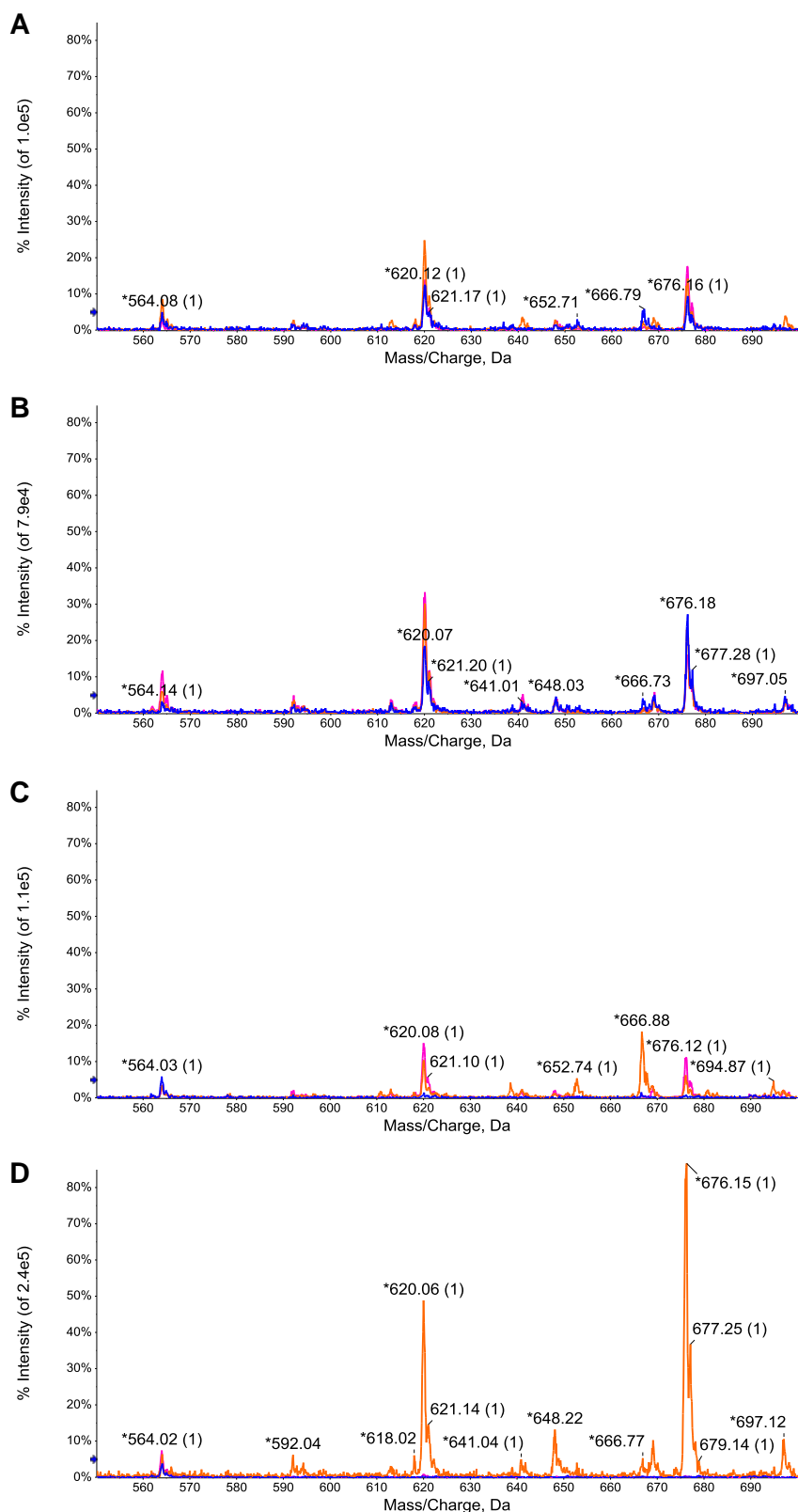


**Figure 6.15 – Detection of chain-shortened PCs from aortae of vehicle- and AICAR-treated C57BL/6 and ApoE<sup>-/-</sup> mice.**

Precursor ion scanning for  $m/z$  184.1 by positive-ionisation ESMS was performed to identify PCs present in aortae from C57BL/6 vehicle- (A) and AICAR-treated mice (B) and ApoE<sup>-/-</sup> vehicle- (C) and AICAR-treated mice (D). Individual spectra were expanded between  $m/z$  550 and 700 to focus on chain-shortened PCs and overlaid to highlight any potential differences in distributions within and between groups.  $n = 3$ .

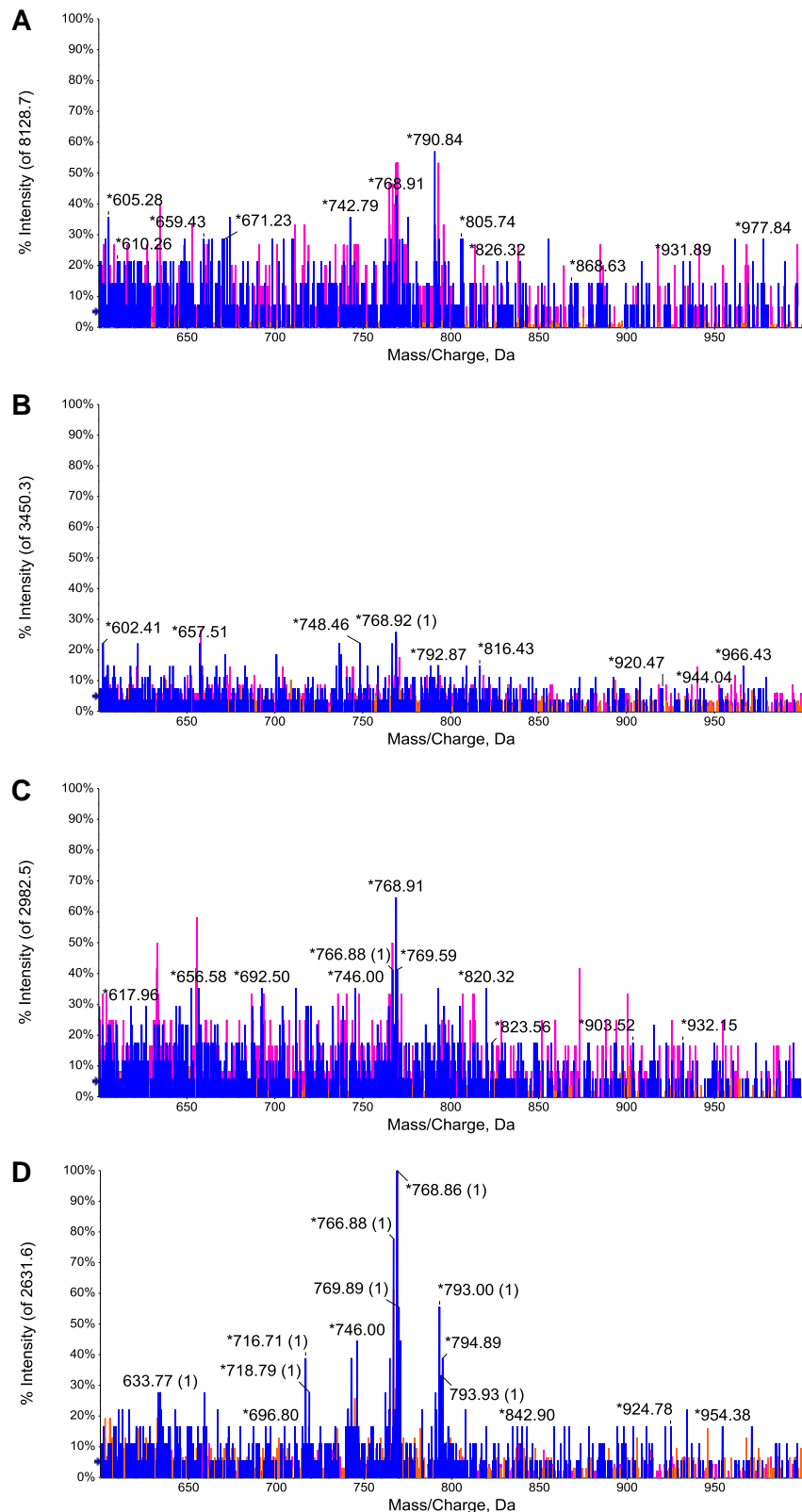


**Figure 6.16 – Detection of PEs from aortae of vehicle- and AICAR-treated C57BL/6 and ApoE<sup>-/-</sup> mice.**

Neutral loss of 141.1 Da by positive-ionisation ESMS was performed to identify PEs present in aortae from C57BL/6 vehicle- (A) and AICAR-treated mice (B) and ApoE<sup>-/-</sup> vehicle- (C) and AICAR-treated mice (D). Individual spectra were overlaid to highlight any differences in distributions within and between groups.  $n = 3$ .

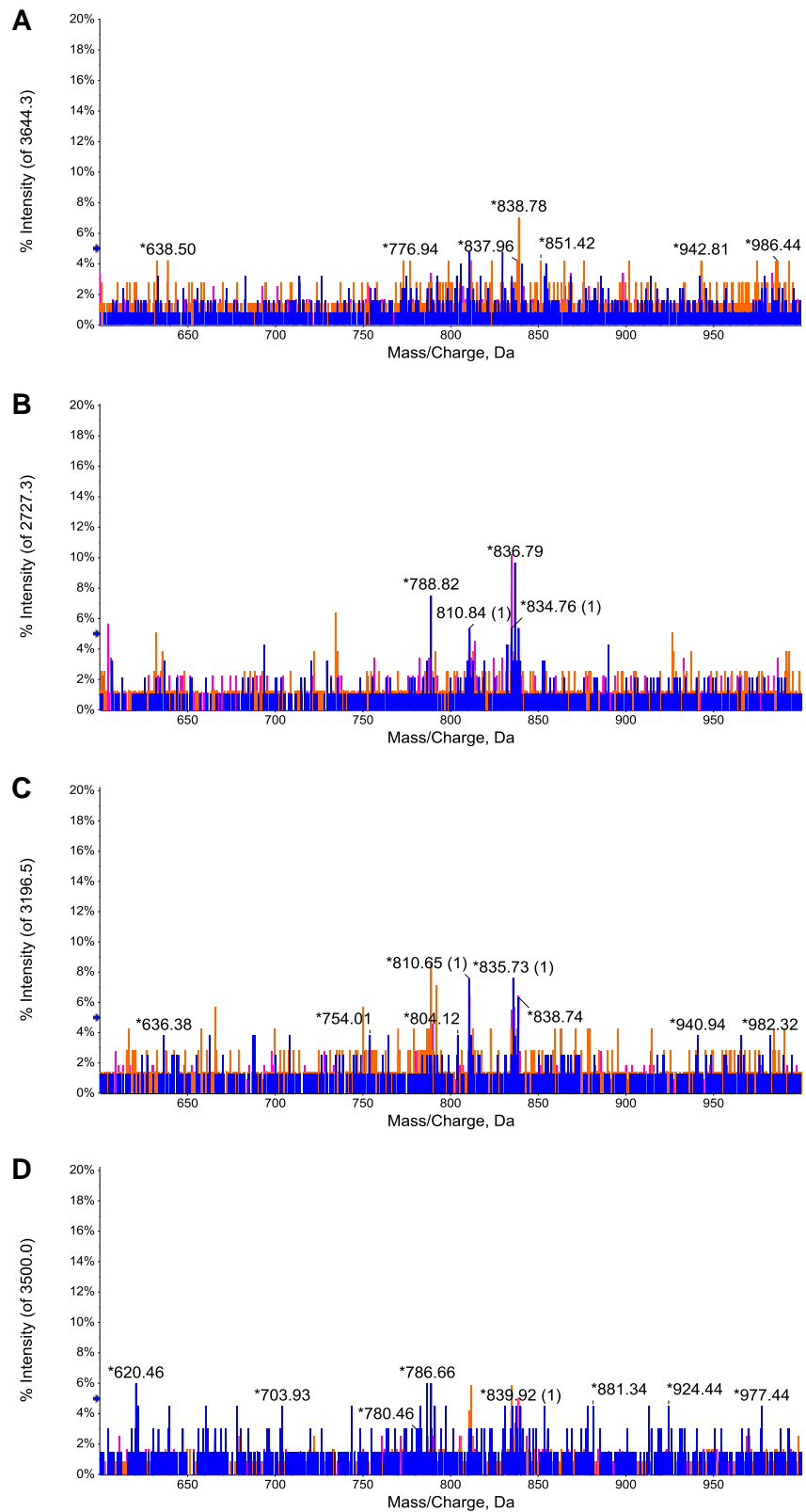


**Figure 6.17 – Detection of PSs from aortae of vehicle- and AICAR-treated C57BL/6 and ApoE<sup>-/-</sup> mice.**

Neutral loss of 87 Da by negative-ionisation ESMS was performed to identify PSs present in aortae from C57BL/6 vehicle- (A) and AICAR-treated mice (B) and ApoE<sup>-/-</sup> vehicle- (C) and AICAR-treated mice (D). Individual spectra were overlaid to highlight any differences in distributions within and between groups. n = 3.

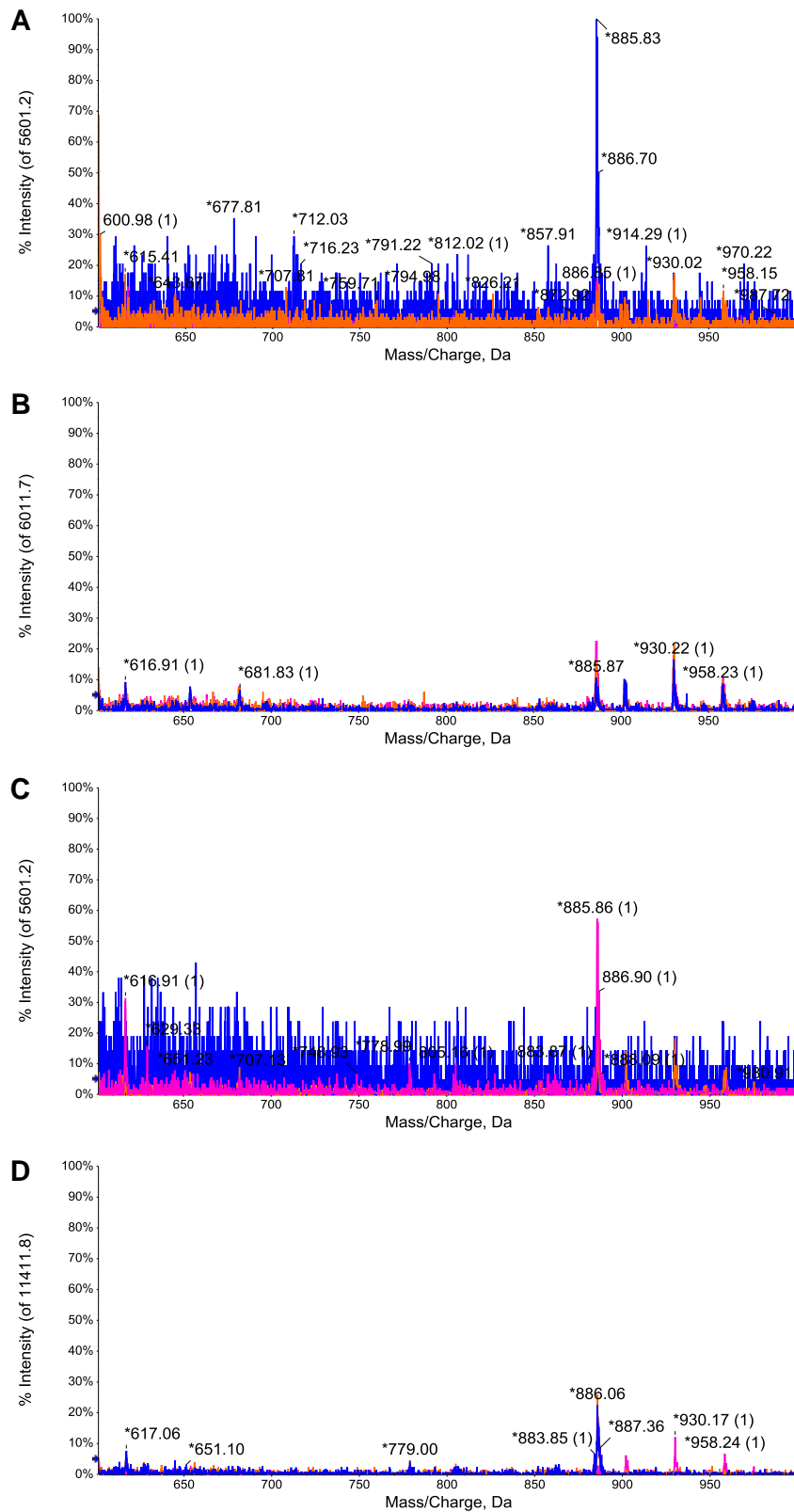


**Figure 6.18 – Detection of PIs from aortae of vehicle- and AICAR-treated C57BL/6 and ApoE<sup>-/-</sup> mice.**

Precursor ion scanning of m/z 241 by negative-ionisation ESMS was performed to identify PIs present in aortae from C57BL/6 vehicle- (A) and AICAR-treated mice (B) and ApoE<sup>-/-</sup> vehicle- (C) and AICAR-treated mice (D). Individual spectra were overlaid to highlight any potential differences in distributions within and between groups. n = 3.

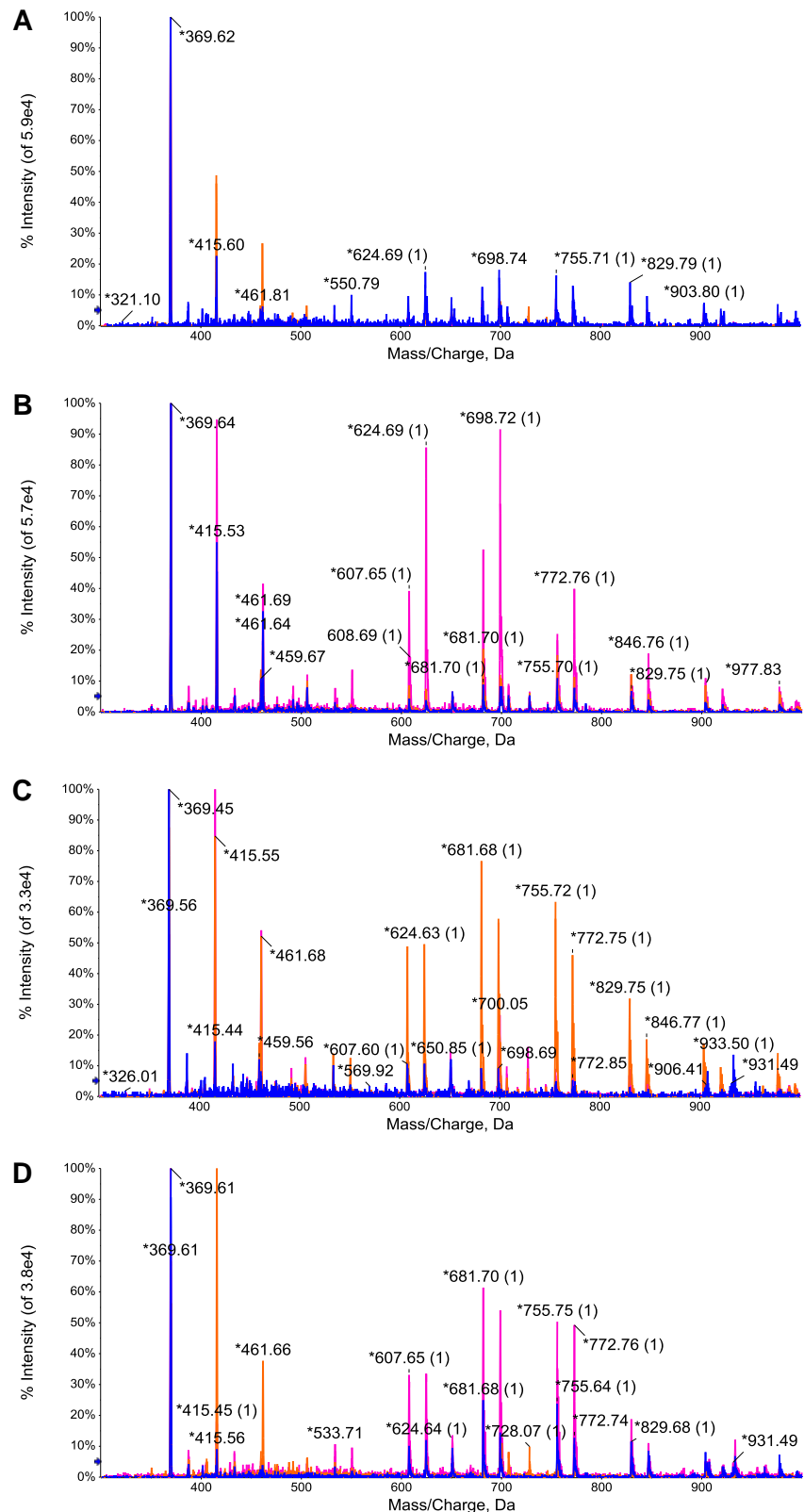


**Figure 6.19 – Detection of cholesterol and cholesteryl esters from aortae of vehicle- and AICAR-treated C57BL/6 and ApoE<sup>-/-</sup> mice.**

Precursor ion scanning for m/z 369.1 by positive-ionisation ESMS was performed to identify cholesterol and cholesteryl esters present in aortae from C57BL/6 vehicle- (A) and AICAR-treated mice (B) and ApoE<sup>-/-</sup> vehicle- (C) and AICAR-treated mice (D). Individual spectra were overlaid to highlight any potential differences in distributions within and between groups. n = 3.

**Table 6.2 – Relative abundances of detected phospholipid species in aortae of vehicle- and AICAR-treated C57BL/6 and ApoE<sup>-/-</sup> mice.**

m/z (H)	PL class	Major species	Relative abundance of ions (% of base peak)			
			C57BL/6 vehicle	C57BL/6 AICAR	ApoE <sup>-/-</sup> vehicle	ApoE <sup>-/-</sup> AICAR
496.7	LPC	16:0	10.9 ± 1.0	12.4 ± 0.0	11.0 ± 0.6	13.6 ± 3.5
524.7	LPC	18:0	5.4 ± 0.1	8.8 ± 0.7	8.0 ± 0.7	8.6 ± 1.7
703.9	SM	16:0	30.6 ± 3.4	36.2 ± 0.6	41.2 ± 9.1	32.8 ± 12.5
<b>732.9</b>	<b>PC</b>	<b>16:0/16:1</b>	<b>17.3 ± 0.8</b>	<b>20.4 ± 1.0</b>	<b>13.7 ± 3.0</b>	<b>11.0 ± 1.4<sup>‡</sup></b>
734.9	PC	16:0/16:0	41.9 ± 4.8	47.2 ± 3.1	35.3 ± 8.4	31.8 ± 4.6
758.9	PC	16:0/18:2	79.5 ± 13.9	62.6 ± 9.0	51.9 ± 6.9	67.2 ± 9.6
760.9	PC	16:0/18:1	70.6 ± 3.0	81.6 ± 4.6	74.9 ± 7.9	87.0 ± 6.7
<b>768.8</b>	<b>PE</b>	<b>18:0/20:4</b>	<b>33.1 ± 13.5</b>	<b>20.2 ± 4.6</b>	<b>40.8 ± 14.1</b>	<b>100 ± 0.0<sup>††,‡‡</sup></b>
782.9	PC	16:0/20:4	93.1 ± 6.9	100 ± 0.0	100 ± 0.0	87.0 ± 10.3
784.9	PC	18:0/18:3	33.0 ± 4.7	27.1 ± 1.3	26.2 ± 2.7	36.4 ± 4.6
786.9	PC	18:0/18:2	40.6 ± 6.2	36.4 ± 4.7	38.6 ± 2.4	74.9 ± 19.5
<b>787.9</b>	<b>SM</b>	<b>22:0</b>	<b>16.0 ± 2.4</b>	<b>12.3 ± 1.7</b>	<b>13.5 ± 2.4</b>	<b>27.7 ± 4.9<sup>†,‡</sup></b>
788.8	PS	18:0/18:1	ND	6.1 ± 0.8	8.0 ± 0.7	2.0 ± 2.5
790.8	PE	18:0/18:0	44.2 ± 13.0	ND	ND	ND
806.9	PC	16:0/22:6	20.1 ± 1.5	22.8 ± 1.1	22.7 ± 0.5	18.1 ± 3.0
<b>810.9</b>	<b>PC</b>	<b>18:0/20:4</b>	<b>48.8 ± 5.7</b>	<b>58.0 ± 1.9</b>	<b>69.7 ± 1.7*</b>	<b>52.6 ± 6.7</b>
813.0	SM	24:1	9.4 ± 0.9	10.5 ± 0.4	13.0 ± 0.8	11.6 ± 2.3
834.9	PC	18:0/22:6	8.5 ± 1.0	10.9 ± 0.6	11.7 ± 0.3	10.1 ± 2.9
838.8	PS	18:0/22:4	2.3 ± 2.3	10.0 ± 0.2	6.2 ± 0.6	5.0 ± 0.0
885.9	PI	18:0/20:4	42.5 ± 28.8	16.5 ± 2.4	38.6 ± 11.1	22.9 ± 3.3
903.1	PI	?	ND	19.4 ± 0.5	ND	ND

Relative abundances for each m/z value (protonated adduct ions) were calculated as a percentage of the largest peak in the individual spectra. Significant differences in distribution of ions are highlighted in bold. PL = phospholipid, ND = not detected. \*p<0.05 vs C57BL/6 vehicle, †p<0.05 and ‡p<0.01 vs C57BL/6 AICAR, †p<0.05 and ††p<0.01 vs ApoE<sup>-/-</sup> vehicle, n = 3.

## 6.4 Discussion

This study is the first to report the effects of AMPK activation on blood pressure regulation in ApoE<sup>-/-</sup> mice and its effect on the lipid profile of aortic tissue. Chronic administration of AICAR resulted in a reduction in mean arterial and diastolic pressures in high fat fed ApoE<sup>-/-</sup> mice. In addition, MPO was elevated in AICAR-treated ApoE<sup>-/-</sup> mice with the lipid profile altered in AMPK activated ApoE<sup>-/-</sup> mice compared to their C57BL/6 mice controls.

As hypertension is both a predisposing risk factor as well as a consequence of the progression of atherosclerosis, investigating potential mechanisms involved in these diseases would be beneficial for the treatment of both hypertension and atherosclerosis. The ability of arteries to maintain vascular tone is altered as a result of atherosclerosis which has serious implications for blood pressure regulation and therefore hypertension. The majority of previous studies examining mean arterial pressure have been in older atherosclerotic mice and little is known about the effect of short-term high fat feeding on these haemodynamic measurements. Mean arterial, diastolic and systolic pressures as well as heart rate were all elevated in ApoE<sup>-/-</sup> mice fed on the high fat diet for 6 weeks compared to their C57BL/6 controls. In addition, pulse pressure was significantly reduced in vehicle-treated ApoE<sup>-/-</sup> mice in relation to their C57BL/6 counterparts. This highlights the altered haemodynamic state found in young high fat fed ApoE<sup>-/-</sup> mice, which has only previously been shown in mice of around 6 or 7 months of age. The first signs of disease can occur as early as 6 to 8 weeks of age in ApoE<sup>-/-</sup> mice, which include monocyte adhesion, disruption of the subendothelial elastic lamina and initial foam cell formation (Nakashima *et al.*, 1994, Coleman *et al.*, 2006). Yang *et al.* (1999) reported no differences in haemodynamic measurements between age-matched 6 week old ApoE<sup>-/-</sup> and C57BL/6 mice but an increase in mean arterial pressure and left ventricular weight to body weight ratio in 7.5 month old ApoE<sup>-/-</sup> mice. Unlike in this study, these mice were not fed on a high fat diet that accelerates the formation and progression of atherosclerosis. Continuous blood pressure measurements over a 24 hour period revealed ApoE<sup>-/-</sup> mice at a similar age to this study having elevated systolic and diastolic pressures as well as increased heart rate compared to C57BL/6 control mice (Pelat *et al.*, 2003). The increase in blood pressure in ApoE<sup>-/-</sup> mice is possibly due to a reduction in arterial elasticity from ECM gene expression which in turn causes arterial stiffening (Kothapalli *et al.*, 2012). This results in the formation of less compliant vessels and the elevated pressures found in hypertension.

ApoE<sup>-/-</sup> mice fed on a high fat diet for 6 weeks also had a significantly larger body weight compared to age-matched C57BL/6 mice at the start of the study. This suggests that 6 weeks of the high fat diet is causing elevated levels of circulating lipoproteins, sufficient for fat storage to occur in these mice. However, older ApoE<sup>-/-</sup> mice have previously been shown to have reduced body weight compared to wild type controls, with the loss of the apoE gene found to be protective against obesity in C57BL/6 mice (Hartley *et al.*, 2000, Karagiannides *et al.*, 2008). In addition, C57BL/6 mice gained weight throughout the two week dosing period while ApoE<sup>-/-</sup> mice consistently lost weight. The steady loss in weight could be due to the heightened state of stress that the atherosclerotic mice are under due to disease progression, therefore making them more likely to lose weight than their C57BL/6 mice counterparts. There was no difference in heart weight normalised to body weight in C57BL/6 or ApoE<sup>-/-</sup> mice, while mature ApoE<sup>-/-</sup> mice display an increased heart to body weight ratio compared to wild type controls (Hartley *et al.*, 2000). Left ventricular hypertrophy did not accompany the elevated mean arterial pressure observed in the ApoE<sup>-/-</sup> mice, which could be due to the short length of time these mice were on the high fat diet. The whole heart weight could also be replaced with a measurement of left ventricular mass which is a routinely used indicator of cardiac hypertrophy. In addition, liver to body weight was reduced in vehicle-treated ApoE<sup>-/-</sup> mice compared to C57BL/6 mice. ApoE is primarily synthesised in the liver therefore the knockout of apoE may result in a reduction in weight due to decreased production. Furthermore, the lack of apoE results in altered cytokine production in young mice livers and lipid metabolism dysfunction, which could also affect the liver size (Yin *et al.*, 2010). Spleen weights normalised to body weight were also substantially larger in both groups of ApoE<sup>-/-</sup> mice, which is thought to be due to altered immune responses in mice deficient in apoE (Laskowitz *et al.*, 2000).

AICAR was chosen as the AMPK activator in this study as it phosphorylates AMPK without altering the levels of ATP (Corton *et al.*, 1994). As the mechanism of action of AICAR occurs by mimicking the effect of AMP, there are also some non-specific effects associated with this agonist via activation of glycogen phosphorylase and fructose-1,6-bisphosphate, both processes involved in the pathology of diabetes (Longnus *et al.*, 2003, Vincent *et al.*, 1996). ZMP formed from the metabolism of AICAR can also either mimic AMP or guanosine monophosphate (GMP) depending on the rotation of the C4 to C6 bond, which induces apoptosis in Jurkat cells independent of AMPK (Lopez *et al.*, 2003). A-769662 is a potent and specific activator of AMPK and was used in the *in vitro* investigation of AMPK in VSM in Chapter 4. However, A-769662 was not utilised for this 2 week dosing study as it is only soluble in DMSO at the concentration needed for

successful *in vivo* AMPK activation. DMSO has several reported detrimental side-effects including nausea, cardiac arrest and hypertension, which would interfere with the observations attributed to AMPK activation over this dosing period (Santos *et al.*, 2003).

AMPK activation by AICAR resulted in a reduction of mean arterial and diastolic pressures in ApoE<sup>-/-</sup> mice, similar to levels found in control C57BL/6 mice. A dramatic elevation in pulse pressure was also witnessed in ApoE<sup>-/-</sup> mice compared to their vehicle-treated controls. These effects have previously been reported with acute AICAR administration in spontaneously hypertensive rats and humans (Foley *et al.*, 1989, Bosselaar *et al.*, 2011, Ford *et al.*, 2012). Long-term AMPK activation has also resulted in a reduction in blood pressure in rats (Buhl *et al.*, 2002, Rivera *et al.*, 2009). The acute reduction in blood pressure has previously been attributed to increased NO bioavailability leading to vasodilatation of arteries (Ford *et al.*, 2012). However, this is a fast, short-lasting response and unlikely to be the only signalling pathway responsible for the effect over the 2 week dosing period. This could therefore suggest a direct action on the VSM which would contribute to a more prolonged period of action, for example, by alterations in the calcium handling machinery in VSM. In contrast, AICAR administration has been shown to have no effect on angiotensin II-induced hypertension in Wistar rats; however, AICAR was found to improve endothelial and vascular function in this study (Schulz *et al.*, 2008). Chronic administration of another AMPK activator, metformin has also displayed a reduction in systolic blood pressure in Otsuka Long-Evans Tokushima fatty rats *in vivo* (Kosegawa *et al.*, 1996).

In addition to the haemodynamic measurements, AICAR administration caused a significant reduction in body weight in ApoE<sup>-/-</sup> mice at the end of the dosing regimen compared to the midpoint measurement. Hypothalamic AMPK activity is involved in modifying food intake and activation of the AMPK pathway has been found to induce hyperphagia and weight gain (Xue and Kahn, 2006, Blanco Martinez de Morentin *et al.*, 2011). This is in contrast to the findings of this study; however, AMPK signalling is thought to be dysfunctional in atherosclerosis and therefore altered responses would not be unusual. In addition, AICAR administration in rats resulted in a lower content of abdominal fat thought to be due to an increase in degradation of adipose tissue (Buhl *et al.*, 2002). Chronic AMPK activation caused a moderate increase in the liver to body weight ratio in both strains of mice. This is consistent with previous published data on the longer term administration of 4 and 7 weeks in non-obese and obese rats respectively (Winder *et al.*, 2000, Buhl *et al.*, 2002). Winder and colleagues hypothesised that this liver

hypertrophy enabled faster metabolism of AICAR to the target tissues after the daily injection. No differences in whole heart to body weight ratio were observed after AICAR treatment. However, left ventricular hypertrophy has been associated with atherosclerosis in hypertensive patients and AMPK activity has also been implicated in a reduction in cardiac hypertrophy (Roman *et al.*, 1995, Chan *et al.*, 2004).

The changes observed in body, organ and haemodynamic measurements were accompanied by alterations in AMPK signalling in aortic and liver tissue in ApoE<sup>-/-</sup> and AICAR-treated mice. Chronic AICAR administration in C57BL/6 mice was found to cause an upregulation of the phosphorylation status of AMPK and its downstream targets in the aorta, which would indicate a potential increase in activity of the enzyme. In comparison with their C57BL/6 counterparts, there was a significant reduction in the amount of phosphorylated and total AMPK $\alpha$  and ACC in ApoE<sup>-/-</sup> mice treated with AICAR. Vehicle-treated ApoE<sup>-/-</sup> mice also had reduced levels of total ACC in relation to their C57BL/6 controls, which resulted in an elevation in the phosphorylated to total ratio of ACC. This suggests that AMPK is dysregulated in the arterial wall in atherosclerosis and the reduced levels leading to reduced AMPK activation, losing the potentially beneficial action of AMPK in the disease. This could be due to higher levels of protein phosphatase 2A, which is partly responsible for inactivating AMPK (Kang *et al.*, 2006). In hypertensive rats, a decrease in phosphorylated AMPK was also observed with no change in the total amount of the enzyme (Ford *et al.*, 2012).

In the liver, there was a reduction in the total amount of AMPK $\alpha$  in both vehicle- and AICAR-treated ApoE<sup>-/-</sup> mice in comparison with their C57BL/6 counterparts. This resulted in a large elevation in the phosphorylated to total ACC ratio with a slight reduction observed in the AICAR-treated group. There were also reduced levels of phosphorylated ACC in vehicle-treated ApoE<sup>-/-</sup> mice. In another study, AMPK activity was increased 3.6-fold in the liver only 1 hour after administration of AICAR and an increase in ZMP up to  $1.59 \pm 0.1$   $\mu\text{mol/g}$  wet muscle weight, with ZMP levels undetectable in control animals (Buhl *et al.*, 2002). This suggests the rapid metabolism of AICAR by the liver into ZMP resulting in the subsequent activation of AMPK signalling. In addition, levels of phosphorylated AMPK in hepatic tissue were reduced in obese Zucker rats by approximately 50 % compared to their lean counterparts (Rivera *et al.*, 2009). AMPK activation has previously been shown to increase hepatic fatty acid oxidation and therefore may facilitate the catabolism of free fatty acids and triglycerides (Velasco *et al.*, 1997). As

ACC is responsible for fatty acid synthesis, inhibition of the enzyme could result in decreased lipid accumulation within the arterial wall.

To investigate the effect of AMPK activation on the circulating inflammatory status, the MPO content of plasma was measured and found to be increased in ApoE<sup>-/-</sup> mice compared to their C57BL/6 mice controls. This is consistent with MPO being elevated in atherosclerosis and a potentially important indicator of CVD progression (Brennan and Hazen, 2003, Baldus *et al.*, 2003, Daugherty *et al.*, 1994). Previously published data on circulating levels of MPO in mouse plasma suggest that the levels observed in this study were dramatically higher at 598.2 ng/ml in ApoE<sup>-/-</sup> mice compared to about 160 ng/ml in LDLr<sup>-/-</sup> mice fed on a high fat diet for 6 weeks. However, these were female animals so there could be potential gender and strain differences (van Leeuwen *et al.*, 2008). In addition, AICAR treatment significantly increased MPO in the plasma of ApoE<sup>-/-</sup> mice compared to the vehicle-treated controls. A previous study has shown AMPK activation to cause a decrease in MPO levels; however, this was measured in lung tissue and not in the circulation (Tsoyi *et al.*, 2011). AMPK is present in neutrophils and phosphorylated by AMPK activators; this could lead to the release of MPO (Alba *et al.*, 2004). However, AICAR was demonstrated to have no effect on MPO levels in the pulmonary circulation (Zhao *et al.*, 2008). As ApoE<sup>-/-</sup> mice have an existing inflammatory state which is highlighted by their enlarged spleens, daily AICAR injections could have exacerbated this and led to higher levels of circulating MPO. In contrast, long-term AICAR administration has been found to reduce plasma triglycerides, free fatty acids and increase HDL by two-fold (Buhl *et al.*, 2002).

In addition, ESMS was utilised to detect different classes of modified lipids in aortic tissue as precursor ion and neutral loss scanning allows the detection of certain types of phospholipids or oxidised products without specifying individual species (Spickett *et al.*, 2011). The precursor ion scan for m/z 184.1 displayed roughly similar distribution of PCs and SMs between groups; however, a decrease in relative abundance of m/z 732.9 in AICAR-treated ApoE<sup>-/-</sup> mice compared to their C57BL/6 controls and an increase in m/z 810.9 in vehicle-treated ApoE<sup>-/-</sup> mice compared with their C57BL/6 controls was observed. These peaks likely corresponds to the protonated adducts of PCs, 16:0/16:1 and 18:0/20:4 respectively. There was a relative increase in m/z 787.9 corresponding to SM 22:0 in ApoE<sup>-/-</sup> mice dosed with AICAR. In addition, in the neutral loss scan for 141.1 Da, an increase in relative intensity of m/z 768.8 (PE 18:0/20:4) was observed in AICAR-treated ApoE<sup>-/-</sup> mice compared to both their vehicle-treated controls and AICAR dosed C57BL/6

mice. This could have resulted from a change in the ratio of  $m/z$  768.8 and 790.9. However, the levels of PEs, PSs and PIs were relatively low in all samples, therefore the differences could be resulting from differing intensities of the signals of the lipid extracts. Further analysis would be needed with the use of suitable standards to characterise these differences fully and to make firm conclusions. Together, this suggests an increase in arachidonoyl-containing species in ApoE<sup>-/-</sup> mice when AMPK is chronically activated. This is in contrast with previous reports; when hepatocytes were incubated with AICAR, there was a reduction in synthesis of PC and PE, thought to be due to a reduction in availability of choline and decreased activity of the pace-setting enzyme, CTP:phosphoethanolamine cytidyltransferase, respectively (Houweling *et al.*, 2002). However, the inhibition of hepatic PC synthesis has also been shown to be independent of AMPK (Jacobs *et al.*, 2007). Moreover, precursor scanning of  $m/z$  369.1 was utilised for detection of cholesterol and cholesteryl esters present in aorta of C57BL/6 and ApoE<sup>-/-</sup> mice. The protonated dehydration product of cholesterol was consistently the largest peak in all samples at  $m/z$  369.6. Activation of AMPK is known to inhibit cholesterol biosynthesis by inactivating HMG-CoA reductase in response to ATP depletion (Kemp *et al.*, 1999). In addition, AMPK activation has previously been implicated in reverse cholesterol transport as activation increased protein levels of ABCG1 and ABCA1, which resulted in cholesterol efflux from macrophage derived foam cells and reduced plaque formation in ApoE<sup>-/-</sup> mice (Li *et al.*, 2010a, Li *et al.*, 2010b). This highlights the effect of AMPK activation on lipid synthesis, which could be influential in reducing the plaque burden in atherosclerosis but further work is required to characterise these modified lipids fully. In addition, the detection of chlorinated lipids in the vessels was not performed due to time constraints. The high levels of plasma MPO in ApoE<sup>-/-</sup> mice would suggest an increase in the presence of HOCl-modified lipids in the vessels and further analysis of these samples would give a better indication of the occurrence of modified lipids in the vascular wall.

## 6.5 Conclusions

In summary, atherosclerotic ApoE<sup>-/-</sup> mice have elevated mean arterial, diastolic and systolic pressures and increased heart rate compared to age-matched healthy C57BL/6 mice as well as a reduction in pulse pressure. AMPK activation by chronic AICAR treatment resulted in a significant reduction in mean arterial and diastolic pressures, in addition to a dramatic increase in pulse pressure in ApoE<sup>-/-</sup> mice compared to their saline-treated counterparts. Plasma MPO levels were elevated in ApoE<sup>-/-</sup> mice and alteration of

the proportion of PCs, SMs and PEs was observed. This is the first study to investigate the effect of AMPK activation on blood pressure regulation in ApoE<sup>-/-</sup> mice. This study also examines for the first time the effect of AMPK activation on the lipid profile of aortic tissue in ApoE<sup>-/-</sup> mice as indicated by differences in the fatty acid chain distribution of PCs, although further work is required to confirm these findings.

# **CHAPTER 7**

## **GENERAL DISCUSSION**

Various physiological effects have previously been attributed to oxLDL, including an exacerbation of the inflammatory response and vascular remodelling processes in atherosclerosis and restenosis. However, little is known to date about the effects of individual modified lipids in these disease phenotypes. The overall aim of this thesis was to investigate the biological effects of modified lipids, both chlorinated and oxidised species, in vascular injury and disease focussing primarily on their effects on VSM. Primary VSMCs were used to examine the effects of these modified lipids at a cellular level. As AMPK has recently been implicated in vascular disease and also lipid synthesis, the impact of AMPK signalling on the effects of individual modified lipids in VSM was also investigated. Subsequently, the occurrence of these modified lipids in neointima lesions was assessed using a carotid artery injury model in healthy and atherosclerotic mice. Finally, *in vivo* AMPK activation in healthy and atherosclerotic mice and its effect on the lipid profile of the aorta were characterised.

As oxLDL is very heterogeneous in its composition, it is important to characterise its effects by using individual modified lipids, in order to attribute the effects seen to each component of the particle. In atherosclerosis, the active form of MPO is present within human lesions and modifies LDL into a form that is readily taken up by macrophages; aiding in the formation of foam cells (Daugherty *et al.*, 1994, Podrez *et al.*, 1999). Chlorinated lipids, phospholipid chlorohydrins and alpha-chloro fatty aldehydes are derived from modification by this MPO/H<sub>2</sub>O<sub>2</sub>/chloride system of both phospholipids and plasmalogens, respectively (Jerlich *et al.*, 2000, Arnhold *et al.*, 2001, Albert *et al.*, 2001). Oxidised phospholipids PGPC and POVPC are the truncated products formed from the autoxidation of PAPC which have previously been found to mimic some of the biological effects of mmLDL (Watson *et al.*, 1995, Watson *et al.*, 1997). The present study found chlorinated lipids to have no effect on VSMC proliferation, viability or migration after 2 hours incubation, whereas oxidised phospholipids caused a concentration-dependent reduction in all of these vascular remodelling processes, with PGPC having the greater effect (Chapter 3). In addition, SOPC ClOH caused a significant reduction in cellular ATP after 6 hours treatment at the highest concentrations. This is the first study to investigate the effects of chlorinated lipids on VSM and to highlight the differing effects between modified lipid species. Chlorinated lipids have previously been shown to induce pro-inflammatory actions such as leukocyte adhesion and generation of ROS (Dever *et al.*, 2006, Dever *et al.*, 2008) but, in the present study, no acute effects on VSMC remodelling processes were found. This could suggest that phospholipid chlorohydrins and alpha-chloro fatty aldehydes could be more involved in the inflammatory response of

atherosclerosis rather than in remodelling processes that result in changes to the vessel architecture. In addition, VSMCs could be more resistant to the actions of chlorinated lipids in comparison to myeloid and endothelial cells. In stark contrast, a biphasic response has previously been reported for oxidised phospholipid effects on remodelling processes with a proliferative action observed at lower concentrations and apoptosis predominating at higher levels (Auge *et al.*, 2002, Fruhwirth *et al.*, 2006, Johnstone *et al.*, 2009). In areas of inflammation, the presence of OCl<sup>-</sup>, the deprotonated form of HOCl, has previously been found to reach concentrations of up to 300 µM (Katrantzis *et al.*, 1991). In human atherosclerotic plaque samples, POVPC was found between 20 to 40 µg per gram of tissue with slightly higher levels, of between 40 to 100 µg per gram of tissue being reported in rabbit aorta for POVPC and PGPC (Ravandi *et al.*, 2004, Watson *et al.*, 1997, Subbanagounder *et al.*, 2000). This suggests that the concentrations of modified lipids used in the present study are relevant to those found within the *in vivo* setting.

AMPK is a key regulator of energy homeostasis and is commonly referred to as a cellular “fuel gauge” (Hardie and Carling, 1997). Activation of AMPK has previously been found to be beneficial in atherosclerosis as it reduced leukocyte adhesion to human aortic endothelial cells and alleviated the plaque burden in ApoE<sup>-/-</sup> mice *in vivo* (Ewart *et al.*, 2008, Li *et al.*, 2010a). In addition, AMPK activation has been found to exert anti-apoptotic effects in a number of cell types including endothelial cells (Ido *et al.*, 2002, Kim *et al.*, 2008, Liu *et al.*, 2010). As the modified lipids used in this study have been found to induce cell death in VSMCs and other cell types, the influence of AMPK on modulating the effects of these lipids was next investigated. Although modified lipid treatment did not phosphorylate AMPK directly, this is the first study to find that modulation of the AMPK pathway changes the response of the VSMCs to modified lipids (Chapter 4). Activation of AMPK prior to incubation of SOPC ClOH and POVPC made VSMCs more susceptible to proliferation and toxicity respectively. This suggests that activation of the AMPK signalling pathway prior to the addition of modified lipids results in greater effects than incubation of the lipids alone. This could be a protective measure to clear damaged or dying cells, resulting from the action of the oxidised phospholipid, more quickly via AMPK signalling while activation of AMPK prior to SOPC ClOH treatment initiates proliferation pathways in VSMCs that the lipid alone cannot stimulate. In addition, differing effects of modified lipids were found on vascular reactivity of mouse carotid arteries in response to activation of AMPK. Similarly to the initial cell experiments, chlorinated lipids were found to have no effect on AICAR-induced relaxation whereas oxidised phospholipids caused a concentration-dependent reduction in relaxation with

PGPC producing a greater reduction. Atherosclerosis significantly reduces the relaxing capacity of arteries with impairment of both endothelium-dependent and -independent actions in arteries isolated from ApoE<sup>-/-</sup> mice. These effects could therefore be partly due to the increased levels of modified lipids in the vascular wall (Crauwels *et al.*, 2003, d'Uscio *et al.*, 2001). This study has therefore produced novel data on the impact of AMPK signalling on the effects of modified lipids and highlighted again the differing effects of modified lipid species in VSMCs.

The divergent effects witnessed with incubation of the different classes of modified lipids used in this study could suggest a different duration of action for each species due to the higher level of toxicity observed with modified lipids at longer treatment times. The modified lipids could also be involved in different cellular processes; for example, the oxidised phospholipids could participate in the primary effects and chlorinated lipids could be involved in the latter stages of remodelling. This could be further enhanced by the activation of the AMPK signalling pathway in VSMCs resulting in enhanced cell death with POVPC and an elevation in proliferation with SOPC ClOH. A schematic diagram displaying the potential interactions of the modified lipids and AMPK signalling is shown in Figure 7.1. This pathway could be activated by cellular changes in ATP evoked by the modified lipids as well as by a stress response to changes in energy homeostasis due to the progression of atherosclerosis. In addition, there could be an interaction of these lipids with upstream kinases known to phosphorylate AMPK such as LKB1 and CAMKK $\beta$ , which with the addition of pharmacological activation of AMPK, result in the observed alteration in the response of modified lipids in VSMCs. PGPC could be responsible for the initial cell death as it induced substantial death after 2 hours in the *in vitro* experiments. This effect could be followed by the action of POVPC as it is less potent than PGPC or additional to the effects of PGPC with prior activation of AMPK. SOPC ClOH and other chlorohydrins may be involved in a proliferative stage with activation of the AMPK signalling pathway or in the last stage of cell death, as a significant reduction in cell death was witnessed after 6 hours treatment at the higher concentrations. This would suggest a cumulative effect of the modified lipids on vascular remodelling processes in the vasculature. Due to their previously reported biphasic response (Auge *et al.*, 2002, Fruhwirth *et al.*, 2006, Johnstone *et al.*, 2009), modified lipids could also be involved in the latter proliferative stages of vascular injury leading to the formation of neointima; however, this would be difficult to measure *in vitro*. MPO has been implicated in all stages of atherosclerosis (Nicholls and Hazen, 2009), therefore with the higher levels of circulating lipoproteins resulting in elevated levels of modified lipids, it would be feasible

for these lipids to be present and involved in all phases of the vascular remodelling processes. Longer incubations with modified lipids would not be possible in quiescing medium, and incubating VSMCs with medium containing growth supplements such as FCS along with modified lipids would lead to the breakdown of these lipids by serum phospholipases (Fruhirth *et al.*, 2006). This is a key limitation of the *in vitro* VSMC model as the effects of longer incubations in quiescing medium with modified lipids could not be attributed solely to the lipids because, in absence of the growth supplements, the cells would likely induce programmed cell death processes due to lack of available nutrients.

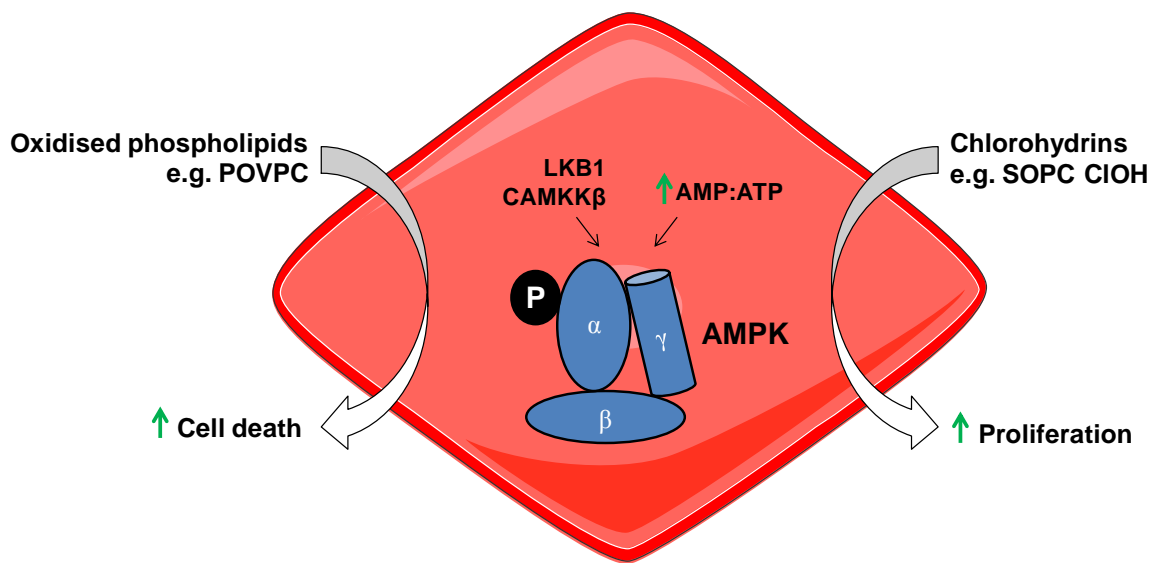


**Figure 7.1 – Schematic diagram of the proposed interaction of modified lipids and AMPK signalling in VSMCs.**

Phosphorylation of AMPK results in VSMCs being more susceptible to cell death and proliferation after treatment with oxidised phospholipids and chlorohydrins, respectively.

Endothelial dysfunction is widely reported to initiate the remodelling process with the intimal layer critical in vascular remodelling due to the release and activation of substances involved in growth, death and migration of vascular and inflammatory cells (Gibbons and Dzau, 1994). Investigation of the effects of the modified lipids used in this study on endothelial cells would aid in the understanding of the actions of these lipids on the vascular remodelling processes, as would the identification of the signalling pathways activated or inhibited by modified lipids in vascular cells. In addition, incubation of modified lipids in a co-culture of endothelial cells and VSMCs would better represent the *in vivo* setting and could highlight novel interactions of the lipids and vascular cells and the potential release of vasoactive substances from the endothelial cells to act on the VSMCs.

As AMPK has previously been found to exert anti-apoptotic effects in endothelial cells, the modulation of this pathway on the effects of the modified lipids used in this study could also further expand the beneficial actions attributed to AMPK in vascular diseases.

To substantiate the observations witnessed in the cellular experiments, *in vivo* analysis was performed to investigate the presence of modified lipids in the arterial wall after both vascular injury and chronic AMPK activation in C57BL/6 and ApoE<sup>-/-</sup> mice. Restenosis is a known complication of the surgical interventions used to treat atherosclerosis and results in neointimal thickening, in part by the action of VSMCs. To investigate the occurrence of different classes of modified lipids in neointima *in vivo*, a carotid artery mouse injury model was used in C57BL/6 and ApoE<sup>-/-</sup> mice. The present study characterises for the first time, the phospholipid molecular species present in the arterial wall of the carotid arteries of C57BL/6 and ApoE<sup>-/-</sup> mice after carotid artery injury (Chapter 5). Neointima formation was greatly increased in ApoE<sup>-/-</sup> mice compared with sham-operated controls and healthy C57BL/6 mice, while no changes were observed in the VSM content of the neointimal growth or on the proliferative and apoptotic processes investigated. In previous studies, apoptosis was found to be elevated immediately after balloon distension injury in ApoE<sup>-/-</sup> mice and via a caspase 3-dependent mechanism in balloon injured rabbits while proliferation was increased 7 and 28 days post injury (Matter *et al.*, 2006, Spiguel *et al.*, 2010). In the present study, it must be remembered that the carotid arteries were injured as well as ligated causing a change in the haemodynamics of the vessel. This in turn could have led to a faster response, explaining the observation that no changes in proliferative or apoptotic processes were detected 14 days after injury. These remodelling mechanisms were occurring to compensate for both the change in vessel diameter as well as the removal of endothelium causing complete occlusion in a number of vessels. Total AMPK $\alpha$  was also found to be significantly increased in the neointimal growth in sham-operated ApoE<sup>-/-</sup> mice compared to their C57BL/6 counterparts. This could be due to an increase in cell number within the neointima resulting in an increase in AMPK present, or could be a protective measure to try and counteract the neointimal hyperplasia.

The interest in the beneficial role of AMPK in vascular diseases has increased substantially over the last few years. This study has revealed for the first time the involvement of AMPK in blood pressure regulation in ApoE<sup>-/-</sup> mice with chronic administration of AICAR resulting in a reduction in mean arterial and diastolic pressures in high fat fed ApoE<sup>-/-</sup> mice (Chapter 6). These effects have previously been reported with acute AICAR administration in spontaneously hypertensive rats and humans (Foley *et al.*, 1989,

Bosselaar *et al.*, 2011, Ford *et al.*, 2012). The acute reduction in blood pressure has previously been attributed to increased NO bioavailability leading to vasodilatation of arteries (Ford *et al.*, 2012). However, this is a fast, short-lasting response and unlikely to be the only signalling pathway responsible for the effect over the 2 week dosing period. This could therefore suggest a direct action on the VSM, which would contribute to a more prolonged period of action, for example, by alterations in the calcium handling machinery in VSM. In comparison with their C57BL/6 counterparts, there was a significant decrease in the amount of phosphorylated and total AMPK $\alpha$  and ACC in ApoE<sup>-/-</sup> mice treated with AICAR compared with their C57BL/6 controls and a reduction in the levels of total ACC in vehicle-treated ApoE<sup>-/-</sup> mice. This suggests that AMPK is dysregulated in the arterial wall in atherosclerosis and the reduced levels could lead to a reduction in AMPK activation, losing the potentially beneficial action of AMPK in halting disease progression. In addition, this is one of the first studies to report an elevation in blood pressure of young ApoE<sup>-/-</sup> mice fed only on a high fat diet for 1 month. Studies have previously focussed on haemodynamic measurements of older mice where the atherosclerotic phenotype would be more pronounced or found no changes at this younger age compared with control mice (Yang *et al.*, 1999, Hartley *et al.*, 2000).

The MPO plasma content was found to be elevated in all groups of ApoE<sup>-/-</sup> mice in both the carotid injury and chronic AMPK activation studies suggesting an increase in the inflammatory status of atherosclerotic mice. This could result in a higher level of modified lipids produced in the arterial wall which are pro-inflammatory and essential in the formation of atherosclerotic lesions. Plasma MPO was further elevated in ApoE<sup>-/-</sup> mice administered AICAR compared to their saline-treated counterparts. Measurement of the levels of circulating neutrophils in C57BL/6 and ApoE<sup>-/-</sup> mice, to see if this accounts for the elevation in plasma MPO, would be beneficial. A novel pharmacological MPO inhibitor, INV-315 has recently been produced which resulted in a reduction in oxidative stress and enhancement of cholesterol efflux in an atherosclerotic mouse model (Liu *et al.*, 2012). This suggests that inhibition of MPO could result in a reduction in atherosclerotic plaque formation and potentially a reduction in modified lipid production. Inhibition of MPO in the carotid injury model could provide valuable information on the formation of neointima and the lipid profile of the arterial wall after inhibition of one of the routes for the production of modified lipids. Recently, AMPK $\alpha$ 2<sup>-/-</sup> mice were crossed with C57BL/6 ApoE<sup>-/-</sup> mice to generate mice with a double knockout of apoE and AMPK $\alpha$ 2 (Wang *et al.*, 2011a). Investigation of the plasma MPO content of these mice would also be beneficial in understanding the relationship between MPO and AMPK in atherosclerotic mice.

In addition, both the carotid injury and chronic AMPK activation studies revealed significant changes in the relative intensities of several phospholipids, primarily PCs, in the arterial tissue of C57BL/6 and ApoE<sup>-/-</sup> mice. In the carotid injury study, a higher proportion of lysolipids was detected in the injured carotid arteries of ApoE<sup>-/-</sup> mice compared to both their uninjured controls as well as the C57BL/6 control mice. This is consistent with a previous study where lysolipids were elevated in the intima and inner media of atherosclerotic aortae of squirrel monkeys, which is likely to be exacerbated in the hyperproliferative state after vascular injury (Portman and Alexander, 1969). Injured carotid arteries also appeared to be enriched with linoleoyl-containing PCs. These unsaturated phospholipids could undergo modification by the MPO system, leading to an increase in modified lipids present at the site of injury. Additional targeted scanning for neutral losses of 36 and 38 Da (H<sup>35</sup>Cl and H<sup>37</sup>Cl) as well as neutral loss of 18 Da, as ions containing –OH groups lose water, could confirm the presence and highlight the relative levels of chlorohydrins and other chlorinated species within the arterial wall after vascular injury. There was not sufficient time to perform this analysis in this study; however, this could form the basis of future work within this area. The distribution of phospholipids was also found to be altered after chronic AICAR administration in ApoE<sup>-/-</sup> mice, suggesting a novel interaction between AMPK activation and the formation of modified lipids. A more pronounced effect may be witnessed with longer term high fat feeding of ApoE<sup>-/-</sup> mice, which would accelerate the progression of atherosclerosis and therefore the levels of circulating and modified lipids. Investigation of the involvement of modified lipids in neointima formation after carotid artery injury in the double knockout mice of apoE and AMPK $\alpha$ 2 could also provide further evidence on the interaction of AMPK signalling and modified lipids in atherosclerosis.

A limitation of the ESMS analysis used in this study is the lack of internal or external standards in the lipid extracts from the injured and uninjured carotid arteries as well as the aortae of mice chronically administered AICAR. Standards are commonly used for quantification of levels within samples by the addition of a lipid at a known concentration. However, there would also be limitations in using standards in these samples as the sizes of the arteries varied and were not pre-weighed before lipid extraction therefore the lipid concentrations cannot be calculated. Additionally, the amount of lipid is likely to vary within the artery and while standards may indicate the absolute concentration, all the lipids should fluctuate together depending on the total lipid content extracted. Comparisons were made instead between the relative intensities of the lipids present in these samples, which generated information about changes in the lipid profile in the different strains and in

response to treatments. It should also be noted that ESMS is not a quantitative technique in itself, due to the different ionisation efficiencies of lipid classes, therefore PC levels cannot be directly compared with PEs or PSs, *etc.* There is also further variation within the PC class as short chains ionise better than long chains. However, all these differences should be the same between samples, therefore it is valid to look for changes in relative intensities and patterns between samples in this study. Additional analysis by liquid chromatography coupled with tandem mass spectrometry would enable the confirmation of the observed changes in proportions of the phospholipids studied in this thesis, as well as provide essential information on the oxidation products present which are critical in the progression of atherosclerosis.

## 7.1 Conclusions

In summary, this thesis has shown for the first time the divergent effects of different classes of modified lipids as well as modulation of AMPK signalling resulting in altered modified lipid responses in VSMCs. The present study has displayed a novel mechanism of blood pressure regulation by chronic activation of AMPK in ApoE<sup>-/-</sup> mice. It has also generated novel data on the relative changes in distribution of PCs in carotid arteries after carotid artery injury as well as in aortic tissue after chronic AMPK activation in both healthy and atherosclerotic mice. Additional analysis is required to confirm the relative differences in PCs which could offer further insight into the involvement of modified lipids in vascular diseases. Furthermore, this study has highlighted a novel interaction of AMPK signalling and modified lipids in VSM and could therefore provide novel therapeutic targets in the treatment of both atherosclerosis and restenosis.

## List of References

(2002) Third report of the National Cholesterol Education Program (NCEP) Expert Panel on detection, evaluation, and treatment of high blood cholesterol in adults (Adult Treatment Panel III) final report. *Circulation*, **106**, 3143-3421.

AIT-OUFELLA, H., KINUGAWA, K., ZOLL, J., SIMON, T., BODDAERT, J., HEENEMAN, S., BLANC-BRUDE, O., BARATEAU, V., POTTEAUX, S., MERVAL, R., ESPOSITO, B., TEISSIER, E., DAEMEN, M. J., LESECHE, G., BOULANGER, C., TEDGUI, A. & MALLAT, Z. (2007) Lactadherin deficiency leads to apoptotic cell accumulation and accelerated atherosclerosis in mice. *Circulation*, **115**, 2168-2177.

AL-SHAWAF, E., NAYLOR, J., TAYLOR, H., RICHES, K., MILLIGAN, C. J., O'REGAN, D., PORTER, K. E., LI, J. & BEECH, D. J. (2010) Short-term stimulation of calcium-permeable transient receptor potential canonical 5-containing channels by oxidized phospholipids. *Arterioscler Thromb Vasc Biol*, **30**, 1453-1459.

ALBA, G., EL BEKAY, R., ALVAREZ-MAQUEDA, M., CHACON, P., VEGA, A., MONTESEIRIN, J., SANTA MARIA, C., PINTADO, E., BEDOYA, F. J., BARTRONS, R. & SOBRINO, F. (2004) Stimulators of AMP-activated protein kinase inhibit the respiratory burst in human neutrophils. *FEBS Lett*, **573**, 219-225.

ALBERT, C. J., CROWLEY, J. R., HSU, F. F., THUKKANI, A. K. & FORD, D. A. (2001) Reactive chlorinating species produced by myeloperoxidase target the vinyl ether bond of plasmalogens - Identification of 2-chlorohexadecanal. *J Biol Chem*, **276**, 23733-23741.

ALEXANDER, R. W. (1995) Theodore Cooper Memorial Lecture. Hypertension and the pathogenesis of atherosclerosis. Oxidative stress and the mediation of arterial inflammatory response: a new perspective. *Hypertension*, **25**, 155-161.

ANBUKUMAR, D. S., SHORNICK, L. P., ALBERT, C. J., STEWARD, M. M., ZOELLER, R. A., NEUMANN, W. L. & FORD, D. A. (2010) Chlorinated lipid species in activated human neutrophils: lipid metabolites of 2-chlorohexadecanal. *J Lipid Res*, **51**, 1085-1092.

ANDREOU, I., TOUSOULIS, D., MILIOU, A., TENTOLOURIS, C., ZISIMOS, K., GOUNARI, P., SIASOS, G., PAPAGEORGIOU, N., PAPADIMITRIOU, C. A., DIMOPOULOS, M. A. & STEFANADIS, C. (2010) Effects of rosuvastatin on myeloperoxidase levels in patients with chronic heart failure: a randomized placebo-controlled study. *Atherosclerosis*, **210**, 194-198.

ANG, A. H., TACHAS, G., CAMPBELL, J. H., BATEMAN, J. F. & CAMPBELL, G. R. (1990) Collagen synthesis by cultured rabbit aortic smooth-muscle cells. Alteration with phenotype. *Biochem J*, **265**, 461-469.

ARNHOLD, J., OSIPOV, A. N., SPALTEHOLZ, H., PANASENKO, O. M. & SCHILLER, J. (2001) Effects of hypochlorous acid on unsaturated phosphatidylcholines. *Free Radic Biol Med*, **31**, 1111-1119.

ARNHOLD, J., OSIPOV, A. N., SPALTEHOLZ, H., PANASENKO, O. M. & SCHILLER, J. (2002) Formation of lysophospholipids from unsaturated

- phosphatidylcholines under the influence of hypochlorous acid. *BBA-Gen Subjects*, **1572**, 91-100.
- AUGE, N., GARCIA, V., MAUPAS-SCHWALM, F., LEVADE, T., SALVAYRE, R. & NEGRE-SALVAYRE, A. (2002) Oxidized LDL-induced smooth muscle cell proliferation involves the EGF receptor/PI-3 kinase/Akt and the sphingolipid signaling pathways. *Arterioscler Thromb Vasc Biol*, **22**, 1990-1995.
- BACKES, A., SEAY, U., SEDDING, D. G., TILLMANN, H. H. & BRAUN-DULLAEUS, R. C. (2010) Inhibition of matrix deposition: a new strategy for prevention of restenosis after balloon angioplasty. *J Cardiovasc Pharmacol*, **55**, 213-218.
- BAIN, J., PLATER, L., ELLIOTT, M., SHPIRO, N., HASTIE, C. J., MCLAUCHLAN, H., KLEVERNIC, I., ARTHUR, J. S., ALESSI, D. R. & COHEN, P. (2007) The selectivity of protein kinase inhibitors: a further update. *Biochem J*, **408**, 297-315.
- BALDUS, S., HEESCHEN, C., MEINERTZ, T., ZEIHNER, A. M., EISERICH, J. P., MUNZEL, T., SIMOONS, M. L. & HAMM, C. W. (2003) Myeloperoxidase serum levels predict risk in patients with acute coronary syndromes. *Circulation*, **108**, 1440-1445.
- BASSIOUNY, H. S., ZARINS, C. K., KADOWAKI, M. H. & GLAGOV, S. (1994) Hemodynamic stress and experimental aortoiliac atherosclerosis. *J Vasc Surg*, **19**, 426-434.
- BATEMAN, A. (1997) The structure of a domain common to archaebacteria and the homocystinuria disease protein. *Trends Biochem Sci*, **22**, 12-13.
- BEDDEL, A., NEGRE-SALVAYRE, A., HEENEMAN, S., GRAZIDE, M. H., THIERS, J. C., SALVAYRE, R. & MAUPAS-SCHWALM, F. (2008) E-cadherin/beta-catenin/T-cell factor pathway is involved in smooth muscle cell proliferation elicited by oxidized low-density lipoprotein. *Circ Res*, **103**, 694-701.
- BEG, Z. H., ALLMANN, D. W. & GIBSON, D. M. (1973) Modulation of 3-hydroxy-3-methylglutaryl coenzyme A reductase activity with cAMP and with protein fractions of rat liver cytosol. *Biochem Biophys Res Commun*, **54**, 1362-1369.
- BELLESIA, F., BONI, M., GHELFI, F., GRANDI, R., PAGNONI, U. M. & PINETTI, A. (1992) Acetal chlorination with  $\text{MNO}_2$ -trimethylchlorosilane. *Tetrahedron*, **48**, 4579-4586.
- BENNETT, M. R. & BOYLE, J. J. (1998) Apoptosis of vascular smooth muscle cells in atherosclerosis. *Atherosclerosis*, **138**, 3-9.
- BENZIANE, B., BJORNHOLM, M., LANTIER, L., VIOLLET, B., ZIERATH, J. R. & CHIBALIN, A. V. (2009) AMP-activated protein kinase activator A-769662 is an inhibitor of the  $\text{Na}^+$ - $\text{K}^+$ -ATPase. *Am J Physiol Cell Physiol*, **297**, C1554-1566.
- BERNE, R. M., LEVY, M. N., KOEPPEN, B. M. & STANTON, B. A. (2004) *Physiology 5th Edition*, USA, Mosby, Elsevier Science.
- BLANCO MARTINEZ DE MORENTIN, P., GONZALEZ, C. R., SAHA, A. K., MARTINS, L., DIEGUEZ, C., VIDAL-PUIG, A., TENA-SEMPERE, M. & LOPEZ, M. (2011) Hypothalamic AMP-activated protein kinase as a mediator of whole body energy balance. *Rev Endocr Metab Disord*, **12**, 127-140.

- BOCHKOV, V. N., KADL, A., HUBER, J., GRUBER, F., BINDER, B. R. & LEITINGER, N. (2002) Protective role of phospholipid oxidation products in endotoxin-induced tissue damage. *Nature*, **419**, 77-81.
- BOSSELAAR, M., SMITS, P., VAN LOON, L. J. & TACK, C. J. (2011) Intravenous AICAR during hyperinsulinemia induces systemic hemodynamic changes but has no local metabolic effect. *J Clin Pharmacol*, **51**, 1449-1458.
- BRADFORD, M. M. (1976) A rapid and sensitive method for the quantitation of microgram quantities of protein utilizing the principle of protein-dye binding. *Anal Biochem*, **72**, 248-254.
- BRENNAN, M. L., ANDERSON, M. M., SHIH, D. M., QU, X. D., WANG, X. P., MEHTA, A. C., LIM, L. L., SHI, W. B., HAZEN, S. L., JACOB, J. S., CROWLEY, J. R., HEINECKE, J. W. & LUSIS, A. J. (2001) Increased atherosclerosis in myeloperoxidase-deficient mice. *J Clin Invest*, **107**, 419-430.
- BRENNAN, M. L. & HAZEN, S. L. (2003) Emerging role of myeloperoxidase and oxidant stress markers in cardiovascular risk assessment. *Curr Opin Lipidol*, **14**, 353-359.
- BRENNAN, M. L., PENN, M. S., VAN LENTE, F., NAMBI, V., SHISHEHBOR, M. H., AVILES, R. J., GOORMASTIC, M., PEPOY, M. L., MCERLEAN, E. S., TOPOL, E. J., NISSEN, S. E. & HAZEN, S. L. (2003) Prognostic value of myeloperoxidase in patients with chest pain. *N Engl J Med*, **349**, 1595-1604.
- BRINDLE, N. P. (1993) Growth factors in endothelial regeneration. *Cardiovasc Res*, **27**, 1162-1172.
- BRITO, P. M., DEVILLARD, R., NEGRE-SALVAYRE, A., ALMEIDA, L. M., DINIS, T. C., SALVAYRE, R. & AUZE, N. (2009) Resveratrol inhibits the mTOR mitogenic signaling evoked by oxidized LDL in smooth muscle cells. *Atherosclerosis*, **205**, 126-134.
- BROWN, B. G., BOLSON, E. L. & DODGE, H. T. (1982) Arteriographic assessment of coronary atherosclerosis. Review of current methods, their limitations, and clinical applications. *Arteriosclerosis*, **2**, 2-15.
- BROWN, M. S. & GOLDSTEIN, J. L. (1983) Lipoprotein metabolism in the macrophage: implications for cholesterol deposition in atherosclerosis. *Annu Rev Biochem*, **52**, 223-261.
- BU, D. X., TARRIO, M., MAGANTO-GARCIA, E., STAVRAKIS, G., TAJIMA, G., LEDERER, J., JAROLIM, P., FREEMAN, G. J., SHARPE, A. H. & LICHTMAN, A. H. (2011) Impairment of the programmed cell death-1 pathway increases atherosclerotic lesion development and inflammation. *Arterioscler Thromb Vasc Biol*, **31**, 1100-1107.
- BUCKLEY, C., BUND, S. J., MCTAGGART, F., BRUCKDORFER, K. R., OLDHAM, A. & JACOBS, M. (1996) Oxidized low-density lipoproteins inhibit endothelium-dependent relaxations in isolated large and small rabbit coronary arteries. *J Auton Pharmacol*, **16**, 261-267.
- BUHL, E. S., JESSEN, N., POLD, R., LEDET, T., FLYVBJERG, A., PEDERSEN, S. B., PEDERSEN, O., SCHMITZ, O. & LUND, S. (2002) Long-term AICAR administration reduces metabolic disturbances and lowers blood pressure in rats displaying features of the insulin resistance syndrome. *Diabetes*, **51**, 2199-2206.

- CAMPBELL, J. H. & CAMPBELL, G. R. (1994) The role of smooth muscle cells in atherosclerosis. *Curr Opin Lipidol*, **5**, 323-330.
- CARLSON, C. A. & KIM, K. H. (1973) Regulation of hepatic acetyl coenzyme A carboxylase by phosphorylation and dephosphorylation. *J Biol Chem*, **248**, 378-380.
- CARR, A. C., VANDENBERG, J. J. M. & WINTERBOURN, C. (1996) Chlorination of cholesterol in cell membranes by hypochlorous acid. *Arch Biochem Biophys*, **332**, 63-69.
- CARR, A. C., VISSERS, M. C., DOMIGAN, N. M. & WINTERBOURN, C. C. (1997) Modification of red cell membrane lipids by hypochlorous acid and haemolysis by preformed lipid chlorohydrins. *Redox Rep*, **3**, 263-271.
- CASSCELLS, W. (1992) Migration of smooth muscle and endothelial cells. Critical events in restenosis. *Circulation*, **86**, 723-729.
- CASTELLANI, L. W., CHANG, J. J., WANG, X., LUSIS, A. J. & REYNOLDS, W. F. (2006) Transgenic mice express human MPO -463G/A alleles at atherosclerotic lesions, developing hyperlipidemia and obesity in -463G males. *J Lipid Res*, **47**, 1366-1377.
- CHAHINE, M. N., BLACKWOOD, D. P., DIBROV, E., RICHARD, M. N. & PIERCE, G. N. (2009) Oxidized LDL affects smooth muscle cell growth through MAPK-mediated actions on nuclear protein import. *J Mol Cell Cardiol*, **46**, 431-441.
- CHAIT, A., BRAZG, R. L., TRIBBLE, D. L. & KRAUSS, R. M. (1993) Susceptibility of small, dense, low-density lipoproteins to oxidative modification in subjects with the atherogenic lipoprotein phenotype, pattern B. *Am J Med*, **94**, 350-356.
- CHAN, A. Y., SOLTYS, C. L., YOUNG, M. E., PROUD, C. G. & DYCK, J. R. (2004) Activation of AMP-activated protein kinase inhibits protein synthesis associated with hypertrophy in the cardiac myocyte. *J Biol Chem*, **279**, 32771-32779.
- CHANG, M. K., BINDER, C. J., MILLER, Y. I., SUBBANAGOUNDER, G., SILVERMAN, G. J., BERLINER, J. A. & WITZTUM, J. L. (2004) Apoptotic cells with oxidation-specific epitopes are immunogenic and proinflammatory. *J Exp Med*, **200**, 1359-1370.
- CHATTERJEE, S., BERLINER, J. A., SUBBANAGOUNDER, G. G., BHUNIA, A. K. & KOH, S. (2004) Identification of a biologically active component in minimally oxidized low density lipoprotein (MM-LDL) responsible for aortic smooth muscle cell proliferation. *Glycoconj J*, **20**, 331-338.
- CHEN, J., MEHTA, J. L., HAIDER, N., ZHANG, X., NARULA, J. & LI, D. (2004) Role of caspases in ox-LDL-induced apoptotic cascade in human coronary artery endothelial cells. *Circ Res*, **94**, 370-376.
- CHENG, G., SALERNO, J. C., CAO, Z., PAGANO, P. J. & LAMBETH, J. D. (2008) Identification and characterization of VPO1, a new animal heme-containing peroxidase. *Free Radic Biol Med*, **45**, 1682-1694.
- CHEREPANOVA, O. A., PIDKOVKA, N. A., SARMENTO, O. F., YOSHIDA, T., GAN, Q., ADIGUZEL, E., BENDECK, M. P., BERLINER, J., LEITINGER, N. & OWENS, G. K. (2009) Oxidized phospholipids induce type VIII collagen expression and vascular smooth muscle cell migration. *Circ Res*, **104**, 609-618.

- CHEUNG, P. C., SALT, I. P., DAVIES, S. P., HARDIE, D. G. & CARLING, D. (2000) Characterization of AMP-activated protein kinase gamma-subunit isoforms and their role in AMP binding. *Biochem J*, **346 Pt 3**, 659-669.
- CHURCH, D. F. & PRYOR, W. A. (1985) Free-radical chemistry of cigarette smoke and its toxicological implications. *Environ Health Perspect*, **64**, 111-126.
- CLARKE, M. C., LITTLEWOOD, T. D., FIGG, N., MAGUIRE, J. J., DAVENPORT, A. P., GODDARD, M. & BENNETT, M. R. (2008) Chronic apoptosis of vascular smooth muscle cells accelerates atherosclerosis and promotes calcification and medial degeneration. *Circ Res*, **102**, 1529-1538.
- CLARKE, M. C., TALIB, S., FIGG, N. L. & BENNETT, M. R. (2010) Vascular smooth muscle cell apoptosis induces interleukin-1-directed inflammation: effects of hyperlipidemia-mediated inhibition of phagocytosis. *Circ Res*, **106**, 363-372.
- CLOWES, A. W. & SCHWARTZ, S. M. (1985) Significance of quiescent smooth muscle migration in the injured rat carotid artery. *Circ Res*, **56**, 139-145.
- COATS, P., KENNEDY, S., PYNE, S., WAINWRIGHT, C. L. & WADSWORTH, R. A. (2008) Inhibition of non-Ras protein farnesylation reduces in-stent restenosis. *Atherosclerosis*, **197**, 515-523.
- COLEMAN, R., HAYEK, T., KEIDAR, S. & AVIRAM, M. (2006) A mouse model for human atherosclerosis: long-term histopathological study of lesion development in the aortic arch of apolipoprotein E-deficient (E0) mice. *Acta Histochem*, **108**, 415-424.
- COLLINS, R. G., VELJI, R., GUEVARA, N. V., HICKS, M. J., CHAN, L. & BEAUDET, A. L. (2000) P-Selectin or intercellular adhesion molecule (ICAM)-1 deficiency substantially protects against atherosclerosis in apolipoprotein E-deficient mice. *J Exp Med*, **191**, 189-194.
- COMINACINI, L., RIGONI, A., PASINI, A. F., GARBIN, U., DAVOLI, A., CAMPAGNOLA, M., PASTORINO, A. M., LO CASCIO, V. & SAWAMURA, T. (2001) The binding of oxidized low density lipoprotein (ox-LDL) to ox-LDL receptor-1 reduces the intracellular concentration of nitric oxide in endothelial cells through an increased production of superoxide. *J Biol Chem*, **276**, 13750-13755.
- CORTON, J. M., GILLESPIE, J. G. & HARDIE, D. G. (1994) Role of the AMP-activated protein kinase in the cellular stress response. *Curr Biol*, **4**, 315-324.
- COSTA, M. A. & SIMON, D. I. (2005) Molecular basis of restenosis and drug-eluting stents. *Circulation*, **111**, 2257-2273.
- CRAUWELS, H. M., VAN HOVE, C. E., HOLVOET, P., HERMAN, A. G. & BULT, H. (2003) Plaque-associated endothelial dysfunction in apolipoprotein E-deficient mice on a regular diet. Effect of human apolipoprotein AI. *Cardiovasc Res*, **59**, 189-199.
- CRIQUI, M. H. & RINGEL, B. L. (1994) Does diet or alcohol explain the French paradox? *Lancet*, **344**, 1719-1723.
- CYRUS, T., WITZTUM, J. L., RADER, D. J., TANGIRALA, R., FAZIO, S., LINTON, M. F. & FUNK, C. D. (1999) Disruption of the 12/15-lipoxygenase gene diminishes atherosclerosis in apo E-deficient mice. *J Clin Invest*, **103**, 1597-1604.

- D'USCIO, L. V., BAKER, T. A., MANTILLA, C. B., SMITH, L., WEILER, D., SIECK, G. C. & KATUSIC, Z. S. (2001) Mechanism of endothelial dysfunction in apolipoprotein E-deficient mice. *Arterioscler Thromb Vasc Biol*, **21**, 1017-1022.
- DAUGHERTY, A., DUNN, J. L., RATERI, D. L. & HEINECKE, J. W. (1994) Myeloperoxidase, a catalyst for lipoprotein oxidation, is expressed in human atherosclerotic lesions. *J Clin Invest*, **94**, 437-444.
- DAVIES, S. P., HAWLEY, S. A., WOODS, A., CARLING, D., HAYSTEAD, T. A. & HARDIE, D. G. (1994) Purification of the AMP-activated protein kinase on ATP-gamma-sepharose and analysis of its subunit structure. *Eur J Biochem*, **223**, 351-357.
- DAVIGNON, J. & GANZ, P. (2004) Role of endothelial dysfunction in atherosclerosis. *Circulation*, **109**, III27-32.
- DAVIS, B. J., XIE, Z., VIOLLET, B. & ZOU, M. H. (2006) Activation of the AMP-activated kinase by antidiabetes drug metformin stimulates nitric oxide synthesis in vivo by promoting the association of heat shock protein 90 and endothelial nitric oxide synthase. *Diabetes*, **55**, 496-505.
- DEVER, G., STEWART, L. J., PITT, A. R. & SPICKETT, C. M. (2003) Phospholipid chlorohydrins cause ATP depletion and toxicity in human myeloid cells. *FEBS Lett*, **540**, 245-250.
- DEVER, G., WAINWRIGHT, C. L., KENNEDY, S. & SPICKETT, C. M. (2006) Fatty acid and phospholipid chlorohydrins cause cell stress and endothelial adhesion. *Acta Biochim Pol* **53**, 761-768.
- DEVER, G. J., BENSON, R., WAINWRIGHT, C. L., KENNEDY, S. & SPICKETT, C. M. (2008) Phospholipid chlorohydrin induces leukocyte adhesion to ApoE<sup>-/-</sup> mouse arteries via upregulation of P-selectin. *Free Radic Biol Med*, **44**, 452-463.
- DOLINSKY, V. W., MORTON, J. S., OKA, T., ROBILLARD-FRAYNE, I., BAGDAN, M., LOPASCHUK, G. D., DES ROSIERS, C., WALSH, K., DAVIDGE, S. T. & DYCK, J. R. (2010) Calorie restriction prevents hypertension and cardiac hypertrophy in the spontaneously hypertensive rat. *Hypertension*, **56**, 412-421.
- DONG, Y., ZHANG, M., WANG, S., LIANG, B., ZHAO, Z., LIU, C., WU, M., CHOI, H. C., LYONS, T. J. & ZOU, M. H. (2010) Activation of AMP-activated protein kinase inhibits oxidized LDL-triggered endoplasmic reticulum stress in vivo. *Diabetes*, **59**, 1386-1396.
- DORAN, A. C., MELLER, N. & MCNAMARA, C. A. (2008) Role of smooth muscle cells in the initiation and early progression of atherosclerosis. *Arterioscler Thromb Vasc Biol*, **28**, 812-819.
- DRACHMAN, D. E., EDELMAN, E. R., SEIFERT, P., GROOTHUIS, A. R., BORNSTEIN, D. A., KAMATH, K. R., PALASIS, M., YANG, D., NOTT, S. H. & ROGERS, C. (2000) Neointimal thickening after stent delivery of paclitaxel: change in composition and arrest of growth over six months. *J Am Coll Cardiol*, **36**, 2325-2332.
- DROBNIK, J., DABROWSKI, R., SZCZEPANOWSKA, A., GIERNAT, L. & LORENC, J. (2000) Response of aorta connective tissue matrix to injury caused by vassopressin-induced hypertension or hypercholesterolemia. *J Physiol Pharmacol*, **51**, 521-533.

- DUBEY, A., KANDULA, S. R. V. & KUMAR, P. (2008) Dimethyl sulfoxide pivaloyl chloride: A new reagent for oxidation of alcohols to carbonyls. *Synthetic Commun*, **38**, 746-753.
- DURAND, E., MALLAT, Z., ADDAD, F., VILDE, F., DESNOS, M., GUEROT, C., TEDGUI, A. & LAFONT, A. (2002) Time courses of apoptosis and cell proliferation and their relationship to arterial remodeling and restenosis after angioplasty in an atherosclerotic rabbit model. *J Am Coll Cardiol*, **39**, 1680-1685.
- DZAU, V. J. & GIBBONS, G. H. (1988) Cell biology of vascular hypertrophy in systemic hypertension. *Am J Cardiol*, **62**, 30G-35G.
- DZAU, V. J., BRAUN-DULLAEUS, R. C. & SEDDING, D. G. (2002) Vascular proliferation and atherosclerosis: new perspectives and therapeutic strategies. *Nat Med*, **8**, 1249-1256.
- ENSELEIT, F., HURLIMANN, D. & LUSCHER, T. F. (2001) Vascular protective effects of angiotensin converting enzyme inhibitors and their relation to clinical events. *J Cardiovasc Pharmacol*, **37 Suppl 1**, S21-30.
- ERRIDGE, C. & SPICKETT, C. M. (2007) Oxidised phospholipid regulation of Toll-like receptor signalling. *Redox Rep*, **12**, 76-80.
- ERRIDGE, C., KENNEDY, S., SPICKETT, C. M. & WEBB, D. J. (2008) Oxidized phospholipid inhibition of toll-like receptor (TLR) signaling is restricted to TLR2 and TLR4: roles for CD14, LPS-binding protein, and MD2 as targets for specificity of inhibition. *J Biol Chem*, **283**, 24748-24759.
- EWART, M. A., KOHLHAAS, C. F. & SALT, I. P. (2008) Inhibition of tumor necrosis factor alpha-stimulated monocyte adhesion to human aortic endothelial cells by AMP-activated protein kinase. *Arterioscler Thromb Vasc Biol*, **28**, 2255-2257.
- EWART, M. A. & KENNEDY, S. (2011) AMPK and vasculoprotection. *Pharmacol Ther*, **131**, 242-253.
- EWART, M. A. & KENNEDY, S. (2012) Diabetic cardiovascular disease - AMP-activated protein kinase (AMPK) as a therapeutic target. *Cardiovasc Hematol Agents Med Chem*, **10**, 190-211.
- FATTORI, R. & PIVA, T. (2003) Drug-eluting stents in vascular intervention. *Lancet*, **361**, 247-249.
- FISCHMAN, D. L., LEON, M. B., BAIM, D. S., SCHATZ, R. A., SAVAGE, M. P., PENN, I., DETRE, K., VELTRI, L., RICCI, D., NOBUYOSHI, M. & ET AL. (1994) A randomized comparison of coronary-stent placement and balloon angioplasty in the treatment of coronary artery disease. Stent Restenosis Study Investigators. *N Engl J Med*, **331**, 496-501.
- FOLEY, J. M., ADAMS, G. R. & MEYER, R. A. (1989) Utility of AICAr for metabolic studies is diminished by systemic effects in situ. *Am J Physiol*, **257**, C488-494.
- FORD, D. A. & GROSS, R. W. (1989) Plasmenylethanolamine is the major storage depot for arachidonic acid in rabbit vascular smooth muscle and is rapidly hydrolyzed after angiotensin II stimulation. *Proc Natl Acad Sci U S A*, **86**, 3479-3483.

- FORD, D. A. & HALE, C. C. (1996) Plasmalogen and anionic phospholipid dependence of the cardiac sarcolemmal sodium-calcium exchanger. *FEBS Lett*, **394**, 99-102.
- FORD, R. J. & RUSH, J. W. (2011) Endothelium-dependent vasorelaxation to the AMPK activator AICAR is enhanced in aorta from hypertensive rats and is NO and EDCF dependent. *Am J Physiol Heart Circ Physiol*, **300**, H64-75.
- FORD, R. J., TESCHKE, S. R., REID, E. B., DURHAM, K. K., KROETSCH, J. T. & RUSH, J. W. (2012) AMP-activated protein kinase activator AICAR acutely lowers blood pressure and relaxes isolated resistance arteries of hypertensive rats. *J Hypertens*, **30**, 725-733.
- FORRESTER, J. S., FISHBEIN, M., HELFANT, R. & FAGIN, J. (1991) A paradigm for restenosis based on cell biology: clues for the development of new preventive therapies. *J Am Coll Cardiol*, **17**, 758-769.
- FRANCO-PONS, N., CASAS, J., FABRIAS, G., GEA-SORLI, S., DE-MADARIA, E., GELPI, E. & CLOSA, D. (2013) Fat necrosis generates proinflammatory halogenated lipids during acute pancreatitis. *Ann Surg*, **257**, 943-951.
- FREIMAN, P. C., MITCHELL, G. G., HEISTAD, D. D., ARMSTRONG, M. L. & HARRISON, D. G. (1986) Atherosclerosis impairs endothelium-dependent vascular relaxation to acetylcholine and thrombin in primates. *Circ Res*, **58**, 783-789.
- FRUHWIRTH, G. O., MOUMTZI, A., LOIDL, A., INGOLIC, E. & HERMETTER, A. (2006) The oxidized phospholipids POVPC and PGPC inhibit growth and induce apoptosis in vascular smooth muscle cells. *BBA-Mol Cell Biol L*, **1761**, 1060-1069.
- FU, X., KASSIM, S. Y., PARKS, W. C. & HEINECKE, J. W. (2001) Hypochlorous acid oxygenates the cysteine switch domain of pro-matrilysin (MMP-7). A mechanism for matrix metalloproteinase activation and atherosclerotic plaque rupture by myeloperoxidase. *J Biol Chem*, **276**, 41279-41287.
- FUKUI, R., AMAKAWA, M., HOSHIGA, M., SHIBATA, N., KOHBAYASHI, E., SETO, M., SASAKI, Y., UENO, T., NEGORO, N., NAKAKOJI, T., II, M., NISHIGUCHI, F., ISHIHARA, T. & OHSAWA, N. (2000) Increased migration in late G(1) phase in cultured smooth muscle cells. *Am J Physiol Cell Physiol*, **279**, C999-1007.
- FURNKRANZ, A., SCHOBER, A., BOCHKOV, V. N., BASHTRYKOV, P., KRONKE, G., KADL, A., BINDER, B. R., WEBER, C. & LEITINGER, N. (2005) Oxidized phospholipids trigger atherogenic inflammation in murine arteries. *Arterioscler Thromb Vasc Biol*, **25**, 633-638.
- GARGALOVIC, P. S., IMURA, M., ZHANG, B., GHARAVI, N. M., CLARK, M. J., PAGNON, J., YANG, W. P., HE, A., TRUONG, A., PATEL, S., NELSON, S. F., HORVATH, S., BERLINER, J. A., KIRCHGESSNER, T. G. & LUSIS, A. J. (2006) Identification of inflammatory gene modules based on variations of human endothelial cell responses to oxidized lipids. *Proc Natl Acad Sci U S A*, **103**, 12741-12746.
- GAUT, J. P. & HEINECKE, J. W. (2001) Mechanisms for oxidizing low-density lipoprotein - Insights from patterns of oxidation products in the artery wall and from mouse models of atherosclerosis. *Trends Cardiovas Med*, **11**, 103-112.
- GEER, J. C. (1965) Fine structure of canine experimental atherosclerosis. *Am J Pathol*, **47**, 241-269.

- GEORGE, S. J. (2000) Therapeutic potential of matrix metalloproteinase inhibitors in atherosclerosis. *Expert Opin Investig Drugs*, **9**, 993-1007.
- GERTHOFFER, W. T. (2007) Mechanisms of vascular smooth muscle cell migration. *Circ Res*, **100**, 607-621.
- GERVAIS, M., PONS, S., NICOLETTI, A., COSSON, C., GIUDICELLI, J. F. & RICHER, C. (2003) Fluvastatin prevents renal dysfunction and vascular NO deficit in apolipoprotein E-deficient mice. *Arterioscler Thromb Vasc Biol*, **23**, 183-189.
- GHARAVI, N. M., BAKER, N. A., MOUILLESSEAU, K. P., YEUNG, W., HONDA, H. M., HSIEH, X., YEH, M., SMART, E. J. & BERLINER, J. A. (2006) Role of endothelial nitric oxide synthase in the regulation of SREBP activation by oxidized phospholipids. *Circ Res*, **98**, 768-776.
- GIBBONS, G. H. & DZAU, V. J. (1994) The emerging concept of vascular remodeling. *N Engl J Med*, **330**, 1431-1438.
- GLASS, C. K. & WITZTUM, J. L. (2001) Atherosclerosis. the road ahead. *Cell*, **104**, 503-516.
- GODIN, D., IVAN, E., JOHNSON, C., MAGID, R. & GALIS, Z. S. (2000) Remodeling of carotid artery is associated with increased expression of matrix metalloproteinases in mouse blood flow cessation model. *Circulation*, **102**, 2861-2866.
- GOIRAND, F., SOLAR, M., ATHEA, Y., VIOLLET, B., MATEO, P., FORTIN, D., LECLERC, J., HOERTER, J., VENTURA-CLAPIER, R. & GARNIER, A. (2007) Activation of AMP kinase alpha1 subunit induces aortic vasorelaxation in mice. *J Physiol*, **581**, 1163-1171.
- GOMEZ, D. & OWENS, G. K. (2012) Smooth muscle cell phenotypic switching in atherosclerosis. *Cardiovasc Res*, **95**, 156-164.
- GÖRANSSON, O., MCBRIDE, A., HAWLEY, S. A., ROSS, F. A., SHPIRO, N., FORETZ, M., VIOLLET, B., HARDIE, D. G. & SAKAMOTO, K. (2007) Mechanism of action of A-769662, a valuable tool for activation of AMP-activated protein kinase. *J Biol Chem*, **282**, 32549-32560.
- GORDON, D., REIDY, M. A., BENDITT, E. P. & SCHWARTZ, S. M. (1990) Cell proliferation in human coronary arteries. *Proc Natl Acad Sci U S A*, **87**, 4600-4604.
- GOTTO, A. M., JR., POWNALL, H. J. & HAVEL, R. J. (1986) Introduction to the plasma lipoproteins. *Methods Enzymol*, **128**, 3-41.
- GRASSIA, G., MADDALUNO, M., GUGLIELMOTTI, A., MANGANO, G., BIONDI, G., MAFFIA, P. & IALENTI, A. (2009) The anti-inflammatory agent bindarit inhibits neointima formation in both rats and hyperlipidaemic mice. *Cardiovasc Res*, **84**, 485-493.
- GREIG, F. H., KENNEDY, S. & SPICKETT, C. M. (2012) Physiological effects of oxidized phospholipids and their cellular signaling mechanisms in inflammation. *Free Radic Biol Med*, **52**, 266-280.
- GRIENDLING, K. K., SORESCU, D. & USHIO-FUKAI, M. (2000) NAD(P)H oxidase: role in cardiovascular biology and disease. *Circ Res*, **86**, 494-501.

- GROSS, R. W. (1984) High plasmalogen and arachidonic acid content of canine myocardial sarcolemma: a fast atom bombardment mass spectroscopic and gas chromatography-mass spectroscopic characterization. *Biochemistry*, **23**, 158-165.
- GRUNTZIG, A. R., SENNING, A. & SIEGENTHALER, W. E. (1979) Nonoperative dilatation of coronary-artery stenosis: percutaneous transluminal coronary angioplasty. *N Engl J Med*, **301**, 61-68.
- HADOKE, P., WAINWRIGHT, C. L., WADSWORTH, R. M., BUTLER, K. & GIDDINGS, M. J. (1995) Characterization of the morphological and functional alterations in rabbit subclavian artery subjected to balloon angioplasty. *Coron Artery Dis*, **6**, 403-415.
- HAMON, M., BAUTERS, C., MCFADDEN, E. P., WERNERT, N., LABLANCHE, J. M., DUPUIS, B. & BERTRAND, M. E. (1995) Restenosis after coronary angioplasty. *Eur Heart J*, **16 Suppl I**, 33-48.
- HANDA, N., TAKAGI, T., SAJO, S., TAKAYA, D., TOYAMA, M., TERADA, T., SHIROUZU, M., SUZUKI, A., LEE, S., YAMAUCHI, T., OKADA-IWABU, M., IWABU, M., KADOWAKI, T., MINOKOSHI, Y. & YOKOYAMA, S. (2011) Structural basis of compound C inhibition of human AMP-activated protein kinase  $\alpha 2$  subunit kinase domain. *Acta Crystallogr D Biol Crystallogr*, **67**, 480-487.
- HANKE, H., STROHSCHNEIDER, T., OBERHOFF, M., BETZ, E. & KARSCH, K. R. (1990) Time course of smooth muscle cell proliferation in the intima and media of arteries following experimental angioplasty. *Circ Res*, **67**, 651-659.
- HANNAN, E. L., RACZ, M., HOLMES, D. R., WALFORD, G., SHARMA, S., KATZ, S., JONES, R. H. & KING, S. B. (2008) Comparison of coronary artery stenting outcomes in the eras before and after the introduction of drug-eluting stents. *Circulation*, **117**, 2071-2078.
- HARDIE, D. G. & CARLING, D. (1997) The AMP-activated protein kinase - fuel gauge of the mammalian cell? *Eur J Biochem*, **246**, 259-273.
- HARDIE, D. G. (2004) The AMP-activated protein kinase pathway--new players upstream and downstream. *J Cell Sci*, **117**, 5479-5487.
- HARDWICK, S. J., HEGYI, L., CLARE, K., LAW, N. S., CARPENTER, K. L., MITCHINSON, M. J. & SKEPPER, J. N. (1996) Apoptosis in human monocyte-macrophages exposed to oxidized low density lipoprotein. *J Pathol*, **179**, 294-302.
- HARTLEY, C. J., REDDY, A. K., MADALA, S., MARTIN-MCNULTY, B., VERGONA, R., SULLIVAN, M. E., HALKS-MILLER, M., TAFFET, G. E., MICHAEL, L. H., ENTMAN, M. L. & WANG, Y. X. (2000) Hemodynamic changes in apolipoprotein E-knockout mice. *Am J Physiol Heart Circ Physiol*, **279**, H2326-2334.
- HAUTMANN, M. B., MADSEN, C. S. & OWENS, G. K. (1997) A transforming growth factor beta (TGFbeta) control element drives TGFbeta-induced stimulation of smooth muscle alpha-actin gene expression in concert with two CArG elements. *J Biol Chem*, **272**, 10948-10956.
- HAVEL, R. J. (1984) The formation of LDL: mechanisms and regulation. *J Lipid Res*, **25**, 1570-1576.

HAWLEY, S. A., DAVISON, M., WOODS, A., DAVIES, S. P., BERI, R. K., CARLING, D. & HARDIE, D. G. (1996) Characterization of the AMP-activated protein kinase from rat liver and identification of threonine 172 as the major site at which it phosphorylates AMP-activated protein kinase. *J Biol Chem*, **271**, 27879-27887.

HAZELL, L. J. & STOCKER, R. (1993) Oxidation of low-density lipoprotein with hypochlorite causes transformation of the lipoprotein into a high-uptake form for macrophages. *Biochem J*, **290** (Pt 1), 165-172.

HAZELL, L. J., VANDENBERG, J. J. M. & STOCKER, R. (1994) Oxidation of low-density lipoprotein by hypochlorite causes aggregation that is mediated by modification of lysine residues rather than lipid oxidation. *Biochem J*, **302**, 297-304.

HAZELL, L. J., ARNOLD, L., FLOWERS, D., WAEG, G., MALLE, E. & STOCKER, R. (1996) Presence of hypochlorite-modified proteins in human atherosclerotic lesions. *J Clin Invest*, **97**, 1535-1544.

HAZELL, L. J., DAVIES, M. J. & STOCKER, R. (1999) Secondary radicals derived from chloramines of apolipoprotein B-100 contribute to HOCl-induced lipid peroxidation of low-density lipoproteins. *Biochem J*, **339**, 489-495.

HAZELL, L. J., BAERNTHALER, G. & STOCKER, R. (2001) Correlation between intima-to-media ratio, apolipoprotein B-100, myeloperoxidase, and hypochlorite-oxidized proteins in human atherosclerosis. *Free Radic Biol Med*, **31**, 1254-1262.

HAZEN, S. L., HALL, C. R., FORD, D. A. & GROSS, R. W. (1993) Isolation of a human myocardial cytosolic phospholipase A2 isoform. Fast atom bombardment mass spectroscopic and reverse-phase high pressure liquid chromatography identification of choline and ethanolamine glycerophospholipid substrates. *J Clin Invest*, **91**, 2513-2522.

HAZEN, S. L., HSU, F. F., DUFFIN, K. & HEINECKE, J. W. (1996) Molecular chlorine generated by the myeloperoxidase hydrogen peroxide chloride system of phagocytes converts low density lipoprotein cholesterol into a family of chlorinated sterols. *J Biol Chem*, **271**, 23080-23088.

HAZEN, S. L. & HEINECKE, J. W. (1997) 3-chlorotyrosine, a specific marker of myeloperoxidase-catalyzed oxidation, is markedly elevated in low density lipoprotein isolated from human atherosclerotic intima. *J Clin Invest*, **99**, 2075-2081.

HEINECKE, J. W., ROSEN, H. & CHAIT, A. (1984) Iron and copper promote modification of low density lipoprotein by human arterial smooth muscle cells in culture. *J Clin Invest*, **74**, 1890-1894.

HEINECKE, J. W., LI, W., MUELLER, D. M., BOHRER, A. & TURK, J. (1994) Cholesterol chlorohydrin synthesis by the myeloperoxidase-hydrogen peroxide-chloride system - Potential markers for lipoproteins oxidatively damaged by phagocytes. *Biochemistry*, **33**, 10127-10136.

HELDMAN, A. W., CHENG, L., JENKINS, G. M., HELLER, P. F., KIM, D. W., WARE, M., JR., NATER, C., HRUBAN, R. H., REZAI, B., ABELLA, B. S., BUNGE, K. E., KINSELLA, J. L., SOLLOTT, S. J., LAKATTA, E. G., BRINKER, J. A., HUNTER, W. L. & FROEHLICH, J. P. (2001) Paclitaxel stent coating inhibits neointimal hyperplasia at 4 weeks in a porcine model of coronary restenosis. *Circulation*, **103**, 2289-2295.

- HENRIKSEN, T., MAHONEY, E. M. & STEINBERG, D. (1981) Enhanced macrophage degradation of low density lipoprotein previously incubated with cultured endothelial cells: recognition by receptors for acetylated low density lipoproteins. *Proc Natl Acad Sci U S A*, **78**, 6499-6503.
- HENRIKSEN, T., MAHONEY, E. M. & STEINBERG, D. (1983) Enhanced macrophage degradation of biologically modified low density lipoprotein. *Arteriosclerosis*, **3**, 149-159.
- HESSLER, J. R., ROBERTSON, A. L., JR. & CHISOLM, G. M., 3RD (1979) LDL-induced cytotoxicity and its inhibition by HDL in human vascular smooth muscle and endothelial cells in culture. *Atherosclerosis*, **32**, 213-229.
- HEVONOJA, T., PENTIKAINEN, M. O., HYVONEN, M. T., KOVANEN, P. T. & ALA-KORPELA, M. (2000) Structure of low density lipoprotein (LDL) particles: basis for understanding molecular changes in modified LDL. *Biochim Biophys Acta*, **1488**, 189-210.
- HOUWELING, M., KLEIN, W. & GEELEN, M. J. (2002) Regulation of phosphatidylcholine and phosphatidylethanolamine synthesis in rat hepatocytes by 5-aminoimidazole-4-carboxamide ribonucleoside (AICAR). *Biochem J*, **362**, 97-104.
- HSIAI, T. K., CHO, S. K., REDDY, S., HAMA, S., NAVAB, M., DEMER, L. L., HONDA, H. M. & HO, C. M. (2001) Pulsatile flow regulates monocyte adhesion to oxidized lipid-induced endothelial cells. *Arterioscler Thromb Vasc Biol*, **21**, 1770-1776.
- HUBER, J., VALES, A., MITULOVIC, G., BLUMER, M., SCHMID, R., WITZTUM, J. L., BINDER, B. R. & LEITINGER, N. (2002) Oxidized membrane vesicles and blebs from apoptotic cells contain biologically active oxidized phospholipids that induce monocyte-endothelial interactions. *Arterioscler Thromb Vasc Biol*, **22**, 101-107.
- HUBER, J., FURNKRANZ, A., BOCHKOV, V. N., PATRICIA, M. K., LEE, H., HEDRICK, C. C., BERLINER, J. A., BINDER, B. R. & LEITINGER, N. (2006) Specific monocyte adhesion to endothelial cells induced by oxidized phospholipids involves activation of cPLA2 and lipoxygenase. *J Lipid Res*, **47**, 1054-1062.
- HUNDAL, R. S., GOMEZ-MUNOZ, A., KONG, J. Y., SALH, B. S., MAROTTA, A., DURONIO, V. & STEINBRECHER, U. P. (2003) Oxidized low density lipoprotein inhibits macrophage apoptosis by blocking ceramide generation, thereby maintaining protein kinase B activation and Bcl-XL levels. *J Biol Chem*, **278**, 24399-24408.
- HURLEY, R. L., ANDERSON, K. A., FRANZONE, J. M., KEMP, B. E., MEANS, A. R. & WITTERS, L. A. (2005) The Ca<sup>2+</sup>/calmodulin-dependent protein kinase kinases are AMP-activated protein kinase kinases. *J Biol Chem*, **280**, 29060-29066.
- IDO, Y., CARLING, D. & RUDERMAN, N. (2002) Hyperglycemia-induced apoptosis in human umbilical vein endothelial cells: inhibition by the AMP-activated protein kinase activation. *Diabetes*, **51**, 159-167.
- IGATA, M., MOTOSHIMA, H., TSURUZOE, K., KOJIMA, K., MATSUMURA, T., KONDO, T., TAGUCHI, T., NAKAMARU, K., YANO, M., KUKIDOME, D., MATSUMOTO, K., TOYONAGA, T., ASANO, T., NISHIKAWA, T. & ARAKI, E. (2005) Adenosine monophosphate-activated protein kinase suppresses vascular smooth muscle cell proliferation through the inhibition of cell cycle progression. *Circ Res*, **97**, 837-844.

INOUE, T., KATO, T., HIKICHI, Y., HASHIMOTO, S., HIRASE, T., MOROOKA, T., IMOTO, Y., TAKEDA, Y., SENDO, F. & NODE, K. (2006) Stent-induced neutrophil activation is associated with an oxidative burst in the inflammatory process, leading to neointimal thickening. *Thromb Haemost*, **95**, 43-48.

INOUE, T. & NODE, K. (2009) Molecular basis of restenosis and novel issues of drug-eluting stents. *Circ J*, **73**, 615-621.

ISHIBASHI, S., BROWN, M. S., GOLDSTEIN, J. L., GERARD, R. D., HAMMER, R. E. & HERZ, J. (1993) Hypercholesterolemia in low density lipoprotein receptor knockout mice and its reversal by adenovirus-mediated gene delivery. *J Clin Invest*, **92**, 883-893.

ISHIGAMI, M., SWERTFEGER, D. K., GRANHOLM, N. A. & HUI, D. Y. (1998) Apolipoprotein E inhibits platelet-derived growth factor-induced vascular smooth muscle cell migration and proliferation by suppressing signal transduction and preventing cell entry to G1 phase. *J Biol Chem*, **273**, 20156-20161.

ISHII, N., MATSUMURA, T., KINOSHITA, H., MOTOSHIMA, H., KOJIMA, K., TSUTSUMI, A., KAWASAKI, S., YANO, M., SENOKUCHI, T., ASANO, T., NISHIKAWA, T. & ARAKI, E. (2009) Activation of AMP-activated protein kinase suppresses oxidized low-density lipoprotein-induced macrophage proliferation. *J Biol Chem*, **284**, 34561-34569.

ISNER, J. M., KEARNEY, M., BORTMAN, S. & PASSERI, J. (1995) Apoptosis in human atherosclerosis and restenosis. *Circulation*, **91**, 2703-2711.

JABER, A. J. & WILKINS, C. L. (2005) Hydrocarbon polymer analysis by external MALDI fourier transform and reflectron time of flight mass spectrometry. *J Am Soc Mass Spectrom*, **16**, 2009-2016.

JACOBS, R. L., LINGRELL, S., DYCK, J. R. & VANCE, D. E. (2007) Inhibition of hepatic phosphatidylcholine synthesis by 5-aminoimidazole-4-carboxamide-1-beta-4-ribofuranoside is independent of AMP-activated protein kinase activation. *J Biol Chem*, **282**, 4516-4523.

JANG, J. H., LEE, T. J., YANG, E. S., MIN DO, S., KIM, Y. H., KIM, S. H., CHOI, Y. H., PARK, J. W., CHOI, K. S. & KWON, T. K. (2010) Compound C sensitizes Caki renal cancer cells to TRAIL-induced apoptosis through reactive oxygen species-mediated down-regulation of c-FLIPL and Mcl-1. *Exp Cell Res*, **316**, 2194-2203.

JAWIEN, J., NASTALEK, P. & KORBUT, R. (2004) Mouse models of experimental atherosclerosis. *J Physiol Pharmacol*, **55**, 503-517.

JERLICH, A., FABJAN, J. S., TSCHABUSCHNIG, S., SMIRNOVA, A. V., HORAKOVA, L., HAYN, M., AUER, H., GUTTENBERGER, H., LEIS, H. J., TATZBER, F., WAEG, G. & SCHAUR, R. J. (1998) Human low density lipoprotein as a target of hypochlorite generated by myeloperoxidase. *Free Radic Biol Med*, **24**, 1139-1148.

JERLICH, A., PITT, A. R., SCHAUR, J. & SPICKETT, C. M. (2000) Pathways of phospholipid oxidation by HOCl in human LDL detected by LC-MS. *Free Radic Biol Med*, **28**, 673-682.

- JIANG, X. C., PAULTRE, F., PEARSON, T. A., REED, R. G., FRANCIS, C. K., LIN, M., BERGLUND, L. & TALL, A. R. (2000) Plasma sphingomyelin level as a risk factor for coronary artery disease. *Arterioscler Thromb Vasc Biol*, **20**, 2614-2618.
- JIN, J., MULLEN, T. D., HOU, Q., BIELAWSKI, J., BIELAWSKA, A., ZHANG, X., OBEID, L. M., HANNUN, Y. A. & HSU, Y. T. (2009) AMPK inhibitor Compound C stimulates ceramide production and promotes Bax redistribution and apoptosis in MCF7 breast carcinoma cells. *J Lipid Res*, **50**, 2389-2397.
- JOHNSTONE, S. R., ROSS, J., RIZZO, M. J., STRAUB, A. C., LAMPE, P. D., LEITINGER, N. & ISAKSON, B. E. (2009) Oxidized phospholipid species promote in vivo differential cx43 phosphorylation and vascular smooth muscle cell proliferation. *Am J Pathol*, **175**, 916-924.
- JUKEMA, J. W., AHMED, T. A., VERSCHUREN, J. J. & QUAX, P. H. (2012a) Restenosis after PCI. Part 2: prevention and therapy. *Nat Rev Cardiol*, **9**, 79-90.
- JUKEMA, J. W., VERSCHUREN, J. J., AHMED, T. A. & QUAX, P. H. (2012b) Restenosis after PCI. Part 1: pathophysiology and risk factors. *Nat Rev Cardiol*, **9**, 53-62.
- KANG, J. H., KIM, H. T., CHOI, M. S., LEE, W. H., HUH, T. L., PARK, Y. B., MOON, B. J. & KWON, O. S. (2006) Proteome analysis of human monocytic THP-1 cells primed with oxidized low-density lipoproteins. *Proteomics*, **6**, 1261-1273.
- KANNEL, W. B., NEATON, J. D., WENTWORTH, D., THOMAS, H. E., STAMLER, J., HULLEY, S. B. & KJELSBURG, M. O. (1986) Overall and coronary heart disease mortality rates in relation to major risk factors in 325,348 men screened for the MRFIT. Multiple Risk Factor Intervention Trial. *Am Heart J*, **112**, 825-836.
- KANTOR, B., ASHAI, K., HOLMES, D. R., JR. & SCHWARTZ, R. S. (1999) The experimental animal models for assessing treatment of restenosis. *Cardiovasc Radiat Med*, **1**, 48-54.
- KARAGIANNIDES, I., ABDOU, R., TZORTZOPOULOU, A., VOSHOL, P. J. & KYPREOS, K. E. (2008) Apolipoprotein E predisposes to obesity and related metabolic dysfunctions in mice. *FEBS J*, **275**, 4796-4809.
- KATRANTZIS, M., BAKER, M. S., HANDLEY, C. J. & LOWTHER, D. A. (1991) The oxidant hypochlorite (OCI<sup>-</sup>), a product of the myeloperoxidase system, degrades articular cartilage proteoglycan aggregate. *Free Radic Biol Med*, **10**, 101-109.
- KAWASAKI, T., DEWERCHIN, M., LIJNEN, H. R., VREYS, I., VERMYLEN, J. & HOYLAERTS, M. F. (2001) Mouse carotid artery ligation induces platelet-leukocyte-dependent luminal fibrin, required for neointima development. *Circ Res*, **88**, 159-166.
- KEMP, B. E., MITCHELHILL, K. I., STAPLETON, D., MICHELL, B. J., CHEN, Z. P. & WITTERS, L. A. (1999) Dealing with energy demand: the AMP-activated protein kinase. *Trends Biochem Sci*, **24**, 22-25.
- KENNEDY, S., MCPHADEN, A. R., WADSWORTH, R. M. & WAINWRIGHT, C. L. (2000) Correlation of leukocyte adhesiveness, adhesion molecule expression and leukocyte-induced contraction following balloon angioplasty. *Br J Pharmacol*, **130**, 95-103.

KENNEDY, S., PRESTON, A. A., MCPHADEN, A. R., MILLER, A. M., WAINWRIGHT, C. L. & WADSWORTH, R. M. (2004) Correlation of changes in nitric oxide synthase, superoxide dismutase and nitrotyrosine with endothelial regeneration and neointimal hyperplasia in the balloon-injured rabbit subclavian artery. *Coron Artery Dis*, **15**, 337-346.

KENNEDY, S., WADSWORTH, R. M. & WAINWRIGHT, C. L. (2006) Locally administered antiproliferative drugs inhibit hypercontractility to serotonin in balloon-injured pig coronary artery. *Vascul Pharmacol*, **44**, 363-371.

KIM, J. E., KIM, Y. W., LEE, I. K., KIM, J. Y., KANG, Y. J. & PARK, S. Y. (2008) AMP-activated protein kinase activation by 5-aminoimidazole-4-carboxamide-1-beta-D-ribofuranoside (AICAR) inhibits palmitate-induced endothelial cell apoptosis through reactive oxygen species suppression. *J Pharmacol Sci*, **106**, 394-403.

KLEBANOFF, S. J. (1980) Oxygen metabolism and the toxic properties of phagocytes. *Ann Intern Med*, **93**, 480-489.

KLEBANOFF, S. J. (2005) Myeloperoxidase: friend and foe. *J Leukoc Biol*, **77**, 598-625.

KNOTT, T. J., PEASE, R. J., POWELL, L. M., WALLIS, S. C., RALL, S. C., JR., INNERARITY, T. L., BLACKHART, B., TAYLOR, W. H., MARCEL, Y., MILNE, R. & ET AL. (1986) Complete protein sequence and identification of structural domains of human apolipoprotein B. *Nature*, **323**, 734-738.

KOSEGAWA, I., KATAYAMA, S., KIKUCHI, C., KASHIWABARA, H., NEGISHI, K., ISHII, J., INUKAI, K. & OKA, Y. (1996) Metformin decreases blood pressure and obesity in OLETF rats via improvement of insulin resistance. *Hypertens Res*, **19**, 37-41.

KOTHAPALLI, D., LIU, S. L., BAE, Y. H., MONSLOW, J., XU, T., HAWTHORNE, E. A., BYFIELD, F. J., CASTAGNINO, P., RAO, S., RADER, D. J., PURE, E., PHILLIPS, M. C., LUND-KATZ, S., JANMEY, P. A. & ASSOIAN, R. K. (2012) Cardiovascular protection by apoE and apoE-HDL linked to suppression of ECM gene expression and arterial stiffening. *Cell Rep*, **2**, 1259-1271.

KU, D. N., GIDDENS, D. P., ZARINS, C. K. & GLAGOV, S. (1985) Pulsatile flow and atherosclerosis in the human carotid bifurcation. Positive correlation between plaque location and low oscillating shear stress. *Arteriosclerosis*, **5**, 293-302.

KUMAR, A. & LINDNER, V. (1997) Remodeling with neointima formation in the mouse carotid artery after cessation of blood flow. *Arterioscler Thromb Vasc Biol*, **17**, 2238-2244.

KUMAR, A. P., PIEDRAFITA, F. J. & REYNOLDS, W. F. (2004) Peroxisome proliferator-activated receptor gamma ligands regulate myeloperoxidase expression in macrophages by an estrogen-dependent mechanism involving the -463GA promoter polymorphism. *J Biol Chem*, **279**, 8300-8315.

KUMAR, V., BUTCHER, S. J., OORNI, K., ENGELHARDT, P., HEIKKONEN, J., KASKI, K., ALA-KORPELA, M. & KOVANEN, P. T. (2011) Three-dimensional cryoEM reconstruction of native LDL particles to 16A resolution at physiological body temperature. *PLoS One*, **6**, e18841.

KUNJATHOOR, V. V., FEBBRAIO, M., PODREZ, E. A., MOORE, K. J., ANDERSSON, L., KOEHN, S., RHEE, J. S., SILVERSTEIN, R., HOFF, H. F. & FREEMAN, M. W. (2002) Scavenger receptors class A-I/II and CD36 are the principal

receptors responsible for the uptake of modified low density lipoprotein leading to lipid loading in macrophages. *J Biol Chem*, **277**, 49982-49988.

KUTTER, D., DEVAQUET, P., VANDERSTOCKEN, G., PAULUS, J. M., MARCHAL, V. & GOTHOT, A. (2000) Consequences of total and subtotal myeloperoxidase deficiency: Risk or benefit? *Acta Haematol-Basel*, **104**, 10-15.

LASKOWITZ, D. T., LEE, D. M., SCHMECHEL, D. & STAATS, H. F. (2000) Altered immune responses in apolipoprotein E-deficient mice. *J Lipid Res*, **41**, 613-620.

LEE, P. C., GIBBONS, G. H. & DZAU, V. J. (1993) Cellular and molecular mechanisms of coronary artery restenosis. *Coron Artery Dis*, **4**, 254-259.

LEITINGER, N., TYNER, T. R., OSLUND, L., RIZZA, C., SUBBANAGOUNDER, G., LEE, H., SHIH, P. T., MACKMAN, N., TIGYI, G., TERRITO, M. C., BERLINER, J. A. & VORA, D. K. (1999) Structurally similar oxidized phospholipids differentially regulate endothelial binding of monocytes and neutrophils. *Proc Natl Acad Sci U S A*, **96**, 12010-12015.

LEITINGER, N. (2005) Oxidized phospholipids as triggers of inflammation in atherosclerosis. *Mol Nutr Food Res*, **49**, 1063-1071.

LESSIG, J., SCHILLER, J., ARNHOLD, J. & FUCHS, B. (2007) Hypochlorous acid-mediated generation of glycerophosphocholine from unsaturated plasmalogen glycerophosphocholine lipids. *J Lipid Res*, **48**, 1316-1324.

LEVICK, J. R. (2003) *An Introduction to Cardiovascular Physiology 4th Edition*, U K, Hodder Arnold.

LI, C. & KEANEY, J. F., JR. (2010) AMP-activated protein kinase: a stress-responsive kinase with implications for cardiovascular disease. *Curr Opin Pharmacol*, **10**, 111-115.

LI, D. & MEHTA, J. L. (2000) Upregulation of endothelial receptor for oxidized LDL (LOX-1) by oxidized LDL and implications in apoptosis of human coronary artery endothelial cells: evidence from use of antisense LOX-1 mRNA and chemical inhibitors. *Arterioscler Thromb Vasc Biol*, **20**, 1116-1122.

LI, D., WANG, D., WANG, Y., LING, W., FENG, X. & XIA, M. (2010a) Adenosine monophosphate-activated protein kinase induces cholesterol efflux from macrophage-derived foam cells and alleviates atherosclerosis in apolipoprotein E-deficient mice. *J Biol Chem*, **285**, 33499-33509.

LI, D., ZHANG, Y., MA, J., LING, W. & XIA, M. (2010b) Adenosine monophosphate activated protein kinase regulates ABCG1-mediated oxysterol efflux from endothelial cells and protects against hypercholesterolemia-induced endothelial dysfunction. *Arterioscler Thromb Vasc Biol*, **30**, 1354-1362.

LI, F. Y., LAM, K. S., TSE, H. F., CHEN, C., WANG, Y., VANHOUTTE, P. M. & XU, A. (2012) Endothelium-selective activation of AMP-activated protein kinase prevents diabetes mellitus-induced impairment in vascular function and re-endothelialization via induction of heme oxygenase-1 in mice. *Circulation*, **126**, 1267-1277.

LIBBY, P., SCHWARTZ, D., BROGI, E., TANAKA, H. & CLINTON, S. K. (1992) A cascade model for restenosis. A special case of atherosclerosis progression. *Circulation*, **86**, III47-52.

- LIBBY, P., EGAN, D. & SKARLATOS, S. (1997) Roles of infectious agents in atherosclerosis and restenosis: an assessment of the evidence and need for future research. *Circulation*, **96**, 4095-4103.
- LIBBY, P. & SIMON, D. I. (2001) Inflammation and thrombosis: the clot thickens. *Circulation*, **103**, 1718-1720.
- LIBBY, P. (2002) Inflammation in atherosclerosis. *Nature*, **420**, 868-874.
- LINDNER, V. & REIDY, M. A. (1991) Proliferation of smooth muscle cells after vascular injury is inhibited by an antibody against basic fibroblast growth factor. *Proc Natl Acad Sci U S A*, **88**, 3739-3743.
- LINDNER, V., FINGERLE, J. & REIDY, M. A. (1993) Mouse model of arterial injury. *Circ Res*, **73**, 792-796.
- LIPPI, G., FRANCHINI, M., FAVALORO, E. J. & TARGHER, G. (2010) Moderate red wine consumption and cardiovascular disease risk: Beyond the "French Paradox". *Semin Thromb Hemost*, **36**, 59-70.
- LITHELL, H. (1994) Pathogenesis and prevalence of atherosclerosis in hypertensive patients. *Am J Hypertens*, **7**, 2S-6S.
- LIU, C., LIANG, B., WANG, Q., WU, J. & ZOU, M. H. (2010) Activation of AMP-activated protein kinase alpha alleviates endothelial cell apoptosis by increasing the expression of anti-apoptotic proteins Bcl-2 and survivin. *J Biol Chem*, **285**, 15346-15355.
- LIU, C., DESIKAN, R., YING, Z., GUSHCHINA, L., KAMPFRATH, T., DEIULIIS, J., WANG, A., XU, X., ZHONG, J., RAO, X., SUN, Q., MAISEYEU, A., PARTHASARATHY, S. & RAJAGOPALAN, S. (2012) Effects of a novel pharmacologic inhibitor of myeloperoxidase in a mouse atherosclerosis model. *PLoS One*, **7**, e50767.
- LOIDL, A., SEVCSIK, E., RIESENHUBER, G., DEIGNER, H. P. & HERMETTER, A. (2003) Oxidized phospholipids in minimally modified low density lipoprotein induce apoptotic signaling via activation of acid sphingomyelinase in arterial smooth muscle cells. *J Biol Chem*, **278**, 32921-32928.
- LOIDL, A., CLAUS, R., INGOLIC, E., DEIGNER, H. P. & HERMETTER, A. (2004) Role of ceramide in activation of stress-associated MAP kinases by minimally modified LDL in vascular smooth muscle cells. *Biochim Biophys Acta*, **1690**, 150-158.
- LONGNUS, S. L., WAMBOLT, R. B., PARSONS, H. L., BROWNSEY, R. W. & ALLARD, M. F. (2003) 5-Aminoimidazole-4-carboxamide 1-beta -D-ribofuranoside (AICAR) stimulates myocardial glycogenolysis by allosteric mechanisms. *Am J Physiol Regul Integr Comp Physiol*, **284**, R936-944.
- LOPEZ, J. M., SANTIDRIAN, A. F., CAMPAS, C. & GIL, J. (2003) 5-Aminoimidazole-4-carboxamide riboside induces apoptosis in Jurkat cells, but the AMP-activated protein kinase is not involved. *Biochem J*, **370**, 1027-1032.
- MA, Z., LI, J., YANG, L., MU, Y., XIE, W., PITT, B. & LI, S. (2004) Inhibition of LPS- and CpG DNA-induced TNF-alpha response by oxidized phospholipids. *Am J Physiol Lung Cell Mol Physiol*, **286**, L808-816.

- MACMAHON, S., SHARPE, N., GAMBLE, G., CLAGUE, A., MHURCHU, C. N., CLARK, T., HART, H., SCOTT, J. & WHITE, H. (2000) Randomized, placebo-controlled trial of the angiotensin-converting enzyme inhibitor, ramipril, in patients with coronary or other occlusive arterial disease. PART-2 Collaborative Research Group. Prevention of Atherosclerosis with Ramipril. *J Am Coll Cardiol*, **36**, 438-443.
- MAGGI, E., MARCHESI, E., RAVETTA, V., FALASCHI, F., FINARDI, G. & BELLOMO, G. (1993) Low-density lipoprotein oxidation in essential hypertension. *J Hypertens*, **11**, 1103-1111.
- MALLAT, Z. & TEDGUI, A. (2000) Apoptosis in the vasculature: mechanisms and functional importance. *Br J Pharmacol*, **130**, 947-962.
- MALLE, E., WAEG, G., SCHREIBER, R., GRONE, E. F., SATTLER, W. S. & GRONE, H. J. (2000) Immunohistochemical evidence for the myeloperoxidase/H<sub>2</sub>O<sub>2</sub>/halide system in human atherosclerotic lesions - Colocalization of myeloperoxidase and hypochlorite-modified proteins. *Eur J Biochem*, **267**, 4495-4503.
- MALLE, E., MARSCHE, G., ARNHOLD, J. & DAVIES, M. J. (2006) Modification of low-density lipoprotein by myeloperoxidase-derived oxidants and reagent hypochlorous acid. *BBA-Mol Cell Biol L*, **1761**, 392-415.
- MANCUSO, A. J., HUANG, S. L. & SWERN, D. (1978) Oxidation of long-chain and related alcohols to carbonyles by dimethyl-sulfoxide activated by oxalyl chloride. *J Org Chem*, **43**, 2480-2482.
- MARSCHE, G., HAMMER, A., OSKOLKOVA, O., KOZARSKY, K. F., SATTLER, W. & MALLE, E. (2002) Hypochlorite-modified high density lipoprotein, a high affinity ligand to scavenger receptor class B, type I, impairs high density lipoprotein-dependent selective lipid uptake and reverse cholesterol transport. *J Biol Chem*, **277**, 32172-32179.
- MARSCHE, G., HELLER, R., FAULER, G., KOVACEVIC, A., NUSZKOWSKI, A., GRAIER, W., SATTLER, W. & MALLE, E. (2004) 2-Chlorohexadecanal derived from hypochlorite-modified high-density lipoprotein-associated plasmalogen is a natural inhibitor of endothelial nitric oxide biosynthesis. *Arterioscler Thromb Vasc Biol*, **24**, 2303-2306.
- MARTINI, F. H. (2006) *Fundamentals of Anatomy & Physiology 7th Edition*, USA, Pearson Benjamin Cummings.
- MATTER, C. M., MA, L., VON LUKOWICZ, T., MEIER, P., LOHMANN, C., ZHANG, D., KILIC, U., HOFMANN, E., HA, S. W., HERSBERGER, M., HERMANN, D. M. & LUSCHER, T. F. (2006) Increased balloon-induced inflammation, proliferation, and neointima formation in apolipoprotein E (ApoE) knockout mice. *Stroke*, **37**, 2625-2632.
- MCMILLEN, T. S., HEINECKE, J. W. & LEBOEUF, R. C. (2005) Expression of human myeloperoxidase by macrophages promotes atherosclerosis in mice. *Circulation*, **111**, 2798-2804.
- MEHRAN, R., DANGAS, G., ABIZAID, A. S., MINTZ, G. S., LANSKY, A. J., SATLER, L. F., PICHARD, A. D., KENT, K. M., STONE, G. W. & LEON, M. B. (1999) Angiographic patterns of in-stent restenosis: classification and implications for long-term outcome. *Circulation*, **100**, 1872-1878.

- MERRILL, G. F., KURTH, E. J., HARDIE, D. G. & WINDER, W. W. (1997) AICA riboside increases AMP-activated protein kinase, fatty acid oxidation, and glucose uptake in rat muscle. *Am J Physiol*, **273**, E1107-1112.
- MESSNER, M. C., ALBERT, C. J. & FORD, D. A. (2008a) 2-Chlorohexadecanal and 2-chlorohexadecanoic acid induce COX-2 expression in human coronary artery endothelial cells. *Lipids*, **43**, 581-588.
- MESSNER, M. C., ALBERT, C. J., MCHOWAT, J. & FORD, D. A. (2008b) Identification of lysophosphatidylcholine-chlorohydrin in human atherosclerotic lesions. *Lipids*, **43**, 243-249.
- METHVEN, L., SIMPSON, P. C. & MCGRATH, J. C. (2009) Alpha1A/B-knockout mice explain the native alpha1D-adrenoceptor's role in vasoconstriction and show that its location is independent of the other alpha1-subtypes. *Br J Pharmacol*, **158**, 1663-1675.
- MILLER, A. M., MCPHADEN, A. R., WADSWORTH, R. M. & WAINWRIGHT, C. L. (2001) Inhibition by leukocyte depletion of neointima formation after balloon angioplasty in a rabbit model of restenosis. *Cardiovasc Res*, **49**, 838-850.
- MITRA, A. K., DHUME, A. S. & AGRAWAL, D. K. (2004) "Vulnerable plaques" - ticking of the time bomb. *Can J Physiol Pharm*, **82**, 860-871.
- MITRA, A. K. & AGRAWAL, D. K. (2006) In stent restenosis: bane of the stent era. *J Clin Pathol*, **59**, 232-239.
- MOORE, K. J., KUNJATHOOR, V. V., KOEHN, S. L., MANNING, J. J., TSENG, A. A., SILVER, J. M., MCKEE, M. & FREEMAN, M. W. (2005) Loss of receptor-mediated lipid uptake via scavenger receptor A or CD36 pathways does not ameliorate atherosclerosis in hyperlipidemic mice. *J Clin Invest*, **115**, 2192-2201.
- MOORE, K. J. & TABAS, I. (2011) Macrophages in the pathogenesis of atherosclerosis. *Cell*, **145**, 341-355.
- MORROW, V. A., FOUFELLE, F., CONNELL, J. M., PETRIE, J. R., GOULD, G. W. & SALT, I. P. (2003) Direct activation of AMP-activated protein kinase stimulates nitric-oxide synthesis in human aortic endothelial cells. *J Biol Chem*, **278**, 31629-31639.
- MOSSE, P. R., CAMPBELL, G. R., WANG, Z. L. & CAMPBELL, J. H. (1985) Smooth muscle phenotypic expression in human carotid arteries. I. Comparison of cells from diffuse intimal thickenings adjacent to atheromatous plaques with those of the media. *Lab Invest*, **53**, 556-562.
- MOTOSHIMA, H., GOLDSTEIN, B. J., IGATA, M. & ARAKI, E. (2006) AMPK and cell proliferation -AMPK as a therapeutic target for atherosclerosis and cancer. *J Physiol*, **574**, 63-71.
- MOUMTZI, A., TRENKER, M., FLICKER, K., ZENZMAIER, E., SAF, R. & HERMETTER, A. (2007) Import and fate of fluorescent analogs of oxidized phospholipids in vascular smooth muscle cells. *J Lipid Res*, **48**, 565-582.
- MOUSSA, I., REIMERS, B., MOSES, J., DIMARIO, C., DIFRANCESCO, L., FERRARO, M. & COLOMBO, A. (1997) Long-term angiographic and clinical outcome of patients undergoing multivessel coronary stenting. *Circulation*, **96**, 3873-3879.

- MULLER, W. A. (2003) Leukocyte-endothelial-cell interactions in leukocyte transmigration and the inflammatory response. *Trends Immunol*, **24**, 327-334.
- NABEL, E. G. (2002) CDKs and CKIs: molecular targets for tissue remodelling. *Nat Rev Drug Discov*, **1**, 587-598.
- NAGATA, D., MOGI, M. & WALSH, K. (2003) AMP-activated protein kinase (AMPK) signaling in endothelial cells is essential for angiogenesis in response to hypoxic stress. *J Biol Chem*, **278**, 31000-31006.
- NAGATA, D., TAKEDA, R., SATA, M., SATONAKA, H., SUZUKI, E., NAGANO, T. & HIRATA, Y. (2004) AMP-activated protein kinase inhibits angiotensin II-stimulated vascular smooth muscle cell proliferation. *Circulation*, **110**, 444-451.
- NAKASHIMA, Y., PLUMP, A. S., RAINES, E. W., BRESLOW, J. L. & ROSS, R. (1994) ApoE-deficient mice develop lesions of all phases of atherosclerosis throughout the arterial tree. *Arterioscler Thromb*, **14**, 133-140.
- NAM, M., LEE, W. H., BAE, E. J. & KIM, S. G. (2008) Compound C inhibits clonal expansion of preadipocytes by increasing p21 level irrespectively of AMPK inhibition. *Arch Biochem Biophys*, **479**, 74-81.
- NELSON, P. R., YAMAMURA, S., MUREEBE, L., ITOH, H. & KENT, K. C. (1998) Smooth muscle cell migration and proliferation are mediated by distinct phases of activation of the intracellular messenger mitogen-activated protein kinase. *J Vasc Surg*, **27**, 117-125.
- NICHOLLS, S. J. & HAZEN, S. L. (2005) Myeloperoxidase and cardiovascular disease. *Arterioscler Thromb Vasc Biol*, **25**, 1102-1111.
- NICHOLLS, S. J. & HAZEN, S. L. (2009) Myeloperoxidase, modified lipoproteins, and atherogenesis. *J Lipid Res*, **50 Suppl**, S346-351.
- NOGUCHI, N., NAKANO, K., ARATANI, Y., KOYAMA, H., KODAMA, T. & NIKI, E. (2000) Role of myeloperoxidase in the neutrophil-induced oxidation of low density lipoprotein as studied by myeloperoxidase-knockout mouse. *J Biochem*, **127**, 971-976.
- NUSSHOLD, C., KOLLROSER, M., KOFELER, H., RECHBERGER, G., REICHER, H., ULLEN, A., BERNHART, E., WALTL, S., KRATZER, I., HERMETTER, A., HACKL, H., TRAJANOSKI, Z., HRZENJAK, A., MALLE, E. & SATTLER, W. (2010) Hypochlorite modification of sphingomyelin generates chlorinated lipid species that induce apoptosis and proteome alterations in dopaminergic PC12 neurons in vitro. *Free Radic Biol Med*, **48**, 1588-1600.
- OLOFSSON, K. E., ANDERSSON, L., NILSSON, J. & BJORKBACKA, H. (2008) Nanomolar concentrations of lysophosphatidylcholine recruit monocytes and induce pro-inflammatory cytokine production in macrophages. *Biochem Biophys Res Commun*, **370**, 348-352.
- OWENS, G. K., KUMAR, M. S. & WAMHOFF, B. R. (2004) Molecular regulation of vascular smooth muscle cell differentiation in development and disease. *Physiol Rev*, **84**, 767-801.
- PANASENKO, O. M., VAKHRUSHEVA, T., TRETAKOV, V., SPALTEHOLZ, H. & ARNHOLD, J. (2007) Influence of chloride on modification of unsaturated

phosphatidylcholines by the myeloperoxidase/hydrogen peroxide/bromide system. *Chem Phys Lipids* **149**, 40-52.

PELAT, M., DESSY, C., MASSION, P., DESAGER, J. P., FERON, O. & BALLIGAND, J. L. (2003) Rosuvastatin decreases caveolin-1 and improves nitric oxide-dependent heart rate and blood pressure variability in apolipoprotein E<sup>-/-</sup> mice in vivo. *Circulation*, **107**, 2480-2486.

PERLMAN, H., MAILLARD, L., KRASINSKI, K. & WALSH, K. (1997) Evidence for the rapid onset of apoptosis in medial smooth muscle cells after balloon injury. *Circulation*, **95**, 981-987.

PEYTON, K. J., YU, Y., YATES, B., SHEBIB, A. R., LIU, X. M., WANG, H. & DURANTE, W. (2011) Compound C inhibits vascular smooth muscle cell proliferation and migration in an AMP-activated protein kinase-independent fashion. *J Pharmacol Exp Ther*, **338**, 476-484.

PIDKOVKA, N. A., CHEREPANOVA, O. A., YOSHIDA, T., ALEXANDER, M. R., DEATON, R. A., THOMAS, J. A., LEITINGER, N. & OWENS, G. K. (2007) Oxidized phospholipids induce phenotypic switching of vascular smooth muscle cells in vivo and in vitro. *Circ Res*, **101**, 792-801.

PIEDRAHITA, J. A., ZHANG, S. H., HAGAMAN, J. R., OLIVER, P. M. & MAEDA, N. (1992) Generation of mice carrying a mutant apolipoprotein E gene inactivated by gene targeting in embryonic stem cells. *Proc Natl Acad Sci U S A*, **89**, 4471-4475.

PITT, B., BYINGTON, R. P., FURBERG, C. D., HUNNINGHAKE, D. B., MANCINI, G. B., MILLER, M. E. & RILEY, W. (2000) Effect of amlodipine on the progression of atherosclerosis and the occurrence of clinical events. PREVENT Investigators. *Circulation*, **102**, 1503-1510.

PLUMP, A. S., SMITH, J. D., HAYEK, T., AALTO-SETALA, K., WALSH, A., VERSTUYFT, J. G., RUBIN, E. M. & BRESLOW, J. L. (1992) Severe hypercholesterolemia and atherosclerosis in apolipoprotein E-deficient mice created by homologous recombination in ES cells. *Cell*, **71**, 343-353.

PODREZ, E. A., SCHMITT, D., HOFF, H. F. & HAZEN, S. L. (1999) Myeloperoxidase-generated reactive nitrogen species convert LDL into an atherogenic form in vitro. *J Clin Invest*, **103**, 1547-1560.

PODREZ, E. A., ABU-SOUD, H. M. & HAZEN, S. L. (2000a) Myeloperoxidase-generated oxidants and atherosclerosis. *Free Radic Biol Med*, **28**, 1717-1725.

PODREZ, E. A., FEBBRAIO, M., SHEIBANI, N., SCHMITT, D., SILVERSTEIN, R. L., HAJJAR, D. P., COHEN, P. A., FRAZIER, W. A., HOFF, H. F. & HAZEN, S. L. (2000b) Macrophage scavenger receptor CD36 is the major receptor for LDL modified by monocyte-generated reactive nitrogen species. *J Clin Invest*, **105**, 1095-1108.

PORTMAN, O. W. & ALEXANDER, M. (1969) Lysophosphatidylcholine concentrations and metabolism in aortic intima plus inner media: effect of nutritionally induced atherosclerosis. *J Lipid Res*, **10**, 158-165.

PRUTZ, W. A. (1996) Hypochlorous acid interactions with thiols, nucleotides, DNA, and other biological substrates. *Arch Biochem Biophys*, **332**, 110-120.

- RAINES, E. W. & ROSS, R. (1993) Smooth muscle cells and the pathogenesis of the lesions of atherosclerosis. *Br Heart J*, **69**, S30-37.
- RANG, H. P., DALE, M. M., RITTER, J. M. & FLOWER, R. J. (2007) *Rang and Dale's Pharmacology 6th Edition*, USA, Churchill Livingstone Elsevier.
- RATCLIFFE, H. L. & LUGINBUHL, H. (1971) The domestic pig: a model for experimental atherosclerosis. *Atherosclerosis*, **13**, 133-136.
- RAUSCH, P. G. & MOORE, T. G. (1975) Granule enzymes of polymorphonuclear neutrophils: A phylogenetic comparison. *Blood*, **46**, 913-919.
- RAVANDI, A., BABAEI, S., LEUNG, R., MONGE, J. C., HOPPE, G., HOFF, H., KAMIDO, H. & KUKSIS, A. (2004) Phospholipids and oxophospholipids in atherosclerotic plaques at different stages of plaque development. *Lipids*, **39**, 97-109.
- REDDICK, R. L., ZHANG, S. H. & MAEDA, N. (1994) Atherosclerosis in mice lacking apoE. Evaluation of lesional development and progression. *Arterioscler Thromb*, **14**, 141-147.
- REDDY, S., HAMA, S., GRIJALVA, V., HASSAN, K., MOTTAHEDEH, R., HOUGH, G., WADLEIGH, D. J., NAVAB, M. & FOGELMAN, A. M. (2001) Mitogen-activated protein kinase phosphatase 1 activity is necessary for oxidized phospholipids to induce monocyte chemotactic activity in human aortic endothelial cells. *J Biol Chem*, **276**, 17030-17035.
- REGAN, C. P., ADAM, P. J., MADSEN, C. S. & OWENS, G. K. (2000) Molecular mechanisms of decreased smooth muscle differentiation marker expression after vascular injury. *J Clin Invest*, **106**, 1139-1147.
- RIVARD, A. & ANDRES, V. (2000) Vascular smooth muscle cell proliferation in the pathogenesis of atherosclerotic cardiovascular diseases. *Histol Histopathol*, **15**, 557-571.
- RIVERA, L., MORON, R., ZARZUELO, A. & GALISTEO, M. (2009) Long-term resveratrol administration reduces metabolic disturbances and lowers blood pressure in obese Zucker rats. *Biochem Pharmacol*, **77**, 1053-1063.
- ROBASZKIEWICZ, A., GREIG, F. H., PITT, A. R., SPICKETT, C. M., BARTOSZ, G. & SOSZYNSKI, M. (2010) Effect of phosphatidylcholine chlorohydrins on human erythrocytes. *Chem Phys Lipids*, **163**, 639-647.
- ROMAN, M. J., PICKERING, T. G., SCHWARTZ, J. E., PINI, R. & DEVEREUX, R. B. (1995) Association of carotid atherosclerosis and left ventricular hypertrophy. *J Am Coll Cardiol*, **25**, 83-90.
- RONG, J. X., BERMAN, J. W., TAUBMAN, M. B. & FISHER, E. A. (2002) Lysophosphatidylcholine stimulates monocyte chemoattractant protein-1 gene expression in rat aortic smooth muscle cells. *Arterioscler Thromb Vasc Biol*, **22**, 1617-1623.
- RONG, J. X., SHAPIRO, M., TROGAN, E. & FISHER, E. A. (2003) Transdifferentiation of mouse aortic smooth muscle cells to a macrophage-like state after cholesterol loading. *Proc Natl Acad Sci U S A*, **100**, 13531-13536.
- ROSS, R. (1995) Cell biology of atherosclerosis. *Annu Rev Physiol*, **57**, 791-804.

- ROSS, R. (1999a) Mechanisms of disease. Atherosclerosis - An inflammatory disease. *N Engl J Med*, **340**, 115-126.
- ROSS, R. (1999b) Atherosclerosis is an inflammatory disease. *Am Heart J*, **138**, S419-S420.
- SAMSAMSHARIAT, S. Z., BASATI, G., MOVAHEDIAN, A., POURFARZAM, M. & SARRAFZADEGAN, N. (2011) Elevated plasma myeloperoxidase levels in relation to circulating inflammatory markers in coronary artery disease. *Biomark Med*, **5**, 377-385.
- SANTOS, N. C., FIGUEIRA-COELHO, J., MARTINS-SILVA, J. & SALDANHA, C. (2003) Multidisciplinary utilization of dimethyl sulfoxide: pharmacological, cellular, and molecular aspects. *Biochem Pharmacol*, **65**, 1035-1041.
- SCHENK, E. A., GAMAN, E. M. & FEIGENBOUM, A. D. (1966) Spontaneous aortic lesions in rabbits. I. Morphological characteristics. *Circ Res*, **19**, 80-88.
- SCHULTZ, J. & KAMINKER, K. (1962) Myeloperoxidase of the leucocyte of normal human blood. I. Content and localization. *Arch Biochem Biophys*, **96**, 465-467.
- SCHULZ, E., DOPHEIDE, J., SCHUHMACHER, S., THOMAS, S. R., CHEN, K., DAIBER, A., WENZEL, P., MUNZEL, T. & KEANEY, J. F., JR. (2008) Suppression of the JNK pathway by induction of a metabolic stress response prevents vascular injury and dysfunction. *Circulation*, **118**, 1347-1357.
- SCHWARTZ, R. S., HUBER, K. C., MURPHY, J. G., EDWARDS, W. D., CAMRUD, A. R., VLIETSTRA, R. E. & HOLMES, D. R. (1992) Restenosis and the proportional neointimal response to coronary artery injury: results in a porcine model. *J Am Coll Cardiol*, **19**, 267-274.
- SCOTT, J. W., HAWLEY, S. A., GREEN, K. A., ANIS, M., STEWART, G., SCULLION, G. A., NORMAN, D. G. & HARDIE, D. G. (2004) CBS domains form energy-sensing modules whose binding of adenosine ligands is disrupted by disease mutations. *J Clin Invest*, **113**, 274-284.
- SENOKUCHI, T., MATSUMURA, T., SAKAI, M., MATSUO, T., YANO, M., KIRITOSHI, S., SONODA, K., KUKIDOME, D., NISHIKAWA, T. & ARAKI, E. (2004) Extracellular signal-regulated kinase and p38 mitogen-activated protein kinase mediate macrophage proliferation induced by oxidized low-density lipoprotein. *Atherosclerosis*, **176**, 233-245.
- SHAO, B., ODA, M. N., BERGT, C., FU, X., GREEN, P. S., BROT, N., ORAM, J. F. & HEINECKE, J. W. (2006) Myeloperoxidase impairs ABCA1-dependent cholesterol efflux through methionine oxidation and site-specific tyrosine chlorination of apolipoprotein A-I. *J Biol Chem*, **281**, 9001-9004.
- SHAO, B., PENNATHUR, S. & HEINECKE, J. W. (2012) Myeloperoxidase targets apolipoprotein A-I, the major high density lipoprotein protein, for site-specific oxidation in human atherosclerotic lesions. *J Biol Chem*, **287**, 6375-6386.
- SHI, R., HU, C., YUAN, Q., YANG, T., PENG, J., LI, Y., BAI, Y., CAO, Z., CHENG, G. & ZHANG, G. (2011) Involvement of vascular peroxidase 1 in angiotensin II-induced vascular smooth muscle cell proliferation. *Cardiovasc Res*, **91**, 27-36.

SHIH, P. T., ELICES, M. J., FANG, Z. T., UGAROVA, T. P., STRAHL, D., TERRITO, M. C., FRANK, J. S., KOVACH, N. L., CABANAS, C., BERLINER, J. A. & VORA, D. K. (1999) Minimally modified low-density lipoprotein induces monocyte adhesion to endothelial connecting segment-1 by activating beta1 integrin. *J Clin Invest*, **103**, 613-625.

SHIMOKAWA, H. & VANHOUTTE, P. M. (1989) Impaired endothelium-dependent relaxation to aggregating platelets and related vasoactive substances in porcine coronary arteries in hypercholesterolemia and atherosclerosis. *Circ Res*, **64**, 900-914.

SIGWART, U., PUEL, J., MIRKOVITCH, V., JOFFRE, F. & KAPPENBERGER, L. (1987) Intravascular stents to prevent occlusion and restenosis after transluminal angioplasty. *N Engl J Med*, **316**, 701-706.

SIMON, B. C., CUNNINGHAM, L. D. & COHEN, R. A. (1990) Oxidized low density lipoproteins cause contraction and inhibit endothelium-dependent relaxation in the pig coronary artery. *J Clin Invest*, **86**, 75-79.

SKALEN, K., GUSTAFSSON, M., RYDBERG, E. K., HULTEN, L. M., WIKLUND, O., INNERARITY, T. L. & BOREN, J. (2002) Subendothelial retention of atherogenic lipoproteins in early atherosclerosis. *Nature*, **417**, 750-754.

SONG, P., WANG, S., HE, C., LIANG, B., VIOLLET, B. & ZOU, M. H. (2011) AMPKalpha2 deletion exacerbates neointima formation by upregulating Skp2 in vascular smooth muscle cells. *Circ Res*, **109**, 1230-1239.

SPICKETT, C. M., RENNIE, N., WINTER, H., ZAMBONIN, L., LANDI, L., JERLICH, A., SCHAUR, R. J. & PITT, A. R. (2001) Detection of phospholipid oxidation in oxidatively stressed cells by reversed-phase HPLC coupled with positive-ionization electrospray MS. *Biochem J*, **355**, 449-457.

SPICKETT, C. M. (2007) Chlorinated lipids and fatty acids: An emerging role in pathology. *Pharmacol Ther*, **115**, 400-409.

SPICKETT, C. M., REIS, A. & PITT, A. R. (2011) Identification of oxidized phospholipids by electrospray ionization mass spectrometry and LC-MS using a QQLIT instrument. *Free Radic Biol Med*, **51**, 2133-2149.

SPIGUEL, L. R., CHANDIWAL, A., VOSICKY, J. E., WEICHSELBAUM, R. R. & SKELLY, C. L. (2010) Concomitant proliferation and caspase-3 mediated apoptosis in response to low shear stress and balloon injury. *J Surg Res*, **161**, 146-155.

STAPLETON, D., GAO, G., MICHELL, B. J., WIDMER, J., MITCHELHILL, K., TEH, T., HOUSE, C. M., WITTERS, L. A. & KEMP, B. E. (1994) Mammalian 5'-AMP-activated protein kinase non-catalytic subunits are homologs of proteins that interact with yeast Snf1 protein kinase. *J Biol Chem*, **269**, 29343-29346.

STAPLETON, D., WOOLLATT, E., MITCHELHILL, K. I., NICHOLL, J. K., FERNANDEZ, C. S., MICHELL, B. J., WITTERS, L. A., POWER, D. A., SUTHERLAND, G. R. & KEMP, B. E. (1997) AMP-activated protein kinase isoenzyme family: subunit structure and chromosomal location. *FEBS Lett*, **409**, 452-456.

STARY, H. C., BLANKENHORN, D. H., CHANDLER, A. B., GLAGOV, S., INSULL, W., JR., RICHARDSON, M., ROSENFELD, M. E., SCHAFFER, S. A., SCHWARTZ, C. J., WAGNER, W. D. & ET AL. (1992) A definition of the intima of human arteries and of its atherosclerosis-prone regions. A report from the Committee on Vascular Lesions of the

Council on Arteriosclerosis, American Heart Association. *Arterioscler Thromb*, **12**, 120-134.

STARY, H. C., CHANDLER, A. B., GLAGOV, S., GUYTON, J. R., INSULL, W., JR., ROSENFELD, M. E., SCHAFFER, S. A., SCHWARTZ, C. J., WAGNER, W. D. & WISSLER, R. W. (1994) A definition of initial, fatty streak, and intermediate lesions of atherosclerosis. A report from the Committee on Vascular Lesions of the Council on Arteriosclerosis, American Heart Association. *Arterioscler Thromb*, **14**, 840-856.

STARY, H. C., CHANDLER, A. B., DINSMORE, R. E., FUSTER, V., GLAGOV, S., INSULL, W., JR., ROSENFELD, M. E., SCHWARTZ, C. J., WAGNER, W. D. & WISSLER, R. W. (1995) A definition of advanced types of atherosclerotic lesions and a histological classification of atherosclerosis. A report from the Committee on Vascular Lesions of the Council on Arteriosclerosis, American Heart Association. *Arterioscler Thromb Vasc Biol*, **15**, 1512-1531.

STARY, H. C. (2000) Natural history and histological classification of atherosclerotic lesions: an update. *Arterioscler Thromb Vasc Biol*, **20**, 1177-1178.

STEINBERG, D. H., GAGLIA, M. A., SLOTTOW, T. L. P., ROY, P., BONELLO, L., DE LABRIOLLE, A., LEMESLE, G., TORGUSON, R., KINESHIGE, K., XUE, Z. Y., SUDDATH, W. O., KENT, K. M., SATLER, L. F., PICHARD, A. D., LINDSAY, J. & WAKSMAN, R. (2009) Outcome differences with the use of drug-eluting stents for the treatment of in-stent restenosis of bare-metal stents versus drug-eluting stents. *Am J Cardiol*, **103**, 491-495.

STEINBRECHER, U. P., PARTHASARATHY, S., LEAKE, D. S., WITZTUM, J. L. & STEINBERG, D. (1984) Modification of low density lipoprotein by endothelial cells involves lipid peroxidation and degradation of low density lipoprotein phospholipids. *Proc Natl Acad Sci U S A*, **81**, 3883-3887.

STEINBRECHER, U. P., ZHANG, H. F. & LOUGHEED, M. (1990) Role of oxidatively modified LDL in atherosclerosis. *Free Radic Biol Med*, **9**, 155-168.

STEMMER, U., DUNAI, Z. A., KOLLER, D., PURSTINGER, G., ZENZMAIER, E., DEIGNER, H. P., AFLAKI, E., KRATKY, D. & HERMETTER, A. (2012) Toxicity of oxidized phospholipids in cultured macrophages. *Lipids Health Dis*, **11**, 110.

STOLL, G. & BENDSZUS, M. (2006) Inflammation and atherosclerosis: Novel insights into plaque formation and destabilization. *Stroke*, **37**, 1923-1932.

STONE, J. D., NARINE, A., SHAVER, P. R., FOX, J. C., VUNCANNON, J. R. & TULIS, D. (2013) AMP-activated protein kinase inhibits vascular smooth muscle cell proliferation and migration and vascular remodeling following injury. *Am J Physiol Heart Circ Physiol*, **304**, H369-H381.

SUBBANAGOUNDER, G., WATSON, A. D. & BERLINER, J. A. (2000) Bioactive products of phospholipid oxidation: isolation, identification, measurement and activities. *Free Radic Biol Med*, **28**, 1751-1761.

SUBBANAGOUNDER, G., DENG, Y. J., BORROMEO, C., DOOLEY, A. N., BELINER, J. A. & SALOMON, R. G. (2002) Hydroxy alkenal phospholipids regulate inflammatory functions of endothelial cells. *Vasc Pharmacol*, **38**, 201-209.

SUN, W., LEE, T. S., ZHU, M., GU, C., WANG, Y., ZHU, Y. & SHYY, J. Y. (2006) Statins activate AMP-activated protein kinase in vitro and in vivo. *Circulation*, **114**, 2655-2662.

SUZUKI, H., KURIHARA, Y., TAKEYA, M., KAMADA, N., KATAOKA, M., JISHAGE, K., UEDA, O., SAKAGUCHI, H., HIGASHI, T., SUZUKI, T., TAKASHIMA, Y., KAWABE, Y., CYNISHI, O., WADA, Y., HONDA, M., KURIHARA, H., ABURATANI, H., DOI, T., MATSUMOTO, A., AZUMA, S., NODA, T., TOYODA, Y., ITAKURA, H., YAZAKI, Y., KODAMA, T. & ET AL. (1997) A role for macrophage scavenger receptors in atherosclerosis and susceptibility to infection. *Nature*, **386**, 292-296.

SWERTFEGER, D. K., BU, G. & HUI, D. Y. (2002) Low density lipoprotein receptor-related protein mediates apolipoprotein E inhibition of smooth muscle cell migration. *J Biol Chem*, **277**, 4141-4146.

SWINDLE, M. M., SMITH, A. C. & HEPBURN, B. J. (1988) Swine as models in experimental surgery. *J Invest Surg*, **1**, 65-79.

TANNER, F. C., YANG, Z. Y., DUCKERS, E., GORDON, D., NABEL, G. J. & NABEL, E. G. (1998) Expression of cyclin-dependent kinase inhibitors in vascular disease. *Circ Res*, **82**, 396-403.

TEIRSTEIN, P. S., MASSULLO, V., JANI, S., POPMA, J. J., MINTZ, G. S., RUSSO, R. J., SCHATZ, R. A., GUARNERI, E. M., STEUTERMAN, S., MORRIS, N. B., LEON, M. B. & TRIPURANENI, P. (1997) Catheter-based radiotherapy to inhibit restenosis after coronary stenting. *N Engl J Med*, **336**, 1697-1703.

TENNANT, G. M., WADSWORTH, R. M. & KENNEDY, S. (2008) PAR-2 mediates increased inflammatory cell adhesion and neointima formation following vascular injury in the mouse. *Atherosclerosis*, **198**, 57-64.

THEILMEIER, G., QUARCK, R., VERHAMME, P., BOCHATON-PIALLAT, M. L., LOX, M., BERNAR, H., JANSSENS, S., KOCKX, M., GABBIANI, G., COLLEN, D. & HOLVOET, P. (2002) Hypercholesterolemia impairs vascular remodelling after porcine coronary angioplasty. *Cardiovasc Res*, **55**, 385-395.

THORNE, G. D., ISHIDA, Y. & PAUL, R. J. (2004) Hypoxic vasorelaxation: Ca<sup>2+</sup>-dependent and Ca<sup>2+</sup>-independent mechanisms. *Cell Calcium*, **36**, 201-208.

THUKKANI, A. K., HSU, F. F., CROWLEY, J. R., WYSOLMERSKI, R. B., ALBERT, C. J. & FORD, D. A. (2002) Reactive chlorinating species produced during neutrophil activation target tissue plasmalogens - Production of the chemoattractant, 2-chlorohexadecanal. *J Biol Chem*, **277**, 3842-3849.

THUKKANI, A. K., ALBERT, C. J., WILDSMITH, K. R., MESSNER, M. C., MARTINSON, B. D., HSU, F.-F. & FORD, D. A. (2003a) Myeloperoxidase-derived reactive chlorinating species from human monocytes target plasmalogens in low density lipoprotein. *J Biol Chem*, **278**, 36365-36372.

THUKKANI, A. K., MCHOWAT, J., HSU, F.-F., BRENNAN, M.-L., HAZEN, S. L. & FORD, D. A. (2003b) Identification of  $\alpha$ -chloro fatty aldehydes and unsaturated lysophosphatidylcholine molecular species in human atherosclerotic lesions. *Circulation*, **108**, 3128-3133.

- THUKKANI, A. K., MARTINSON, B. D., ALBERT, C. J., VOGLER, G. A. & FORD, D. A. (2005) Neutrophil-mediated accumulation of 2-CIHDA during myocardial infarction: 2-CIHDA-mediated myocardial injury. *Am J Physiol Heart Circ Physiol*, **288**, H2955-H2964.
- THYBERG, J. & HULTGARDH-NILSSON, A. (1994) Fibronectin and the basement membrane components laminin and collagen type IV influence the phenotypic properties of subcultured rat aortic smooth muscle cells differently. *Cell Tissue Res*, **276**, 263-271.
- TOWLER, M. C. & HARDIE, D. G. (2007) AMP-activated protein kinase in metabolic control and insulin signaling. *Circ Res*, **100**, 328-341.
- TSOYI, K., JANG, H. J., NIZAMUTDINOVA, I. T., KIM, Y. M., LEE, Y. S., KIM, H. J., SEO, H. G., LEE, J. H. & CHANG, K. C. (2011) Metformin inhibits HMGB1 release in LPS-treated RAW 264.7 cells and increases survival rate of endotoxaemic mice. *Br J Pharmacol*, **162**, 1498-1508.
- ULLEN, A., FAULER, G., KOFELER, H., WALTL, S., NUSSHOLD, C., BERNHART, E., REICHER, H., LEIS, H. J., WINTERSPERGER, A., MALLE, E. & SATTLER, W. (2010) Mouse brain plasmalogens are targets for hypochlorous acid-mediated modification in vitro and in vivo. *Free Radic Biol Med*, **49**, 1655-1665.
- VAN DEN BERG, J. J., WINTERBOURN, C. C. & KUYPERS, F. A. (1993) Hypochlorous acid-mediated modification of cholesterol and phospholipid: analysis of reaction products by gas chromatography-mass spectrometry. *J Lipid Res*, **34**, 2005-2012.
- VAN LEEUWEN, M., GIJBELS, M. J., DUIJVESTIJN, A., SMOOK, M., VAN DE GAAR, M. J., HEERINGA, P., DE WINTHER, M. P. & TERVAERT, J. W. (2008) Accumulation of myeloperoxidase-positive neutrophils in atherosclerotic lesions in LDL<sup>r</sup>- mice. *Arterioscler Thromb Vasc Biol*, **28**, 84-89.
- VAN TITS, L. J., STIENSTRA, R., VAN LENT, P. L., NETEA, M. G., JOOSTEN, L. A. & STALENHOF, A. F. (2011) Oxidized LDL enhances pro-inflammatory responses of alternatively activated M2 macrophages: a crucial role for Krüppel-like factor 2. *Atherosclerosis*, **214**, 345-349.
- VASQUEZ-VIVAR, J., KALYANARAMAN, B., MARTASEK, P., HOGG, N., MASTERS, B. S., KAROUI, H., TORDO, P. & PRITCHARD, K. A., JR. (1998) Superoxide generation by endothelial nitric oxide synthase: the influence of cofactors. *Proc Natl Acad Sci U S A*, **95**, 9220-9225.
- VELASCO, G., GEELLEN, M. J. & GUZMAN, M. (1997) Control of hepatic fatty acid oxidation by 5'-AMP-activated protein kinase involves a malonyl-CoA-dependent and a malonyl-CoA-independent mechanism. *Arch Biochem Biophys*, **337**, 169-175.
- VINCENT, M. F., ERION, M. D., GRUBER, H. E. & VAN DEN BERGHE, G. (1996) Hypoglycaemic effect of AICariboside in mice. *Diabetologia*, **39**, 1148-1155.
- VISSERS, M. C. M., PULLAR, J. M. & HAMPTON, M. B. (1999) Hypochlorous acid causes caspase activation and apoptosis or growth arrest in human endothelial cells. *Biochem J*, **344 Pt 2**, 443-449.
- VISSERS, M. C. M., CARR, A. C. & WINTERBOURN, C. C. (2001) Fatty acid chlorohydrins and bromohydrins are cytotoxic to human endothelial cells. *Redox Rep*, **6**, 49-56.

VUCICEVIC, L., MISIRKIC, M., JANJETOVIC, K., HARHAJI-TRAJKOVIC, L., PRICA, M., STEVANOVIC, D., ISENOVIC, E., SUDAR, E., SUMARAC-DUMANOVIC, M., MICIC, D. & TRAJKOVIC, V. (2009) AMP-activated protein kinase-dependent and -independent mechanisms underlying in vitro antiglioma action of compound C. *Biochem Pharmacol*, **77**, 1684-1693.

WALKER, L. N., BOWEN-POPE, D. F., ROSS, R. & REIDY, M. A. (1986) Production of platelet-derived growth factor-like molecules by cultured arterial smooth muscle cells accompanies proliferation after arterial injury. *Proc Natl Acad Sci U S A*, **83**, 7311-7315.

WALTON, K. A., COLE, A. L., YEH, M., SUBBANAGOUNDER, G., KRUTZIK, S. R., MODLIN, R. L., LUCAS, R. M., NAKAI, J., SMART, E. J., VORA, D. K. & BERLINER, J. A. (2003) Specific phospholipid oxidation products inhibit ligand activation of toll-like receptors 4 and 2. *Arterioscler Thromb Vasc Biol*, **23**, 1197-1203.

WANG, Q., ZHANG, M., LIANG, B., SHIRWANY, N., ZHU, Y. & ZOU, M. H. (2011a) Activation of AMP-activated protein kinase is required for berberine-induced reduction of atherosclerosis in mice: the role of uncoupling protein 2. *PLoS One*, **6**, e25436.

WANG, S., LIANG, B., VIOLLET, B. & ZOU, M. H. (2011b) Inhibition of the AMP-activated protein kinase- $\alpha$ 2 accentuates agonist-induced vascular smooth muscle contraction and high blood pressure in mice. *Hypertension*, **57**, 1010-1017.

WARDLE, R. L., GU, M., ISHIDA, Y. & PAUL, R. J. (2006)  $Ca^{2+}$ -desensitizing hypoxic vasorelaxation: pivotal role for the myosin binding subunit of myosin phosphatase (MYPT1) in porcine coronary artery. *J Physiol*, **572**, 259-267.

WATSON, A. D., BERLINER, J. A., HAMA, S. Y., LA DU, B. N., FAULL, K. F., FOGELMAN, A. M. & NAVAB, M. (1995) Protective effect of high density lipoprotein associated paraoxonase. Inhibition of the biological activity of minimally oxidized low density lipoprotein. *J Clin Invest*, **96**, 2882-2891.

WATSON, A. D., LEITINGER, N., NAVAB, M., FAULL, K. F., HORKKO, S., WITZTUM, J. L., PALINSKI, W., SCHWENKE, D., SALOMON, R. G., SHA, W., SUBBANAGOUNDER, G., FOGELMAN, A. M. & BERLINER, J. A. (1997) Structural identification by mass spectrometry of oxidized phospholipids in minimally oxidized low density lipoprotein that induce monocyte/endothelial interactions and evidence for their presence in vivo. *J Biol Chem*, **272**, 13597-13607.

WEIDINGER, F. F., MCLENACHAN, J. M., CYBULSKY, M. I., GORDON, J. B., RENNKE, H. G., HOLLENBERG, N. K., FALLON, J. T., GANZ, P. & COOKE, J. P. (1990) Persistent dysfunction of regenerated endothelium after balloon angioplasty of rabbit iliac artery. *Circulation*, **81**, 1667-1679.

WEISS, D., KOOLS, J. J. & TAYLOR, W. R. (2001) Angiotensin II-induced hypertension accelerates the development of atherosclerosis in apoE-deficient mice. *Circulation*, **103**, 448-454.

WELT, F. G. & ROGERS, C. (2002) Inflammation and restenosis in the stent era. *Arterioscler Thromb Vasc Biol*, **22**, 1769-1776.

WILDSMITH, K. R., ALBERT, C. J., ANBUKUMAR, D. S. & FORD, D. A. (2006) Metabolism of myeloperoxidase-derived 2-chlorohexadecanal. *J Biol Chem*, **281**, 16849-16860.

- WINDER, W. W., HOLMES, B. F., RUBINK, D. S., JENSEN, E. B., CHEN, M. & HOLLOSZY, J. O. (2000) Activation of AMP-activated protein kinase increases mitochondrial enzymes in skeletal muscle. *J Appl Physiol*, **88**, 2219-2226.
- WINTERBOURN, C. C., VANDENBERG, J. J. M., ROITMAN, E. & KUYPERS, F. A. (1992) Chlorohydrin formation from unsaturated fatty-acids reacted with hypochlorous acid. *Arch Biochem Biophys*, **296**, 547-555.
- WITZTUM, J. L. & STEINBERG, D. (1991) Role of oxidized low density lipoprotein in atherogenesis. *J Clin Invest*, **88**, 1785-1792.
- WITZTUM, J. L. (1994) The oxidation hypothesis of atherosclerosis. *Lancet*, **344**, 793-795.
- WOODS, A., SALT, I., SCOTT, J., HARDIE, D. G. & CARLING, D. (1996) The alpha1 and alpha2 isoforms of the AMP-activated protein kinase have similar activities in rat liver but exhibit differences in substrate specificity in vitro. *FEBS Lett*, **397**, 347-351.
- WOODS, A., JOHNSTONE, S. R., DICKERSON, K., LEIPER, F. C., FRYER, L. G., NEUMANN, D., SCHLATTNER, U., WALLIMANN, T., CARLSON, M. & CARLING, D. (2003a) LKB1 is the upstream kinase in the AMP-activated protein kinase cascade. *Curr Biol*, **13**, 2004-2008.
- WOODS, A. A., LINTON, S. M. & DAVIES, M. J. (2003b) Detection of HOCl-mediated protein oxidation products in the extracellular matrix of human atherosclerotic plaques. *Biochem J*, **370**, 729-735.
- XUE, B. & KAHN, B. B. (2006) AMPK integrates nutrient and hormonal signals to regulate food intake and energy balance through effects in the hypothalamus and peripheral tissues. *J Physiol*, **574**, 73-83.
- YAN, Z. Q. & HANSSON, G. K. (2007) Innate immunity, macrophage activation, and atherosclerosis. *Immunol Rev*, **219**, 187-203.
- YANG, C. Y., CHEN, S. H., GIANTURCO, S. H., BRADLEY, W. A., SPARROW, J. T., TANIMURA, M., LI, W. H., SPARROW, D. A., DELOOF, H., ROSSENEU, M. & ET AL. (1986) Sequence, structure, receptor-binding domains and internal repeats of human apolipoprotein B-100. *Nature*, **323**, 738-742.
- YANG, J., CHENG, Y., JI, R. & ZHANG, C. (2006) Novel model of inflammatory neointima formation reveals a potential role of myeloperoxidase in neointimal hyperplasia. *Am J Physiol Heart Circ Physiol*, **291**, H3087-3093.
- YANG, R., POWELL-BRAXTON, L., OGAOAWARA, A. K., DYBDAL, N., BUNTING, S., OHNEDA, O. & JIN, H. (1999) Hypertension and endothelial dysfunction in apolipoprotein E knockout mice. *Arterioscler Thromb Vasc Biol*, **19**, 2762-2768.
- YEH, M., LEITINGER, N., DE MARTIN, R., ONAI, N., MATSUSHIMA, K., VORA, D. K., BERLINER, J. A. & REDDY, S. T. (2001) Increased transcription of IL-8 in endothelial cells is differentially regulated by TNF-alpha and oxidized phospholipids. *Arterioscler Thromb Vasc Biol*, **21**, 1585-1591.
- YEH, M., COLE, A. L., CHOI, J., LIU, Y., TULCHINSKY, D., QIAO, J. H., FISHBEIN, M. C., DOOLEY, A. N., HOVNANIAN, T., MOUILLESEAUX, K., VORA, D. K., YANG, W. P., GARGALOVIC, P., KIRCHGESSNER, T., SHYY, J. Y. & BERLINER, J.

- A. (2004) Role for sterol regulatory element-binding protein in activation of endothelial cells by phospholipid oxidation products. *Circ Res*, **95**, 780-788.
- YIN, M., ZHANG, L., SUN, X. M., MAO, L. F. & PAN, J. (2010) Lack of apoE causes alteration of cytokines expression in young mice liver. *Mol Biol Rep*, **37**, 2049-2054.
- YOSHIDA, T., GAN, Q. & OWENS, G. K. (2008) Kruppel-like factor 4, Elk-1, and histone deacetylases cooperatively suppress smooth muscle cell differentiation markers in response to oxidized phospholipids. *Am J Physiol Cell Physiol*, **295**, C1175-1182.
- YU, S., WONG, S. L., LAU, C. W., HUANG, Y. & YU, C. M. (2011) Oxidized LDL at low concentration promotes in-vitro angiogenesis and activates nitric oxide synthase through PI3K/Akt/eNOS pathway in human coronary artery endothelial cells. *Biochem Biophys Res Commun*, **407**, 44-48.
- YU, W., LIU-BRYAN, R., STEVENS, S., DAMANAHALLI, J. K. & TERKELTAUB, R. (2012) RAGE signaling mediates post-injury arterial neointima formation by suppression of liver kinase B1 and AMPK activity. *Atherosclerosis*, **222**, 417-425.
- ZADELAAR, S., KLEEMANN, R., VERSCHUREN, L., DE VRIES-VAN DER WEIJ, J., VAN DER HOORN, J., PRINCEN, H. M. & KOOISTRA, T. (2007) Mouse models for atherosclerosis and pharmaceutical modifiers. *Arterioscler Thromb Vasc Biol*, **27**, 1706-1721.
- ZETTLER, M. E., PROCIUK, M. A., AUSTRIA, J. A., MASSAELI, H., ZHONG, G. M. & PIERCE, G. N. (2003) OxLDL stimulates cell proliferation through a general induction of cell cycle proteins. *Am J Physiol Heart Circ Physiol*, **284**, H644-H653.
- ZHANG, R., BRENNAN, M. L., FU, X., AVILES, R. J., PEARCE, G. L., PENN, M. S., TOPOL, E. J., SPRECHER, D. L. & HAZEN, S. L. (2001) Association between myeloperoxidase levels and risk of coronary artery disease. *JAMA*, **286**, 2136-2142.
- ZHAO, X., ZMIJEWSKI, J. W., LORNE, E., LIU, G., PARK, Y. J., TSURUTA, Y. & ABRAHAM, E. (2008) Activation of AMPK attenuates neutrophil proinflammatory activity and decreases the severity of acute lung injury. *Am J Physiol Lung Cell Mol Physiol*, **295**, L497-504.
- ZHOU, G., MYERS, R., LI, Y., CHEN, Y., SHEN, X., FENYK-MELODY, J., WU, M., VENTRE, J., DOEBBER, T., FUJII, N., MUSI, N., HIRSHMAN, M. F., GOODYEAR, L. J. & MOLLER, D. E. (2001) Role of AMP-activated protein kinase in mechanism of metformin action. *J Clin Invest*, **108**, 1167-1174.
- ZHU, B., KUHEL, D. G., WITTE, D. P. & HUI, D. Y. (2000) Apolipoprotein E inhibits neointimal hyperplasia after arterial injury in mice. *Am J Pathol*, **157**, 1839-1848.
- ZIOUZENKOVA, O., ASATRYAN, L., AKMAL, M., TETTA, C., WRATTEN, M. L., LOSETO-WICH, G., JURGENS, G., HEINECKE, J. & SEVANIAN, A. (1999) Oxidative cross-linking of ApoB100 and hemoglobin results in low density lipoprotein modification in blood. Relevance to atherogenesis caused by hemodialysis. *J Biol Chem*, **274**, 18916-18924.

# Appendices

## Appendix 1:

**F.H. Greig**, S. Kennedy and C.M. Spickett (2012) Physiological effects of oxidized phospholipids and their cellular signaling mechanisms in inflammation. *Free Radic Biol Med*, **52**, 266-280.

## Appendix 2:

A. Robaszekiewicz, **F.H. Greig**, A.R. Pitt, C.M. Spickett, G. Bartosz and M. Soszyński (2010) Effect of phosphatidylcholine chlorohydrins on human erythrocytes. *Chem Phys Lipids*, **163**, 639-647.